A STUDY OF STRUCTURE STABILITY USING THE FINITE ELEMENT METHOD AND MINIMUM WEIGHT DESIGN OF COMPOSITE PANEL

by

ALI HASAN SURI

Thesis presented for the degree of Ph.D. to the Faculty of Engineering, the University of Glasgow

Department of Aeronautics and Fluid Mechanics

1983

To The Memory of My Father

A C K N O W L E D G E M E N T S.

The Author wishes to express his deep gratitude to his Supervisor, Mr. T. Cain, M.R.Ae.S., for his continuous guidance and unfailing support throughtout the period in which this work was conducted, and for the large amount of time he spent in reading the manuscript and for the correction of the Thesis.

A debt of gratitude is also owed to Professor Bryan Richards and to all members of the Department of Aeronautics of Glasgow University, for their encouragement and support.

The Author wishes to thank Al Fateh University for the financial support and for providing the scholar fees and for the Scholarship.

Finally, thanks and appreciation to Mrs. A. Leishman for the typing of the manuscript.

SUMMARY

A general study of the finite element approach and its application to structural analysis is conducted and methods of derivation of element properties are reviewed.

It is found that the method has the advantage of generality of application and that the direct approach is easier to programme than the force method. A unified and simple formula is derived for the computation of element elastic and geometric stiffness matrices and is found to be much easier to apply than existing methods.

The standard finite element displacement method is used to study overall buckling of beams, plates, and stiffened plates. The results show that the method can provide accurate answers as compared with the existing analytical approaches.

The exact finite strip, the approximate finite strip, and the finite strip for local buckling analysis are reviewed and are found to economise greatly in computer time, needing less storage space because of their narrow band width as compared with the standard finite element method.

In particular, the finite strip for local stability which uses a standard eigenvalue subroutine and is based on the concept of geometric stiffness matrices is used to study local buckling and buckling of plates and plates supported elastically by continuous elastic medium. The results obtained are shown to be very close to those obtained analytically, the effect of the elastic support being to increase greatly the buckling stress relative to the unsupported plates.

The results of compression tests on 21 steel strips supported elastically by core material represented by balsa wood and foam Polystyrene with one side free and the other clamped, show good agreement with the theoretical analysis.

The results of the study conducted on stabilised plates suggest that a composite panel made up of thin stiffeners and light core may provide a structure which performs better under in-plane loadings.

The study of local buckling of a composite panel reveals that high local buckling stresses can be obtained relative to an integrally stiffened panel of the same geometry using a relatively low value of the core stiffness. It also shows that for each cross-section geometry there is a value for the stiffness of the core at which the local buckling stress reaches a value beyond which a large increase in core stiffness will only produce a small increase in buckling stress; these values, which can be used to find the necessary core stiffness to fully stabilise the stiffeners against the onset of local buckling, are given in terms of the cross-section parameters.

Minimum weight design of a composite panel is considered, the minimum weight design of a panel with an isotropic core using the results obtained from the local study is found to be more efficient than either the integrally stiffened panel or the truss-core stiffened panel or the Z stiffened panel over a full range of the structural index.

The minimum weight panel made up of very thin stiffeners and orthotropic core is found to be efficient only in the intermediate and high range of the structural index.

C O N T E N T S

INTRODUCTION

In the field of aircraft construction, thin-walled components loaded in-plane have an important role and their failure by local or overall instability would constitute an immediate threat to safety.

The presence of stiffening webs, cut-outs and varying plate thickness in the structural components added to the variety of types of loading to be considered and the necessity of close interpretation of the boundary conditions, makes the use of conventional methods of analysis extremely difficult.

An alternative approach is now available in the finite element method formulated in matrix form and achieving a numerical solution without using the differential equation or the analytical expression of the total potential energy.

The object of this study will be first to conduct a general survey of the finite element method, examining the variety of approaches employed, and second, having chosen the most appropriate approach, the overall and local instability types of failure of a variety of structural forms will be studied.

Particular attention will be given to the use of the finite element method for the purpose of the determination of the buckling load for stabilised plates and for the determination of the nondimensional quantities necessary for minimum weight design.

An efficiency study based on the results obtained from the analysis of a structural component built up from thin high strength material and light-weight core will be included.

The finite element method has evolved basically along two main divisions, identified as the "force" and "displacement" methods.

The first of these considers internal forces to be the unknowns (1) and uses element flexibilities to construct the mathematical model of the complete structure. Its application to stability analysis has been considered in Reference (2).

The second, considers displacements to be the unknowns and formulates the mathematical model in terms of element stiffnesses. There are two sub-divisions within this second method, Argyris' approach (1) and the direct approach (3) and the application of this method to stability study first appeared in (4) when, unlike the force method, it received wide acceptance.

There are a variety of methods available for the derivation of element stiffnesses, some involving rather complicated procedures, and there is a need for a more unified approach.

Since continuous support was known to be the best method of stabilising a structure, this problem received a great deal of attention in the nineteen-forties (5), (6). Subsequently, attention was focused on other types of construction and the sandwich construction made of two materials was abandoned. I believe this to have been because the analytical approaches used were not convenient to explore fully the advantages of using core material with various boundary conditions and the assumptions used to interpret the core stiffness, unless greatly simplified, could not be accommodated in the analysis. For this reason, a large part of this study was devoted to theoretical experimental analysis of stabilised plates.

CHAPTER 1.

FINITE ELEMENT METHOD

1.1. Introduction:

The exact solution of an elasticity problem is obtained by integrating the differential equation expressed in terms of either the displacement or the stress resultant taking into account the associated boundary conditions. For some structures the setting up of the differential equation is difficult if not impossible, and sometimes, even if the differential equation can be found the mathematical representation for the actual boundary conditions is not easy to obtain.

As a result it is only in special cases that a closed form solution can be found, and for complex structures numerical methods must be employed.

These numerical methods can solve the structural problem either by finding a numerical solution to the differential equation (Finite difference method) or, after transforming the structure into finite elements connected together at the nodes, according to theory of elasticity equilibrium and compatibility laws (Finite element method), by applying the equilibrium and compatibility conditions to these nodes.

The finite difference method can be used if the differential equation and the associated boundary conditions are known but, as has been said, this is not always the case.

In the finite element method in its two principal divisions, the force approach and the displacement approach, the boundary conditions do not constitute a difficulty.

1.1.1 The Finite Element Method.

The finite element method of structural analysis, developed for use on high speed computers has now become universally accepted as a valid aid to designers. The method provides accurate and rapid solutions to many of the problems encountered in engineering.

In addition to stress analysis, vibration (7) and buckling (8) are areas where the method is efficiently used.

The finite element method is based on the concept of replacing the actual continuous structure by an equivalent model made up from discrete structural elements for which the elastic and inertial properties are expressed in matrix form.

The matrices representing the single components are then fitted together according to rules established by the theory of elasticity to represent the static and dynamic properties of the actual structure.

The points or lines where the discrete elements are joined are known as nodes. The elastic properties of an element are found by assuming either a form for the displacement variation or for the stress distribution within its boundaries.

The complete solution is then found by combining the individual approximate displacement or stress distributions in a manner which satisfies the force equilibrium and displacement compatibility at the junction between these elements.

Two of the sub-divisions within the finite element method are (1) the force or flexibility method where forces are the unknowns and (2) the displacement method where the displacements are the unknowns.

In this chapter and in the next these two methods will be looked at in reasonable detail and in later chapters the displacement method will be used in a stability study of some structural elements and in the design for minimum weight of a panel.

1.1.2. Finite Elements in Stability of Structures.

Geometric nonlinearity can be dealt with equally well by the finite element method. When deflections are so large that the equilibrium equations must be referred ro the deformed configuration then nonlinear terms in the matrix formulation for a structure mean that a solution can only be obtained by an iteration procedure.

The buckling load for a structure can be obtained as a particular application of large deflection theory.

Thus buckling loads for a structure idealised into an assembly of discrete elements can be determined as the eigenvalues of a determinantal equation (9).

Although both approaches can be used for stability analysis the direct displacement approach has been found to be more attractive and easier to programme for the computer.

In the displacement approach the stability of the structure is analysed by introducing the geometrical stiffness which is added to the elastic stiffness to form a combined stiffness matrix. Since the geometric stiffness matrix is a function of the initial linear stress distribution in the structure, the addition of elastic and geometric stiffnesses leads to an equilibrium equation of standard eigenvalue type for which the buckling stress can be found.

Chapter 2 and Chapter 3 will present the study of the finite element method in dealing with structural stability and the buckling loads for some particular structures will be found by the displacement approach .

1.2 THE FORCE METHOD

1.2.1 General:

The force method was very popular in the early fifties. In reference (10) Argyris traced the origins of this approach, and in a series of papers published in "Aircraft Engineering" Volumes 26 and 27 (11), he developed in detail this method which proved to be very powerful for the analysis of a complex structure.

For completeness, a brief resumé of Argyris' presentation is given in the following sections.

In this method the internal forces in the structure are chosen as unknowns and the flexibilities of the elements are used in the analysis.

The internal forces and displacements in a structure can be found by simple matrix operations for any set of external loads and the matrix of thermal effects or initial lack of fit once the matrices $\mathbf{B}_0$, $\mathbf{B}_1$ and $\mathbf{f}$ are determined.

In the following paragraphs, the matrices $\mathbf{B}_0$, $\mathbf{B}_1$, $\mathbf{f}$ will be discussed and the analysis procedure of the force method will be presented together with the application of the force method to the solution of some particular problems.

1.2.1a Force Method Solution Procedure for Statically Determinate Structure.

Given an elastic structure subjected to the applied loads $\mathbf{P}$ where $\mathbf{P}$ is a column of $\mathbf{m}$ elements, $\mathbf{P}=\{ p_1\ p_2 \cdots p_m \}$.

The structure is idealised into an assemblage of finite elements for which the displacement-force relationships are known.

The internal generalised forces $\mathbf{S}$ for the structure are given as a column matrix, each element of which is a submatrix representing the applied juncture forces for a structural element

$$\mathbf{S} = \{ \mathbf{S}_1 \ \mathbf{S}_2 \cdots\cdots \mathbf{S}_s \}$$

For the element j then $\mathbf{S}_j = \mathbf{B}_j \mathbf{P}$

The matrix $\mathbf{B}_j$ is a rectangular matrix with as many rows as $\mathbf{S}_j$ and as many columns as the number of elements in $\mathbf{P}$ and the elements of the i^{th} column of $\mathbf{B}_j$ are the juncture forces corresponding to the applied load $\mathbf{P}_i = 1$.

Then for the entire structure the relation between the applied forces and the internal generalised forces becomes

$$\mathbf{S} = \mathbf{B} \mathbf{P}$$

where $\mathbf{B}$ is now the partioned matrix $\mathbf{B} = \{ \mathbf{B}_1 \ \mathbf{B}_2 \cdots \mathbf{B}_s \}$

For a statically determinate structure the elements of $\mathbf{B}$ are found from the equilibrium conditions alone.

To find the column of external displacement $\mathbf{U} = \{ u_1 u_2 \ldots u_m \}$, $\mathbf{f}$, the diagonal matrix, is formed. This has the element flexibility matrices as submatrices and has the form:

$$\mathbf{f} = \begin{bmatrix} \mathbf{f}_1 & \mathbf{f}_2 & \cdots & \mathbf{f}_s \end{bmatrix}$$

For a single element the displacement at its boundary is:

$$\mathbf{V}_j = \mathbf{f}_j \mathbf{S}_j$$

This can be written:

$$\mathbf{V}_j = \mathbf{f}_j \mathbf{B}_j \mathbf{P}$$

Analogously, for the complete structure:

$$\mathbf{V} = \mathbf{f}\,\mathbf{B}\,\mathbf{P}$$

The column matrix of internal deformation $\mathbf{V}$ is related to the external deformation column $\mathbf{U}$ by the relation:

$$\mathbf{U} = \mathbf{B}^{T}\mathbf{V}$$

(matrix form of unit load theorem)
See Appendix (A.1)

Substituting for $\mathbf{V}$:

$$\mathbf{U} = \mathbf{B}^{T}\mathbf{f}\,\mathbf{B}\,\mathbf{P}$$

The last equation can be written as:

$$\mathbf{U} = \mathbf{F}_{o}\,\mathbf{P}$$

Where $\mathbf{F}_{o}$ represents the flexibility of the statically determinate structure.

$\mathbf{U}$ the column matrix of external deformation.

and $\mathbf{P}$ the column matrix of the external loads.

It is worth noticing that:

$$\mathbf{F}_{o} = \mathbf{K}_{e}^{-1}$$

Where $\mathbf{K}_{e}$ is the reduced elastic stiffness to be encountered later on in the displacement method.

1.2.1b
Force Method Solution Procedure for Statically Indeterminate Structure.

In the case of a statically indeterminate structure, the condition of compatibility of deformation must be introduced.

For a structure g times redundant, the internal generalised forces are devided into a basic system which is in equilibrium with the applied loadsand g independent systems each forming one of/

/of the self-equilibrating force systems of the redundant structures.

If $\mathbf{X}$ is the column matrix of the generalised redundant forces $\{x_1 - - x_g\}$

then the matrix equation $\mathbf{S} = \mathbf{B}\,\mathbf{P}$ must be expanded

in the form:

$$\mathbf{S} = \mathbf{B}_0\mathbf{P} + \mathbf{B}_1\mathbf{X}$$

Where $\mathbf{B}_1$ is the matrix of the generalised forces on elements arising from unit values of the redundancies.

For simple structures $\mathbf{X}$ can be found by assuming hypothetical cuts in the structure and applying the compatibility conditions then the matrix $\mathbf{B}_1$ will be found by giving each of the chosen redundancies unit value one at a time.

For more complex structures the matrix $\mathbf{X}$ need not be associated with hypothetical cuts. In this case the redundancies are regarded as self-equilibrating localised groups of internal forces. The procedure for selecting such systems for wings or fuselages and specific relationships for the evaluation of $\mathbf{B}_1$ is well documented (1).

The expression for the generalised element displacements becomes :

$$\mathbf{V} = \mathbf{f}\,\mathbf{B}_0\mathbf{P} + \mathbf{f}\,\mathbf{B}_1\mathbf{X}$$

To find $\mathbf{X}$ the compatibility condition is introduced in the form:

$$\mathbf{B}_1^T\mathbf{V} = \mathbf{0}$$

Substituting for $\mathbf{V}$ this equation will become:

$$\mathbf{B}_1^T\mathbf{f}\,\mathbf{B}_0\,\mathbf{P} + \mathbf{B}_1^T\mathbf{f}\,\mathbf{B}_1\,\mathbf{X} = \mathbf{0}$$

Introducing

$$\mathbf{F}_{11} = \mathbf{B}_1^T\mathbf{f}\,\mathbf{B}_1$$

$$\mathbf{F}_{10} = \mathbf{B}_1^T\mathbf{f}\,\mathbf{B}_0$$

Then:

$$\mathbf{X} = -\mathbf{F}_{11}^{-1}\,\mathbf{F}_{10}\,\mathbf{P}$$

Hence $\mathbf{S}$ can still be written as

$$\mathbf{S} = \mathbf{B}\ \mathbf{P}$$

Where $\mathbf{B}$ now is given as

$$\mathbf{B} = \mathbf{B}_o - \mathbf{B}_1 \mathbf{F}_{11}^{-1} \mathbf{F}_{1o}$$

$\mathbf{B}_o$ is the $\mathbf{B}$ found for the chosen statically determinate sub-structure.

From the principal of virtual work applied to the statically determinate sub-structure *

$$\mathbf{U} = \mathbf{B}_o^T \mathbf{V}$$

Then by substituting for $\mathbf{V}$ and writing $\mathbf{F}_{oo} = \mathbf{B}_o^T \mathbf{f}\ \mathbf{B}_o$ we have

$$\mathbf{U} = \mathbf{F}_{oo}\mathbf{P} + \mathbf{F}_{1o}^T \mathbf{X}$$

$$\mathbf{U} = \mathbf{F}\ \mathbf{P}$$

Where $\mathbf{F}$, the flexibility matrix of the assembled structure, is given as:

$$\mathbf{F} = \mathbf{F}_{oo} - \mathbf{F}_{1o}^T \mathbf{F}_{11}^{-1} \mathbf{F}_{1o}$$

---

* See Appendix (A. 1)

1.3 THE DISPLACEMENT METHOD.

1.3.1. General:

Two significant contributions in the final development of the displacement method are attributed to the work of Argyris in a series of papers published in (Aircraft Engineering 1954 to 1955 (1)), and to Turner and al. 1956 (3)).

Although both approaches lead to the final set of equations relating displacements at the nodes to the external applied forces, they differ in the assembly procedure of the stiffness matrix of the whole structure from the stiffnesses of the single components.

In the first approach, following a procedure very similar to that adopted in the previous section, the stiffness matrices formulated with respect to their individual local coordinate system are first arrayed in a large single matrix $\mathbf{k}$ then to produce the assembled stiffness matrix, the following matrix operation takes place:

$$\mathbf{K} = \tilde{\mathbf{A}}\,\mathbf{k}\,\mathbf{A}$$

Where the matrix $\mathbf{A}$ represents relationships between external and the internal displacements. This approach is dual to the force method and has the advantage that a computer programme developed for one method can be used without much alteration for the other. This approach will be named as Argyris approach.

In the second case, stiffness matrices for single components which are referred to local coordinate axes are transformed to the overall structure coordinate axes and the stiffness matrix for the whole structure can be assembled by merely adding element stiffness coefficients having identical subscripts.

This approach can be seen to score over the first in that it can be programmed for the computer with much less effort. This approach is known as the direct approach. In this section, these two approaches will be looked at in some detail.

1.3.2. Argyris Approach.

For a particular element of the idealised structure, the force displacement approach relationships can be written as:

$$\mathbf{S}_i = \mathbf{k}_i \mathbf{V}_i$$

where $\mathbf{V}_i$ is the column of nodal deformations relative to the junctures considered acting as a support*, $\mathbf{K}_i$ the element stiffness matrix, and $\mathbf{S}_i$ is the column of nodal forces.

For the whole structure composed of $\mathbf{s}$ elements, the force-displacement relationships take the following form:

$$\mathbf{S} = \mathbf{k}\,\mathbf{V}$$

where $\mathbf{S}$, $\mathbf{k}$ and $\mathbf{V}$ take the forms given below:

$$\mathbf{S}=\{\mathbf{S}_1 \text{ ---- } \mathbf{S}_s\} \quad , \quad \mathbf{k}=\lceil \mathbf{k}_1 \text{ - - - } \mathbf{k}_s \rfloor \quad , \quad \mathbf{V}=\{\mathbf{V}_1 \text{ -- --- } \mathbf{V}_s\}$$

if we indicate by p the number of elements in $\mathbf{V}$ and by m the number of elements in $\mathbf{U}$, for small displacement the relation between external displacements $\mathbf{U}$ and internal displacements $\mathbf{V}$ can be written as

$$\mathbf{V} = \mathbf{A}_0 \mathbf{U} \qquad \text{(see Appendix (A.1))}$$

where the matrix $\mathbf{A}_0$ is of order $(p \times m)$,

if $\mathbf{U}$ is specified at all juncture points, so that m=p, then the matrix $\mathbf{A}_0$ can be found from geometric reasoning.

---

* The element matrix need not include the rigid body displacement modes so that the degree of freedom corresponding to a statically determinate stable support may be excluded and in writing $\mathbf{V}_i$ we do not include the displacements of all the juncture points, instead we consider some of the junctures to be supports for the element.

If m is less than p so that (p - m) = r, the total of all joint displacement in this case can be written as

$$\begin{bmatrix} \mathbf{U} \\ \mathbf{Z} \end{bmatrix}$$

which is a column matrix of order p.

Where the elements of the matrix Z are known as kinematic redundancies in an analogy with the force method,

and the relation between internal and external displacement becomes:

$$\mathbf{V} = \mathbf{A_o}\ \mathbf{U} + \mathbf{A_1}\ \mathbf{Z}$$

Where the matrix $\mathbf{A_o}$ is of order ($^{p \times m}$) and the ith column of it represents a set of element deformation that are produced or compatible with unit deformation $u_i = 1$ with all other displacements $u_j = 0$ for $j \neq i$ and all the elements of **Z** are equal to zero.

$\mathbf{A_1}$ is of order ($p \times r$) and its ith column represents a set of element deformations that are produced or compatible with a unit deformation $z_i = 1$ while all $z_j = 0$ for $j \neq i$; and all the elements of **U** are zeros.

$\mathbf{A_1}$ can also be found by geometric reasoning alone.

These two matrices can be written as:

$$\mathbf{A_o} = \{\mathbf{A_{o_1}} \cdots \mathbf{A_{o_s}}\} \qquad \mathbf{A_1} = \{\mathbf{A_{1_1}} \cdots \mathbf{A_{1_s}}\}$$

where $\mathbf{A}_{oi}$, $\mathbf{A}_{1i}$ are row matrices of order m and r.

As in the case of the force method there are different choices for determining the matrix $\mathbf{V_i}$ and for each $\mathbf{V_i}$ chosen there will correspond certain $\mathbf{k_i}$ and $\mathbf{S_i}$ matrices.

To maintain the specified displacement $\mathbf{U}$ a set of forces must be applied at the juncture points, $\mathbf{P} = \{\mathbf{p_1} \cdots \mathbf{p_m}\}$.

To determine the kinematic redundancies $\mathbf{Z}$ we impose equilibrium between the internal and the external forces.

Substituting for $\mathbf{V}$ in the above equation gives:

$$\mathbf{S} = \mathbf{k}\,\mathbf{A_o}\mathbf{U} + \mathbf{k}\,\mathbf{A_1}\mathbf{Z} \qquad (1.1)$$

If we indicate by U_E the strain energy of the system and by V the potential energy of the applied forces, then from the principal of the stationary value of the total potential energy:

$$\delta(U_E + V) = o$$

Because the displacement vector $\mathbf{U}$ is specified at the m points, then the virtual displacement must vanish at these points and as a result:

$$\delta V = o$$

and the above condition reduces to

$$\delta U_E = o$$

For the unspecified displacements we take as a virtual displacement, the deformationsthat are compatible with unit variation of the r elements in $\mathbf{Z}$.

By successively taking $Z_i = 1$ with $i = 1, r$ and considering all other elements of $\mathbf{Z}$ and all elements of $\mathbf{U}$ equal to zero the matrix $\mathbf{A}_1$ will have been found.

Then from the condition that $\delta U_E = -\delta W_i = 0$ the equilibrium condition can be written as:

$$\mathbf{A}_1^T \mathbf{S} = \mathbf{O}$$

Where the $i^{th}_{col.}$ $\mathbf{A}_1$ is effectively the set of virtual displacement $\mathbf{V}$ corresponding to a virtual displacement of the i^{th} unspecified displacement.

Substituting for $\mathbf{S}$ from equation (1. 1)

$$\mathbf{A}_1^T(\mathbf{k}\,\mathbf{A}_0\mathbf{U} + \mathbf{k}\,\mathbf{A}_1\mathbf{Z}) = \mathbf{O} \qquad (1.\ 2)$$

or

$$\mathbf{C}_{11}\mathbf{Z} = -\ \mathbf{C}_{10}\mathbf{U}$$

where the notation $\mathbf{C}_{ij} = \mathbf{A}_i^T \mathbf{k}\, \mathbf{A}_j$ is used.

hence

$$\mathbf{Z} = -\ \mathbf{C}_{11}^{-1}\mathbf{C}_{10}\mathbf{U}$$

to obtain $\mathbf{S}$ we substitute in equation

Also the internal deformations can be obtained now by substitution for $\mathbf{Z}$ and the final result can be put into the following form:

$$\mathbf{V} = \mathbf{A}\,\mathbf{U}$$

$$\mathbf{S} = \mathbf{k}\mathbf{A}\mathbf{U} \qquad (1.\ 3)$$

where

$$\mathbf{A} = \mathbf{A}_0 - \mathbf{A}_1\mathbf{C}_{11}^{-1}\mathbf{C}_{10}$$

then from the principal of the stationary value of the total potential energy

$$\delta\ (\ U_E + V\ ) = 0$$

which expresses the equilibrium of internal forces $\mathbf{S}$ and external forces $\mathbf{P}$, and by taking a virtual displacement $u_i=1$ and $u_j=0$, $\mathbf{Z}=\mathbf{O}$ for all $j\neq i$, we find

$$\delta V = - P_i$$

The i^{th} column of $\mathbf{A_o}$ is a set of deformations which are compatible with $u_i=1$.

The product of the trnaspose of this column with $\mathbf{S}$ is

$$\mathbf{A}_{o_1}^{T}\mathbf{S} = -\delta W_{i\lambda} = \delta U_{E\lambda}$$

Repeating the procedure for all the values of U_i which are different from the first and from

$$-\delta V = \delta U_E$$

leads to

$$\mathbf{P} = \mathbf{A}_o^{T}\mathbf{S}$$

substituting on $\mathbf{S}$ by (1. 3)

gives

$$\mathbf{P} = \mathbf{k}\,\mathbf{U} \qquad (1.4)$$

where

$$\mathbf{k} = \mathbf{C}_{oo} - \mathbf{C}_{1o}^{T}\mathbf{C}_{11}^{-1}\mathbf{C}_{1o}$$

is the assembled stiffnes matrix.

So far it was assumed that $\mathbf{U}$ was given and $\mathbf{P}$ represents the unknown loads.

But in practice, the load matrix is given and it is the displacement which are the unknowns.

To find the displacement vector in terms of the external load vector invert equation(1.4) give

$$\mathbf{U} = \mathbf{k}^{-1}\mathbf{P}$$

To find $\mathbf{S}$ using (1.3)and(1.4)

$$\mathbf{S} = \mathbf{K}\,\mathbf{A}\,\mathbf{k}^{-1}\,\mathbf{P}$$

1.3.3. Direct Approach.

Suppose we have the relationships which relate element forces to element displacements in matrix from:

$$\mathbf{F} = \mathbf{k}_e \mathbf{U}$$

where $\mathbf{k}_e$ is elastic stiffness matrix for the finite element to be used to construct the finite element model.

The elements are assembled to form the finite element model for the whole structure by joining all elements at their respective nodal points and in the process the compatability of node displacement and equilibrium requirements must be satisfied throughout.

Thus at node i the equilibrium of forces in the x direction for example must be

$$\mathbf{P}_{ix} = \Sigma \mathbf{F}_{ix}$$

The fact that the displacements of the nodes of all the elements which meet at node i must be equal ensure that the compatability requirement is satisfied.

It follows that the elastic stiffness matrix for the complete structure can be obtained simply by adding the elements stiffness coefficients having identical subscripts. This will lead to the relation:

$$\mathbf{P} = \mathbf{K_S}\ \mathbf{U}$$

This equation includes all the displacement components of all nodes, represents a completely free body and the displacement can not be uniquely determined by the forces.

Mathematically the determinant of matrix $\mathbf{K_S}$ is zero and the matrix is singular which means it cannot be inverted .

To obtain a solution it is necessary to eliminate a certain number of degrees of freedom (in plane: three, in space: six),

This can be done by the prescription of appropriate displacements after the assembly stage, and deleting the rows and columns relative to these displacements and $\mathbf{K_S}$ become $\mathbf{K_r}$.

The displacement can be given by:

$$\mathbf{U} = \mathbf{K_r^{-1}}\mathbf{P}$$

For computer use the above procedure can be translated into the following steps: (3),(8),(11)

a - Each element stiffness is evaluated and each element of each stiffness matrix is given a double subscript i and j, the first refers to force component and the second to the displacement component.

b - An array of order equal to the number of degrees of freedom for the complete structure is prepared and named the assembly array.

c - A relation must be established between the element stiffness matrix labels i, j and the labels of the single components of the assembly array l, m.

d - Each element from the element stiffness matrix is sent to a place in the assembly stiffness matrix and summed up to the previous value of the assembly stiffness element.

e - This procedure is repeated for all the elements forming the idealised structure.

f - If different types of elements are involved, to satisfy the rulesof matrices summation the stiffnesses of these elements have to be of the same order and the individual sub-matrices to be added have therefore to be built up of same number of individual components of force or displacement.

g - Having built up the assembly matrix, the constraint condition which is equivalent to zero displacements at certain nodes can be taken into account by eliminating the columns of stiffness coefficients multiplying these degrees of freedom.

h - The result from the previous step is more equations than unknowns, the rows corresponding to the eliminated columns are set aside for later use to find support reactions.

i - The set of equations remaining after the elimination of rows and columns relative to the support conditions are solved for the displacements.

j - The internal force system is found by back substitution of the displacements found in the previous step into the force displacement relationships for the elements.

k - If it is necessary,the transformation from the global co-ordinate system to local co-ordinates must be performed before the stress computation is accomplished.

Summarising, for the displacement direct approach the following matrix operations must be performed:

$$\mathbf{P} = \mathbf{K}_s \mathbf{U} \cdot$$

by partitioning:

$$\begin{bmatrix} \mathbf{P}_f \\ \mathbf{P}_c \end{bmatrix} = \begin{bmatrix} \mathbf{K}_{ff} & \mathbf{K}_{fc} \\ \mathbf{K}_{cf} & \mathbf{K}_{cc} \end{bmatrix} \begin{bmatrix} \mathbf{U}_f \\ \mathbf{U}_c \end{bmatrix}$$

where subscripts **c** denote degrees of freedom relative to support condition, **f** for the unsupported.

Then for $\mathbf{U}_c = \mathbf{O}$

$$\mathbf{P}_f = \mathbf{K}_{ff} \mathbf{U}_f$$

and

$$\mathbf{P}_c = \mathbf{K}_{cf} \mathbf{U}_f$$

The solution for the displacement

$$\mathbf{U}_f = \mathbf{K}^{-1}_{ff} \mathbf{P}_f$$

and the support reactions

$$\mathbf{P}_c = \mathbf{K}_{cf} \mathbf{K}^{-1}_{ff} \mathbf{P}_f$$

1.3.4. SOME PARTICULAR APPLICATIONS OF THE DISPLACEMENT METHOD.

1.3.4.1. Analysis of Structures Subject to Heat:

Suppose that all the elements or some of them are subject to heat represented by the temperature distribution $T = T(x, y, z)$.

From unit displacement theorem

$$F_i = \int_V \epsilon_i^T \sigma \, dV$$

where ϵ_i represents the column matrix of compatible strains due to unit displacement in the direction of F_i and σ is the exact stress matrix due to the applied forces F_i and temperature T.

Applying the unit displacement in turn to all points we have:

$$\mathbf{F} = \int_V \underline{\epsilon}^T \sigma \, dV \qquad \text{where } \underline{\epsilon}^T \text{ is now of order } n \times 6$$

Introducing the matrix of total strains

$$e = \epsilon + e_T$$

From Hook's law generalised for thermal strains,

$$\sigma = \mathbf{E}\, e + \mathbf{E}_T \alpha T$$

For linear system

$$e = \mathbf{b}\,\mathbf{U}$$

Substituting

$$\mathbf{F} = \int_V \underline{\epsilon}^T \mathbf{E}\,\mathbf{b}\,\mathbf{U}\, dV + \int_V \underline{\epsilon}^T \mathbf{E}_T \alpha T \, dV$$

Then following either the Argyris approach of 1.3.2. or the direct approach of 1.3.3., the relation for one element between forces and displacements will take the following form

$$\mathbf{F} = \mathbf{k}_e \mathbf{U} + \mathbf{h}$$

Carrying out the assembly procedure as explained before, again transforming from local to global axes when necessary, for the complete structure we can write:

$$\mathbf{P} = \mathbf{K}_e \mathbf{U} + \mathbf{H}$$

Partitioning the matrices to take into account the condition at the supports:

$$\begin{bmatrix} \mathbf{P}_f \\ \mathbf{P}_c \end{bmatrix} = \begin{bmatrix} \mathbf{K}_{ff} & \mathbf{K}_{fc} \\ \mathbf{K}_{cf} & \mathbf{K}_{cc} \end{bmatrix} \begin{bmatrix} \mathbf{U}_f \\ \mathbf{U}_c \end{bmatrix} + \begin{bmatrix} \mathbf{H}_f \\ \mathbf{H}_c \end{bmatrix}$$

leads to the final solution in the form:

$$\mathbf{U}_f = \mathbf{K}_{ff}^{-1} (\mathbf{P}_f - \mathbf{H}_f)$$

1.3.4.2. Displacement Approach to Large Deformation.

When deflections are large enough to cause significant changes in geometry so that the equations of equilibrium must be referred to the deformed configuration the relations between forces and deflections become nonlinear.

In the displacement method a geometric stiffness matrix which relates the applied loads to the geometric configuration of the structure is introduced. The dependence of the geometric stiffness on the level of loading introduces nonlinear terms, so that a solution to the governing matrix equation can no longer be obtained directly and an iterative procedure is necessary.

The first treatment of this problem by the displacement method was by Turner and al. in a paper published by the Journal of Aerospace (4) Science Vol. 27 No. 2, 1960. Other important references are (12), (13) and (14), which treat the same problem with more detail and include also some particular solution procedures.

Suppose that the elastic and the geometric stiffness matrices for an element of a structure have been found and are given by ($\mathbf{k_e}$) and ($\mathbf{k_g}$). Methods for the derivation of the elastic and geometric stiffness matrices will be examined later.

The total stiffness of the complete structure will be given by

$$\mathbf{K} = \mathbf{K_e} + \mathbf{K_g}$$

where $\mathbf{K_e}$ is the elastic stiffness matrix encountered in the linear analysis and $\mathbf{K_g}$, the geometric stiffness matrix, is formed from the element geometric stiffness matrices.

Starting from the unloaded condition then, for the load increment $\Delta \mathbf{P}$, the displacement increment $\mathbf{U}_1$, and internal forces per element $\mathbf{F}_1$ are found.

It is to be noticed that in this first step, a linear analysis is used since $\mathbf{K_g = O}$ initially because no internal forces are present.

In the next step, the results from step one are used to find the new geometric stiffness. Another incremental displacement $\mathbf{U}_2$, and internal force for element $\mathbf{F}_2$, are found.

This procedure is repeated until the full load is applied. The number of steps used depends on the accuracy required, the accuracy increasing with the number of steps.

Finally, the total displacement of the structure will be given as the summation of the series of incremental displacements.

In the following Table a summary of the procedure is given:

TABLE (1.1) - STEP BY STEP PROCEDURE FOR LARGE DEFLECTION ANALYSIS.

STEP	TOTAL STIFFNESS	DISPLACEMENT INC.	ELEMENT FORCES
1	K_e	ΔU_1	F_1
2	$K_e + K_g$	ΔU_2	F_2
⋮	⋮	⋮	⋮
n	$K_e + K_g$	ΔU_n	F_n
	TOTAL DISPLACEMENT	$U = \sum_i \Delta U_i$	

1.3.4.3. DISPLACEMENT METHOD FOR STRUCTURE STABILITY ANALYSIS.

In the previous subsection, it was found that by expressing the stiffness of the structure as $(\mathbf{K}_e + \mathbf{K}_g)$ where $\mathbf{K}_e$ is the elastic stiffness and $\mathbf{K}_g$ is the geometric stiffness, the large deflection analysis can be carried out by a step by step procedure, at each step the following matrix equation must be considered:

$$\mathbf{U} = (\mathbf{K}_e + \mathbf{K}_g)^{-1} \mathbf{P}$$

Suppose that instead of $\mathbf{P}$ we substitute $\lambda \mathbf{P}^*$ where λ is a constant proportionality of $\mathbf{P}$ and $\mathbf{P}^*$ defines the relative magnitudes of the applied loads.

Since the geometrical stiffness is proportional to the applied loads, it can be written as $\lambda \mathbf{K}_g^*$ where $\mathbf{K}_g^*$ is the geometric stiffness matrix for unit value of λ . For a small displacement $\mathbf{K}_e$ the elastic stiffness matrix can be treated as constant, and the above equation can be written as:

$$\mathbf{U} = (\mathbf{K}_e + \lambda \mathbf{K}_g^*)^{-1} \lambda \mathbf{P}^*$$

It follows that for displacement tending to infinity

$$|\mathbf{K}_e + \lambda \mathbf{K}_g^*| = 0$$

Where the last equation represents the linear stability determinant for a structure idealised into an assembly of discrete elements (8).

λ is known also as load factor .

1.3.5. METHODS OF DETERMINATION OF ELEMENT ELASTIC STIFFNESSES.

Some of the methods used for the determination of the force-displacement relationships for the finite elements employed as basic elements in the construction ofafinite element model for the complete structure are:

1.3.5.1. The Unit Displacement Theorem.

1.3.5.2. Castigliano's Theorem.

1.3.5.3. Solution of the Differential Equation.

1.3.5.4. Inversion of the Displacement Force Relationships.

These methods will be examined briefly in the following sections and then used to find the elastic stiffnesses for some structural elements.

Further reading on this subject can be found in (11), (15) and (16).

1.3.5.1. The Unit Displacement Theorem:

Let us suppose that an elastic element is subject to a set of n forces

$$\mathbf{F} = \{ F_1 \ldots\ldots F_n \}$$

and then

$$\mathbf{U} = \{ U_1 \ldots\ldots U_n \}$$

is the corresponding column of displacement components.

Then from the unit displacement theorem,

$$F_i = \int_v \underline{\epsilon}_i^T \boldsymbol{\sigma} \, dV$$

Where ($\underline{\epsilon}_i$) is the matrix of compatible strains due to unit displacement (U_i) in the direction of F_i, and $\boldsymbol{\sigma}$ is the exact stress distribution corresponding to the applied forces $\mathbf{F}$.

Applying the unit displacement at all points from $i = 1$ to n, the following system of equations can be obtained:

$$\mathbf{F} = \int_V \underline{\epsilon}^T \sigma \, dV$$

where

$$\underline{\epsilon}^T = \{ \underline{\epsilon}_1 \quad \underline{\epsilon}_2 \quad \ldots\ldots \quad \underline{\epsilon}_n \}$$

, in general a (nx6) matrix.

For a linear structure, neglecting temperature effects $e_T = 0$, the exact strains (ϵ), can be written as:

$$\epsilon = \mathbf{b}\,\mathbf{U}$$

where **b** is matrix of exact strains due to unit displacement **U**.

Hence

$$\sigma = \mathbf{E}\,\mathbf{b}\,\mathbf{U}$$

and substituting in the above equation for element forces gives

$$\mathbf{F} = \int_V \underline{\epsilon}^T \mathbf{E}\,\mathbf{b}\,\mathbf{U} \, dV \cdot$$

Since

$$\mathbf{F} = \mathbf{k}\,\mathbf{U}$$

where **k** represents the element stiffness matrix,

then

$$\mathbf{k} = \int_V \underline{\epsilon}^T \mathbf{E}\,\mathbf{b} \, dV$$

The matrix ($\underline{\epsilon}$) of compatible strains can be evaluated without any appreciable difficulties, but the matrix (**b**) which relates the exact strains to the displacement vector is usually difficult to find and an approximate procedure has to be adopted.

This requires that approximate functions relating strains and displacements must be found and the degree of approximation depends on the extent to which these functions satisfy equilibrium and compatibility.

One approach is to use the strain-displacement function which satisfies compatibility of deformation only, so that, denoting this approximate matrix by $\underline{\mathbf{b}}$ and noting that $\underline{\mathbf{b}} = \underline{\epsilon}$, the following equation for the elastic stiffness of the structural element is obtained:

$$\mathbf{k} = \int_V \underline{\mathbf{b}}^T \mathbf{E}\, \underline{\mathbf{b}} \; dV$$

This approach will be used to obtain the stiffness matrix for a two dimensional beam element, and for a rectangular plate in bending.

1.3.5.2. Derivation of Element Elastic Stiffness Using Castigliano's Theorem.

Castigliano's theorem part one can be used for the determination of element force-displacement relationships as follows.

Again, suppose that the element is subject to the system of loads:

$$\mathbf{F} = \{F_1 \ldots\ldots F_n\}$$

Then if U_E is the strain energy of the element, the following system of equations can be written:

$$F_i = \delta U_E / \delta U_i \qquad i=1,n$$

Where the strain energy U_E is expressed as a function of U_i.

But $$U_E = \tfrac{1}{2}\int_V \sigma^T \epsilon \; dV$$

and

$$\sigma = \mathbf{E}\,\epsilon$$

so that

$$U_E = \tfrac{1}{2}\int_V \epsilon^T \mathbf{E}\, \epsilon \; dV.$$

Using the relationship

$$\epsilon \cong \underline{b}\, U$$

The strain energy becomes

$$U_E = \tfrac{1}{2}\int_V U^T \underline{b}^T E \underline{b}\, U \; dV$$

and from Castigliano's theorem

$$F = \partial U_E / \partial U$$

$$F = k\, U$$

where $$k = \int_V \underline{b}^T E \underline{b} \; dV$$

Which is the same result as that obtained in the previous section.

This approach will be used to find the elastic stiffness matrix for rectangular plate element for in-plane loading.

The previous two methods led to the same expression for the elastic stiffness matrix and because of the linearity assumptions used, the application is limited to linearly elastic structures.

They have the advantage of being suitable for use by computer since they consist of a sequence of matrix operations, and because of the congruent transformation implicit in the final form of the expression of the elastic stiffness matrix, the result is always a symmetric matrix.

1.3.5.3.
Derivation of Elastic Stiffness Matrix from the Solution of the Differential Equation.

In the case of a structural element for which there is available a solution to the governing differential equation the elastic stiffness matrix can be found directly.

This method can best be illustrated by the derivation of the stiffness matrix for a three dimensional beam element in a later section.

1.3.5.4. Derivation of Elastic Stiffness from Flexibility.

Suppose that for a structural element the relation

$$U_f = f \quad F_f$$

is known, where

U_f is the displacement of the unsupported nodes

f is the element flexibility matrix

F_f is the nodal forces

In terms of stiffnesses, for the same element the displacement-force relationship can be written as

$$\begin{bmatrix} F_f \\ F_c \end{bmatrix} = \begin{bmatrix} k_{ff} & k_{fc} \\ k_{cf} & k_{cc} \end{bmatrix} \begin{bmatrix} U_f \\ U_c \end{bmatrix}$$

where the subscripts f and c are to indicate quantities related to unsupported and supported nodes.

It can be seen that

$$k_{ff} = f^{-1}$$

To find k_{fc} use the condition of static equilibrium between the support forces F_c and the applied external forces F_f, which can be written as

$$F_c = \bar{w} \quad F_f$$

Then, because $U_c = O$

$$F_f = k_{ff} \; U_f = f^{-1} U_f$$

so that

$$F_c = \bar{w} \; f^{-1} U_f$$

Again, because $U_c = O$

$$F_c = k_{cf} U_f$$

From the equivalence of the two equations for F_c , we find

$$k_{cf} = \bar{w}\, f^{-1}$$

and from reciprocity

$$k_{fc} = k_{cf}^{T} = f^{-1}\, \bar{w}^{T} \qquad \text{since } f^{-1} \text{ is symmetrical .}$$

Finally to find k_{cc} ,

$$F_c = \bar{w}\, F_f$$

$$F_c = \bar{w}\,(k_{ff} U_f + k_{fc} U_c)$$

$$= \bar{w}\,(k_{ff} U_f + f^{-1} \bar{w}^{T} U_c)$$

but

$$F_c = k_{cf} U_f + k_{cc} U_c$$

$$= \bar{w}\, f^{-1} U_f + k_{cc} U_c$$

and

$$k_{ff} = f^{-1}$$

$$\therefore \quad k_{cc} = \bar{w}\, f^{-1} \bar{w}^{T}$$

and finally, the matrix k_e in function of f the flexibility matrix of the stable supported element will have the following form:

$$k_e = \begin{bmatrix} f^{-1} & f^{-1} \bar{w}^{T} \\ \bar{w} f^{-1} & \bar{w} f^{-1} \bar{w}^{T} \end{bmatrix}$$

1.3.6. ELASTIC STIFFNESS MATRICES FOR SOME STRUCTURAL ELEMENTS.

In the previous section, some of the methods currently in use for the derivation of element stiffness matrices were reviewed, in this section these methods will be applied to derive some structural elements which will be used for the study which follows .

In addition to the references cited in the previous section, (17), (18) were also consulted.

1.3.6.1 Two Dimensional Beam Element:

The unit displacement method will be used to find the elastic stiffness matrix for the two dimensional beam.

This beam has two degrees of freedom per node, one translational and one rotational, the associated moments are shown in Fig. (1.1).

Assuming a displacement function given by the equation:

$$v = a_1 x^3 + a_2 x^2 + a_3 x + a_4$$

In matrix form

$$v = \mathbf{R}\ \mathbf{a}$$

The rotational displacement is then:

$$\theta_z = d\ v/dx = 3\ a_1 x^2 + 2\ a_2 x + a_3$$

Substituting the nodal co-ordinates into the equations for the deflection and rotation, the following set of equations can be obtained:

$$U_1 = a_4$$

$$U_2 = a_3$$

$$U_3 = a_1 L^3 + a_2 L^2 + a_3 L + a_4$$

$$U_4 = 3\ a_1 L^2 + 2\ a_2 L + a_3$$

which in matrical form can be written

$$\mathbf{U} = \mathbf{L}\ \mathbf{a}$$

where $\mathbf{U}$ is the node displacement vector.

Substituting $\mathbf{a} = \mathbf{L}^{-1}\mathbf{U}$ in the equation for v gives

$$v = \mathbf{R}\ \mathbf{L}^{-1}\mathbf{U}$$

$$\equiv \mathbf{N}\ \mathbf{U}$$

The inversion of the matrix ($\mathbf{L}$) is straight forward and ($\mathbf{L}^{-1}$) is given in Table (1.2), Table (1.3) gives the form of ($\mathbf{N}$), the shape function.

Elastic strains for a beam can be written as $\varepsilon_x = \frac{d\ u}{d\ x} - y\ \frac{d^2 v}{d\ x^2} + \frac{1}{2}\left(\frac{d\ v}{d\ x}\right)^2$

The term of interest is the second on the right hand side which become

$$= -\ y\mathbf{N}''\mathbf{U}$$

or $$= \mathbf{b}\ \mathbf{U}$$

The row matrix $\mathbf{b}$ is derived immediately from the matrix $\mathbf{N}$ and the stiffness matrix $\mathbf{k}$ is then given by

$$\mathbf{k} = \int_V \mathbf{b}^T E\ \mathbf{b}\ dV = E\ I_z \int_L \mathbf{N}'^T \mathbf{N}''\ dL$$

The final form of the stiffness matrix is given in Table (1.5).

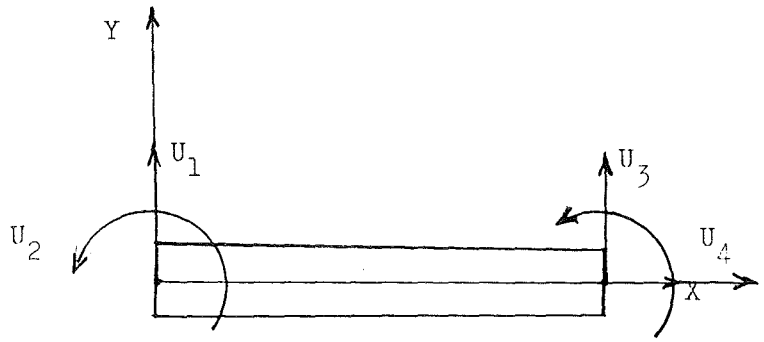

Fig. (1.1) - two dimensional beam element.

$$\frac{1}{L^3}\begin{bmatrix} 2 & L & -2 & L \\ -3L & -2L^2 & 3L & -L^2 \\ 0 & L^3 & 0 & 0 \\ L^3 & 0 & 0 & 0 \end{bmatrix}$$

Table (1.2)- Matrix $\mathbf{L}^{-1}$ for two dimensional beam element.

$$\mathbf{N}^T = \begin{bmatrix} 2X^3 - 3X^2 + 1 \\ LX^3 - 2LX^2 + LX \\ -2X^3 + 3X^2 \\ LX^3 - LX^2 \end{bmatrix}$$

$$X = x/L$$

Table (1.3) - Matrix of shape functions for two dimensional beam element.

$$\mathbf{b}^{T} = -y \begin{bmatrix} -6 / L^2 + 12\,x / L^3 \\ -4 / L + 6\,x / L^2 \\ -12\,x / L^3 + 6 / L^2 \\ 6\,x / L^2 - 2 / L \end{bmatrix}$$

$$\mathbf{b} = -y\,\mathbf{N}''$$

Table (1.4) - Matrix **b** for two dimensional beam element.

$$\mathbf{k_e} = E\,I_z \begin{bmatrix} 12 / L^3 & & & \\ 6 / L^2 & 4 / L & \text{Symm.} & \\ -12 / L^3 & -6 / L^2 & 12 / L^3 & \\ 6 / L^2 & 2 / L & -6 / L^2 & 4 / L \end{bmatrix}$$

Table (1.5) - Two dimensional elastic stiffness for beam .

1.3.6.2. Threedimensional Beam Element

The elastic stiffness matrix for this type of element will be derived from the use of the solution of the differential equation for displacement.

The beam element under consideration and the applied system of forces is given in Figure (1.2)the assumptions of the engineering theory for beams applies.

The following forces applied : Axial forces (F_1 , F_7), shearing forces (F_2 , F_3 , F_8 , F_9), bending moments (F_5 , F_6 , F_{11}, F_{12}) and twisting moments (F_4 , F_{10}).

The corresponding displacements : U_1 toU_{12} will be taken positive in the positive directions of the applied forces.

The local axes will be considered to coincide with the axis of the beam and with the directions of the principal axes of inertia of the cross section, this will enable the computation to be carried out for six groups of forces which can be considered independently from each other.

a - Axial forces (F_1 , F_7) :

For the uniform beam shown in Figure(1.2), the differential equation when axial forces are applied:

$F = -(du/dx)\ E\ A$

at $x = 0$ $F = F_1$

so $F_1 = -(du/dx) E\ A$ = constant

integrating

$F_1\ x = -\ u\ E\ A + c_1$

at $x = 0$

$0 = -U_1\ E\ A + c_1$

so $c_1 = U_1 E\ A$

so that

$F_1\ x = E\ A\ (\ U_1 - u)$

then $\quad$ at x=L $\quad u = U_7$

so that

$$F_1 L = E A (U_1 - U_7) = - F_7 L$$

then

$$k(i,j) = d F_i / d U_j$$

so that

$$k(1,1) = d F_1 / dU_1 = EA/L$$

$$k(1,7) = d F_1 / d U_7 = - EA/L$$

$$k(7,1) = d F_7 / d U_1 = - EA/L$$

$$k(7,7) = d F_7 / d U_7 = EA/L$$

b - Twisting moments (F_4 and F_{10}) :

Considering first the beam is constrained at one end so that the rotation at that end is zero, while the remaining rotation and moments are different from zero.

Then if by G J we indicate the torsional stiffness of this beam, then

$$F_4 = - \quad G J (d \theta / dx)$$

Integrating

$$F_4 x = - \quad G J \theta + c_2$$

Then from the boundary condition

$$\text{at } x = 0 \qquad \theta = U_4$$

substituting

$$0 = - GJ U_4 + \quad c_2$$

and

$$c_2 = GJ U_4$$

substituting on c_2

$$F_4 x = G J(U_4 - \theta)$$

then at x = L $\quad \theta = U_{10}$ $\quad$ so $\quad F_4 L = GJ (U_4 - U_{10})$

From equilibrium $\quad F_4 + F_{10} = 0$

we can write

$$F_{10} L = - GJ (U_4 - U_{10})$$

then from

$$k(i,j) = dF_i/d\ U_j$$

we have

$$k(4,4) = GJ/L$$

$$k(4,10) = - GJ/L$$

$$k(10,10) = GJ/L$$

$$k(10,4) = - GJ/L$$

c - Shearing forces (F_2 , F_8) :

The lateral deflection in the plane of a beam subjected to shearing forces and bending moments, which are associated with these shearing forces,is given by:

$$v = v_b + v_s$$

where v_b is the lateral deflections due to bending and v_s is the deflection due to shear, such that:

$$d\ v_s/dx = - F_2/G\ A_s$$

Where A_s is the effective cross section area in shear.

The bending deflection is given by the following equation:

$$E\ I_z(d^2y_b/dx^2) = F_2\ x - F_6$$

integrating

$$E\ I_z\ (dy_b/dx) = \tfrac{1}{2}\ F_2\ x^2 - F_6\ x + c_3$$

then

$$E\ I_z\ (dv/dx) = E\ I_z\ (dv_b/dx) + E\ I_z(dv_s/dx)$$

$$= \tfrac{1}{2}\ F_2\ x^2 - F_6\ x + c_3 - (F_2/G\ A_s)(E\ I_z)$$

and since

$dv_b/dx = 0$ at $x = 0$ $\quad c_3 = 0$

$d\ v_b/dx = 0$ at $x = L$ $\quad F_6 = F_2\ L\ /2$

so that

$$E\ I_z\ (dv/dx) = F_2\ (\tfrac{1}{2}\ x^2 - \tfrac{1}{2}\ x\ L - (E\ I_z/G\ A_s))$$

integrating again gives

$$E I_z v = F_2(x^3/6 - x^2 L/4 - (E I_z/ G A_s) x) + c_4$$

Introducing the third boundary condition, namely, v = 0 at x = L gives

$$c_4 = F_2 (L^3/12 + (E I_z / G A_s) L)$$

so that

$$E I_z v = F_2(x^3/6 - x^2L/4 -(E I_z/GA_s)x) + F_2(L^3/12 +(\frac{E I_z}{})L)$$
$$= F_2(x^3/6 - x^2L/4 - \phi L^2x/12 + (1 +\phi) L^3/12^{G A_s}$$

where $\phi = 12 (E I_z/(G A_s L^2))$

From equilibrium

$$F_2 + F_8 = 0 \qquad F_8 = -F_2$$

$$F_{12} = - F_6 + F_2 L = - F_2 L /2$$

Now at $x = 0 \qquad v = U_2$

then

$$U_2 = (1 +\phi) L^3 F_2 /(12 E I_z)$$

so that

$$k(2,2) = F_2/U_2 = 12 E I_z /((1 +\phi) L^3)$$

$$k(6,2) = F_6/U_2 = \tfrac{1}{2} F_2 L/U_2 = 6 E I_z/((1 + \phi) L^2)$$

$$k(8,2) = F_8/U_2 = - F_2 / U_2 = - 12 E I_z /((1 + \phi) L^3)$$

$$k (12,2) = F_{12} /U_2 = (F_2 L/(2U_2)) = 6 E I_z/((1 +\phi) L^2)$$

Repeating the procedure again for the beam when constrained at end $x = 0$ and the only displacement allowed is U_8, then

the following stiffness coefficients will be found:

$$k(8,8) = k(2,2) = 12\ E\ I_z /((1+\phi)\ L^3)$$

$$k(12,8) = -\ k(6,2) = -\ 6\ E\ I_z /((1+\phi)\ L^2)$$

d - Bending moments (F_6, F_{12}) :

To find the stiffness coefficients corresponding to displacements U_6 and U_{12} we will refer to the drawings given in Fig. (1.3.b), in which forces and displacements are shown for beams constrained at the ends.

For the beam constrained from rotating at edge $x = L$, under the action of moments F_6 and F_{12}, and shear forces F_2 and F_8 the differential equation is given by the following:

$$E\ I_z\ (dv_b/dx) = F_2\ x^2/2 - F_6\ x + c_5$$

$$E\ I_z(dv/dx) = E\ I_z(dv_b/dx) + E\ I_z(dv_s/dx)$$

$$= \tfrac{1}{2}\ F_2\ x^2 - F_6\ x + c_5 - F_2\ E\ I_z/G\ A_s$$

Then from the boundary conditions

$$d\ v_b/dx = 0 \quad \text{at } x = L$$

$$c_5 = -\ F_2\ L^2/2 + F_6\ L$$

Substituting

$$E\ I_z\ dv_b/dx = \tfrac{1}{2}\ F_2(x^2 - L^2) - F_6(x - L) - F_2\ E\ I_z/(G\ A_s)$$

Integrating,

$$E\ I_z\ v = \tfrac{1}{2}\ F_2\ (x^3/3 - L^2\ x) - F_6\ (x^2/2 - L\ x) - F_2\left(\frac{E\ I_z}{G\ A_s}\right)x + c_6$$

Then from

$$v = 0 \quad \text{at} \quad x=0 \text{ and } \quad \text{at} \quad x= L$$

we find

$$c_6 = 0$$

and

$$0 = \tfrac{1}{2} F_2 (- 2 L^3 /3) - F_6 (- L^2/2) - F_2 E I_z L/(G A_s)$$

$$= - F_2 (L^3/3 + E I_z L/G A_s) + F_6 L^2/2$$

$$F_6 = F_2 (2 L/3 + 2 E I_z/(G A_s L))$$

or

$$F_2 = 6 F_6/ (4L + (12 E I_z L/(G A_s L^2))) = 6F_6/(L (4 + \phi))$$

From equilibrium

$$F_2 = - F_8$$

and

$$F_6 = - F_{12} + F_2 L$$

and from $x=0$ $\quad U_6 = d v_b/dx$

$$U_6 = dv/dx - dv_s/dx$$

$$= dv/dx + F_2/(G A_s)$$

substituting

$$U_6 = F_6(1 + \phi)L / E I_z (4 + \phi)$$

so

$$k(6,6) = F_6/U_6 = (4 + \phi) E I_z/((1 + \phi) L)$$

$$k(8,6) = - F_2/ U_6 = - 6 E I_z/((1 + \phi) L^2)$$

$$k(12,6) = F_{12}/ U_6 = (- F_6 + F_2 L)/U_6 = (2 - \phi) E I_z /((1 + \phi)L)$$

Operating similarly on the beam with the other end clamped we obtain

$$k(12,12) = k(6,6) = (4 + \phi) E I_z /((1 + \phi)L)$$

Repeating the procedure again for the beam subject to shearing forces F_3 and F_9 and bending moments F_5 and F_{11}, noting that the flexural stiffness in this case is given by EI_y and maintaining the sign convention adopted so far, the following stiffness coefficients can be found:

$$k(3,3) = f\ k(2,2)$$

$$k(5,3) = -f\ k(6,2)$$

$$k(9,3) = f\ k(8,2)$$

$$k(11,3) = f\ k(12,2)$$

$$k(9,9) = f\ k(8,8)$$

$$k(11,9) = -f\ k(12,8)$$

$$k(5,5) = f\ k(6,6)$$

$$k(9,5) = -f\ k(8,6)$$

$$k(11,5) = f\ k(12,6)$$

where $f = I_y\ (1+\phi_y)/(I_z(1+\phi_z))$

and $\phi_y = EI_z/G\ A_{sy}\ L^2$ $\qquad$ $\phi_z = E\ I_y / G\ A_{s_z}\ L^2$

and for the complete beam element the elastic stiffness can be arranged in Table (1.6)

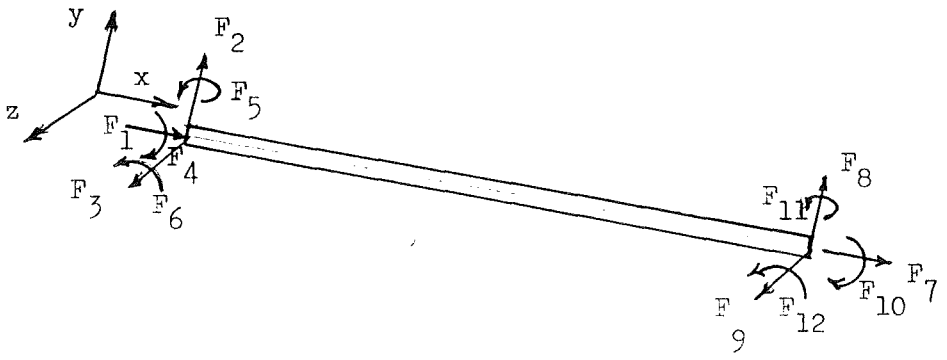

Fig. (1.2) - Beam element.

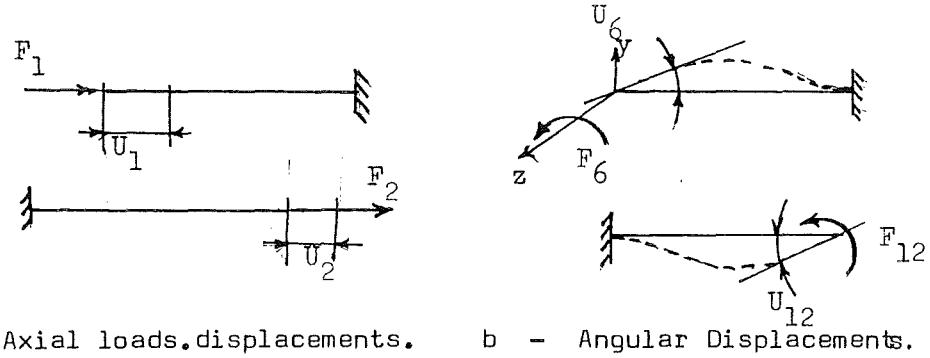

a - Axial loads.displacements.

b - Angular Displacements.

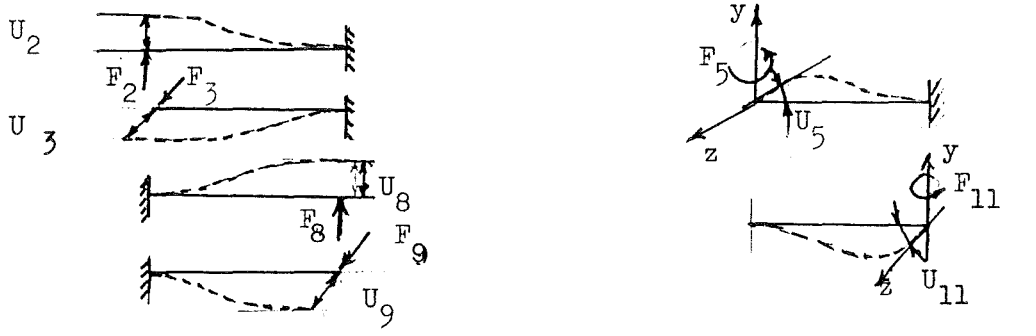

c - Transverse bending displacement.

d - Angular displacements.

Fig. (1.3) - Forces and deflections on beam element.

Table (1.6) - Elastic stiffness for beam element.

$$
\begin{bmatrix}
EA/L & & & & & & & & & & & \\
0 & 12I_z/L^3S & & & & & & & & & & \\
0 & 0 & 12I_y/L^3Q & & & & & & & & & \\
0 & 0 & 0 & GJ/L & & & & & & & & \\
0 & 0 & -6I_y/L^2Q & 0 & VI_y/LQ & & & & & & & \\
0 & 6I_z/L^2S & 0 & 0 & 0 & WI_z/LS & & & & & & \\
-EA/L & 0 & 0 & 0 & 0 & 0 & EA/L & & & & & \\
0 & -12I_z/L^3S & 0 & 0 & 0 & -6I_z/L^2S & 0 & 12I_z/L^3S & & & & \\
0 & 0 & -12I_y/L^3Q & 0 & 6I_y/L^2Q & 0 & 0 & 0 & 12I_y/L^3Q & & & \\
0 & 0 & 0 & -GJ/L & 0 & 0 & 0 & 0 & 0 & GJ/L & & \\
0 & 0 & -6I_y/L^2Q & 0 & 4I_y/LQ & 0 & 0 & 0 & 6I_y/L^2Q & 0 & VI_y/LQ & \\
0 & 6I_z/L^2S & 0 & 0 & 0 & YI_z/LS & 0 & -6I_z/L^2S & 0 & 0 & 0 & WI_z/LS
\end{bmatrix}
$$

SYM.

$S = 1 + \phi_y$, $R = 1 + \phi_z$, $V = 4 + \phi_z$

$W = 4 + \phi_y$, $X = 2 - \phi_z$, $Y = 2 - \phi_y$

$\phi_y = 12\ E\ I_z / G\ A_{sy}\ L^2$

$\phi_z = 12\ E\ I_y / G\ A_{sz}\ L^2$

1.3.6.3. Rectangular Plate Element- Membrane Stresses

The plate element is shown in Fig. (1.4) the coordinate system used is as shown, but in the analysis nondimensional coordinates will be used so that if A and B are the length of the plate in the x direction and the width of the plate in the y direction, the non-dimensional coordinates will be

$$X = x/A \qquad Y = y/B$$

As it was shown, there are eight degrees of freedom, two at each node, and they consist of a displacement in x direction and a displacement in y direction. These displacements are positive or negative according to the direction of the coordinate axis.

Assuming the displacement functions which satisfy the assumption of linearly varying boundary displacement (16), namely,

$$u = c_1 X + c_2 X Y + c_3 Y + c_4$$
$$v = c_5 X + c_6 X Y + c_7 Y + c_8$$

and using the displacements at the nodes, $U_1, U_2, \ldots\ldots U_8$, to evaluate the constants c_i leads to displacement functions in the following form:

$$u = (1-X)(1-Y)U_1 + (1-X)YU_3 + XYU_5 + X(1-Y)U_7$$
$$v = (1-X)(1-Y)U_2 + (1-X)YU_4 + XYU_6 + X(1-Y)U_8$$

The strains corresponding to the assumed displacement functions are:

$$\varepsilon_x = du/dx = \frac{1}{A}\, du/dX = (1/A)(- (1-Y)U_1 - YU_3 + YU_5 + (1-Y)U_7)$$
$$\varepsilon_y = dv/dy = \frac{1}{B}(-(1-X)U_2 + (1-X)U_4 + X U_6 - XU_8)$$
$$\gamma_{xy} = du/dy + dv/dx = \frac{1}{B}\, du/dY + \frac{1}{A}\, dv/dX$$
$$= (1/B)(-(1-X)U_1 + (1-X)U_3 + XU_5 + (-1)XU_7) + (1/A)(-(1-Y)U_2 - YU_4 +$$

or $$+YU_6 + (1-Y)U_8)$$

$$\epsilon = \mathbf{b}\, U$$

and the matrix ($\mathbf{b}$) is given in Table (1.8)

From the energy approach to the determination of the elastic stiffness the matrix of elastic stiffness is given from the following equation:

$$\mathbf{k_e} = \int_V \mathbf{b}^T \mathbf{E}\ \mathbf{b}\ dV$$

The matrix of elastic stiffness for the rectangular plate element is given in full in Table (1.9)

$$\mathbf{E} = \frac{E}{1-\nu^2}\begin{bmatrix} 1 & \nu & 0 \\ \nu & 1 & 0 \\ 0 & 0 & \frac{1-\nu}{2} \end{bmatrix}$$

Table(1.7) - Elasticity matrix for plate element.

$-(1-Y)/A$	0	$-Y/A$	0	Y/A	0	$(1-Y)/A$	0
0	$-(1-X)/B$	0	$(1-X)/B$	0	X/B	0	$-X/B$
$-(1-X)/B$	$-(1-Y)/A$	$(1-X)/B$	$-Y/A$	X/B	Y/A	$-X/B$	$(1-Y)/A$

Table (1.8) - Matrix **b**, relating strains to nodal displacements for Rectangular Plate Element (in-plane).

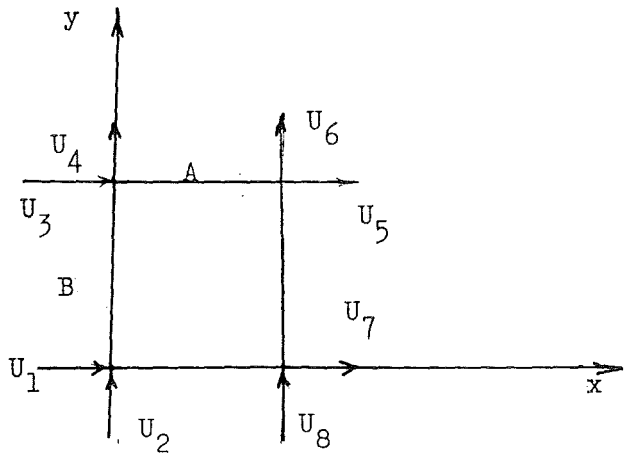

Fig. (1.4)- Rectangular Plate Element (in-plane).

Table (1.9) - Elastic Stiffness Matrix for Rectangular Plate Element (in-plane).

$$k = \frac{E\,T}{12(1-\nu^2)} \begin{bmatrix} a & & & & & & \\ b & g & & & & \text{SYM.} & \\ c & -d & a & & & & \\ d & h & b & g & & & \\ e & -b & f & -d & a & & \\ -b & i & d & j & b & a & \\ f & d & e & b & c & d & a \\ -d & j & b & i & d & h & -b & g \end{bmatrix}$$

$a = 4p + 2yq$ $\quad c = 2p-2yq$ $\quad e = -2p-yq$ $\quad g=4q+2yp$ $\quad i = -2q -yp$ $\quad A=$ plate length

$b = 3x/2$ $\quad d = 3z/2$ $\quad f = -4p +yq$ $\quad h= -4q+yp$ $\quad j = 2q-2yp$ $\quad B =$ plate width

$p = B/A$ $\quad q = A/B$ $\quad x = 1+\nu$ $\quad y= 1 -\nu$ $\quad z = 1 - 3\nu$ $\quad T =$ plate thicness

1.3.6.4. Rectangular Plate Element (in bending).

In the previous section, the in-plane stiffness of a rectangular plate element which has eight degrees of freedom representing the translations u and v at the four corner nodes in the x and y directions was considered.

In this section, the out-of-plane stiffness of a rectangular plate element which has twelve degrees of freedom, eight rotations and four translations, will be considered. The element coordinate axes and the nodal displacements are shown in Fig. (1.5) Here also nondimensional coordinates X and Y will be used.

In this case, the assumed displacement function for the median plane is given by the following polynomial (13) :

$$w = c_1 + c_2 X + c_3 Y + c_4 X^2 + c_5 X Y + c_6 Y^2 + c_7 X^3 + c_8 X^2 Y + c_9 X Y^2 + c_{10} Y^3 + c_{11} X^3 Y + c_{12} X Y^3$$

The displacements U_1, to U_{12} can be related to the displacement by the following matrical equation:

$$w = \mathbf{N}_z \mathbf{U}$$

Where the transpose of $\mathbf{N}_z$ is the matrix given in Table (1. 10)

Then the matrix b which relates strains to displacements can be found from the following considerations:

The strains are given by:

$$\varepsilon_x = - z \partial^2 w/\partial x^2$$

$$\varepsilon_y = - z \partial^2 w /\partial y^2$$

$$\gamma_{xy} = - 2 z \partial^2 w/\partial x \partial y$$

then substituting for w , the matrix **b** in compact form can be written as:

$$\mathbf{b} = - z \begin{bmatrix} \partial^2 \mathbf{N}_z/\partial x^2 \\ \partial^2 \mathbf{N}_z/\partial y^2 \\ 2 \partial^2 \mathbf{N}_z/\partial x \partial y \end{bmatrix}$$

3×12

This is given explicity in Table (1.11)

Then from the Castigliano's approach discussed in previous section the matrix $\mathbf{b}$ of elastic stiffness is given from the equation:

$$\mathbf{k_e} = \int_V \mathbf{b}^T \mathbf{E}\, \mathbf{b}\ dV$$

Where the matrix $\mathbf{k_e}$ is given in Table (1.12)

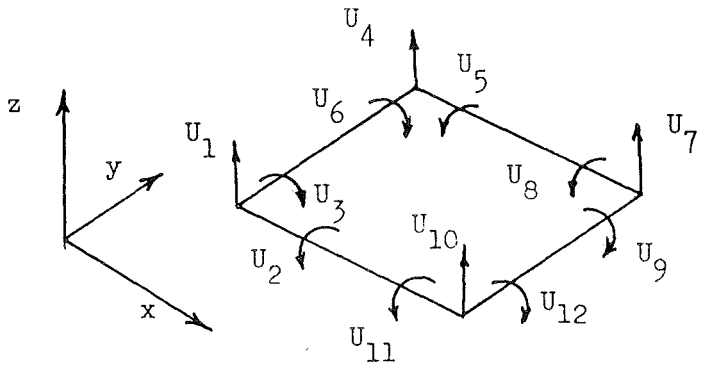

Fig. (1.5) - Rectangular Plate Element (in-bending).

$$\mathbf{N}_z^T = \begin{bmatrix} 1 - XY - S\,X^2 Q - P T Y^2 \\ P Y Q^2 B \\ -X\,P^2\,Q\,A \\ P\,T\,Y^2 + X\,P\,V\,W \\ -P\,Q\,Y^2\,B \\ -X\,P^2\,Y\,A \\ S\,X^2\,Y - X\,Y\,Q\,W \\ -X\,Q\,Y^2\,B \\ P\,X^2 Y\,A \\ S\,X^2\,Q + X\,Y\,Q\,W \\ X\,Y\,Q^2\,B \\ P\,X^2\,Q\,A \end{bmatrix}$$

where

$P = 1 - X$ $\quad S = 3 - 2X$ $\quad V = 1 - 2X$

$Q = 1 - Y$ $\quad T = 3 - 2Y$ $\quad W = 1 - 2Y$

$X = x/A$ $\quad Y = y/B$ $\quad$ A,B are length and width of the plate.

Table (1.10) - Matrix $\mathbf{N}_z^T$ for Rectangular Plate Element (in-bending).

$$\mathbf{b}^T = \begin{bmatrix}
V\,Q\,L & P\,W\,N & (1 - 6XP - 6YQ)\,J \\
0 & P\,G\,U & (1 - 4Y + 3Y^2)M \\
-F\,Q\,M & 0 & -(1 - 4X + 3X^2)U \\
V\,Y\,L & -PWN & (-1 + 6XP + 6YQ)J \\
0 & P\,I\,U & -Y\,G\,M \\
-F\,Y\,M & 0 & (1 - 4X + 3X^2)\,U \\
-V\,Y\,L & -X\,W\,N & (1 - 6XP - 6YQ)J \\
0 & X\,I\,U & Y\,G\,M \\
-H\,Y\,M & 0 & -X\,F\,U \\
-V\,Q\,L & X\,W\,N & (-1 + 6X\,P + 6YQ)J \\
0 & X\,G\,U & -(1 - 4Y + 3Y^2)M \\
-H\,Q\,M & 0 & X\,F\,U
\end{bmatrix}$$

where

$P = 1 - X$

$Q = 1 - Y$

$V = 1 - 2X$

$W = 1 - 2Y$

$F = 2 - 3X$

$G = 2 - 3Y$

$L = 6z/A^2$

$M = 2z/A$

$N = 6z/B^2$

$U = 2z/B$

$J = 2z/AB$

A = plate length

B=plate width

$X = x/A$

$Y = y/B$

Table (1.11) - Matrix $\mathbf{b}^T$ for Rectangular Plate (in-bending).

Table (1.12) - Matrix $\mathbf{k}_e$ for Rectangular Plate Element.

$\mathbf{k}_e = L$

a											
b	g										
c	h	j									
d	-e	f	a								
e	i	0	-b	g							
f	0	k	c	-h	j						
m	s	w	p	-q	-u	a					
n	t	0	-q	v	0	-b	g				
o	0	x	u	0	z	-c	h	j			
p	u	y	m	n	w	d	e	-f	a		
q	v	0	-n	t	0	-e	i	0	b	g	
u	0	z	s	0	x	-f	0	k	-c	-h	j

SYM.

where

$a = 4(C + D) + E$

$b = (2D + F)B$

$c = -(2C + F)A$

$d = 2(C - 2D) - E$

$e = (2D + G)B$

$f = (-C + F)A$

$g = (4D/3 + 4H$

$h = -AB$

$i = (2D/3 - H)B^2$

$j = (4C/3 + 4H)A^2$

$k = (2C/3 - 4H)A^2$

$m = -2(C + D) + E$

$n = (D - G)B$

$o = (-C + G)A$

$p = -2(2C - D) - E$

$q = (D - F)B$

$u = -(2C + G)A$

$v = (2D/3 - 4H)B^2$

$w = (C - G)A$

$x = (C/3 + H)A^2$

$y = (2C + G)A$

$z = (2C/3 - H)A^2$

and

$C = (B/A)^2$

$D = (A/B)^2$

A = plate length

B = plate width

ν = Poison's ratio

$E = (14 - 4\nu)/5$

$F = (1 + 4\nu)/5$

$G = (1 - \nu)/5$

$H = (1 - \nu)/15$

0 = zero

$L = \bar{E}T^3/(12(1 - \nu^2)AB)$

$\bar{E}$ = is Young's modulus for the material of the plate

T = is the plate thickness.

1.3.6.5. Elastic Stiffness Matrix for Pin-jointed Bar.

Here the stiffness matrix relating axial forces to axial displacements for pin-jointed bar will be derived from flexibility.

From the equilibrium condition the matrix $\bar{\mathbf{w}}$ will be found and this will be used together with flexibility matrix to find the elastic stiffness matrix.(see section 1.3.5.4)

In this case $\bar{\mathbf{w}}$ is composed of just one element and equal to - 1

The flexibility matrix for pin-jointed bar element $\mathbf{f}$ = L/(EA) and $\mathbf{f}^{-1}$ = EA/L.

Substituting in the terms of the matrix given in article 1.3.5.3., the elastic stiffness matrix becomes:

$$\mathbf{k}_e = \begin{bmatrix} \mathbf{f}^{-1} & \mathbf{f}^{-1}\bar{\mathbf{w}}^{T} \\ \bar{\mathbf{w}}\mathbf{f}^{-1} & \bar{\mathbf{w}}\,\mathbf{f}^{-1}\bar{\mathbf{w}}^{T} \end{bmatrix} = \frac{A\,E}{L}\begin{bmatrix} 1 & -1 \\ -1 & 1 \end{bmatrix}$$

where

A is the cross section area of the bar

L is the length of the bar

E is Young's modulus of the material

1.3.6.6. Rectangular Plate Element in Bending (Orthotropic Plate).

In Section 1.3.6.4. the elastic stiffness matrix for isotropic plate in bending was derived using the following equation:

$$\mathbf{k_e} = \int_V \mathbf{b}^T \mathbf{E}\, \mathbf{b}\ dV$$

The matrix $\mathbf{b}$ is given in Table (1.11).

To find the elastic stiffness matrix for orthotropic plate the same form of the above equation is still applied, except here the matrix $\mathbf{E}$ is replaced by the matrix $\mathbf{D}$ and we may write

$$\mathbf{k_e} = \int_V \mathbf{b}^T \mathbf{D}\, \mathbf{b}\ dV$$

Where $\mathbf{D}$ is the matrix which expresses the orthotropic properties of the plate as will be seen in the Third Chapter.

The derivation of this elastic matrix was carried out in (19) but it was found that the derivation was referred to a system of axes in which the direction of the z axes is opposite to the direction of the z axes of the system adopted in this project.

To obtain the elastic matrix referenced to the system of axes adopted the elastic matrix of Reference (19) has to be pre and post multiplied by the following matrix:-

$$\mathbf{J} = \begin{bmatrix} \mathbf{j} & \mathbf{0} & \mathbf{0} & \mathbf{0} \\ \mathbf{0} & \mathbf{j} & \mathbf{0} & \mathbf{0} \\ \mathbf{0} & \mathbf{0} & \mathbf{j} & \mathbf{0} \\ \mathbf{0} & \mathbf{0} & \mathbf{0} & \mathbf{j} \end{bmatrix}$$

where

$$\mathbf{j} = \begin{bmatrix} 1 & 0 & 0 \\ 0 & 1 & 0 \\ 0 & 0 & -1 \end{bmatrix}$$

The elastic matrix for orthotropic plate is given (14) as

$$\mathbf{k_e} = (1/(60AB))\tilde{\mathbf{L}} \left[D_x \mathbf{k_1} + D_y \mathbf{k_2} + D_1 \mathbf{k_3} + D_{xy} \mathbf{k_4} \right] \tilde{\mathbf{L}}$$

Where matrices $\mathbf{k_1}$, $\mathbf{k_2}$, $\mathbf{k_3}$, $\mathbf{k_4}$, and $\tilde{\mathbf{L}}$ are given in Table (1.13), (1.14), (1.15), (1.16) and Table (1.17).

Table(1.13)

$k_1 = (\frac{B}{A})^2$

60											
0	0										
30	0	20									
30	0	15	60								
0	0	0	0	0			SYM.				
15	0	10	30	0	20						
-60	0	-30	-30	0	-15	60					
0	0	0	0	0	0	0	0				
30	0	10	15	0	5	-30	0	20			
-30	0	-15	-60	0	-30	30	0	-15	60		
0	0	0	0	0	0	0	0	0	0	0	
15	0	5	15	0	10	-15	0	10	-30	0	0

Table(1. 14)

$k_2 = (\frac{A}{B})^2$

60											
-30	20										
0	0	0									
-60	30	0	60								
-30	10	0	30	20			SYM.				
0	0	0	0	0	0						
30	-15	0	-30	-15	0	60					
-15	10	0	15	5	0	-30	20				
0	0	0	0	0	0	0	0	0			
-30	15	0	30	15	0	-60	30	0	60		
-15	5	0	15	10	0	-30	10	0	30	20	
0	0	0	0	0	0	0	0	0	0	0	0

where

A is the length of the plate

B is the width of the plate

Table(1.15)

$$k_3 = \begin{bmatrix}
30 & & & & & & & & & & & \\
-15 & 0 & & & & & & & & & & \\
15 & -15 & 0 & & & & & & & & & \\
-30 & 0 & -15 & 30 & & & & & & & & \\
0 & 0 & 0 & 15 & 0 & & & & & & & \\
-15 & 0 & 0 & 15 & 15 & 0 & & & & & & \\
-30 & 15 & 0 & 30 & 0 & 0 & 30 & & & & & \\
15 & 0 & 0 & 0 & 0 & 0 & -15 & 0 & & & & \\
0 & 0 & 0 & 0 & 0 & 0 & -15 & 15 & 0 & & & \\
30 & 0 & 0 & -30 & -15 & 0 & -30 & 0 & 15 & 30 & & \\
0 & 0 & 0 & -15 & 0 & 0 & 0 & 0 & 0 & 15 & 0 & \\
0 & 0 & 0 & 0 & 0 & 0 & 15 & 0 & 0 & -15 & -15 & 0
\end{bmatrix}$$

SYM.

Table(1.16)

$$k_4 = \begin{bmatrix}
84 & & & & & & & & & & & \\
-6 & 8 & & & & & & & & & & \\
6 & 0 & 8 & & & & & & & & & \\
-84 & 6 & -6 & 84 & & & & & & & & \\
-6 & -2 & 0 & 6 & 8 & & & & & & & \\
-6 & 0 & -8 & 6 & 0 & 8 & & & & & & \\
-84 & 6 & -6 & 84 & 6 & 6 & 84 & & & & & \\
6 & -8 & 0 & -6 & 2 & 0 & -6 & 8 & & & & \\
6 & 0 & -2 & -6 & 0 & 2 & -6 & 0 & 8 & & & \\
84 & -6 & 6 & -84 & -6 & -6 & -84 & 6 & 6 & 84 & & \\
6 & 2 & 0 & -6 & -8 & 0 & -6 & -2 & 0 & 6 & 8 & \\
-6 & 0 & 2 & -6 & 0 & -2 & 6 & 0 & -8 & -6 & 0 & 8
\end{bmatrix}$$

SYM.

Table(1.17)

$$\bar{L} = \begin{bmatrix}
I & O & O & O \\
O & I & O & O \\
O & O & I & O \\
O & O & O & I
\end{bmatrix} \quad \text{and} \quad I = \begin{bmatrix}
1 & 0 & 0 \\
0 & B & 0 \\
0 & 0 & A
\end{bmatrix}$$

1.3.6.7. Elastic Stiffness Matrix for Beam in Torsion.

The cross-section of the thin walled beam considered, is shown in Figure (1.6a).

This elastic matrix which is about to be derived, may find application in the study of torsional buckling.

From Figure (1.6b) we find that two degrees of freedom at each node were considered, two rotation (U_1, U_3) and two expressed by the first derivations of rotations (U_2, U_4), the latter were included to account for warping of cross-sections.

To use Castiglian's theorem for the derivation of the elastic matrix the strain energy of the cross-section is derived as follows:

Strain Energy:

For the beam considered the strain energy is composed of two parts

$$U_{E_1} + U_{E_2}$$

where

U_{E_1} is the strain energy due to Saint Venant twisting.

U_{E_2} is the strain energy due to twisting produced by warping cross-section.

From Reference (20) the strain energy can be expressed as follows:

$$U_E = U_{E_1} + U_{E_2} = \tfrac{1}{2}\int_L \left(G\,J\,(d\theta/dx)^2 + E\,\Gamma\,(d^2\theta/dx^2)^2 \right) dx$$

Assuming for the θ the displacement function (21)

$$\theta = a_1 x^3 + a_2 x^2 + a_3 x + a_4$$

and from

at $x = 0$ $\theta = U_1$ and $d\theta/dx = U_2$

and

at $x = L$ $\theta = U_3$ and $d\theta/dx = U_4$

we find

$$\mathbf{U} = \mathbf{L}\,\mathbf{a}$$

so

$$\mathbf{a} = \mathbf{L}^{-1}\mathbf{U}$$

Substituting on a_i in the assumed displacement function we obtain

$$\theta = \mathbf{N}\,\mathbf{U}$$

Where $\mathbf{N}$ is the row matrix of shape functions given in Table (1. 3).

Substituting in the expression of the strain energy we obtain

$$U_E = \tfrac{1}{2}\int_L GJ\,\mathbf{U}^T\mathbf{N}'^T\mathbf{N}'\mathbf{U}\,dx + \tfrac{1}{2}\int_L E\Gamma\,\mathbf{U}^T\mathbf{N}''^T\mathbf{N}''\mathbf{U}\,dx$$

where primes indicate differentiation.

then from

$$\partial U_E / \partial U_i = F_i \qquad i = 1.4$$

We obtain

$$\mathbf{k}_e\,\mathbf{U} = \mathbf{F}$$

where

$$\mathbf{k}_e = \int_L \left(GJ\,\mathbf{N}'^T\mathbf{N}' + \Gamma E\,\mathbf{N}''^T\mathbf{N}'' \right) dx$$

$\mathbf{N}'$ and $\mathbf{N}''$ are given in Table (1.18).

Substituting and integrating we obtain the matrix given in Table (1.19).

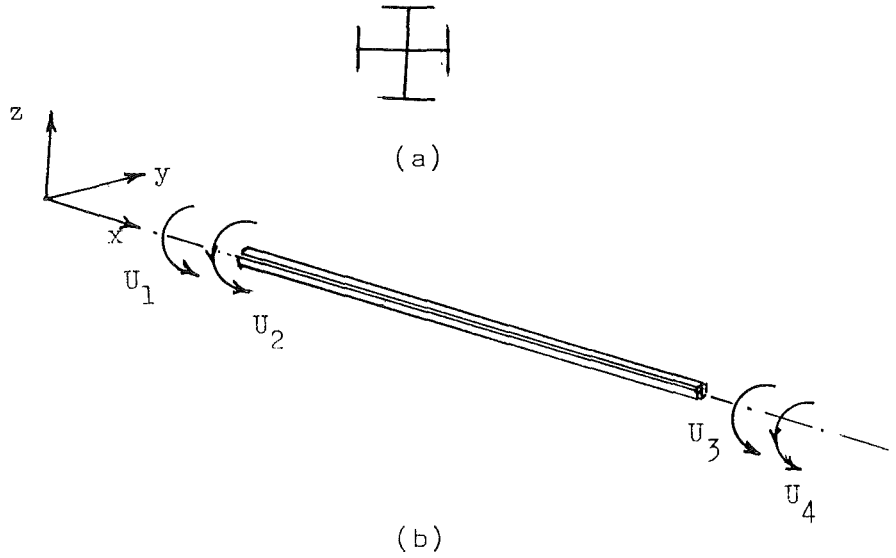

FIGURE (1.6) - CROSS-SECTION (a) AND NODAL DEGREE OF FREEDOM (b) FOR BEAM IN TORSION.

$$\mathbf{N}' = \begin{bmatrix} N_1' & N_2' & N_3' & N_4' \end{bmatrix}$$

$$\mathbf{N}'' = \begin{bmatrix} N_1'' & N_2'' & N_3'' & N_4'' \end{bmatrix}$$

where

$$N_1' = \left(-6x/L^2 + 6x^2/L^3 \right)$$

$$N_2' = \left(1 - 4x/L + 3x^2/L^2 \right)$$

$$N_3' = \left(-6x^2/L^3 + 6x/L^2 \right)$$

$$N_4' = \left(3x^2/L^2 - 2x/L \right)$$

$$N_1'' = \left(-6/L + 12x/L^3 \right)$$

$$N_2'' = \left(-4/L + 6x/L^2 \right)$$

$$N_3'' = \left(-12x/L^3 + 6/L^2 \right)$$

$$N_4'' = \left(6x/L^2 - 2/L \right)$$

TABLE (1.18) - MATRIX $\mathbf{N}'$ AND $\mathbf{N}''$ FOR BEAM ELEMENT IN TORSION.

$$\mathbf{k_e} = \mathbf{k_1} + \mathbf{k_2}$$

where

$$\mathbf{k_1} = GJ \begin{bmatrix} 6/5L & & & \\ 1/10 & 2L/15 & \text{SYM.} & \\ -6/5L & -1/10 & 6/5L & \\ 1/10 & -L/30 & -1/10 & 2L/15 \end{bmatrix}$$

and

$$\mathbf{k_2} = E\Gamma \begin{bmatrix} 12/L^3 & & & \\ 6/L^2 & 4/L & \text{SYM.} & \\ -12/L^3 & -6/L^2 & 12/L^3 & \\ 6/L^2 & 2/L & -6/L^2 & 4/L \end{bmatrix}$$

where

G is the shearing modulus of elasticity

J is the torsional constant

GJ is the torsional rigidity of the cross section

E is Young's modulus of elasticity

Γ is the warping constant

$E\Gamma$ is the warping rigidity of the section

TABLE (1.19) - ELASTIC STIFFNESS MATRIX $\mathbf{k_e}$ FOR THIN WALLED BEAM ELEMENT IN TORSION.

1.4. Conclusions.

1. The finite element method is a powerful technique of general application, once element stiffnesses are derived the finite element model of the complete structure is obtained, a variety of problems can be dealt with very efficiently.
2. Because the finite element method uses elements of different sizes and shapes and of different material properties, it can be used for the analysis of structures with complicated geometries, composed of parts which have different temperatures, and for structures of non-isotropic material properties.
3. The way in which the finite element method accommodates the boundary conditions in the analysis, introduces a broader interpretation of the effect of constraints.
4. The displacement direct approach is easier to programme and to apply than the force method and than Argyris' approach.
5. Among the methods used for the derivation of the elastic stiffness matrices encountered in this Chapter, those based on the principal of virtual work (Unit displacement method, Castigliano's theorem) are more advantageous because they consist of a series of matrical operations and can be extended to derive the geometric stiffness matrices necessary for stability analysis.

CHAPTER 2.

STRUCTURE STABILITY.

2.1. Introduction:

In general, the literature in structure stability can be roughly divided into two main topics:

a. Linear Study : Which is primarily concerned with critical equilibrium states.

b. Nonlinear Study : Which is concerned with the equilibrium path configuration in the vicinity of the equilibrium state.

A great contribution to the first topic is due to H. Ziegler and some of his work is summarised in (22).

In the study of linear stability of structures, he first classified systems into conservative systems and nonconservative systems.

Conservative systems are systems subject to conservative forces.

A nonconservative system is one which is subject to at least one nonconservative force.

Where conservative forces are forces which when their point of application is displaced from point A to point B, the work done is only a function of the initial and final positions and does not depend on the displacement path.

Forces are then classified as reactions, and external loads.

Reactions can be considered conservative if they are nonworking (ex. frictionless normal pressure).

Nonconservative reactions are dissipative or doing negative work. (ex. Kinetic dry friction). (It is to be noted here, that nonworking reactions are considered as conservative, although they do not admit potential energy).

Loads are classified as follows:

Stationary loads, which are independent of time but may be velocity dependent.

Nonstationary loads, which depend explicity on time and are nonconservative (e.g. pulsating loads).

Velocity dependent stationary loads include those which do zero work (e.g. gyroscopic) and are conservative and those which do negative work i.e. are dissipative (e.g. air drag) and are non-conservative.

Stationary velocity independent loads also fall into both categories. Those which can be derived from a potential (e.g. gravitational forces) and are conservative are called non-circulatory whilst all others are nonconservative and known as circulatory.

Examples of nonconservative systems are those which have a dissipative reaction, or dissipative load, circulatory or non-stationary type.

Charts (2.1), (2.2) summarise the above classifications of forces and systems and can be used as a guide to find the appropriate solution to the stability of any elastic system encountered in a structure ([22]).

In the analysis which follows, the systems which will be treated as those which are classified as nongyroscopic in which reactions are nonworking and loads are stationary and noncirculatory.

This category can be treated using the energy approach and the finite element method, which will be adopted throughout.

For axially loaded structures, the buckling load is defined as the load at which small disturbances of the position of equilibrium of the structure will lead to large deformations which exceed the allowable limits specified under certain working conditions and working time.

Since in practical structures the object of design is to retain a well defined shape, the critical buckling study will define the load at which this well defined shape is lost, and consequently, the use of small perturbation theory from equilibrium has an actual practical meaning.

In aircraft structures, for example, large use is made of slender columns and thin plates which are very likely to fail by buckling and thus the determination of buckling stress is a problem of extreme importance.

In this Chapter, a comparative study of different methods applied to this category of problem of elastic stability will be undertaken, emphasis being placed on the finite element method.

In the next Chapter, the method will be used to study the stability of some structures under axial loading and, where possible, comparison with existing solutions or with experimental results will be made.

In addition, the buckling of a new structural element will be studied and conclusions will be drawn.

CHART (2.1)

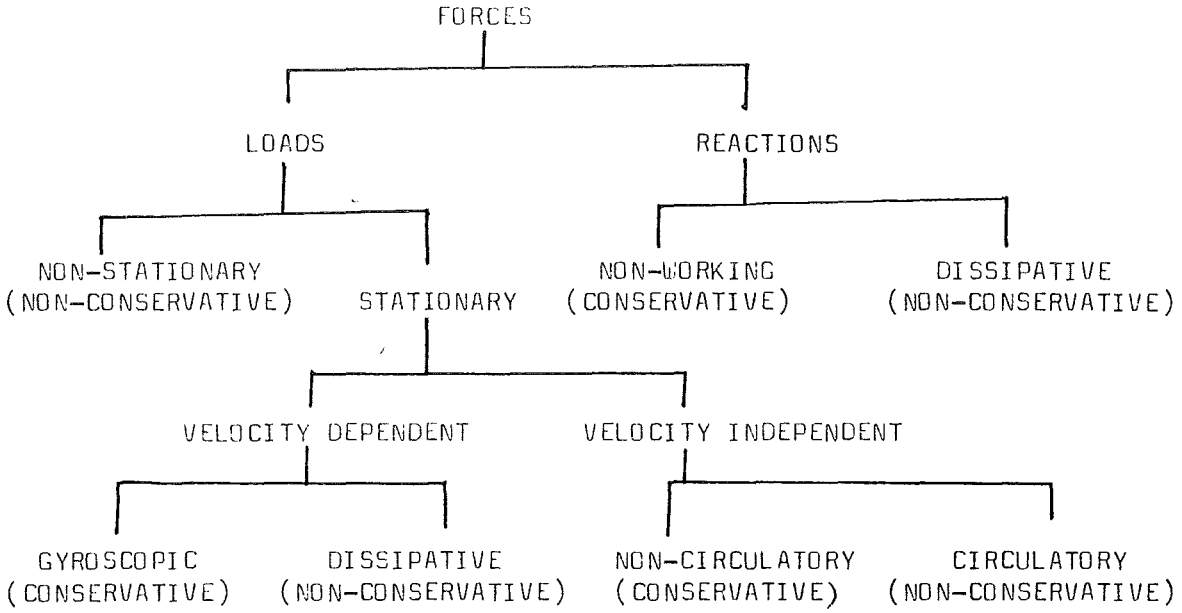

CHART (2.2)

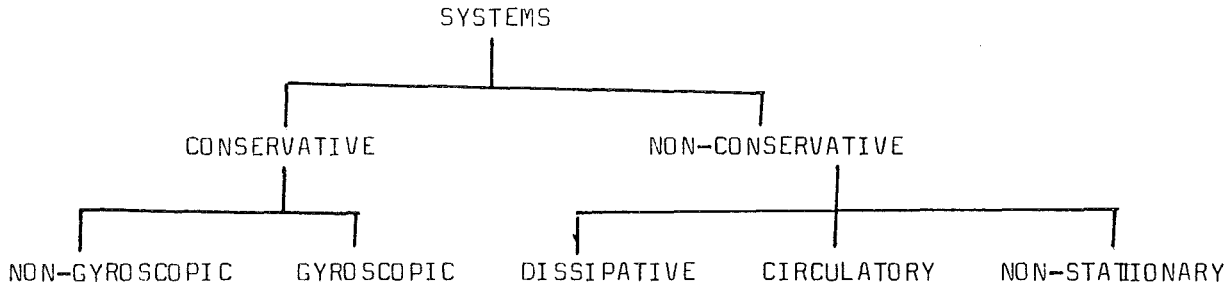

2.2. The Equilibrium Method. (Euler - 1744).

This method is mostly encountered in the analysis of simple structural forms, for example, the axially loaded bar and the rectangular plate carrying in-plane edge loadings, and it is based on the concept of the condition of neutral equilibrium.

This means that there is no loss of equilibrium when the bar or plate is displaced slightly from its initial straight or plane form.

The bent position is used to establish equilibrium between the external applied forces and the internal forces, and the analysis can be outlined as follows:

a - The basic equilibrium equation between internal forces and external applied forces is set up,

b - This equation is transformed in terms of stresses,

c - From Hooke's Law the basic equation is transformed into an equation in terms of strains,

d - By expressing the strains in terms of the displacement, the equilibrium equation will become the differential equation which governs the deflection of the structure,

e - Since it is a stability problem, the integration of the differential equation will lead to a set of eigenvalues and corresponding eigenvectors and the critical load will be the smallest of the eigenvalues.

2.3. Determination of Buckling Load by the Principal of Total Potential Energy.

It is based on the equation:-

$$\delta(U_E + V) = 0$$

Where U_E is the strain energy of the elastic structure, and V is the potential energy and their sum is known as the total potential energy.

The above equation can be stated as follows:-

"((An elastic body is in equilibrium if no change occurs in the total potential energy of the system for any small arbitary displacement.))"

In the determination of the buckling load this method can be used in either one of the following procedures.

1. Assumed Deflection Shape:

This procedure is attributed to Navier (1820) and applied to several examples in (23).

The analysis is carried out as follows:-

a. The analytical expression of the total potential energy is found.

b. A suitable displacement function is chosen in terms of unknown coefficients and in the choice of displacement function it is important that it satisfies both the geometric boundary conditions represented by slope and deflection and the natural boundary conditions represented by shear and bending moment. If it is not possible to satisfy both, at least the geometric boundary condition must be satisfied.

c. The total potential energy is then calculated in terms of the unknown parameters.

d. The expression of minimum total potential energy ($\delta(U_E + V) = 0$) is then obtained by equating to zero the partial differentials of this energy with respect to each one of those unknown coefficients.

e. The critical load is found by elimination of the unknown parameters.

This procedure depends in the first place on the choice of the displacement function, if it is the exact one then the buckling load will be exact, if the assumed displacement function is not exact then the buckling load determined will be approximate and the degree of approximation depends on how closely the true buckling shape is represented.

2. Variational Approach:

This procedure first appeared in 1891 in a paper by G.H. Bryan (24).

In the previous procedure, an important feature is the choice of buckling shape which must, at least, satisfy the geometric boundary conditions.

This second procedure is principally suitable for the study of the case when the assumed deflection shape can not be easily found.

In this procedure, the variation calculus is used to find the conditions represented by the <u>differential equation and the natural boundary conditions</u> which the exact deflection shape must satisfy so that the total potential energy of the system become stationary ($\delta(U_E + V) = 0$).

It leads only to the governing differential equations of the problem.

An application can be found in the above reference where a circular plate was studied and in Ref. ([20])., in which this procedure was applied to the simple case of axially loaded simply supported column p 89.

2.4. Determination of Buckling Load Using the Ritz Method.

This method is referred to by W. Ritz and first appeared in the literature in 1909.

In the Ritz method, an assumed shape is used to represent the deformation of the system. This reduces the number of degrees of freedom and the critical load is found by using only ordinary calculus (25).

Application of this method proceeds as follows:-

1. The analytical expression of the total potential energy is obtained.

2. The deflection surface is expressed in expanded form as the sum of an infinite set of functions having undetermined coefficients.

Each term of the expansion must satisfy the boundary condition of the problem.

3. The total energy of the structure is computed for the deflection surface and then minimised with respect to the undetermined coefficients.

4. This minimisation procedure leads to a set of linear homogeneous equations in the undetermined coefficients.

5. These equations have non-vanishing solutions only if their coefficients vanish.

The vanishing of this stability determinant provides the equation that may be solved for the buckling load.

6. If the set of functions is complete and capable of representing slope, deflection, shape and curvature of any possible deformation, the solution is exact.

For the exact analysis the order of the determinant will be infinite, and if only a reduced nember of terms are used, an approximate buckling load will be obtained, which will be higher/

/higher than the exact value.

An application of this method can be found in (26) where the lateral buckling of deep beam was analysed.

2.5. Determination of the Buckling Load by the Principal of Conservation of Energy.

This method is referred to as the Timoshenko method having been developed by Timoshenko, S. ([27]), 1910, and used extensively in (28) for the solution of a variety of instability problems.

This method is based on the energy concept which can best be explained by taking the axially loaded column as a particular example. This column when subjected to gradually increasing load remains stable in the straight form as long as the load is lower than the buckling load.

During this stage, the load does work by virtue of the shortening of the bar.

When the buckling load is reached, the straight form of equilibrium is no longer unique and another equilibrium condition represented by a bent form of the bar appears.

The work done by the load is now associated with a displacement arising in part from the bending of the bar and in part from the axial deformation of the bar.

Because of the bending, the strain energy of the bar is also increased by an amount due to the bending deformation and so it can be said that at the instant prior to buckling, the increase in external work is equal to the increase in strain energy.

In mathematical terms, before buckling the system is stable and we have

$$U_E - W_e > 0$$

after buckling stability is lost and

$$U_E - W_e < 0$$

whilst at transition

$$U_E - W_e = 0$$

This last condition is characteristic of the incipient state of buckling, and can be stated in the following form:-

"((A conservative system is in equilibrium if the strain energy stored is equal to the work performed by the external loads.))"

Analysis procedure for the general problem is:-

1. Expressions for the strain energy and the external work are obtained.

In general, the deformation of the structure prior to buckling is neglected, because it is considered to be much smaller than the bending deformation.

2. An assumed displacement function is chosen which must satisfy as many as possible of the boundary conditions. Generally, the function will involve n coefficients a_i or parameters.

3. From the equality $U_E = W_e$
this equation is derived

$$P = U_E(a_1, a_2, \ldots\ldots a_n)/\bar{W}_e(a_1, a_2, \ldots\ldots a_n)$$

The parameters are then adjusted until P becomes a minimum; this leads to n equations of this type

$$\partial P / \partial a_i = (1/\bar{W}_e^{\,2})\left[(\partial U_E / \partial a_i)\,\bar{W}_e - (\partial \bar{W}_e / \partial a_i)\,U_E\right] = 0$$

which become $\partial U_E / \partial a_i - P(\partial W_e / \partial a_i) = 0 \quad (i = 1, n)$

This final set of equations gives the n constants a_i and the buckling load.

It can be seen that there is a striking similarity between the various energy approaches:

a. All of them lead to a buckling load higher than the exact one if a limited number of terms is considered.

b. All lead to the exact buckling load if the assumed displacement function represents exactly the true buckled shape and satisfies the boundary condition.

2.6 The Determination of Buckling Load by Galerkin's Method.

This method is attributed to B.G. Galerkin, and first appeared in 1915, see (29).

In the previous method a trial function was assumed for the deflection and then substituted in the analytical expression of total potential energy to find the buckling load.

This method also uses a trial function to represent the deflection shape, the trial functions satisfying term by term the geometric and natural boundary conditions.

The undetermined constants in which the trial function is expressed are then determined by considering each term of the trial function in turn to be a weighing function, and then setting the weighted average of the residual function to zero.

The physical meaning of this condition is that if the trial function is representing exactly the buckled shape then the residual become zero. If the trial function does not represent exactly the buckled shape then the weighted averages when set up equal to zero will provide the conditions which the trial function must satisfy so that the error of approximation becomes a minimum.

Another method of obtaining Galerkin's conditions which is based on the principal of least square can be found in (30).

Once the Galerkin's conditions are obtained, which are in number equal to the number of the unknowns in the assumed trial function, a set of the necessary number of equations is obtained. The determinant of the coefficients of the undetermined constants will give the buckling load.

This method can be summarised as follows:-

1. The differential equation is obtained from equilibrium or the principal of total potential energy.

Suppose this to be

$$\mathcal{L}(W) = 0$$

2. A trial function which satisfies geometric and natural boundary conditions is selected

$$\Theta = \sum_{i=1}^{n} a_i \psi_i$$

3. The equation residual is then found from

$$R = \mathcal{L}(\Theta) = \sum_{i=1}^{n} a_i \mathcal{L}(\psi_i)$$

4. In general, if $W(x)$ is a weighing function, the weighted average of a function $f(x)$ in an interval $a < x < b$ is

$$\int_a^b W f \, dx \Big/ \int_a^b W \, dx$$

In this case, setting the weighted averages of the residual R equal to zero equivalent to

$$\int_D \psi_i \mathcal{L}(\Theta) = 0 \qquad i = 1 \ldots\ldots n$$

Where D is the domain of the differential equations.

5. This last step provides a system of n equations for the n undetermined coefficients. The determinant of the coefficients of these unknowns provide the buckling load.

An application of this method to the buckling of a column and to the buckling of a plate in shear can be found in (20).

2.7. The Determination of Buckling Load by Finite Difference Method.*

In the previous article, the solution to a buckling problem is found by approximating the shape by properly selecting a displacement function.

In addition to the problem of setting up the differential equation itself, there is also the problem of finding the right function to be used for the approximation, which must satisfy both geometric and natural boundary conditions. Unless a great deal of physical intuition is exercised the solution may differ greatly from the exact.

The finite difference method overcomes the second part of the problem associated with the differential equation by replacing the differential equation and the boundary condition by their finite difference approximations (31).

The result is that instead of dealing with the differential equation the solution to the problem is found by analysing a set of equivalent algebraic equations.

The basis of this method is that a derivative of a function at a point can be replaced by an algebraic expression formed by the value of the function at that point and several nearby points. Instead of analysing a system of infinite degree of freedom an idealised structure formed by discrete element is used, even with a relatively large mesh a good approximation to the exact solution can be obtained.

In buckling analysis, by using the finite difference expressions to replace the derivatives at the number of points chosen, and introducing the boundary conditions, we form a system of homogeneous equations. The determinant of the coefficients of these equations, will be transformed into a characteristic equation and the smallest root will define the buckling load.

---

* L. F. Richardson - 1911 , see (25) pp. 87 .

For the function f (x), the derivatives can be replaced as follows:-

$$\left[\frac{df}{dx}\right]_{x=i} = \frac{f_{i+h} - f_i}{h}$$

Where f_i, f_{i+h} are the values of f (x) at x = i and at x = i + h, and h is the distance between those two points

$$\left[\frac{d^2 f}{d x^2}\right]_{x=i} = \frac{f_{i+h} - 2 f_i + f_{i-h}}{h^2}$$

$$\left[\frac{d^4 f}{d x^4}\right]_{x=i} = \frac{f_{i+2h} - 4f_{i+h} + 6f_i - 4 f_{i-h} + f_{i-2h}}{h^4}$$

For the function f (x, y), the derivatives in the governing differential equation assume the following expressions:-

Relative to x at point j, K

$$\left[\frac{\partial^2 w}{\partial x^2}\right]_{j,K} = \frac{w_{j+h,K} - 2 w_{j,K} + w_{j-h,K}}{h^2}$$

and

$$\left[\frac{\partial^4 w}{\partial x^4}\right]_{j,K} = \frac{w_{j+2h,K} - 4 w_{j+h,K} + 6 w_{j,K} - 4 w_{j-h,K} + w_{j-2h,K}}{h^4}$$

relative to y at point j, K

$$\left[\frac{\partial^2 w}{\partial y^2}\right]_{j,K} = \frac{w_{j,K+h} - 2 w_{j,K} + w_{j,K-h}}{h^2}$$

and

$$\left[\frac{\partial^4 w}{\partial y^4}\right]_{j,K} = \frac{w_{j,K+2h} - 4 w_{j,K+h} + 6w_{j,K} - 4w_{j,K-h} + w_{j,K-2h}}{h^4}$$

An application can be found in (20).

2.7.1.

Conclusion:

From the previous introductory study of these well established methods used in the determination of buckling load, the following conclusions can be drawn:-

1. For a solution to be obtained using any one of the above methods, either it is necessary to find the differential equation or the analytical expressions of the strain and potential energies with the obvious difficulty involved.

2. A closed form solution to the differential equation is rarely obtained and an approximate solution procedure has to be adopted which, in general, involves an assumed displacement function. The degree of approximation depends a great deal on the proper choice of the assumed displacement function.

3. The similarity of the various methods may lead to some confusion in the proper selection of the procedure suitable for the problem in hand, and failure to make the correct choice will lead to error in the result.

4. As will be seen, the finite element approach to this problem is less problem dependent and once a programme is set up a variety of problems can be solved with minimum effort and time.

Clearly the finite element method also involves the employment of an assumed displacement function but in general, this comes at a very early stage and is limited in the sense that it is applied to the finite element and its deflected form not to the deflection of the structure as a whole.

2.8. Determination of the Buckling Load by the Finite Element Method.

In the previous article, the finite difference method overcame the difficulty of finding a solution to the differential equation of a structure by replacing the governing differential equation by a set of equivalent algebraic equations that are usually easier to solve. When an adequate computer is available, this method has the advantage of generality of application although we still have the problem of setting up the differential equation which describes the behaviour of the structure and of finding the associated boundary conditions.

In the previous Chapter, it was shown how the finite element method overcomes all the problems encountered above.

The finite element method transforms the structure into an assembly of finite elements connected at nodes, and, using the stiffnesses of the single elements, the elastic stiffness of the complete structure is built up according to equilibrium and compatability conditions dictated by the theory of elasticity and under the assumption of small displacements. For the elastic structure, the following equation which relates applied forces on the complete structure to the displacements, can be given:-

$$\mathbf{P = K U}$$

For buckling analysis, in the displacement approach, the stiffness of the structure is no longer constant but is a function of the axial or in-plane load of the various elements and can be considered to be formed of two parts, one the constant elastic stiffness and the other the geometric stiffness, which is a function of the axial or in-plane loads.

In the previous Chapter, the stability determinant for a structure idealised into an assembly of **discrete** elements and in the absence of temperature effects, was found to be:-

$$\left|\mathbf{K}_e + \lambda \mathbf{K}_g^*\right| = 0$$

Where $\mathbf{K}_e$ is the elastic stiffness matrix

$\mathbf{K}_g^*$ is the geometric stiffness matrix

λ is a proportionality constant

The elastic stiffness matrices were discussed in that Chapter.

In the following sections, the derivation of geometric stiffness matrices for some structural elements will be considered.

2.8.1 Derivation of Geometric Stiffness Matrices from the Principal of Virtual Work.

An elastic body in equilibrium under a set of applied forces

$$\mathbf{F} = \{F_1 \; F_2 \; \ldots\ldots \; F_n\}$$

is subject to small virtual displacements which are compatible with the constraint system and are represented by the vector

$$\delta\mathbf{U} = \{\delta U_1 \; \delta U_2 \; \ldots\ldots \delta U_n\}$$

Each is applied in turn at the point of application of the corresponding force F.

Then the virtual work produced by these forces is equal to the increase in strain energy of the body.

This can be written as

$$\delta W_e = \delta U_E$$

or

$$\mathbf{F}^T \delta\mathbf{U} = \int_V \sigma^T \delta\epsilon \; dV \qquad (2.1)$$

Where σ are the stresses which are produced by the applied forces $\mathbf{F}$ and ϵ are the strains compatible with the virtual displacements $\delta\mathbf{U}$.

This method was considered in the previous Chapter, for the derivation of the elastic stiffness matrix under the name of the unit displacement method.

In order to provide, a general formula for the derivation of geometric stiffness matrices which is easier to apply than that proposed in (8) the following study has been conducted on the strain-displacement relationships.

Consider the standard strain-displacement expressions:-

$$\varepsilon_x = du/dx + \tfrac{1}{2}\left((du/dx)^2 + (dv/dx)^2 + (dw/dx)^2\right)$$

$$\varepsilon_y = dv/dy + \tfrac{1}{2}\left((du/dy)^2 + (dv/dy)^2 + (dw/dy)^2\right)$$

$$\varepsilon_z = dw/dz + \tfrac{1}{2}\left((du/dz)^2 + (dv/dz)^2 + (dw/dz)^2\right)$$

$$\gamma_{xy} = du/dy + dv/dx + \left((du/dx)(du/dy) + (dv/dx)(dv/dy) + (dw/dx)(dw/dy)\right)$$

$$\gamma_{yz} = dv/dz + dw/dy + \left((du/dz)(du/dy) + (dv/dz)(dv/dy) + (dw/dz)(dw/dy)\right)$$

$$\gamma_{zx} = dw/dx + du/dz + \left((du/dz)(du/dx) + (dv/dz)(dv/dx) + (dw/dz)(dw/dx)\right)$$

or

$$\epsilon = \epsilon_0 + \epsilon_L$$

Using matrix notations the second term on the right hand side can be written as (14) :

$$\epsilon_L = \tfrac{1}{2} \begin{bmatrix} \mathbf{G}_x^T & \mathbf{0} & \mathbf{0} \\ \mathbf{0} & \mathbf{G}_y^T & \mathbf{0} \\ \mathbf{0} & \mathbf{0} & \mathbf{G}_z^T \\ \mathbf{G}_y^T & \mathbf{G}_x^T & \mathbf{0} \\ \mathbf{0} & \mathbf{G}_z^T & \mathbf{G}_y^T \\ \mathbf{G}_z^T & \mathbf{0} & \mathbf{G}_x^T \end{bmatrix}_{6\times 9} \begin{bmatrix} \mathbf{G}_x \\ \mathbf{G}_y \\ \mathbf{G}_z \end{bmatrix}_{9\times 1} \qquad (2.2)$$

and in compact form

$$\epsilon_L = \frac{1}{2} \psi \theta \qquad (2.3)$$

so that the strains can be expressed as

$$\epsilon = \epsilon_o + \frac{1}{2} \psi \theta$$

where

$$\mathbf{G}_x = \{ du/dx \quad dv/dx \quad dw/dx \}$$

$$\mathbf{G}_y = \{ du/dy \quad dv/dy \quad dw/dy \}$$

$$\mathbf{G}_z = \{ du/dz \quad dv/dz \quad dw/dz \}$$

Using the notations

$$u = \mathbf{N}_x \mathbf{U}$$

$$v = \mathbf{N}_y \mathbf{U}$$

$$w = \mathbf{N}_z \mathbf{U}$$

Where $\mathbf{U}$ is the node displacement vector of order $(n \times 1)$ and $\mathbf{N}_x$, $\mathbf{N}_y$ and $\mathbf{N}_z$ are the shape functions, each being a row vector of order $(1 \times n)$ so that

$$\begin{aligned} \mathbf{G}_x &= \{ d\mathbf{N}_x/dx\,\mathbf{U} \quad d\mathbf{N}_y/dx\,\mathbf{U} \quad d\mathbf{N}_z/dx\,\mathbf{U} \} \\ \mathbf{G}_y &= \{ d\mathbf{N}_x/dy\,\mathbf{U} \quad d\mathbf{N}_y/dy\,\mathbf{U} \quad d\mathbf{N}_z/dy\,\mathbf{U} \} \\ \mathbf{G}_z &= \{ d\mathbf{N}_x/dz\,\mathbf{U} \quad d\mathbf{N}_y/dz\,\mathbf{U} \quad d\mathbf{N}_z/dz\,\mathbf{U} \} \end{aligned} \qquad (2.4)$$

Considering the principal of virtual work

$$\int_V \sigma^T \delta\epsilon = \mathbf{F}^T \delta\mathbf{U}$$

Substituting for ϵ we have

$$\int_V \sigma^T (\delta\epsilon_o + \delta\epsilon_L) \, dV = \mathbf{F}^T \delta\mathbf{U}$$

so that it can be written as

$$\int_V (\sigma^T \delta\epsilon_o + \sigma^T \delta\epsilon_L) \, dV = \mathbf{F}^T \delta\mathbf{U}$$

considering first the first term on the left hand side, from previous Chapter

$$\delta\epsilon_o = \mathbf{b}\,\delta\mathbf{U}$$

and from

$$\sigma = \mathbf{E}\,\mathbf{b}\,\mathbf{U}$$

taking the transpose and substituting

$$\int_V \mathbf{U}^T \mathbf{b}^T \mathbf{E}\,\mathbf{b}\,\delta\mathbf{U} \, dV$$

then considering the second term on the left hand side

$$\int_V \sigma^T \delta\epsilon_L \, dV$$

from

$$\delta\epsilon_L = \delta(\tfrac{1}{2}\,\psi\,\theta)$$

we have

$$\delta\epsilon_L = \tfrac{1}{2}\delta\psi\,\theta + \tfrac{1}{2}\,\psi\,\delta\theta$$

and then from (14)

$$\delta\psi\,\theta = \psi\,\delta\theta$$

so that

$$\delta\epsilon_L = \psi\,\delta\theta \qquad (2.5)$$

where

$$\delta\theta = \{\, dN_x/dx \quad dN_y/dx \quad dN_z/dx \quad dN_x/dy \quad dN_y/dy$$
$$dN_z/dy \quad dN_x/dz \quad dN_y/dz \quad dN_z/dz \,\} \delta U$$

substituting on ψ and on $\delta\theta$ using equation (2.5) we find

$$\delta\epsilon_L = \{\, U^T B_{Lx} \delta U \quad U^T B_{Ly} \delta U \quad U^T B_{Lz} \delta U \quad U^T B_{Lxy} \delta U \quad U^T B_{Lyz} \delta U \quad U^T B_{Lzx} \delta U \,\}$$

where

$$B_{Lx} = dN_x^T/dx \; dN_x/dx + dN_y^T/dx \; dN_y/dx + dN_z^T/dx \; dN_z/dx$$

$$B_{Ly} = dN_x^T/dy \; dN_x/dy + dN_y^T/dy \; dN_y/dy + dN_z^T/dy \; dN_z/dy$$

$$B_{Lz} = dN_x^T/dz \; dN_x/dz + dN_y^T/dz \; dN_y/dz + dN_z^T/dz \; dN_z/dz$$

$$B_{Lxy} = dN_x^T/dy \; dN_x/dx + dN_y^T/dy \; dN_y/dx + dN_z^T/dy \; dN_z/dx +$$
$$+ dN_x^T/dx \; dN_x/dy + dN_y^T/dx \; dN_y/dy + dN_z^T/dx \; dN_z/dy$$

$$B_{Lyz} = dN_x^T/dz \; dN_x/dy + dN_y^T/dz \; dN_y/dy + dN_z^T/dz \; dN_z/dy +$$
$$+ dN_x^T/dy \; dN_x/dz + dN_y^T/dy \; dN_y/dz + dN_z^T/dy \; dN_z/dz$$

$$B_{Lzx} = dN_x^T/dz \; dN_x/dx + dN_y^T/dz \; dN_y/dx + dN_z^T/dz \; dN_z/dx +$$
$$+ dN_x^T/dx \; dN_x/dz + dN_y^T/dx \; dN_y/dz + dN_z^T/dx \; dN_z/dz ,$$

The principal of virtual work after eliminating δU can be written as follows:-

$$F^T = \int_V U^T b^T E \, b \, dV + \int_V U^T \Big[\sigma_x B_{Lx} + \sigma_y B_{Ly} + \sigma_z B_{Lz} + \tau_{xy} B_{Lxy} +$$
$$+ \tau_{yz} B_{Lyz} + \tau_{zx} B_{Lzx} \Big] dV$$

after taking the transpose we have

$$F = \int_V b^T E b \, U \, dV + \int_V \Big[\sigma_x B_{Lx} + \sigma_y B_{Ly} + \sigma_z B_{Lz} + \tau_{xy} B_{Lxy} +$$
$$+ \tau_{yz} B_{Lyz} + \tau_{zx} B_{Lzx} \Big] U \, dV$$

where

$$\int_V \mathbf{b}^T \mathbf{E}\, \mathbf{b} \; dV$$

is the elastic stiffness matrix $\mathbf{k_e}$

and

$$\int_V \left[\sigma_x \; \mathbf{B}_{Lx} + \sigma_y \; \mathbf{B}_{Ly} + \sigma_z \; \mathbf{B}_{Lz} + \right.$$

$$\left. + \tau_{xy} \; \mathbf{B}_{Lxy} + \tau_{yz} \; \mathbf{B}_{Lyz} + \tau_{zx} \; \mathbf{B}_{Lzx} \right] dV \qquad (2.6)$$

is the general form of the geometric stiffness matrix $\mathbf{k_g}$.

In the following sections, the above formula will be used to derive the geometric stiffness matrices for some structural elements.

2.8.1.1 Derivation of the Geometric Stiffness Matrix for a Pin Jointed Bar Element.

For the pin-jointed bar element which is shown in Figure (2.1), where a large displacement of the element in the plane (z, x) is shown, the lateral displacement will be given by the following equations:-

$$w = (1 - X)\,U_2 + U_4 X$$

Where $X = x/L$ and L is the length of the element.
This can be written as

$$w = \mathbf{N}_z\,\mathbf{U}$$

where

$$\mathbf{N}_z = \begin{bmatrix} 0 & (1 - X) & 0 & X \end{bmatrix}$$

and

$$d\mathbf{N}_z/dx = \mathbf{N}'_z = \begin{bmatrix} 0 & -1/L & 0 & 1/L \end{bmatrix}$$

From the general formula for the geometric matrix (2.6) for only σ_x we obtain

$$\mathbf{k_g} = \int_V \sigma_x\,\mathbf{B}_{Lx}\,dV = \int_V \sigma_x\,d\mathbf{N}_z/dx\;d\mathbf{N}_z/dx\;dV$$

Substituting

$$\mathbf{k_g} = F_x \int_L \begin{bmatrix} 0 \\ 1/L \\ 0 \\ 1/L \end{bmatrix} \begin{bmatrix} 0 & -1/L & 0 & 1/L \end{bmatrix} dx$$

Integrating we obtain the geometric stiffness matrix given in Table (2.1).

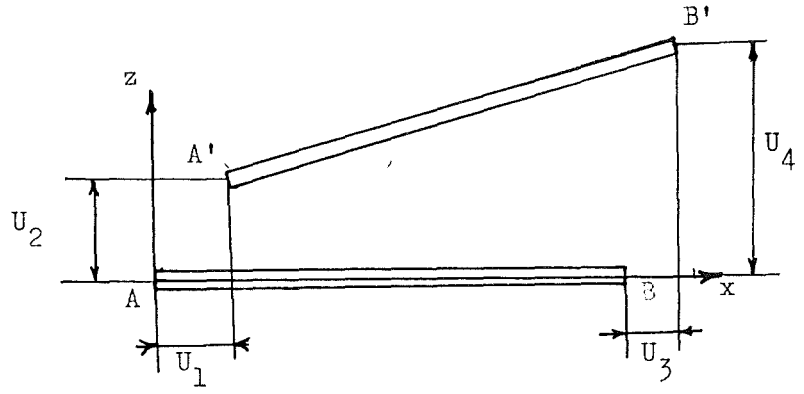

FIGURE (2.1) - LARGE DISPLACEMENT OF PIN-JOINTED BAR ELEMENT.

$$\mathbf{k_g} = \frac{F_x}{L} \begin{bmatrix} 0 & 0 & 0 & 0 \\ 0 & 1 & 0 & -1 \\ 0 & 0 & 0 & 0 \\ 0 & -1 & 0 & 1 \end{bmatrix}$$

TABLE (2.1) - GEOMETRIC STIFFNESS MATRIX FOR PIN-JOINTED BAR ELEMENT.

2.8.1.2 Derivation of the Geometric Stiffness Matrix for a Beam Element, in Flexure in the xy Plane.

Assuming a displacement function (17)

$$v = a_1 x^3 + a_2 x^2 + a_3 x + a_4$$

at node 1 and 2 a positive rotation produce positive

d w/dx so at node 1

$$x = 0$$

$$U_1 = v\Big|_{x=0} \quad , \quad U_2 = dv/dx\Big|_{x=0}$$

and at node 2

$$x = L$$

$$U_3 = v\Big|_{x=L} \quad , \quad U_4 = dv/dx\Big|_{x=L}$$

U are the nodal displacements shown in Figure (2. 2)

Substituting, we obtain:

$$\begin{bmatrix} U_1 \\ U_2 \\ U_3 \\ U_4 \end{bmatrix} = \begin{bmatrix} 0 & 0 & 0 & 1 \\ 0 & 0 & 1 & 0 \\ L^3 & L^2 & L & 1 \\ 3L^2 & 2L & 1 & 0 \end{bmatrix} \begin{bmatrix} a_1 \\ a_2 \\ a_3 \\ a_4 \end{bmatrix} \quad \text{or} \quad \mathbf{U = l\ a}$$

Then from

$$\mathbf{a = l^{-1} U}$$

We have

$$a_1 = (2/L^3)\,U_1 + (1/L^2)\,U_2 + (-2/L^3)\,U_3 + (1/L^2)\,U_4$$

$$a_2 = (-3/L^2)\,U_1 + (-2/L)\,U_2 + (3/L^2)\,U_3 + (-1/L)\,U_4$$

$$a_3 = U_2$$

$$a_4 = U_1$$

Substituting on a_i in the displacement function and taking the coefficients of the nodal displacements we obtain the shape functions

$$N_1 = 2X^3 - 3X^2 + 1$$

$$N_2 = L\,X\,(X-1)^2$$

$$N_3 = -2X^3 + 3X^2 \qquad (2.7)$$

$$N_4 = L\,(X^3 - x^2)$$

Where $X = x/L$ is the nondimensional co-ordinate.

The displacement function can now be written as:

$$v = \mathbf{N}_y\,\mathbf{U}$$

Where $\mathbf{N}_y$ is the row vector of shape functions and $\mathbf{U}$ is the column vector of nodal displacement from the standard formula derived (2.6)

$$\mathbf{k_g} = \int_v \sigma_x\,\mathbf{B}_{Lx} = \int_v \sigma_x\,\mathbf{N}_y'^{T}\mathbf{N}_y'\,dV$$

where

$$d\,\mathbf{N}_y/dx = \mathbf{N}'$$

For combined axial and bending of the beam

$$\sigma_x = \sigma_0 + \sigma_1\,y$$

Where

σ_o is the stress at the centroide in the x direction

σ_1 is the rate of change of σ with respect to y which is assumed to vary linearly with x.

Substituting on σ

$$\mathbf{k_g} = \int_v \sigma_o \mathbf{N}_y'^T \mathbf{N}_y' \, dV + \int_v \sigma_1 \, y \, \mathbf{N}_y'^T \mathbf{N}_y' \, dV$$

the second term on the right hand side becomes zero because

$$\int_A y \, dA = 0$$

and the geometric stiffness for the beam will be given from

$$\mathbf{k_g} = \sigma_o A \int_L \mathbf{N}_y'^T \mathbf{N}_y' \, dx$$

Substituting on $\mathbf{N}_y'$

$$\mathbf{k_g} = F_x \begin{bmatrix} N_1'^2 & & \text{Sym.} & \\ N_2'N_1' & N_2'^2 & & \\ N_3'N_1' & N_3'N_2' & N_3'^2 & \\ N_4'N_1' & N_4'N_2' & N_4'N_3' & N_4'^2 \end{bmatrix}$$

which give the geometric stiffness matrix given in Table (2.2).

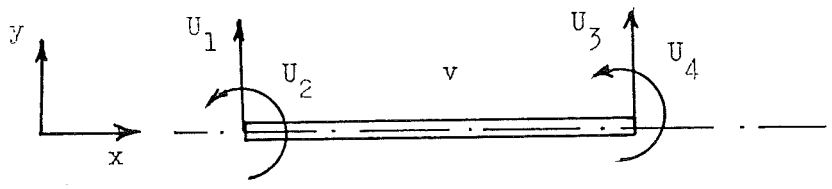

FIGURE (2.2) - LARGE DISPLACEMENT FOR BEAM ELEMENT.

$$\mathbf{k_g} = \frac{F_x}{30L}\begin{bmatrix} 36 & & & \\ 3L & 4L^2 & & \\ -36 & -3L & 36 & \\ 3L & -L^2 & -3L & 4L^2 \end{bmatrix}$$

TABLE (2.2) - GEOMETRIC STIFFNESS MATRIX FOR BEAM ELEMENT.

2.8.1.3 Derivation of the Geometric Stiffness Matrix for Three-Dimensional Beam Element in Flexure.

For the beam shown in Figure assuming displacement functions given by

(see Figure(2.3))

$$v = a_1 x^3 + a_2 x^2 + a_3 x + a_4$$
$$w = b_1 x^3 + b_2 x^3 + b_3 x + b_4$$

and following the same procedure adopted in the previous section for the two cases, we arrive at the following equation:-

$$\begin{bmatrix} v \\ w \end{bmatrix} = \begin{bmatrix} \mathbf{N}_y \\ \mathbf{N}_z \end{bmatrix} \mathbf{U}$$

where

U is shown in figure(2.3)

$\mathbf{N}_y$ is a row matrix of order (1 x 12) and the nonzero elements $N_y(1,2)$, $N_y(1,6)$, $N_y(1,8)$ and $N_y(1,12)$ are equal to N_1, N_2, N_3, and N_4 which are given in(2.7) .

$\mathbf{N}_z$ is a row matrix of order (1, 12) contain zeros everywhere except the following elements which are defined as follows:-

$$N_z(1,3) = N_y(1,2)$$
$$N_z(1,5) = N_y(1,6)$$
$$N_z(1,9) = N_y(1,8)$$
$$N_z(1,11) = -N_y(1,12)$$

Then from

$$\mathbf{k_g} = \int_v \sigma_x \quad \mathbf{B}_{Lx} \quad dV = \int_v \sigma_x (\mathbf{N}'^{T}_y \mathbf{N}'_y + \mathbf{N}'^{T}_z \mathbf{N}'_z) \, d\,V$$

Where primes indicate differentiation relative to x, and

$\sigma_x = \sigma_o + \sigma_1 y + \sigma_2 z$

where σ_o is the stress at the centroid , σ_1 is the rate of change of σ_x with respect to y , and σ_2 is the rate of change of σ_x with respect to z .

and observing that

$$\int_A y \, dA = 0$$

and $$\int_A z \, dA = 0$$

we find

$$\mathbf{k_g} = \sigma_o \int_V (\mathbf{N}_y'^{\top} \mathbf{N}_y' + \mathbf{N}_z'^{\top} \mathbf{N}_z') \, dV$$

the geometric stiffness matrix is given in Table (2. 3).

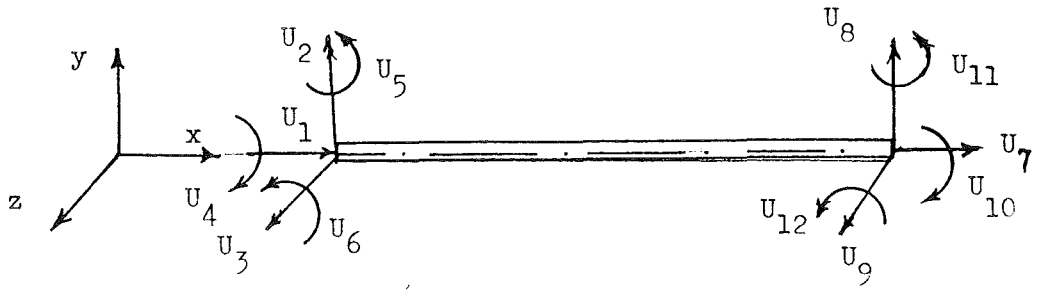

FIGURE (2.3) - THREE DIMENSIONAL BEAM ELEMENT NODAL DISPLACEMENT.

$$\frac{F_x}{30L}\begin{bmatrix}
0 & & & & & & & & & & & \\
0 & 36 & & & & & & & & & & \\
0 & 0 & 36 & & & & \text{SYM.} & & & & & \\
0 & 0 & 0 & 0 & & & & & & & & \\
0 & 0 & -3L & 0 & 4L^2 & & & & & & & \\
0 & 3L & 0 & 0 & 0 & 4L^2 & & & & & & \\
0 & 0 & 0 & 0 & 0 & 0 & 0 & & & & & \\
0 & -36 & 0 & 0 & 0 & -3L & 0 & 36 & & & & \\
0 & 0 & -36 & 0 & 3L & 0 & 0 & 0 & 36 & & & \\
0 & 0 & 0 & 0 & 0 & 0 & 0 & 0 & 0 & 0 & & \\
0 & 0 & -3L & 0 & -L^2 & 0 & 0 & 0 & 3L & 0 & 4L^2 & \\
0 & 3L & 0 & 0 & 0 & -3L & 0 & -3L & 0 & 0 & 0 & 4L^2
\end{bmatrix}$$

TABLE (2.3) - GEOMETRIC STIFFNESS MATRIX FOR BEAM ELEMENT.

2.8.1.4 Derivation of the Geometric Stiffness Matrix for Beam in Torsion with End Constraint Effects .

From Figure (2.4) (b), we have

$$\Delta = r\theta$$

$$v = -a = -\Delta \sin\alpha = -r\theta\sin\alpha$$

$$w = b = \Delta\cos\alpha = r\theta\cos\alpha$$

Then from

$$r\sin\alpha = z$$

$$r\cos\alpha = y$$

we obtain

$$v = -z\theta$$

$$w = y\theta$$

Assuming for the rotation the displacement function (21),

$$\theta = c_1 x^3 + c_2 x^2 + c_3 x + c_4$$

and for the large displacement deformations shown in Figure (2.4) where U_1 and U_3 are rotations at node 1 and 2 and U_2 and U_4 represent the first derivatives of the rotation relative to the longitudinal axis x, we may write:-

$$\begin{bmatrix} v \\ w \end{bmatrix} = \begin{bmatrix} \mathbf{N}_y \\ \mathbf{N}_z \end{bmatrix} \mathbf{U}$$

Where v and w are deformations in y and z direction respectively and where

$$\mathbf{N}_y = -z\mathbf{N}$$

$$\mathbf{N}_z = y\mathbf{N}$$

and N_i with i = 1, 4 are given in Equation (2.7).

Then from

$$d\mathbf{N}_y/dx = \mathbf{N}'_y = -z\mathbf{N}'$$

$$d\mathbf{N}_z/dx = \mathbf{N}'_z = y\mathbf{N}'$$

and from the general formula (2.6)

$$\mathbf{k_g} = \int_V \sigma_x \mathbf{B}_{Lx} \, dV = \int_V \sigma_x \left(\mathbf{N}_y'^T \mathbf{N}_y' + \mathbf{N}_z'^T \mathbf{N}_z' \right) dV$$

we find

$$\mathbf{k_g} = \int_L \sigma_x \left(\int_A (y^2 + z^2) \, dA \right) \mathbf{N}'^T \mathbf{N}' \, dx$$

$\int_A (y^2 + z^2) dA = I_o$, is the polar moment of inertia relative to the centre of twist .

Substituting we obtain

$$\mathbf{k_g} = \sigma_x \, I_o \int_L \mathbf{N}'^T \mathbf{N}' \, dx$$

The integration has already been carried out and the resulting geometric stiffness matrix is listed in table (2.4) .

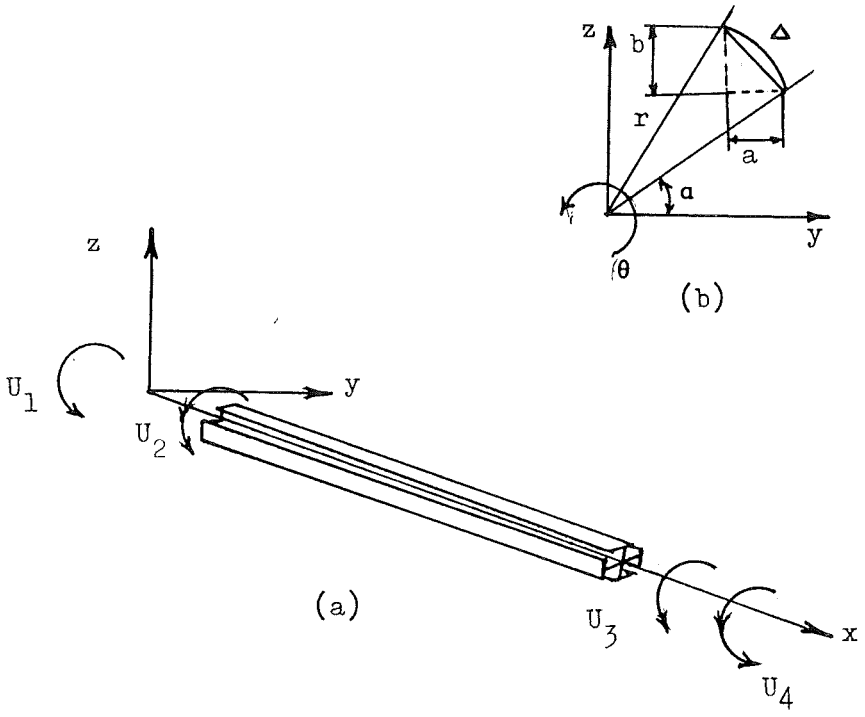

FIGURE (2.4) - DEFORMATION FOR BEAM ELEMENT IN TORSION .

$$\mathbf{k_g} = \frac{\sigma_x}{30L} I_o \begin{bmatrix} 36 & & & \\ 3L & 4L^2 & & \\ 36 & -3L & 36 & \\ 3L & -L^2 & -3L & 4L^2 \end{bmatrix}$$

TABLE (2.4) - GEOMETRIC STIFFNESS MATRIX FOR BEAM ELEMENT IN PURE TORSION.

2.8.1.5 Derivation of the Geometric Stiffness Matrix for a Rectangular Plate Element (Without Bending).

For a plate subject only to membrane stresses the geometric stiffness matrix can be derived as follows:-

The displacement distribution is assumed to be represented by (16):

$$w = \left[(1 - X)(1 - Y) \quad (1 - X)Y \quad X Y \quad X (1 - Y) \right] \mathbf{U}$$

where

$$X = x/A$$

$$Y = y/B$$

and

$$\mathbf{U} = \{ U_1 \quad U_2 \quad U_3 \quad U_4 \}$$

Where $\mathbf{U}$ represent the nodal displacements shown in Figure (2.5).

The assumed displacement function can be written as

$$w = \mathbf{N} \quad \mathbf{U}$$

If a general loading represented by

$$\sigma = \{ \sigma_x \quad \sigma_y \quad \tau_{xy} \}$$

is applied, then from formula (2.6) we have

$$\mathbf{k_g} = \int_V \left[\sigma_x \ \mathbf{B}_{Lx} + \sigma_y \ \mathbf{B}_{Ly} + \tau_{xy} \ \mathbf{B}_{Lxy} \right] dV$$

Where in this case

$$\mathbf{B}_{Lx} = \mathbf{N}_z'^{T}\ \mathbf{N}_z'$$
$$\mathbf{B}_{Ly} = \hat{\mathbf{N}}_z^{T}\ \hat{\mathbf{N}}_z$$
$$\mathbf{B}_{Lxy} = \mathbf{N}_z'^{T}\ \hat{\mathbf{N}}_z + \hat{\mathbf{N}}_z^{T}\ \mathbf{N}_z'$$

$$\mathbf{N}_z' = d\,\mathbf{N}_z/dx = (1/A)\begin{bmatrix} -(1-Y) & -Y & Y & (1-Y) \end{bmatrix}$$

and

$$\hat{\mathbf{N}}_z = d\,\mathbf{N}_z/dy = (1/B)\begin{bmatrix} -(1-X) & (1-X) & X & -X \end{bmatrix}$$

then from

$$\mathbf{k_g} = \int_V \left[\sigma_x\ \mathbf{N}_z'^{T}\ \mathbf{N}_z' + \sigma_y\ \hat{\mathbf{N}}_z^{T}\ \hat{\mathbf{N}}_z + \tau_{xy}(\mathbf{N}_z'^{T}\ \hat{\mathbf{N}}_z + \hat{\mathbf{N}}_z^{T}\ \mathbf{N}_z') \right] dV$$

Carrying out the integration we obtain the geometric stiffness matrix given in Table (2.5) .

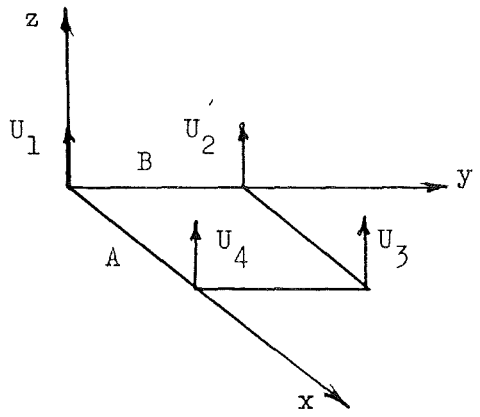

Thicness of plate = T

FIGURE (2.5) - RECTANGULAR PLATE ELEMENT LARGE DISPLACEMENT. (IN-PLANE FORCES).

$$k_g = \frac{\sigma_x T B}{6A}\begin{bmatrix} 2 & & & \\ 1 & 2 & \text{SYM.} & \\ -1 & -2 & 2 & \\ -2 & -1 & 1 & 2 \end{bmatrix} + \frac{\sigma_y T A}{6B}\begin{bmatrix} 2 & & & \\ -2 & 2 & \text{SYM.} & \\ -1 & 1 & 2 & \\ 1 & -1 & -2 & 2 \end{bmatrix}$$

$$+ \frac{\tau_{xy} T}{4}\begin{bmatrix} 2 & & & \\ 0 & -2 & \text{SYM.} & \\ -2 & 0 & 2 & \\ 0 & 2 & 0 & -2 \end{bmatrix}$$

TABLE (2.5) - GEOMETRIC STIFFNESS MATRIX FOR RECTANGULAR PLATE (IN-PLANE FORCES).

2.8.1.6 Derivation of Geometric Stiffness Matrix for a Plate in Bending.

Those component displacements at the four nodes which will define the large deformations are shown in Figure (2.6).

The lateral deflection can be represented by (13):

$$w = c_1 + c_2 X + c_3 Y + c_4 X^2 + c_5 X Y + c_6 Y^2 + c_7 X^3 + c_8 X^2 Y + c_9 X Y^2 + c_{10} Y^3 + c_{11} X^3 Y + c_{12} X Y^3$$

where

$X = x/A$ where A is the plate length

$Y = y/B$ B is the plate width

It must be noticed that this assumed displacement function satisfies compatibility of displacements along the common boundaries with other elements, and does not satisfy compatibility of slopes but, as will be seen, its use in buckling analysis gives relatively good results.

Considering a uniform axial loading in the x direction acting on the sides , the geometric stiffness matrix, becomes:

$$\mathbf{k_g} = \int_V \sigma_x \, \mathbf{B}_{Lx} \, dV = \int_V \sigma_x \, \mathbf{N}_z'^{T} \mathbf{N}_z' \, dV$$

where primes indicate differentiation relative to x.

Variation of σ across depth being neglected.

The shape function matrix was given in Table (1.10) and $d\mathbf{N}_z^T/dx$ is given in Table (2.6).

Substituting in the above equation for $\mathbf{N}_z'$ and carrying out the integration term by term the geometric stiffness matrix given in Table (2.7) will be obtained which is identical to that given in (8).

$$\mathbf{N}_Z^T = \begin{bmatrix}
(1/A)\,(-Y-(6X-6X^2)(1-Y)+(3-2Y)\,Y^2) & 1\\
-(1/A)\,(Y\,(1-Y)^2\,B) & 2\\
((-1+4X-3X^2)\,(1-Y)) & 3\\
(1/A)\,(-(3Y^2-2Y^3)+(1-6X+6X^2))\,Y & 4\\
(1/A)\,(1-Y)\,Y^2)\,B & 5\\
-(1-4X+3X^2)\,Y & 6\\
(1/A)\,((6X-6X^2)\,Y-Y\,(1-Y)\,(1-2Y)) & 7\\
(1/A)\,((1-Y)\,Y^2)\,B & 8\\
((2X-3X^2)\,Y) & 9\\
(1/A)\,(6X-6X^2)\,(1-Y)+Y\,(1-Y)\,(1-2Y)) & 10\\
(1/A)\,(Y\,(1-Y)^2\,B) & 11\\
((2X-3X^2)\,(1-Y) & 12
\end{bmatrix}$$

TABLE (2.6) - MATRIX FOR RECTANGULAR PLATE IN BENDING.

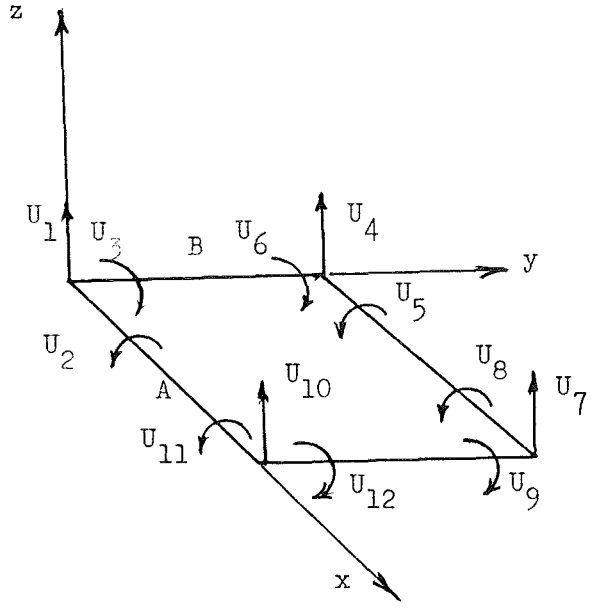

FIGURE (2.6) - LARGE DEFORMATION OF RECTANGULAR PLATE IN BENDING.

TABLE (2.7) - GEOMETRIC STIFFNESS FOR RECTANGULAR PLATE LOADED IN x DIRECTION. (OUT-OF-PLANE DEFORMATION).

$\mathbf{k_g}$ = G

a											
b	h										
c		j									
e	-f	g	a								
f	k		-b	h							
g		l	c		j						
-e	f	-g	-a	b	-c	a					
-f	-k		b	-h		-b	h				
g		m	c		n	-c		j			
-a	-b	-c	-e	-f	-g	e	f	-g	a		
- b	-h		f	-k		-f	k		b	h	
c		n	g		m	-g		l	-c		j

SYM.

Where

$$G = \sigma_x T B/(1260A)$$

and

a =	552	h =	$12B^2$
b =	66B	j =	$56A^2$
c =	- 42A	k =	$-9B^2$
e =	204	l =	$28A^2$
f =	- 39B	m =	$-7A^2$
g =	- 21A	n =	$-14A^2$

T is the plate thicness

Blank spaces are zeros.

2.8.2 Derivation of the Geometric Stiffness Matrix Using Castigliano's Theorem (Part - I).

In the previous Chapter, it was found that by using the principal of virtual work a direct and general formula for the determination of the geometric stiffness matrix was obtained.

This general formula is then applied to some structural elements and the geometric matrices derived found to be identical with those obtained by more complicated and elaborate approaches.

In this section, it will be shown that the same general formula can be derived from Castigliano's theorem (Part - I).

This theorem is expressed as

$$F_i = \delta U_E / \delta U_i \qquad i = 1, n$$

This can be written as

$$F_i \, \delta U_i = \delta U_E \qquad i = 1, n$$

Using matrix notation we may write

$$\mathbf{F}^T \delta \mathbf{U} = \delta U_E \qquad (2.8)$$

then from

$$U_E = \int_V \boldsymbol{\epsilon}^T \boldsymbol{\sigma} \, dV = \int_V \boldsymbol{\sigma}^T \boldsymbol{\epsilon} \, dV$$

and

$$\delta U_E = \int_V \boldsymbol{\sigma}^T \delta \boldsymbol{\epsilon} \, dV$$

Substituting in equation (2.8) we find

$$\mathbf{F}^T \delta \mathbf{U} = \int_V \boldsymbol{\sigma}^T \delta \boldsymbol{\epsilon} \, dV$$

which is the same equation of virtual work used in the previous section to find the general expression of the geometric matrix.

CHAPTER 3.

BUCKLING ANALYSIS

PART 1.

3.1.1. Introduction.

In Chapter One the finite element method in general was considered and elastic stiffness matrices were derived for some structural elements.

In Chapter Two the derivation of the geometric stiffness matrices for those elements was undertaken using the direct formula obtained from the analysis of the non-linear expression of the principal of virtual work.

In this first part of Chapter Three, the standard finite element is used to find buckling loads for structures idealised into beams and plates. Flexural and torsional buckling modes of beams are analysed first and the results are compared with the analytical solutions, then isotropic and orthotropic plates and panels are considered.

The results using different finite element grids are compared with those obtained analytically for the plates and obtained experimentally for stiffened panels.

For better assessment of the efficiency of the finite element method computation times are included and results and conclusions are presented at the end of each section.

In the second part, a new version of the finite element in which the structure is idealised into finite strips, a procedure which has been found very advantageous, will be considered.

The finite strip approach will be used to study the local buckling mode for a variety of plate type structures and, in particular, the buckling of plates stabilised by an elastic medium and the local buckling of a composite panel.

3.1.2. Buckling of Beams Using the Finite Element Method.

The method will be applied first to beams which buckle in the flexural mode then to beams which buckle in the torsional mode.

There is a vast literature on the subject of buckling of beams Reference (28) contains a generalised treatment, the application of the finite element method to this class of problems received attention in (9), (21) and (32).

The elastic and geometric stiffness matrices were derived in the previous Chapters and here their application to the buckling analysis will be studied.

3.1.2.1. Flexural Buckling of the Axially Loaded Beam.

This section, the finite element method approach to structural stability will be applied, using the elastic and the geometric stiffnesses which are in Table (1.5) and (2.2).

a. Critical Load for the Axially Loaded Beam with Ends Clamped.

The beam is idealised as shown in Figure (3.1). The form of the assembled elastic and geometrical stiffness matrices of the idealised beam is shown in Table (3.1).

Because ends are assumed to be clamped which corresponds to rotation and displacement at node 1 and 3 being zero the first, second, fifth and sixth rows and columns will be eliminated from the assembly matrices.

U_1	U_2	U_3	U_4	U_5	U_6	
$K(1,1)_I$	$K(1,2)_I$	$K(1,3)_I$	$K(1,4)_I$	0	0	U_1
$K(2,1)_I$	$K(2,2)_I$	$K(2,3)_I$	$K(2,4)_I$	0	0	U_2
$K(3,1)_I$	$K(3,2)_I$	$K(3,3)_I + K(1,1)_I$	$K(3,4)_I + K(1,2)_{II}$	$K(1,3)_{II}$	$K(1,4)_{II}$	U_3
$K(4,1)_I$	$K(4,2)_I$	$K(4,3)_I + K(2,1)_{II}$	$K(4,4)_I + K(2,2)_{II}$	$K(2,3)_{II}$	$K(2,4)_{II}$	U_4
0	0	$K(3,1)_{II}$	$K(3,2)_{II}$	$K(3,3)_{II}$	$K(3,4)_{II}$	U_5
0	0	$K(4,1)_{II}$	$K(4,2)_{II}$	$K(4,3)_{II}$	$K(4,4)_{II}$	U_6

TABLE (3.1)- ASSEMBLY MATRIX FOR BEAM ELEMENT REPRESENTED BY TWO FINITE ELEMENTS .

$K(3,3)_I$ + $K(1,1)_{II}$	$K(3,4)_I$ + $K(1,2)_{II}$
$K(4,3)_I$ + $K(2,1)_{II}$	$K(4,4)_I$ + $K(2,2)_{II}$

TABLE (3.2) THE REDUCED ASSEMBLY MATRIX FOR THE BEAM ELEMENT IDEALISED INTO TWO ELEMENTS.

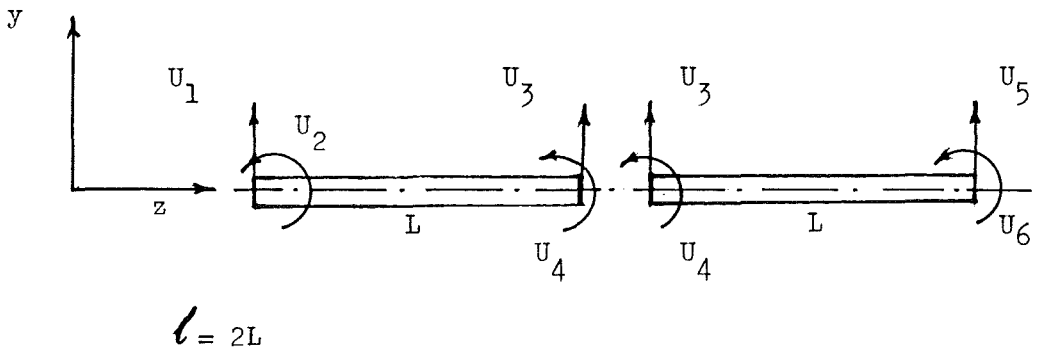

FIGURE(3.1)- Beam Idealisation .

The form of the reduced matrix is given in Table (3.2)

Then from the determinental equation:

$$\left| \mathbf{K}_e + \mathbf{K}_g \right| = 0$$

Substituting we obtain:-

$$\left| \frac{E\,I}{L^3} \begin{bmatrix} 24 & 0 \\ 0 & 8L^2 \end{bmatrix} - \frac{Fx}{L} \begin{bmatrix} \frac{12}{5} & 0 \\ 0 & \frac{4L^2}{15} \end{bmatrix} \right| = 0$$

For $Fx = 1$ $\quad \mathbf{K}_g \rightarrow \mathbf{K}_g^*$

$$\left| \frac{EI}{L^3} \begin{bmatrix} 24 & 0 \\ 0 & 8L^2 \end{bmatrix} - \frac{\lambda}{L} \begin{bmatrix} \frac{12}{5} & 0 \\ 0 & \frac{4L^2}{15} \end{bmatrix} \right| = 0$$

$$\left(24 \frac{EI}{L^3} - \frac{12\lambda}{5L} \right)\left(\frac{8EI}{L} - \frac{4L\lambda}{15} \right) = 0$$

$$\lambda_1 = 24\frac{EI}{L^2} \left[\frac{5}{12} \right] = 10 \frac{EI}{(0.5\ell)^2} = 40 \frac{EI}{\ell^2}$$

$$\lambda_2 = \frac{2EI}{L} \left[\frac{15}{L} \right] = 30 \frac{EI}{L^2} = 30 \frac{EI}{(0.5\ell)^2} = 120 \frac{EI}{\ell^2}$$

ℓ is the length of the beam.

The second value for λ corresponds to the higher buckling mode.

Comparing the primary mode end-load, the value given by the classic analytical solution shows that the error is less then 2%.

b. Critical Load for the Axially Loaded Beam with Ends Simply Supported

In this case, to reduce the computation time by exploiting the symmetrical buckling shape, only one element will be used, as shown in Figure (3.2)

The reduced matrices can be obtained by eliminating the first and fourth rows and columns which corresponds to considering the displacement at node one and rotation at node two being zero.

Using the elastic and geometric stiffness matrices as before, lead to:

$$\left| \frac{EI}{L^3} \begin{bmatrix} 4L^2 & -6L \\ -6L & 12 \end{bmatrix} - \frac{\lambda}{L} \begin{bmatrix} \frac{2L^2}{15} & -\frac{L}{10} \\ -\frac{L}{10} & \frac{6}{5} \end{bmatrix} \right| = 0$$

which has the two roots

$$\lambda_1 = 2.5 \quad EI/(0.5\ell)^2$$

$$\lambda_2 = 3\,0.1 \quad EI/(0.5\ell)^2$$

The buckling load is the smallest of these, that is

$$P_{cr} = 10. \frac{EI}{\ell^2}$$

Comparing this with

$$P_{cr} = \pi^2 \frac{EI}{\ell^2}$$

one can see that the error is only 1.41%.

c. Conclusion:

1. For beams which buckle in flexure under axial load the finite element can be very advantageous in providing accurate solutions.
2. Although only one element is used, the results are less than 2% in error compared with those obtained using the exact method.

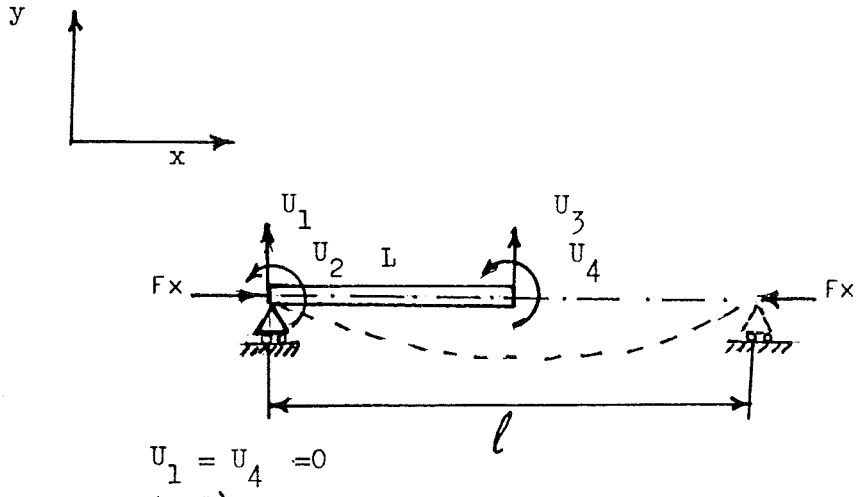

FIGURE (3.2)- ONE ELEMENT IDEALISATION OF SIMPLY SUPPORTED AXIALLY LOADED BEAM.

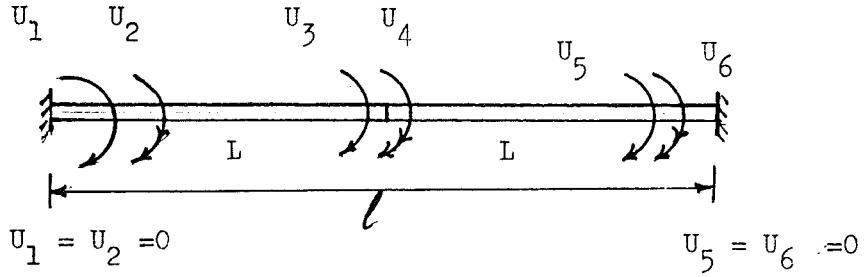

FIGURE (3.3)- TWO ELEMENT IDEALISATION OF BUILT IN BEAM FOR TORSIONAL BUCKLING ANALYSIS.

3.1.2.2 Buckling of Thin Walled Beam by Pure Torsion.

Beams having double symmetry of cross section and which are subjected to an axial compressive force, buckle in any one of the following modes:

1. Buckling by bending in one of the two planes of symmetry.
2. Pure torsional buckling.

Buckling by bending was studied in the previous two sections.

The torsional buckling will be studied in this section and a comparison will be made between the finite element solution and the continuous function solution.

a. Finite Element.

The elastic and geometric stiffness matrices for pure torsion of a beam are given in Table (1.19) and Table (2.4).

Two elements will be used to represent the full length of the beam.

The beam is assumed to be built in at the ends, this implies no rotation about any axis and zero warping

The reduced elastic and geometric matrices will have the same form as that represented in Table (3.2)

The determinental equation will be:

$$\left| \begin{bmatrix} 2a & 0 \\ 0 & 2b \end{bmatrix} - \lambda \begin{bmatrix} 2c & 0 \\ 0 & 2d \end{bmatrix} \right| = 0$$

where

$a = 12GJ/(10L) + 12E\Gamma/L^3$, $b = 12GJ/(10L) + 12E\Gamma/L^3$

$c = 12S_o/(10L)$, $d = 12S_o/(10L)$

$S_o = I_o/A$

Re-writing

$$\begin{vmatrix} (2a - \lambda 2c) & 0 \\ 0 & (2b - \lambda 2d) \end{vmatrix} = 0$$

which corresponds to

$$\lambda_1 = \lambda_2 = \left[12GJ/(10L)\right] \Big/ (10L/12S_o) + \left[12E\Gamma/L^3\right] \Big/ (10L/12S_o)$$

$$= GJ/S_o + 10E\Gamma/(S_o L^2)$$

and gives

$$P_{cr} = \frac{A}{I_o}\left[(GJ + \frac{40E\Gamma}{\ell^2})\right]$$

The solution to the same problem using the equilibrium method Ref. (28) Page 229 was found to be:

$$P_{cr} = \frac{A}{I_o} (GJ + 4\pi^2 E\Gamma/\ell^2)$$

which showed that the difference is less than 2%.

b. Conclusion:

1. The finite element method can be used for the analysis of the buckling in pure torsion of thin-walled beams which are built in at the ends giving accurate results with a minimum of computation.

2. The use in this problem, of elastic and geometric stiffness matrices derived using a third degree polynomial as the assumed displacement function is a suitable choice.

3. The other boundary condition associated with torsion, which is interpreted as zero rotation and free warping that is

$$\begin{cases} \theta = 0 \\ \partial^2\theta/\partial x^2 = 0 \end{cases}$$

cannot be properly accommodated in the analysis as the second quantity does not appear in the displacement vector. An analysis based on $\theta_x = 0, \partial\theta/\partial x = 0$ might be expected to produce a large error especially if the beam has a large value of $E\Gamma$, as shown in Reference (17), Page 395.

3.1.3 Buckling of Isotropic Plates using the Finite Element Method.

1. Introduction:

In the previous two sections, the finite element method was applied to the determination of critical buckling loads for columns.

In this section, the method will be applied to find the solution to a plate buckling problem, the solution will be compared with the existing solution by other method, and the number of elements necessary to achieve a good accuracy will be found.

For this analysis, a plate simply supported on all four sides will be used. Its dimensions are (A = 50, B = 25, T = 0.5 mm), and it is axially loaded in its plane in the x direction.

Using the computer programme developed for the method, the plate will be analysed using the finite element grid shown in Figure (3.4).

2. Finite Element Procedure:

1. The elastic stiffness matrix for the full plate is assembled using the elastic stiffness matrix derived in the first chapter and given in Table (1.12).

2. The geometric stiffness matrix for the plate is also assembled using the geometric stiffness matrix for the plate element given in Table (2. 7).

3. The assembly procedure was described in Chapter 1.

4. For each of the five cases to be studied, the nodal system and the boundary conditions had to be prepared and introduced as programme input.

5. In Figure (3.5) is shown a typical plate element with nodal displacements, and the finite element grid for the thirty-six finite element idealisation with the nodal numbering system adopted.

6. After deleting the rows and columns corresponding to the boundary conditions the reduced elastic and geometric stiffness matrices are then substituted into the determinant

$$\left| \mathbf{K}_e + \lambda \mathbf{K}_g^* \right| = 0$$

and by using the appropriate subroutine (Appendix*) the smallest buckling load is found as the lowest eigenvalue and the buckling shape represented by the associated eigenvector will be determined.

3. Computer Programme:

The computer progrqmme used for the analysis in which the above steps were incorporated is listed in Chapter Five and name PROGRAMME (3.1).

4. Conclusions:

1. For the four different finite element grids analysed the following results were obtained and compared with the buckling stress coefficient obtained from the classical theory: See Table (3.3).

2. For these cases, the computer time required using PROGRAMME (3.1) is given in Table (3.3).

3. From 1. and 2., it can be seen that the finite element can be used equally well for the buckling analysis of isotropic plates and the degree of accuracy increases with the increase of the number of elements employed.

4. As can be seen from Table (3.3), the accuracy achieved by using 36 finite element grid for one quarter of the plate was obtained at the expense of using much more computer time and storage space. It may be worthwhile to sacrifice some degree of accuracy for the sake of economy.

---

* See APPENDIX (A.2)

TABLE (3.3) - FINITE ELEMENT ANALYSIS OF BUCKLING OF SIMPLY SUPPORTED AXIALLY LOAD ISOTROPIC PLATE (A/B = 2).

	FULL PLATE 4 ELEMENTS	FULL PLATE 9 ELEMENTS	$\frac{1}{4}$ PLATE 4 ELEMENTS	FULL PLATE 36 ELEMENTS	$\frac{1}{4}$ PLATE 36 ELEMENTS	CLASSICAL THEORY
BUCKLING STRESS COEFFICIENT K	2.92	3.31	3.50	3.82	3.89	4.0
SIZE OF ASSEMBLY MATRIX	27 x 27	48 x 48	27 x 27	147x147	147x147	
SIZE OF REDUCED MATRIX	7 x 7	20 x 20	9 x 9	95x 95	100x100	
COMPUTER TIME (SECONDS)	4.113	15.451	4.388	68.772	69.650	

$$K = \frac{\sigma}{\frac{\pi^2 E}{12(1-\nu^2)}}$$

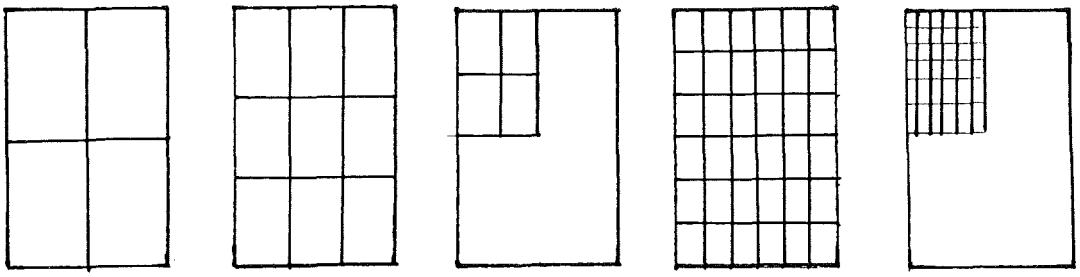

(2 x 2) (3 x 3) (4 x 4) (6 x 6) (12 x 12)

Figure (3. 4) - The Five Finite Element Grids Used to Study the Buckling of the Plate which has A = 50 mm., B = 25 mm and A/B = 2).

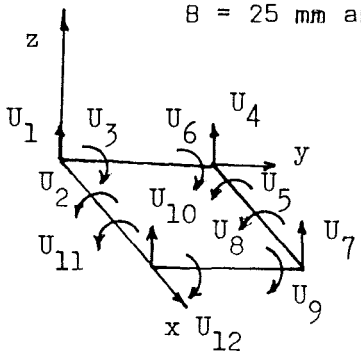

Figure(3.5)- Finite Element Idealisation of Plate

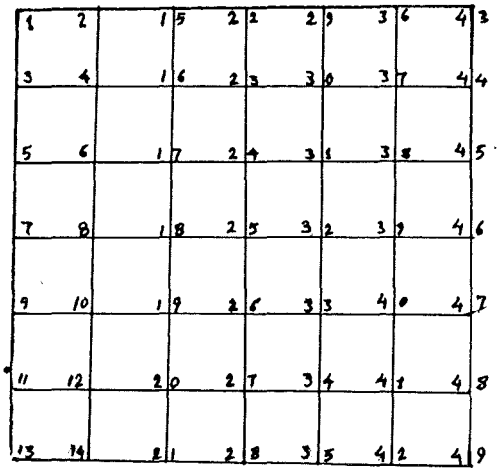

3.1.4. ORTHOTROPIC PLATES.

3.1.4.1 Introduction:

In the previous section, a plate was studied using the finite element. The plate was isotropic, which means that it had in all directions, the same elastic properties.

Many plates encountered in engineering can not be considered to be isotropic. It may be because they possess natural material anisotropy as would plates made of wood or plywood or fibre reinforced plastics, or perhaps because they may possess structural anisotropy caused by the presence of stiffeners or corrugations or because they are sandwich plates made of skin core combinations.

In this section, the use of the finite element method for the buckling analysis of this type of plate will be studied and the application of the orthotropic analogy to the overall buckling of multiplate type of construction will be reviewed.

3.1.4.2 Differential Equation Solution:

For general anisotropic plate we have (33)

$$\begin{bmatrix} \varepsilon_x \\ \varepsilon_y \\ \gamma_{xy} \end{bmatrix} = \begin{bmatrix} S_{11} & S_{12} & S_{13} \\ S_{21} & S_{22} & S_{23} \\ S_{31} & S_{32} & S_{33} \end{bmatrix} \begin{bmatrix} \sigma_x \\ \sigma_y \\ \tau_{xy} \end{bmatrix} \qquad \text{or} \quad \epsilon = S_{\alpha} \sigma \qquad (3.1)$$

where S_{ij} are the elastic compliances which obey the reciprocity law

$$S_{ij} = S_{ji}$$

and

$$S_{11} = 1/E_x, \quad S_{22} = 1/E_y,$$
$$S_{12} = -\nu_{xy}/E_x = -\nu_{yx}/E_y = 1/E_1$$
$$S_{33} = 1/G_{xy}$$

and E_x, E_y, G_{xy} are the elastic properties in x and y directions.

Anisotropic plates which have three mutually perpendicular planes of symmetry with respect to the elastic properties are called orthotropic and for this type of plate

$$S_{13} = S_{23} = 0$$

From (3. 1)

$$\sigma = S_o^{-1} \epsilon$$

or in explicit form,

$$\sigma_x = E'_x \varepsilon_x + E''_1 \varepsilon_y$$

$$\sigma_y = E'_y \varepsilon_y + E''_1 \varepsilon_x$$

$$\tau_{xy} = G'_{xy} \gamma_{xy}$$

where $E'_x = E_x/(1 - \nu_{xy} \nu_{yx})$, $E'_y = E_y/(1 - \nu_{xy} \nu_{yx})$,

$E''_1 = \nu_{yx} E_x/(1 - \nu_{xy} \nu_{yx}) = \nu_{xy} E_y/(1 - \nu_{xy} \nu_{yx})$

and $G'_{xy} = G_{xy} = G$

then from $\varepsilon_x = -z \partial^2 w/\partial x^2$

$\varepsilon_y = -z \partial^2 w/\partial y^2$

$\gamma_{xy} = -2z \partial^2 w/\partial x \partial y$

Substituting we obtain:

$$\sigma_x = - z (E'_x \partial^2 w/\partial x^2 + E''_1 \partial^2 w/\partial y^2)$$

$$\sigma_y = - z\,(E_y'\,\partial^2 w/\partial y^2 + E_1''\,\partial^2 w/\partial x^2)$$

$$\tau_{xy} = - 2G\,z\,\partial^2 w/\partial x\,\partial y$$

and from

$$Mx = \int_{-h/2}^{h/2} \sigma_x\, z\, dz \quad , \qquad My = \int_{-h/2}^{h/2} \sigma_y\, z\, dz$$

$$Mxy = \int_{-h/2}^{h/2} \tau_{xy}\, z\, dz$$

h = Thicness

we obtain:

$$\begin{aligned} Mx &= - (Dx\,\partial^2 w/\partial x^2 + D_1\,\partial^2 w/\partial y^2) \\ My &= - (Dy\,\partial^2 w/\partial y^2 + D_1\,\partial^2 w/\partial x^2) \\ Mxy &= 2\,Dxy\,\partial^2 w/\partial x\,\partial y \end{aligned} \qquad (3.2)$$

where

$$Dx = E_x' h^3/12, \quad Dy = E_y' h^3/12, \quad D_1 = E_1'' h^3/12$$

$$Dxy = G h^3/12$$

From the general theory , the differential equation for a plate loaded in compression takes the form:

$$\partial^2 Mx/\partial x^2 + 2\,\partial^2 Mxy/\partial x\partial y + \partial^2 My/\partial y^2 =$$

$$+ Nx\,\partial^2 w/\partial x^2 + Ny\,\partial^2 w/\partial y^2$$

Substituting from (3.2) we obtain

$$Dx\,\partial^4 w/\partial x^4 + 2\,(2Dxy + D_1)\,\partial^4 w/\partial x^2\partial y^2 + Dy\,\partial^4 w/\partial y^4 = - Nx\,\partial^2 w/\partial x^2 \qquad (3.3)$$

(only compression in x direction)

In reference (3.4) the case of an orthotropic plate subject either to uniaxial compression in the x direction or to compression in both the x and y directions, was studied for the following boundary conditions.

1. All edges simply supported.

2. All edges clamped.

3. Ends simply supported, sides clamped.

4. Ends clamped, sides simply supported.

The following important results were found:

1. The buckling stress can be presented in a simple formula as a function of the geometry and material properties of the orthotropic plate.

2. The curves for an isotropic plate can be used for an orthotropic plate except that on the abscissa instead of A/B, we plot

$$A/B\ (Do/Dx)^{0.25}$$

and on the ordinate, instead of the buckling stress coefficient

$$K = B^2 N_x /(\pi^2 D)$$

for the orthotropic plate

$$K = B^2 N_x / (\pi^2 (Dx\ Dy)^{0.5}) + 2 (1 - (2Dxy + D_1)/(Dx\ Dy)^{0.5}) \qquad (3.4)$$

3. For boundary condition 1. and 4. above putting

$$Dy = Dx = D$$

$$D_1 = \nu D$$

and $$Dxy = \tfrac{1}{2} (1 - \nu) D$$

in equation (3.3) confirms that the isotropic is only a particular case of the more general orthotropic plate.

For the purpose of this study, only the formula for the buckling stress of an axially loaded orthotropic plate simply supported at the sides, will be considered.

4. For cases of boundary condition 2. and 3. the exact solution leads to a family of curves relating K and λ for each value of $(2Dxy + D_1)/(Dx\ Dy)^{0.5}$.

But each of the two cases can also be reduced to a single curve which closely approximate the exact relation if in the following equation in which

$$K = B^2 Nx/(\pi^2 (Dx\ Dy)^{0.5}) + C (1 - (2Dxy + D1)/(Dx\ Dy)^{0.5})$$

For boundary condition 3 (sides clamped, ends simply supported)

C = 2.4 and for boundary condition 2. (all edges clamped)

C = 2.46.

5. The curves of the results of the study are presented in E.S.D.U. Data Sheet Item Number 71015 and reproduced for completeness in Graph (3.1).

In this graph, it must be remembered that curves (a) and (b) are exact and curves (c) and (d) are approximate ahd there appears to be a typing error in the value of C for curve(c), which should be 2.4 according to the cited reference.

For axially loaded orthotropic plate in compression the solution of the differential equation proceeds as follows (34):

From the differential equation (3.3), if only axial compression in x direction is applied, we have:-

$$Dx (\partial^4 w/\partial x^4) + 2\left[2Dxy + D1 \right] (\partial^4 w/\partial x^2 \partial y^2) + Dy (\partial^4 w/\partial y^4) = - Nx (\partial^2 w/\partial x^2)$$

Taking the origin of the coordinate x,y as shown below and writing

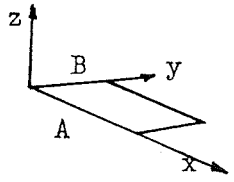

$$AX = x$$

$$BY = y$$

the differential equation (3.3) becomes:

$$1/\beta^4 (\partial^4 w/\partial X^4) + 2\alpha/\beta^2 (\partial^4 w/\partial X^2 \partial Y^2) + \partial^4 w/\partial Y^4 = - B^2/Dy\ (N_x/\beta^2)\ (D_y / D_x)^{0.5} \partial^2 W/\partial X^2$$

where

$$\beta = (A/B)\,(Dy/Dx)^{0.25}, \quad \alpha = (2Dxy + D1)/(Dy\ Dx)^{0.5}$$

Then from the boundary conditions:-

$$W = Mx = 0 \quad \text{at} \quad X = 0,\ 1$$

$$W = My = 0 \quad \text{at} \quad Y = 0,\ 1$$

which can also be written as

$$W = \partial^2 w/\partial X^2 = 0 \quad \text{at} \quad X = 0,\ 1$$

$$W = \partial^2 w/\partial Y^2 = 0 \quad \text{at} \quad Y = 0,\ 1$$

By assuming a deflection shape the function

$$W = C_1 \sin m\pi X \sin n\pi Y$$

which will satisfy the boundary condition listed above and substituting into the differential equation using the derivatives

$$\partial^2 w/\partial X^2 = -C_1 (m\pi)^2 \sin m\pi X \sin n\pi Y$$

$$\partial^4 w/\partial X^4 = C_1 (m\pi)^4 \sin m\pi X \sin n\pi Y$$

$$\partial^4 w/\partial X^2 \partial Y^2 = C_1 (m\pi)^2 (n\pi)^2 \sin m\pi X \sin n\pi Y$$

$$\partial^4 w/\partial Y^4 = C_1 (n\pi)^4 \sin m\pi X \sin n\pi Y$$

we obtain

$$(m\pi)^4/\beta^4 + (2\alpha/\beta^2)(m\pi)^2 (n\pi)^2 + (n\pi)^4 = (m\pi)^2 \left(B^2 Nx/(Dy\,\beta^2)\right)\left(\frac{Dy}{Dx}\right)^{0.5}$$

which leads to

$$Nx = \left[\pi^2 (Dx\ Dy)^{0.5}/B^2\right]\left[(m^2/\beta^2) + 2\alpha n^2 + \beta^2 n^4/m^2\right]$$

As can be seen, the value of Nx is increasing with n and since n is an integer, the smallest value of Nx for each m is when $n = 1$.

To find the value of m which gives the smallest value of Nx:

$$\partial Nx / \partial m = 0$$

becomes

$$(2m/\beta^2) - 2\beta^2/m^3 = 0$$

or $$m^4 = \beta^4$$

so that

$$m_{cr} = \beta$$

$$= (A/B) \left(Dy/Dx \right)^{0.25}$$

Substituting for m in the expression of Nx:

$$N_{cr} = 2\pi^2 (Dx\ Dy)^{0.5}/\beta \left[1 + \alpha \right]$$

where

$$\alpha = (2\ Dxy + D1) / (Dx\ Dy)^{0.5}$$

$$N_{cr} = 2\pi^2 (Dx\ Dy)^{0.5}/B^2 + (2\pi^2/B^2)(2\ Dxy + D1)$$

where N_{cr} is the buckling load per unit width for orthotropic plate.

In general

$$Nx = \pi^2 (Dx\ Dy)^{0.5}/B^2 \left[(m/\beta)^2 + 2\alpha + (\beta/m)^2 \right] \qquad (3.5)$$

This can be transformed to:-

$$B^2 Nx/(\pi^2 (Dx\ Dy)^{0.5}) - 2\alpha = (m/\beta)^2 + (\beta/m)^2$$

or

$$B^2 Nx/(\pi^2 (Dx\ Dy)^{0.5}) - 2(2\ Dxy + D1)/(Dx\ Dy)^{0.5} = (m/\beta + \beta/m)^2 - 2$$

This can be put into the alternative form by writing:

$$K = \left((m/\beta) + (\beta/m) \right)^2 \qquad (3.6)$$

so that

$$K = B^2 Nx/(\pi^2 (Dx\ Dy)^{0.5}) + 2\left[1 - (2Dxy + D1)/(Dx\ Dy)^{0.5}\right]$$

if K in equation (3.6) is plotted for different values of β it will give for each value of m a curve which will intersect the curves for other values of m .

The lower envelope curve will then give Nx for plates of all degrees of orthotropy including, of course, the isotropic plate. Equation (3.5), can be written as:

$$B^2 Nx/(\pi^2 (Dx\ Dy)^{0.5}) - 2\alpha = K'$$

where

$$K' = \left((m/\beta)^2 + (\beta/m)^2 \right)$$

and

$$\alpha = (2\ Dxy + D1) / (Dx\ Dy)^{0.5}$$

or

$$Nx = K'\ \pi^2 (Dx\ Dy)^{0.5}/B^2 + 2\ \pi^2 (Dx\ Dy)^{0.5}\ \alpha /B^2$$

$$Nx = Ko\ (Dx\ Dy)^{0.5}/B^2 + 2\ \pi^2\ Do/B^2 \qquad (3.7)$$

where

$$Do = 2\ Dxy + D1 \quad , \quad Ko = \pi^2 K'$$

equation (3.7) is the formula used in E.S.D.U. Data Sheet Item Number 71015.

3.1.4.3 BUCKLING ANALYSIS OF AN ORTHOTROPIC PLATE USING THE FINITE ELEMENT METHOD.

3.1.4.3.1 Introduction:

In the first part of this section, the analysis using the differential equation for an orthotropic plate was carried out and the formula for finding the buckling stress was found. This formula and the curves which give the buckling stress for different values of the boundary conditions are included in E.S.D.U. Data Sheet Item 71015.

In this section, the finite element method will be used to find the buckling stress for an orthotropic plate and the results will be compared with those obtained from the solution of the differential equation for the purpose of gaining confidence in the method, and evaluating the accuracy of the programme developed specially for this type of plate.

3.1.4.3.2 Finite Element Procedure:

1. The elastic stiffness matrix for the orthotropic plate is represented in CHAPTER 1 and the geometric stiffness matrix is given in Table (2. 7).

2. For each finite element grid used, the elastic and geometric stiffness matrices are assembled according to the standard procedure.

3. Because the direction of the axis of reference for the elastic stiffness matrix was not the same as that for the geometric stiffness matrix, a small subroutine was used in the programme to change the direction of the axis of the elastic stiffness into the direction adopted throughout.

4. As in the case of the isotropic plate the grid numbering system and the boundary condition matrix for each grid were introduced as an input data.

5. The reduced matrices obtained after elimination of the displacement at the boundary are presented to the solving subroutine to find the smallest eigenvalue and the corresponding eigenvector.

6. The computer programme used is listed in Chapter Five and named PROGRAMME (3.2).

3.1.4.3.3 Presentation of the Results of the Study:

1. In Table (3. 4) is shown the accuracy obtained using different finite element grids for the analysis of a particular orthotropic plate which has the following rigidities and geometry:

Dx	= 3779026.3	N.mm	3.779 kNm
Dy	= 3006090.0	N.mm	3.006 kNm
Dxy	= 1019556.0	N.mm	1.019 kNm
D1	= 842391.	N.mm	0.8414 kNm

B = 76.2mm and A/B vary between 0.8 and 2.

For simply supported sides the following finite element meshs were used:

1. Full plate nine elements.
2. Full plate sixteen elements.
3. Full plate thirty-six elements.
4. One quarter of plate thirty-six elements.

Table (3. 4) also includes the solution for the same plate as obtained from E.S.D.U. Data Sheet Number 71015.

2. Table (3.5) gives the finite element and the continuous function theory solutions to the buckling of the same plate but with sides clamped and ends simply supported for a range of $\frac{A}{B}$ from 0.6 to 1.8, using thirty-six elements to represent the full plate.

3. In Table (3. 6), the results of the finite element and continuous function theory buckling analysis for the same plate with all sides clamped for $\frac{A}{B}$ from 0.8 to 1.2 are presented.

TABLE (3.4) - COMPARISON BETWEEN THE BUCKLING STRESS COEFFICIENT FOR SIMPLY SUPPORTED ORTHOTROPIC PLATE AS DETERMINED BY THE FINITE ELEMENT METHOD AND FROM THE SOLUTION OF THE DIFFERENTIAL EQUATION.

	FULL PLATE: 9 ELEMENTS.		16 ELEMENTS.		36 ELEMENTS.		ONE QUARTER: 36 ELEMENTS.		E.S.D.U. ITEM 71015 FIGURE 1	
A/B	Ko	m	Ko	m	Ko	m	Ko	m	Ko	m
.8	26.18	1	26.18	1	24.51	1	23.46	1	22.13	1
1.	22.94	1	22.94	1	21.34	1	20.34	1	20.12	1
1.2	23.44	1	23.44	1	21.82	1	20.81	1	21.13	1
1.6	24.03	2	23.77	2	23.42	2	23.18	2	20.83	2
2.	19.00	2	19.60	2	19.83	2	19.95	2	20.12	2

TABLE (3.5) - BUCKLING STRESS COEFFICIENT FOR ORTHOTROPIC PLATE WITH SIDES CLAMPED AND ENDS SIMPLY SUPPORTED.

A/B	FINITE ELEMENT (6 x 6)	THEORY E.S.D.U. 71015
.60	50.00	48.00
.80	49.00	46.00
1.00	56.00	54.00
1.40	44.00	45.00
1.80	43.00	46.00

TABLE (3.6) - BUCKLING STRESS COEFFICIENT FOR CLAMPED ORTHOTROPIC PLATE.

A/B	FINITE ELEMENT (6 x 6)	THEORY E.S.D.U. 71015
.8	94.	90.
1.	79.	76.
1.2	76.	74.

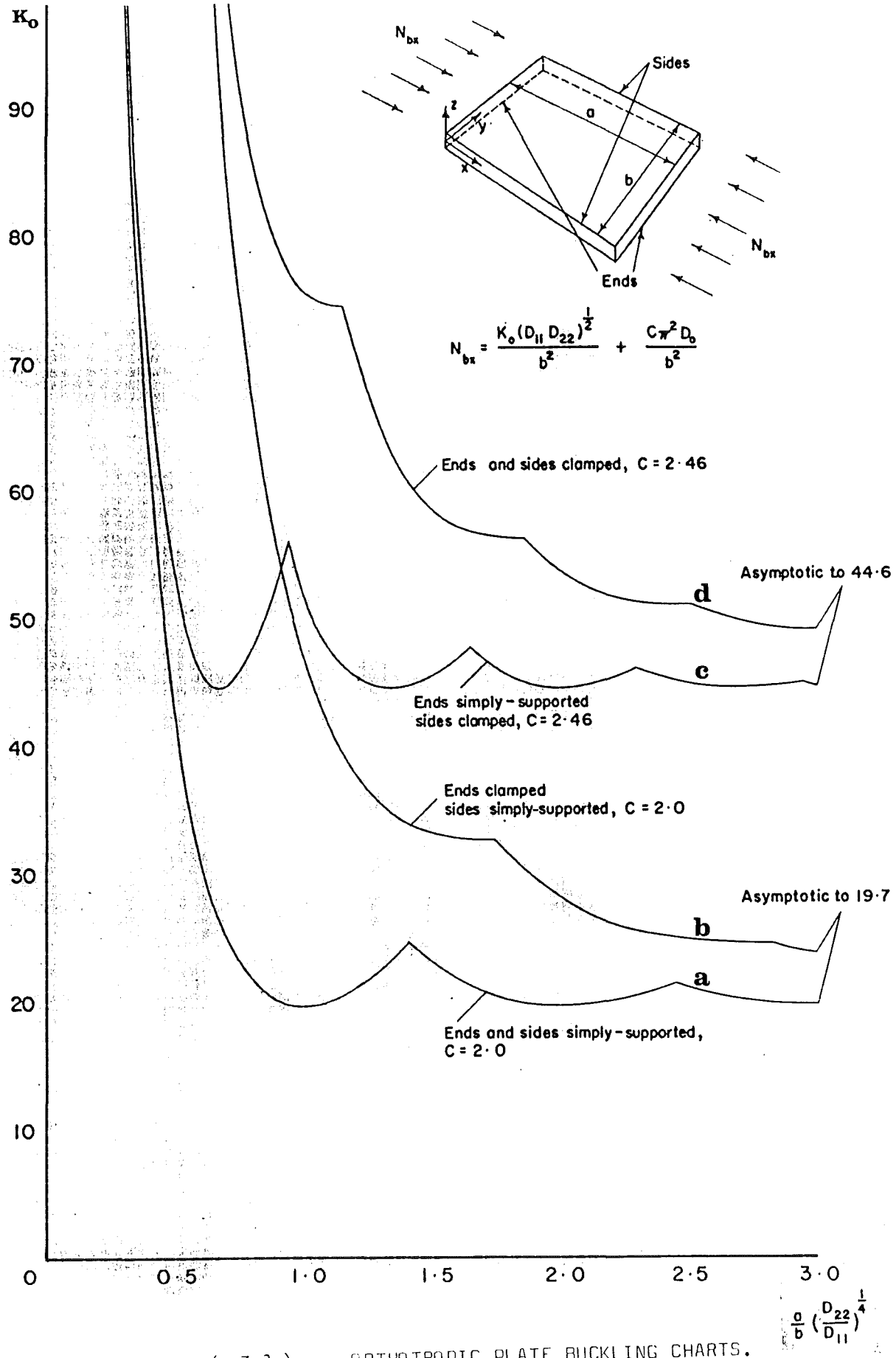

GRAPH (3.1) - ORTHOTROPIC PLATE BUCKLING CHARTS.

E.S.D.U. DATA ITEM (71015).

3.1.4.3.4 Rsults and Conclusions.

1. The results of the buckling analysis of an orthotropic plate using the finite element method showed good agreement with the E.S.D.U. theory for the boundary conditions considered.

2. The computer time for the orthotropic plate buckling analysis was found to be very much the same as that for isotropic plate with an equivalent finite grid.

3. The finite element also predicted the same critical shape as that described by the continuous function theory.

4. Next, the orthotropic plate programme will be used for the determination of the overall buckling stress for stiffened panels using appropriate expressions for the rigidities Dx, Dy, Dxy and D_1.

3.1.5. Overall Buckling of Stiffened Panels.

3.1.5.1. Introduction:

A stiffened panel is an example of a composite action type of construction employed particularly in the construction of high performance airplanes.

The use of such panels in thin wings is found to be very advantageous where the cover performs the contouring functions as well as the load carrying function.

It consists of a plate divided by a series of longitudinal stringers, these stringers serve to carry part of the axial load, increase the flexural stiffness, and to divide the plate forming the skin into a series of narrow strips each having a relatively low value of the width to thickness ratio.

These can be manufactured by milling from the solid slab (integrally stiffened) or by fabrication from sheet and stiffener sections. The minimum weight design of such panels has received much attention in the past (35), (36), and the optimum geometry, which is based on simultaneous buckling modes has been found to be characterised by rather sturdy stiffeners.

In this Section, the overall buckling of stiffened panels will be studied using standard finite element methods.

The two methods to be considered are based on:-

1. The stiffened panel considered as an orthotropic panel.

2. The stiffened panel considered as formed by beams and isotropic plates acting together.

Both methods have received attention in the past, but here a comparative study is attempted and light will be thrown on the problems related to the application of these methods. For this purpose, the results for some integrally stiffened panels which

/which were tested in compression and elastically buckled in the flexural mode, are used.

The experimental results which are listed in Table (3.13) together with material and geometric configurations are obtained from (37) and from (38).

It is to be noted that in addition to the standard finite element approaches mentioned above, there are another three methods based on finite strip approach which can be used for initial buckling of stiffened panels and these are:

1. The exact finite strip in which the panel is idealised into a series of finite strips (39).

2. The approximate finite strip where the panel can be idealised into a finite strips and finite beams (40).

3. The finite strip for local buckling analysis (41).

These methods will be summarised in the second part of this Chapter.

3.1.5.2. The Stiffened Panel as an Orthotropic plate:

If there are a relatively large number of stiffeners, the method of analysis which was described in the previous Section and applied to an orthotropic plate can be used for the analysis of stiffened panels provided the rigidity constants which occur in the theory of orthotropic plates are properly derived from the material properties and geometry of the stiffened panel.

Although accurate expressions of the rigidity constants can only be obtained by experimental procedures, the analytical expressions given below show a very good agreement with those determined experimentally (42).

(a) Expression for D_x:

D_x is the flexural stiffness of the stiffened plate/

/plate per unit width in x direction and given as

$$D_x = (EI_x)/B_s$$

where E is the Young's Modulus in compression of the material.

I_x is the second moment of area of plate-stiffener combination.

B_s is the stiffener spacing.

If we assume that the neutral axis of the cross-section lies at distance z from the middle plane of the skin, the above relation can be written as:

$$D_x = (E I_{xp} + EI_{xs})/B_s$$

where I_{xp} is the moment of inertia of the skin about the neutral axis and I_{xs} is the moment of inertia of the stiffener about the neutral axis and this can be written as:

$$D_x = (E B_s T_s^3 /12 (1 - \nu^2) + E B_s T_s z^2/(1 - \nu^2) + E I_{xs}) /B_s$$

When the stiffener has a simple rectangular cross-section this expression becomes:-

$$D_x = D + E T_s z^2/(1 - \nu^2) + (E (T_w B_w^3/12) + E T_w B_w \left(\frac{T_s + B_w}{2} - z\right)^2)/ B_s$$

In the above formula the full width of plate between stiffeners was considered as resisting the bending of the panel.

(b) Expression for D_y:

If the stiffened panel has also a series of stiffeners in the trnasverse direction, then a formula similar to that above can be used.

If stiffeners lie only in the longitudinal direction x it is reasonable to assume that the flexural stiffness in y direction is equal to:

$$D_y = D$$

(c) Expression for D_{xy}:

The twisting rigidity D_{xy} for the stiffened panel is given as

$$D_{xy} = D_{xy_s} + (GJ)/B_s$$

where D_{xy_s} is the twisting rigidity of the plate skin and given by $G\ T_s^3/3$ and GJ is the torsional stiffness of the stringers and equal to $G\ B_w\ T_w^3/3$ and for the stiffened panel we can write:

$$D_{xy} = G\ T_s^3/3 + G\ B_w\ T_w^3/3\ B_s$$

(d) Expression for D_1:

In Reference (43) D_1 was assumed zero. To assess the effect of D_1 on the buckling stress the simply supported orthotropic plate considered in the previous Section, was analysed for different values of D_1 and it was found that a variation of D_1 equal to 50% produced only a very small variation in the critical buckling stress obtained. See Table (3.7).

However, for the investigation which follows, D_1 will be taken to be νD.

This seems to be a reasonable assumption since for an isotropic plate D_1 is equal to νD.

TABLE (3.7) - THE EFFECT OF THE VARIATION OF D_1 ON THE BUCKLING STRESS FOR ORTHOTROPIC PLATE.

n	$\frac{D_1 + n \frac{D_1}{10}}{D_1}$	$\frac{N_{crf}}{N_{cri}}$
- 5	0.5	0.93
- 4	0.6	0.95
- 3	0.7	0.96
- 2	0.8	0.97
- 1	0.9	0.99
0	1.0	1.0
1	1.1	1.01
2	1.2	1.03
3	1.3	1.04
4	1.4	1.05
5	1.5	1.07

(e) Finite Element Procedure:

1. The elastic and geometric stiffness matrices used are given in section 1.3.6.6. and section 2.8.1.6. .

2. The computer programme which was used for the study of orthotropic plate is used except that here, instead of giving the rigidities as constant numbers on the input card, the expressions given above are introduced into the programme.

3. The finite element mesh is that given in Figure (3.5) except that the boundary value matrix is now representative of a panel free on both sides but clamped at the ends.

4. The clamped ends is interpreted by considering the out-of-plane displacements and rotations for all the nodes on the ends to be zero.

(f) Presentation of the Results of the Study.

1. For each of the panels considered, the buckling stress co-efficient k is given for different values of B_{se}, which is the part of skin considered in the computation of the flexural rigidities, in Table (3.8).

2. Table (3.8) includes the values of k which correspond to the experimental determined stresses and also those obtained from the strut formula.

3. The buckling stress co-efficient for the panels determined by using the strut formula were those obtained by considering $B_{se} = B_s$ where B_s is the stiffeners spacing.

(g) Results and Conclusions:

1. For the smaller values of B_{se} the buckling load rises sharply as B_{se} increases but for higher values of B_{se} the rate of increase of the buckling stress becomes less marked.

2. The orthotropic plate idealisation can be used for the buckling analysis of panels which have four or more stiffeners if the appropriate value for B_{se} is used.

3. This value of B_{se} can be obtained by analysing the results of tests on geometrically similar structures in which the geometric parameters are varied one at a time.

4. From this very limited study it seems that when B_w/B_s is small a larger part of the skin is involved in resisting buckling. (Panel C).

5. Computation time (75.203 secs.)

6. The solution obtained by the strut formula is in agreement only with Panel B, while it over estimates by a great deal the buckling stress for Panels A and C.

7. If the same value of B_{se} is used for both the strut formula and the finite element approach, similar results will be obtained.

TABLE (3.8) - THEORETICAL AND EXPERIMENTAL BUCKLING STRESS COEFFICIENTS FOR STIFFENED PANELS.

(ORTHOTROPIC ANALOGY)

PANEL	$\frac{T_w}{T_s}$	$\frac{B_w}{B_s}$	$\frac{B_s}{T_s}$	B_{se} (FINITE ELEMENT)					TEST RESULTS	STRUT FORMULA WITH $B_{se} = B_s$
				$2.5T_s$	$5.0T_s$	$7.5T_s$	$10.0T_s$	$12.5T_s$		
A	1.6	0.78	13.5	8.2	10.25	11.86	13.13	14.5	6.96	13.76
B	1.32	0.49	24.0	12.3	15.46	17.9	19.6	21.16	20.93	24.58
C	0.79	0.314	23.5	28.5	36.3	41.03	42.4	46.8	36.77	54.73

$$K = N_{cr} B^2/(\pi^2 D)$$

$$D = E \bar{T}^3/(12\,(1 - \nu^2))$$

STRUT FORMULA: $\sigma_{cr} = 4\,\frac{\pi^2 E\, I}{A\, L^2}$

3.1.5.3. Overall Buckling Stress for Stiffened Panel Using Beam-Plate Idealisation:

In the previous section, three panels for which the experimental buckling stresses are known were studied using the orthotropic analogy, the buckling stress co-efficient being found for different values of B_{se}.

In this section, the same panels will be studied using a finite element mesh which is formed by beams and plates.

(a) Finite Element Idealisation:

1. The panel is idealised into a mesh of plate bending elements and with the stringers represented by T cross-section beams. The beam and the adjacent plates assumed to have the same neutral axis.

Although different types of elements are used, the assembly procedure is the same as that used in the previous section, because both elements have the same number of degrees of freedom per node.

2. The elastic and geometric stiffness matrices for the plate elements are given in Table (1.11) and (2. 7).

3. The elastic and geometric stiffness matrices for the beam elements are given in Table (3. 9) and (3.10) and as can be seen from those Tables, only three nodal displacement components are considered at each node, namely one translational displacement in the direction normal to the plane of the panel and two rotations about the x and y axes respectively.

4. Figure (3. 6) shows two plate elements and a beam element which join at one node.

5. It is worth noting that by using this type of beam to represent the stringers, the stringer will deform only in the zx plane, and the only stiffness involved is the flexural/

/flexural stiffness about the y axis.

6. Computer programme PROGRAMME (3.3) was used, and the computation was carried out for a simply supported plate with only one stringer and for the three clamped panels considered in the previous section.

As in the previous section, the object was to find for each panel, the width of the effective flange of the beam representing the stringers necessary to produce the same buckling stress as that found experimentally.

(b) Presentation of the Study:

1. For the simply supported plate with central stringer studied the results using the finite element method and the results using the analysis of Timoshenko (28) are given in Table (3.11) and here also the buckling stress co-efficient is used. In both theoretical and finite element analysis the same effective flange width is used.

2. For panels A, B and C the geometric non-dimensional parameters and the effective flange width and the buckling stress co-efficient are given in Table (3.12).

(c) Results and Conclusions:

1. The result of the analysis of the simply supported plate with only one stiffener, using four plate elements and two beam elements, agrees with the solution obtained in Reference (28) using the energy approach.

This suggests that the idealisation should prove to be satisfactory for panels with a small number of stiffeners.

2. The results obtained by applying this method agree with those obtained by the orthotropic analogy for Panels A, B .

3. Since some Authors suggest the use of an effective flange a width equal to just the thickness of the panel, while others suggest values between 20 and 40 times the thickness, an answer may be found by applying this procedure to more experimental panels.

4. The effective flange widths for the beams used in this method does not differ from those found using the orthotropic panel theory. This was to be expected since in both cases the expression of the flexural stiffness, which is the determining factor for the buckling of an axially loaded panel (EI_x), is the same.

5. Computer time in this method is higher, for example, to find the buckling stress for Panel A required 314.841 sec. which is about four times the time needed using the orthotropic analogy.

a					
o	o		SYM.		
- b	o	c			
- a	o	b	a		
o	o	o	o	o	
- b	o	d	b	o	c

where

$a = 12 E I_y / (L^3 (1 + S_z))$

$b = 6 E I_y / (L^2 (1 + S_z))$

$c = (4 + S_z) E I_y / (L (1 + S_z))$

$d = (2 - S_z) E I_y / (L (1 + S_z))$

$S_z = 12 E I_y / (G A_s L^2)$

I_y is moment of inertia about y axis.

TABLE (3.9)- Elastic stiffness for beam element.

a					
o	o		SYM.		
- b	o	c			
- a	o	b	a		
o	o	o	o	o	
- b	o	- d	b	o	c

where

$a = 36\ F_x/(30L)$

$b = 3\ F_x L/(30L)$

$c = 4\ F_x L^2/(30L)$

$d = F_x L^2/(30L)$

TABLE (3.10)- Geometric Stiffness Matrix
For Beam Element .

TABLE (3.11) - SIMPLY SUPPORTED PLATE WITH CENTRAL STRINGER, FINITE ELEMENTS AND ENERGY APPROACH BUCKLING STRESS CO-EFFICIENTS:

((B = 80 mm, T_s = 0.5, T_w = 0.5, B_w = 5 mm, B_{se} = 20 mm)).

$A/_B$	K FINITE ELEMENT	K Ref. (28)
1.0	22.46	23.85
1.2	17.23	20.26
1.4	13.91	16.12
1.6	11.88	13.61
1.8	10.63	11.88
2.0	9.61	10.74

TABLE (3. 12) - THEORETICAL AND EXPERIMENTAL BUCKLING STRESS COEFFICIENTS FOR STIFFENED PANELS.

(BEAM-PLATE IDEALISATION)

PANEL	$\frac{T_w}{T_s}$	$\frac{B_w}{B_s}$	$\frac{B_s}{T_s}$	B_{se}						TEST RESULTS	STRUT FORMULA $B_{se} = B_s$
				o	$2.5T_s$	$5.0T_s$	$7.5T_s$	$10.0T_s$	$12.5T_s$		
A	1.6	0.78	13.5	5.63	8.08	9.91	10.6	12.32	13.13	6.96	13.76
B	1.32	0.49	24.0	7.37	9.62	13.46	18.32	21.34	24.05	20.93	24.58
C	0.79	0.314	23.5	11.96	24.60	34.4	43.13	51.17	56.85	36.77	54.73

$K = N_{cr} B^2 / (\pi^2 D)$

$D = E \bar{T}^3 / (12 (1 - \nu^2))$

STRUT FORMULA : $\sigma = 4 \frac{\pi^2 E I}{A L^2}$

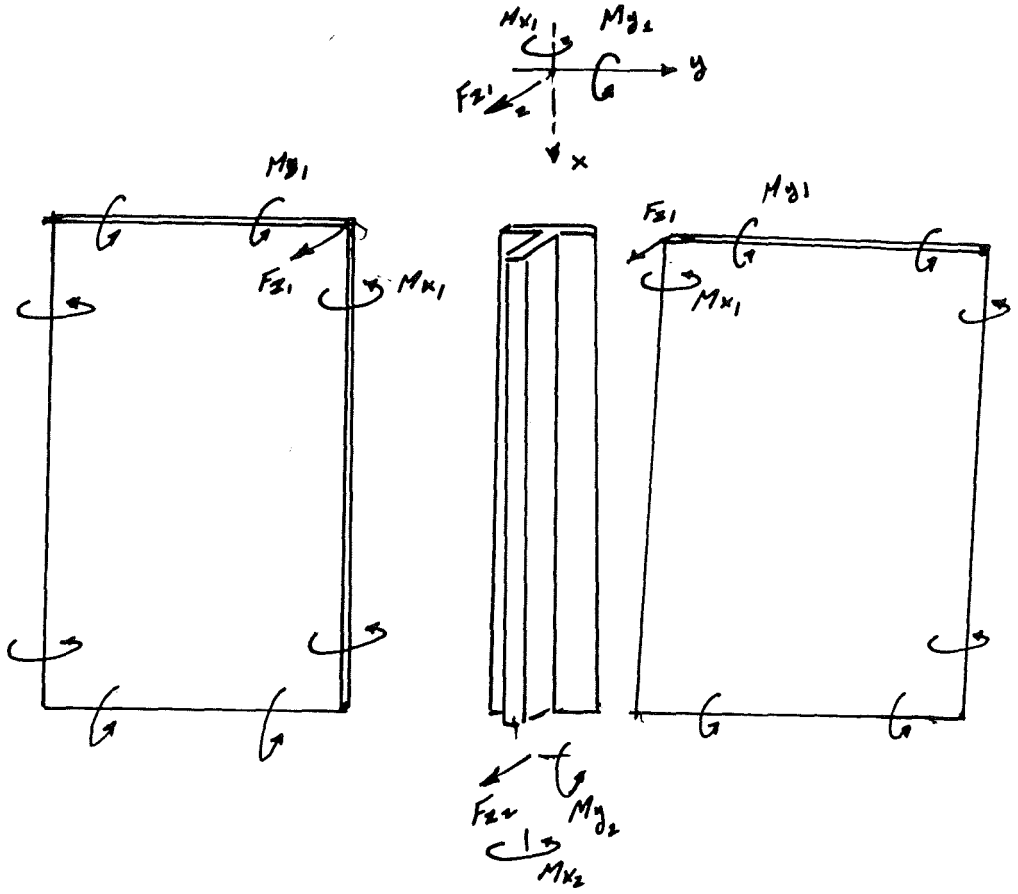

FIGURE (3.6) - BEAM-PLATE IDEALISATION OF STIFFENED PANEL.

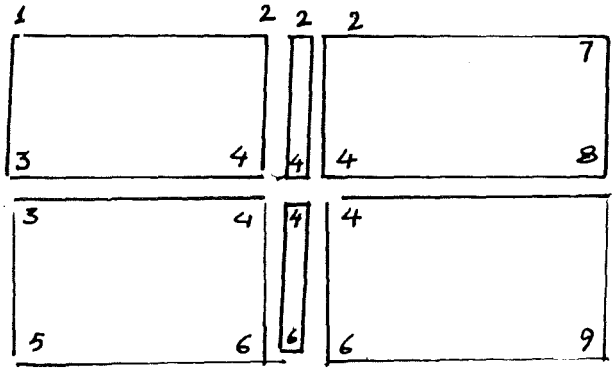

FIGURE (3.7) - PLATE WITH CENTRAL STRINGER FINITE ELEMENT IDEALISATION.

TABLE (3. 13) - GEOMETRY, MATERIAL CHARACTERISTICS AND EXPERIMENTALLY DETERMINED BUCKLING STRESSES FOR THE THREE SPECIMENS.

	A	B	C
MATERIAL	D T D 5050 ref.(37)	D T D 687 ref.(38)	D T D 687 ref.(38)
$E \left(\frac{N}{mm^2}\right)$	71791.0	72100. *	73700. *
$\sigma_{.1\%}$	414.0	518.0 *	511.0 *
σ_u	490.0	592.0 *	592.0 *
L (mm)	1140.0	629.0	241.0
B	390.0	211.0	178.0
B_w	53.0	26.0	14.0
B_s	68.0	52.0	44.0
T_w	8.0	2.92	1.5
T_s	5.0	2.2	1.9
$\bar{T}$	11.2	3.66	2.37
B_w/B_s	0.78	0.49	0.314
T_w/T_s	1.6	1.32	0.79
B_w/T_s	10.6	11.8	7.29
B_s/T_s	13.5	24.08	23.5
AREA	4494.0	858.0	421.9
$n_{stif.}$	6.0	4.0	4.0
σ_{EXP}	366.0	410.0	375.0
$\pi^2 D$	91066934.0	3191649.0	765633.0
$K = \frac{N_{cr} B^2}{D \pi^2}$	6.8	20.93	36.77

* ARE QUANTITIES DETERMINED FROM TESTS ON THE MATERIAL. $D = \frac{E \bar{T}^3}{12 (1-\nu^2)}$

PART 2.

3.2. Introduction.

In this part, another aspect of instability of structure will be examined, in particular, the local buckling of plate type structure and a method of improving the buckling behaviour of thin walled structures will be introduced.

Because of the importance of the revolutionary new field of finite element known as finite strip, a brief study of three different methods based on the finite strip idealisation is included and these are:

1. The exact finite strip (Wittrick)
2. The approximate finite strip (Cheung)
3. The finite strip for local instability (Przemieniecki)

Although the three methods share many common features and can be considered to belong to one family, the underlying theory involved in the development and the assumptions used are very much different as will be seen.

The first method is based on large deformation theory and the de-stabilising effect of the in-plane stresses is considered.

As a result, all modes of buckling regardless of the critical wave length can be singled out in the results of the analysis.

In the second small deflection theory is used and an approximate deflection pattern is assumed,in the longitudinal direction the deflection shape is approximate by a Fourier series and in the transverse direction a polynomial is assumed and only overall buckling is computed.

The third method which is also based on small deflection theory is particularly devised for use in study of the class of problems which fail by local instability and for this reason much use is made of it in this part.

These method have the advantages of:

1. Great saving in computer time.

2. Less storage space because of the very narrow band width.

3. A relatively large range of application, since many structures have geometric and matrial properties which do not vary along one direction.

4. Less input data because of the lower number of nodes involved.

3.2.1. The Exact Finite Strip (Wittrick).

This method was first presented by W.H. Wittrick in 1968 (39).

The method can be applied to the buckling and vibration of panels which consist of a series of thin flat plates connected together along their longitudinal edges.

The structure is idealised into long rectangular finite strips joined edge to edge at each common edge, which is considered as a nodal line. Four components of displacement are considered, one rotational and three translational.

One moment and three forces are associated with these displacements.

At buckling, both the forces and the displacements vary sinusoidally.

A finite strip on which forces and displacements are shown is presented in Figure (3.8).

The following assumptions are used:-

1. Thin plate theory.

2. Whatever the mode of buckling, the structure buckles sinusoidally in the longitudinal direction.

3. The structure is subjected to a system of basic stresses which are uniform in the longitudinal direction.

4. End cross-section are free to warp.

The edge generalised forces are related to the edge generalised displacements through a stiffness matrix which is formed of two uncoupled submatrices.

The first is the out-of-plane submatrix whose elements are derived by considering the differential equation for a plate in bending under the action of out-of-plane generalised forces with the ends simply supported.

The second is the in-plane stiffness submatrix in which the destabilising effect of the basic stress distribution is taken into account, the nonlinear theory of elasticity being used to set up the large displacement differential equation for a plate axially loaded in its own plane.

Then, after the stiffness of all the strips have been derived, these are assembled to produce the stiffness matrix of the whole structure.

From the equilibrium equations at all line junctions a set of homogeneous simultaneous equations is obtained.

The stability criterion is that the determinant of all coefficients of this system becomes zero.

The elements of the stability determinant are transcendental functions of the critical buckling stress σ and the critical wave length λ. For any assumed value of λ there are an infinite number of values of σ for which the stability determinant becomes zero.

To converge in a short computer time to the exact solution within prescribed errors an iteration procedure is employed (44).

Comments:

1. This method can be used as a tool for the study of the interaction problem of different modes of buckling of plate type structure.
2. The fact that this method needs a special solving subroutine limit its use as compared to other methods which use a standard eigenvalue/eigenvector procedure.
3. In Ref. (45), the theoretical solution is compared with experimental results for a panel and shows very close agreement.
4. Using this method, it is found (46), that the conventional approach to local stability is accurate if the number of stiffeners is more than three, and the use of strut formula for overall buckling analysis of stiffened panels is acceptable for the range of $8 \leq \frac{\lambda}{B_s} \leq 32$.
5. Because in this method, fewer constraints are imposed on the mode of deformation at buckling, it will accurately identify the true lowest buckling load which makes it of great practical value to the structural engineer.
6. The derivation of elastic matrix is more difficult than in the standard finite element, and the elements are complicated transcendental functions of the critical wave length and the compressive stress.

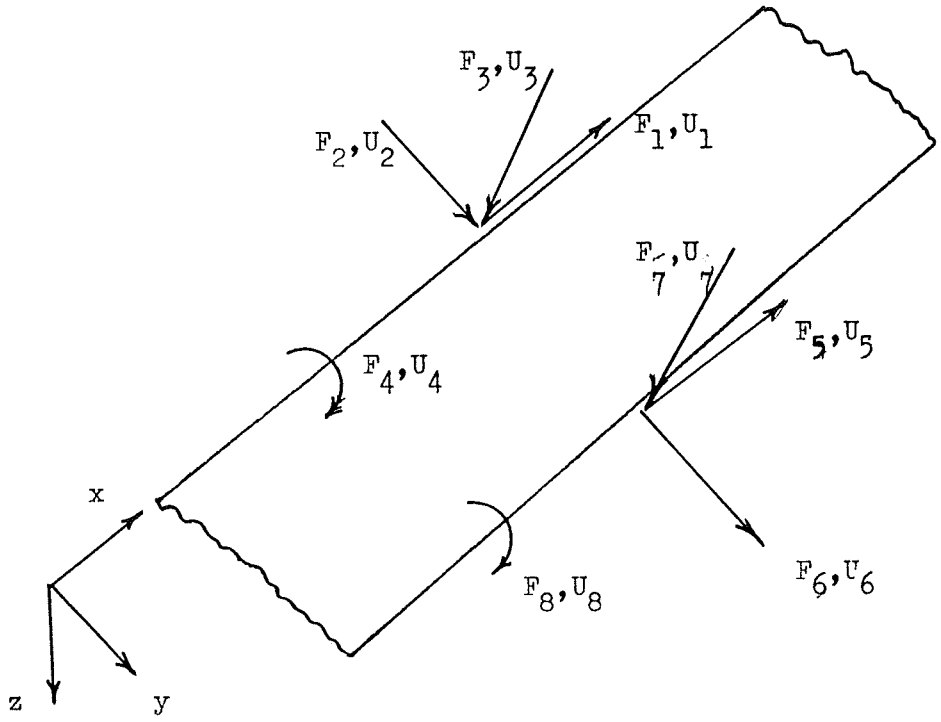

Each pair of F_i and U_i has to be multiplied by $e^{i\pi x/\lambda}$.

FIGURE (3.8) - GENERALISED FORCE AND DISPLACEMENTS FOR EXACT FINITE STRIP.

3.2.2. Finite Strip Method as Developed by Cheung.

This method was first presented by Y.K. Cheung in 1968 (47), and a full treatment can be found in (40). It can be used for linear analysis as well as for vibration and buckling.

For the representation of deflected shape this method uses a displacement function formed by the product of a polynomial and a series having the form:-

$$w = \sum_{n=1}^{r} f_n(y) \sin \frac{n \pi x}{A}$$

where A is the length of the strip.

The series is differentiable and satisfies the boundary condition in the longitudinal direction at the ends besides representing the deflected shape in that direction.

The polynomial represents the deflected shape in the transverse direction and, as in the standard finite element method, it must satisfy the requirement of completeness, and also the requirement that the strains derived using this displacement function must remain finite at the interface between two adjacent strips.

For buckling analysis, it follows the same procedure used for the standard finite element method.

1. Using the assumed displacement function and after deciding on the number of terms in the series, the elastic and geometric stiffness matrices are derived.

2. The overall stiffness matrices are assembled from the contributions of all the strips.

3. The assembled matrices are then reduced according to the boundary conditions.

4. Finally, using a standard eigenvalue-eigenvector sub-routine the buckling load is found.

Comments:

1. This method needs more storage space and more computation time than the exact finite strip since accuracy is obtained by using more elements and more terms of the series.
2. For the analysis of stiffened panels using this method, a combination of beams and plates was used, an assumed flange width being adopted for the beam.
3. A search of the literature has not revealed any experimental verification of the results of the finite strip buckling analysis.
4. The method uses a standard eigenvalue-eigenvector subroutine, so that the solution procedure is easier to programme than that of the previous method.
5. The buckling load found corresponds to overall buckling and the method does not apply to problems in which the critical wave length is small.
6. Improvement in the performance was obtained (48),
   a. By using high order polynomials so that compatability of moments and shears was assured.
   b. By using internal nodes in the strip.

   But in each case, at the expense of storage space.

3.2.3 FINITE STRIP FOR LOCAL STABILITY

(a) Introduction:

In the previous sections, two finite strip methods were briefly introduced, the exact finite strip method which is based on the nonlinear theory of elasticity and which can be used for general buckling analysis as well as in vibration analysis and the approximate finite strip which is applicable to linear analysis, overall buckling,and vibration. It was found that these methods share the property of great saving in computer time and cost relative to the standard finite element procedure.

Another finite strip method of interest, which is primarily designed to deal with problems of local buckling of thin walled structures, is the finite strip for local stability method which was presented by J.S. Przemieniecki (41) in 1973.

By us ing the same assumptions of Chilver (49) 1953, which were discussed by H.L. Cox (50), he used the finite strip elastic and geometric stiffnesses in a standard eigenvalue/eigenvector procedure to find the buckling load which corresponds to the local buckling mode. The results showed good agreement with the material presented in E.S.D.U. Data Sheet 01.02.82.

Assumptions:

1. Edge lines at junctions between flat plate components remain fixed in space.

2. Component flat plates rotate about these edge lines.

3. Angles between elements of junctions before and after buckling remain the same.

4. Effect of side constraint is neglected.

5. Ends of structure are constrained to remain straight.

(b) Elastic Stiffness Matrix.

For the analysis, the structure is divided into a series of finite strips, each of length equivalent to half wave length L as shown in Figure (3.9). A single strip with the relevant nodal displacements is represented in Figure (3.10).

The deflected shape for each strip is assumed to be given by:

$$w = f(Y) \sin(\pi x/L),$$
$$Y = y/b$$

where a cubic polynomial is used to represent the deflection in the transverse direction and the trigonometric term is to describe deflection in the longitudinal direction.

The deflected shape as a function of the nodal displacement will be

$$w = \mathbf{N}_z \mathbf{U}$$

$$w = \left[(1 - 3Y^2 + 2Y^3)\ (Y - 2Y^2 + Y^3)b\ (2Y^2 - 2Y^3)\ (-Y^2 + Y^3)b\right] s\ \mathbf{U}$$

where

$$s = \sin(\pi x/L) \quad \text{and} \quad \mathbf{U} = \begin{bmatrix} U_1 \\ U_2 \\ U_3 \\ U_4 \end{bmatrix}.$$

Then from the expression for strain for a plate in bending

$$\epsilon = \begin{bmatrix} \epsilon_x \\ \epsilon_y \\ \gamma_{xy} \end{bmatrix} = \begin{bmatrix} -z\dfrac{\partial^2 w}{\partial x^2} \\ -z\dfrac{\partial^2 w}{\partial y^2} \\ -2z\dfrac{\partial^2 w}{\partial x \partial y} \end{bmatrix} = z \begin{bmatrix} \pi^2/L^2 & \mathbf{N}_z & \sin(\pi x/L) \\ -(1/b^2) & \mathbf{N}_z'' & \sin(\pi x/L) \\ -(2\pi/bL) & \mathbf{N}_z' & \cos(\pi x/L) \end{bmatrix} \mathbf{U}$$

where primes indicate differentiation relative to y, or in matrix form,

$$\epsilon = \mathbf{b}\ \mathbf{U}$$

From Chapter 2

$$\mathbf{k_e} = \int_V \mathbf{b}^T \mathbf{E}\ \mathbf{b}\ dV$$

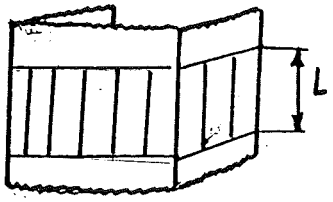

FIGURE (3.9) - FINITE STRIP FOR LOCAL STABILITY IDEALISATION.

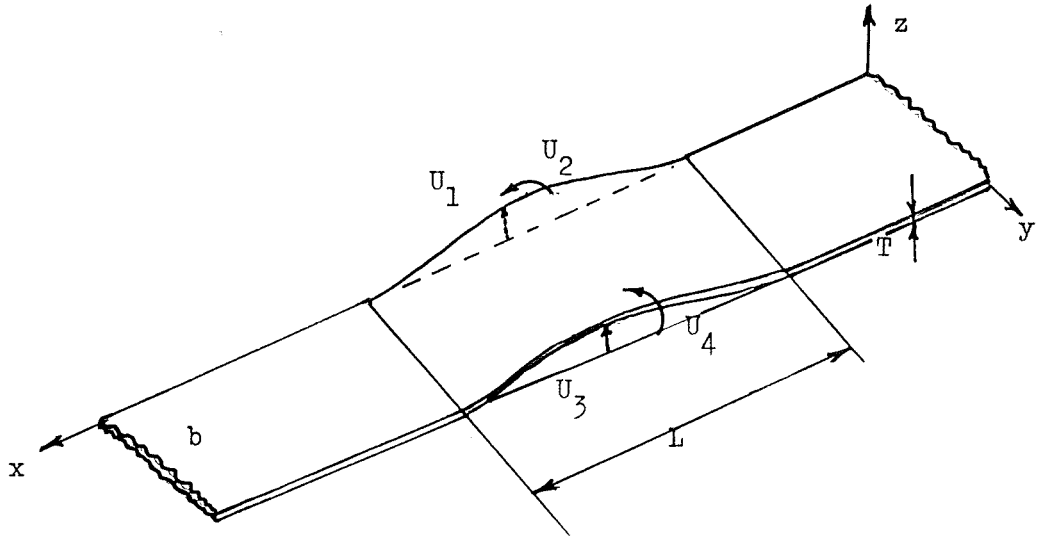

FIGURE (3.10) - SINGLE FINITE STRIP WITH NODAL DISPLACEMENT.

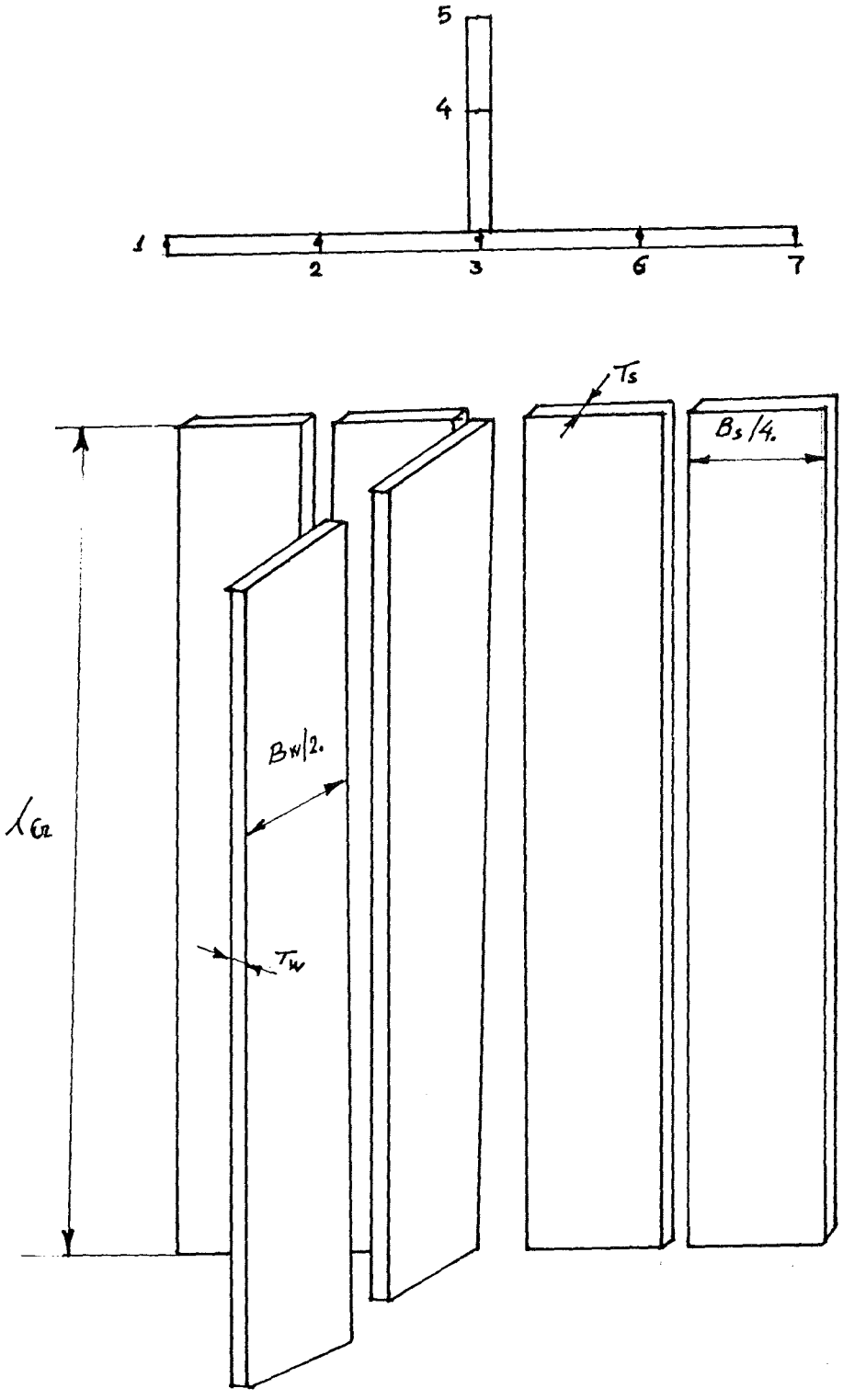

FIGURE (3.11) - FINITE ELEMENT IDEALISATION.

where

$$E = \frac{E}{(1-\nu^2)} \begin{bmatrix} 1 & \nu & 0 \\ \nu & 1 & 0 \\ 0 & 0 & (1-\nu)/2 \end{bmatrix}$$

Integrating, the elastic stiffness matrix dependent on half wave length will be .

$$\mathbf{k_e} = K_{E1} + K_{E2} + K_{E3}$$

where K_{E1}, K_{E2} and K_{E3} are given in Table (3.14).

3. The Geometric Stiffness Matrix.

The geometric stiffness matrix for the finite atrip can be derived following the same procedure used in the prevous Chapter and assuming a middle plane constant stress σ_x acting in the x direction and no shearing stress at the middle plane. The geometric stiffness matrix will then be given by:

$$= \sigma_x \int_0^L \int_0^b \int_{-T/2}^{T/2} \mathbf{N}'^{T}_{z..} \mathbf{N}'_{z..} \, dx \, dy \, dz ,$$

where

$$\mathbf{N}'_z = (\partial/\partial x) \mathbf{N}(Y) \sin\left(\frac{\pi x}{L}\right) = (\pi/L) \mathbf{N}(Y) \cos\left(\frac{\pi x}{L}\right)$$

Substituting and integrating leads to the geometric stiffness matrix given in Table (3.15).

(d) Buckling Mode Determination:

Once the elastic stiffness matrix and the geometric stiffness matrix has been found for all single strips forming the structure, the elastic and the geometric stiffness matrices for the complete structure are assembled and the free body degrees of freedom are eliminated.

$$\mathbf{k_e} = K_{E1} + K_{E2} + K_{E3}$$

where

$$K_{E1} = \frac{\pi^4 Ebt^3}{10080(1-\nu^2)L^3}\begin{bmatrix} 156 & & & \\ 22b & 4b^2 & \text{Sym.} & \\ 54 & 13b & 156 & \\ -13b & -3b^2 & -22b & 4b^2 \end{bmatrix}$$

$$K_{E2} = \frac{\pi^2 Et^3}{360(1-\nu^2)bL}\begin{bmatrix} 36 & & & \\ (3+15\nu)b & 4b^2 & \text{Sym.} & \\ -36 & -3b & 36 & \\ 3b & -b^2 & -(3+15\nu)b & 4b^2 \end{bmatrix}$$

$$K_{E3} = \frac{ELt^3}{24(1-\nu^2)b^3}\begin{bmatrix} 12 & & & \\ 6b & 4b^2 & \text{Sym.} & \\ -12 & -6b & 12 & \\ 6b & 2b^2 & -6b & 4b^2 \end{bmatrix}$$

where

L is the length of the buckling wave length

b is the width of strip

TABLE (3.14) - ELASTIC STIFFNESS MATRIX FOR FINITE STRIP.(41)

$$\frac{\sigma_x \pi^2 bt}{840\ L}\begin{bmatrix} 156 & & & \\ 22b & 4b^2 & \text{Sym.} & \\ 54 & 13b & 156 & \\ -13b & -3b^2 & -22b & 4b^2 \end{bmatrix}$$

TABLE (3.15) - GEOMETRIC STIFFNESS MATRIX FOR FINITE STRIP.

The equilibrium equation for the complete structure will be

$$(\mathbf{K_e} + \mathbf{K_g})\ \mathbf{U} = \mathbf{P}$$

Introducing the constant λ so that

$$\mathbf{P} = \lambda \mathbf{P}^*$$

and the geometric stiffness matrix becomes

$$\mathbf{K_g} = \lambda \mathbf{K_g}^*$$

where $\mathbf{K_g}^*$ is the geometric stiffness matrix for unit value of λ .

$$(\mathbf{K_e} + \lambda \mathbf{K_g}^*)\ \mathbf{U} = \lambda \mathbf{P}^*$$

and

$$\mathbf{U} = (\mathbf{K_e} + \lambda \mathbf{K_g}^*)^{-1} \lambda \mathbf{P}^*$$

which means that the displacement tends to infinity when

$$\left| \mathbf{K_e} + \lambda \mathbf{K_g}^* \right| = \mathbf{0}$$

$\left| \mathbf{K_e} + \lambda \mathbf{K_g}^* \right|$ is the stability determinant, a nd the smallest value of its roots will be the buckling load for the structure.

Alternatively, as in previous analysis, the eigenvalue and eigenvectors of this system

$$(\mathbf{K_e} + \lambda \mathbf{K_g}^*)\ \mathbf{U} = \mathbf{O}$$

will be found and the smallest eigenvalue will be the buckling load and associated eigenvector will define the buckling shape.

Since the buckling wave length is unknown, the following procedure is used to find the buckling stress and mode.

(e) Solution Procedures.

1. First Procedure.

The graphical procedure suggested in (41) has the disadvantage of not being suitable for continuous computer use,

/use, and an alternative procedure has been found to be more efficient.

This procedure has the following outline:

From a preliminary study it was found that the relation between buckling stresses and associated half wave lengths is of a parabolic form.

For a particular structure, the minimum point of this parabola represent the buckling stress and the critical wave length.

This suggested a simple iterative procedure in which the minimum of the parabola is found using Cramer's rule for a series of values of σ a nd L:

1. The relation between σ and L is represented by this equation:

$$\sigma = aL^2 + bL + C$$

2. A typical plate component width is chosen, and three fractions of it, say L, .8L, .6L, are used to find three corresponding stresses.

By substitution of these three pairs of values in the parabolic equation given above, a system of three equations in three unknowns, a, b and c are found.

3. Cramer's rule is used to find the values of these unknowns.

4. Substitution of these values for a, b and c in the parabolic equation gives the actual parabolic equation for the structure.

5. From

$$\frac{\partial \sigma}{\partial L} = 0$$

a critical wave length is found.

6. Using this critical wave length another buckling stress is determined.

7. Among these four pairs of values of stresses and the associated critical wave lengths a comparison is made and the pair of highest stress is neglected and the remainder used again in the parabolic equation to find new values of a, b and c.

8. The procedure is repeated until convergence is obtained; only six steps were found to lead to very accurate results using PROGRAMME (3.5).

2. Second Procedure.

As it will be seen when the above procedure was applied for local buckling of thin-walled structures, the results in all cases were very satisfactory. However, for thin short plates the solutions were not quite accurate and another solution procedure had to be dopted. This can be applied equally well to all the different types of thin-walled structures of finite length.

This second procedure has the following outline:

From the analysis of local buckling modes it appears that the structure will buckle into an integral number of half-waves common to all flat plate components. By using integral numbers of half wave lengths, the buckling stress computed for a structure is found to vary over the band of half-waves used describing a curve with minimum defined by the appropriate critical number of half-waves.

This method has been incorporated into PROGRAMME (3.4), which was used for the analysis of flat plates and for plates supported on the two sides by an elastic medium which reacts only in compression. The latter application is discussed fully at a later stage.

f. Conclusion:

1. This method is very efficient for the study of a structure which fails by local buckling.

2. Band width is very small and computation time is, as can be seen, shorter than the previous two methods.

3. In the following analyses, two finite strips were used to represent each component plate for the study of a variety of structures (channel section, stiffened plates and sandwich panels) and in each case the results were very accurate.

4. It is based on the concept of the geometric stiffness matrix, and the solution procedure converges in six iterations to the exact value.

5. To find a buckling stress in the above cases, less than one second of computer time was used operating on the 2976* machine.

6. When used in the analysis of plates of finite length, the critical stress computed was found to be very accurate and computation time found to be 0.01 of the computation time for the standard finite element method.

7. For the study which follows, this method was found to be more suitable and less cumbersome to manipulate than the other two methods presented earlier on.

---

* the Glasgow University ICI 2976 Computer .

3.2.3.1 Local Buckling of Thin-walled Channel Section Columns.

(a) Introduction:

The local buckling instability analysis for a thin-walled column of channel section will be studied using the finite element method, assuming that the column will buckle according to the local buckling mode described above.

In Graph (3. 2), the local buckling stress coefficient is plotted against a range of B_w/B_s and T_w/T_s using PROGRAMME (3.5).

(b) Finite element idealisation:

The column is idealised into six elements, two for each component flat plate, with each strip half the width of the plate and of length equal to the assumed wave-length,

The elastic and geometric stiffness matrices are given in Table(3.14) Table (3.15), and nodal matrix **ND** (I,J) and a boundary matrix **NB** (I) are given in Table (3.16a). The cross-section idealisation is given in Figure (3.12).

(c) Conclusion:

1. The results obtained using the finite element method agree reasonably well with the theoretical results obtained by classical approach ([51]).

2. The computer time for the complete analysis using 2976 computer, was found to be 23 seconds.

3. Channel sections which have relatively long and thin webs are very weak from the local instability point of view.

3.2.3.2. Local Buckling of Stiffened Plate.

(a) Introduction:

In this section the finite element strip will be used to study the local instability of longitudinally siffened plate.

Buckling is assumed to occur with component flat plates rotating around the junction lines which remain straight. The structure will buckle into a complete number of half-waves and end and side constraint effects are neglected.

(b) Procedure:

The local buckling stress coefficient is plotted against values of B_w/B_s which vary between .2 and 1.2, for values of T_w/T_s from the range (.25 to 1.5) using PROGRAMME (3.5) and the results are given in Graph (3.3).

(c) Finite element idealisation:

The finite element grid is shown in Figure (3.12), six finite strips are used two for the web, each of width equal to .5 B_w, and four finite strips for the skin, two at each side of the web, each strip having .25 B_s as width.

The elastic and geometric stiffness matrices are given in Table (3.14) and Table (3.15)

The first solution procedure is adopted and the nodal displacement matrix and boundary condition matrices are as given in Table (3.16).

(d) Conclusion:

1. The results obtained by the finite strip method agree remarkably well with E.S.D.U. Data Sheet Number 70003 with amendment A September, 1976.

2. Six finite strips were used with total degree of freedom equal to just 14. and were found to be sufficient to obtain this high degree of accuracy.

3. Solution procedures (1) and (2) were found to converge to the same buckling stress.

4. Stiffened panels with long and or thin webs are very weak and, as can be seen from Graph (3.3), the buckling stress for stiffened panels which are characterised by T_w/T_s = .25 lose stiffness very rapidly with increase of the B_w/B_s

3.2.3.3. Local Buckling of Web Core Sandwich Panel.

(a) Introduction:

This panel is shown in Figure (3.12) and it consists of two face sheets separated by vertical webs, the face sheets provide the necessary stiffness for overall buckling and the webs act as stabilisers against plate buckling.

The local buckling mode analysed here is given in Figure (3.12), and the buckling stress coefficient as a function of B_w/B_s and T_w/T_s is given in Graph (3.4).

The results agree very well with the results obtained using the E.S.D.U. Data Sheets method

(b) Finite element idealisation:

Taking advantage of the symmetric shape six elements are used, four on the skin, two on either side of the web, each of width equal to $0.25B_s$ and two on the web with width $0.25B_w$ Figure (3.12).

The values of T_w/T_s and B_w/B_s used are the same as in the previous example and the matrix **ND** (I,J) and **NB** (I) are as given in Table (3.16).

(c) Conclusion:

1. The results obtained using the finite element method agree very well with the results obtained using the E.S.D.U. Data Sheets method.

2. The order of the assembled matrix is (14 x 14), and computation time found to be 20. seconds using PROGRAMME (3.5).

3. For the same values of the ratios T_w/T_s and B_w/B_s this panel showed better behaviour than the stiffened panel from local instability point of view, provided it buckles in this mode.

4. For $\frac{T_w}{T_s} = 0.25$, the local buckling stress remains quite high till $\frac{B_w}{B_s} = .8$ after which the buckling stress drops sharply as in the previous structures examined.

1	2
2	3
3	4
4	5
5	6
6	7

ND

5
9

NB

a . Channel Section

1	2
2	3
3	4
4	5
3	6
6	7

ND

2
5
14

NB

b. Integrally Stiffened Panel

1	2
2	3
3	4
4	5
3	6
6	7

ND

2
5
10
14

NB

c. Web Core Sandwich Panel

TABLE (3.16) - NODAL NUMBERING AND BOUNDARY MATRICES.

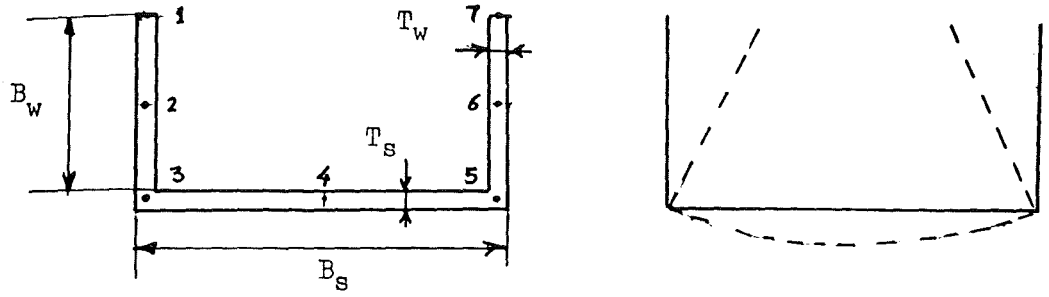

a. Channel Section

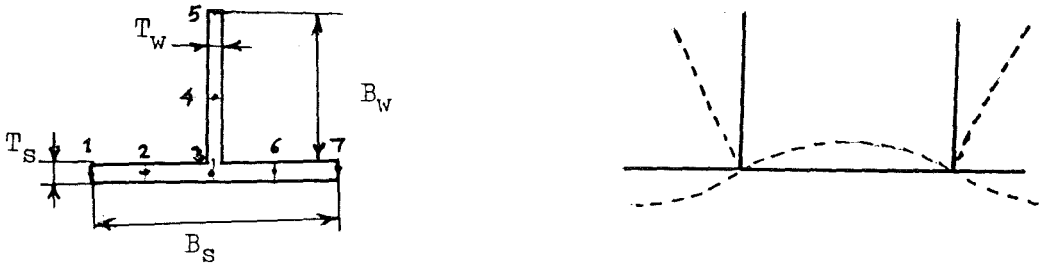

b. Integrally Stiffened Panel

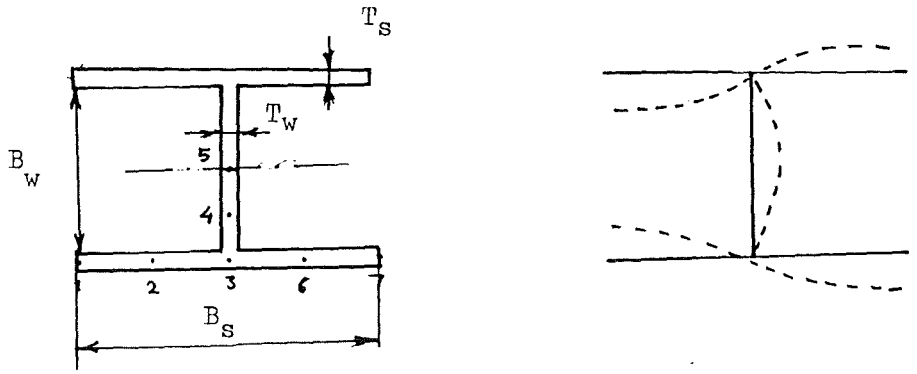

c. Web Core Sandwich Panel

FIGURE (3.12) - FINITE STRIP IDEALISATION AND LOCAL BUCKLING MODE.

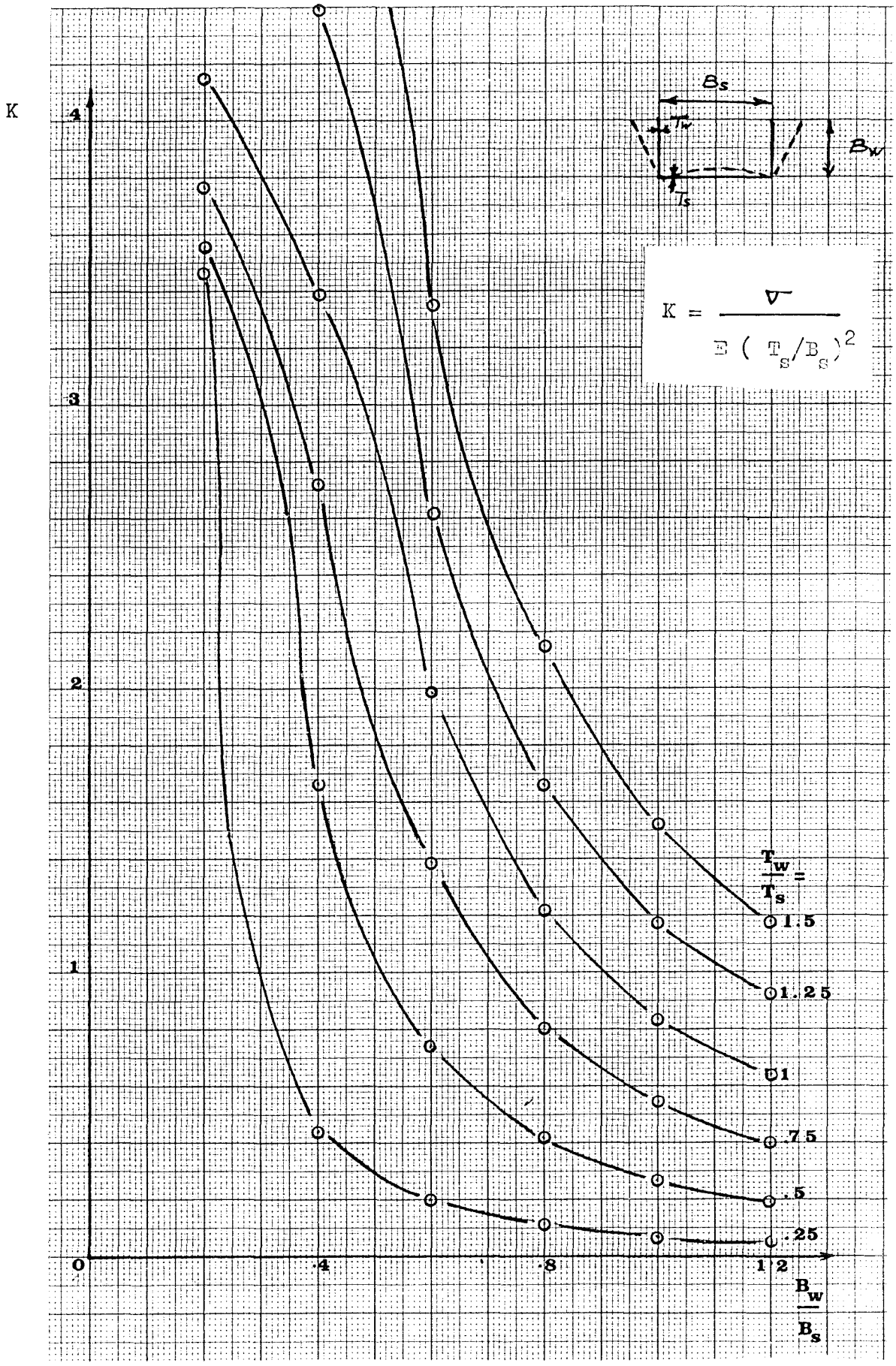

GRAPH (3.2) - LOCAL BUCKLING ANALYSIS OF THIN-WALLED CHANNEL SECTION BY FINITE STRIP METHOD.

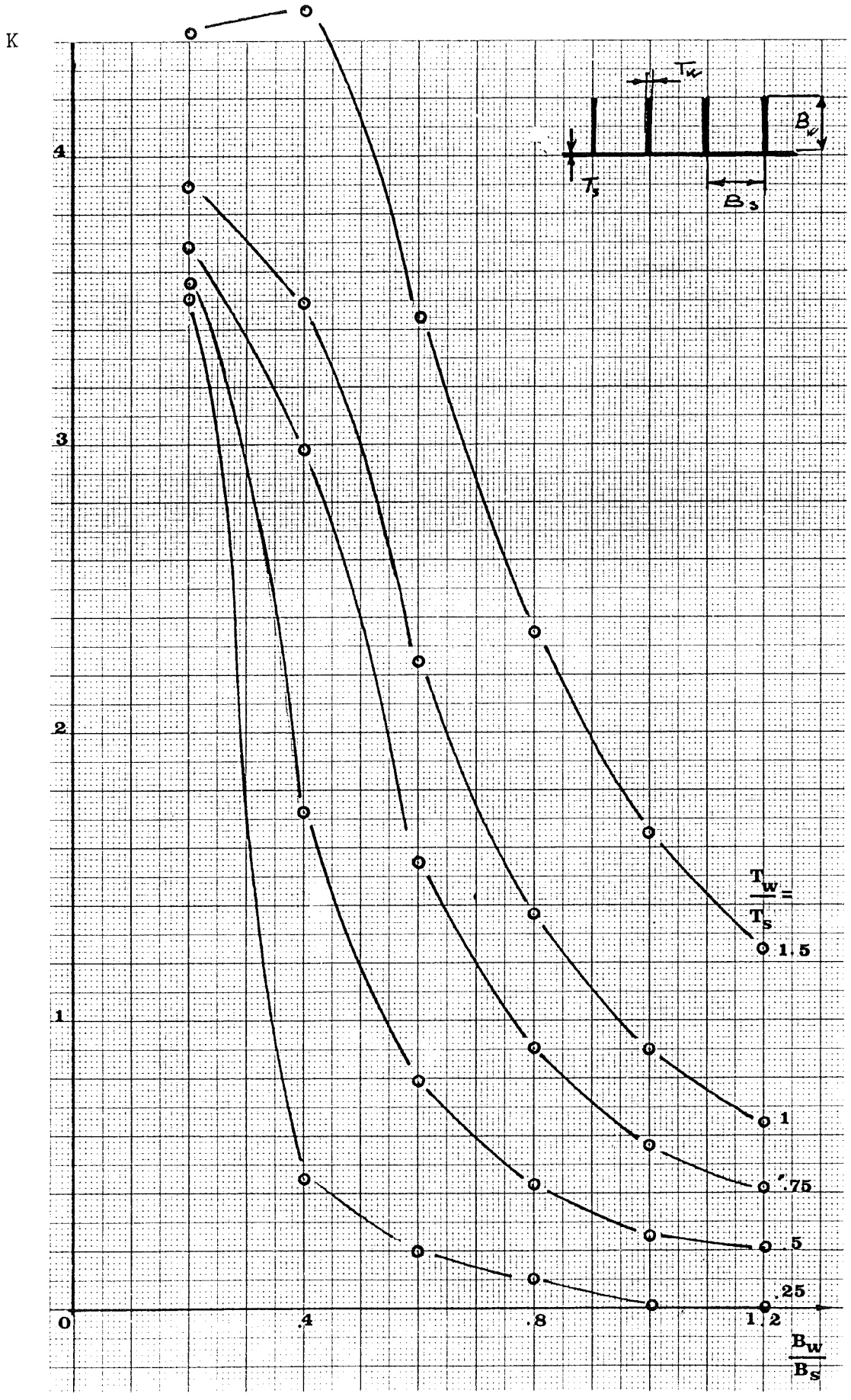

GRAPH (3.3) - LOCAL BUCKLING ANALYSIS OF STIFFENED PANEL.

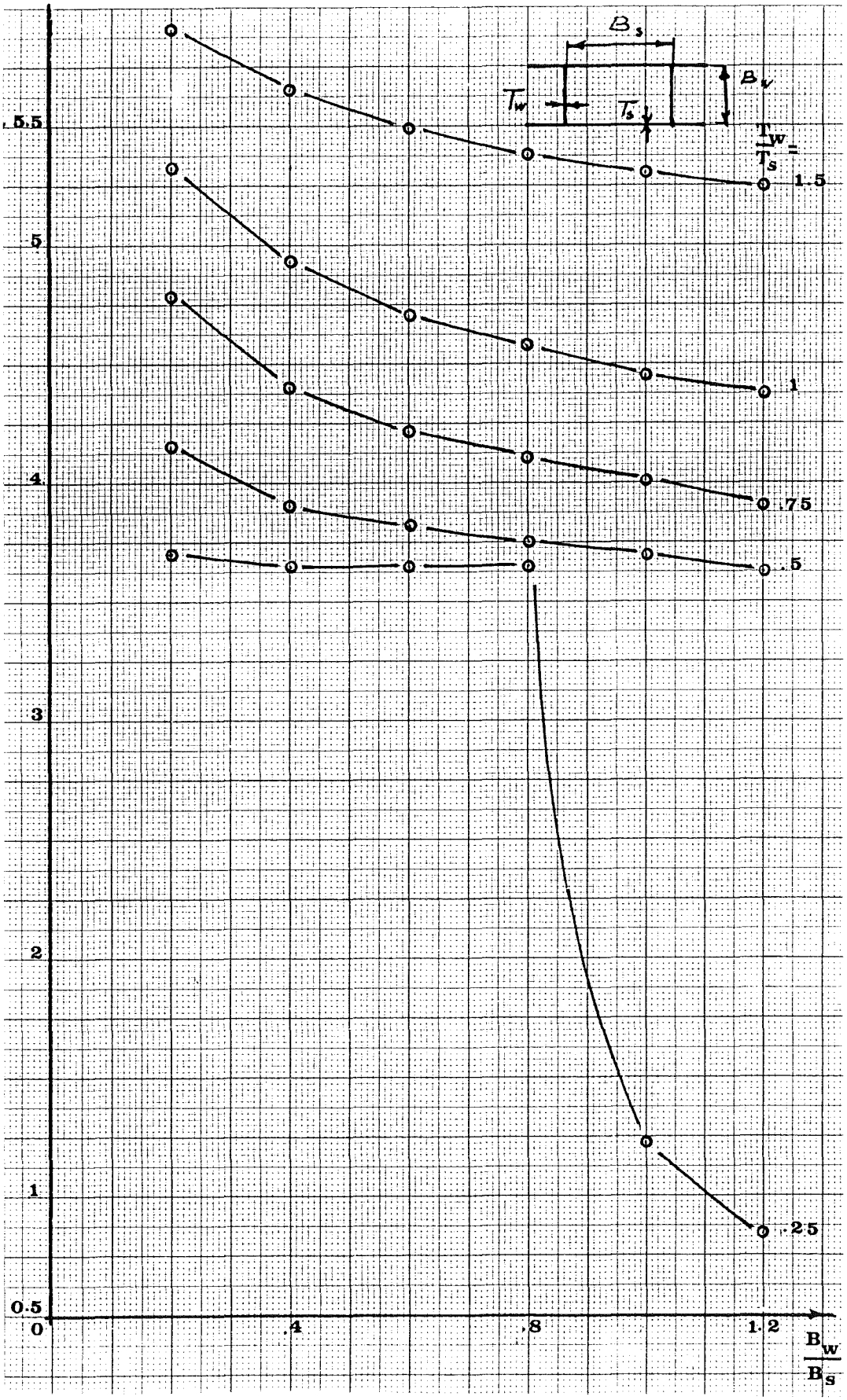

GRAPH (3.4) - LOCAL BUCKLING ANALYSIS OF WEB CORE SANDWICH PANEL.

3.2.4. Buckling of Plates.

(a) Introduction:

In the preceding section, the finite strip method was used for the analysis of the local instability of some structural elements, and it can be seen that the results of the computations agree very well with the existing solutions obtained by other methods.

In this section, the finite strip is applied to the buckling analysis of plates of finite length, supported at the ends and with different boundary conditions at the lateral sides. As it will be seen, not only are the results very accurate, but also the reduction in computer time is remarkable.

For example, in the case of buckling of a simply supported plate, using the conventional finite element procedure, as in the previous part , to obtain the same degree of accuracy as that obtained here, 36 finite elements were used to represent one quarter of the plate. This corresponds to forty-nine degrees of freedom and assembly matrices of order of (147 x 147) and a computation time of 69 seconds.

The same plate buckling problem when treated here, using six finite strips to represent the plate involved seven nodes with 14 degrees of freedom and required a computation time of .78 seconds.

(b) Finite Strip Idealisation:

The plate is idealised into 6 finite strips joined edge to edge, the elastic and geometric stiffness matrices are given in Table (3.14) and Table (3.15) and the finite grid is represented in Figure (3.13). The matrix of nodal displacements **ND** (I,J) and the matrices of boundary conditions **NB** (I) for sides simply supported, clamped-clamped, and clamped-free are given in Table (3.17).

The computer programme listed in Chapter Five, PROGRAMME (3. 4), is used and the results are given in Graph (3. 5).

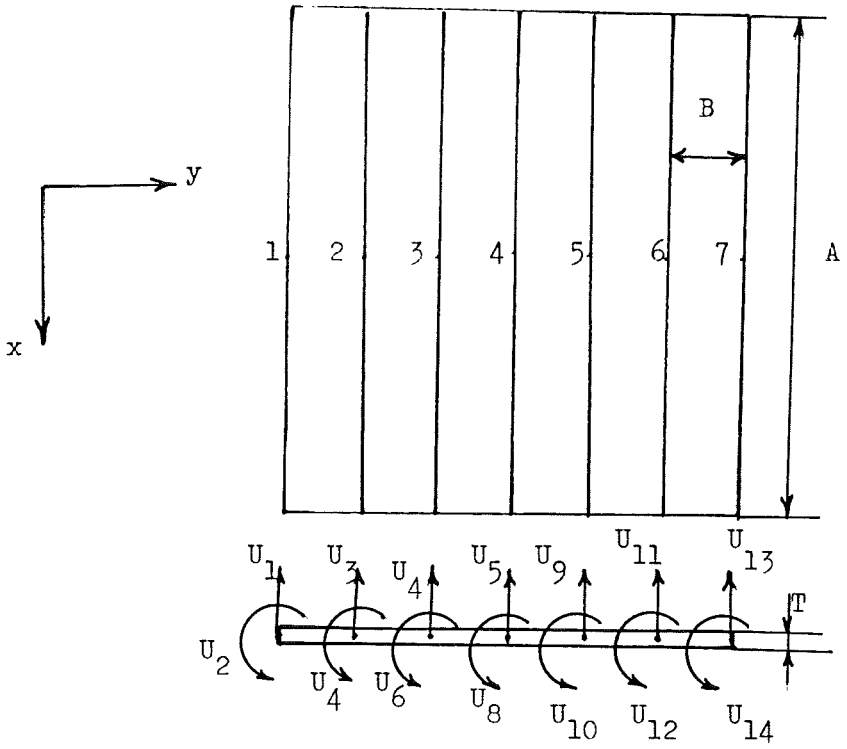

FIGURE (3.13) - FINITE STRIP IDEALISATION FOR PLATE BUCKLING.

$$\mathbf{ND}(I,J) = \begin{bmatrix} 1 & 2 \\ 2 & 3 \\ 3 & 4 \\ 4 & 5 \\ 5 & 6 \\ 6 & 7 \end{bmatrix}$$

$$\mathbf{NB}(I) = \begin{bmatrix} 1 \\ \\ 13 \end{bmatrix}$$

sides simple supported.

$$\mathbf{NB}(I) = \begin{bmatrix} 1 \\ 2 \\ 13 \\ 14 \end{bmatrix}$$

clamped-clamped

$$\mathbf{NB}(I) = \begin{bmatrix} 1 \\ \\ 2 \end{bmatrix}$$

clamped-free

TABLE (3.17) - NODAL DISPLACEMENT AND BOUNDARY MATRICES FOR THE ANALYSIS OF PLATE BUCKLING.

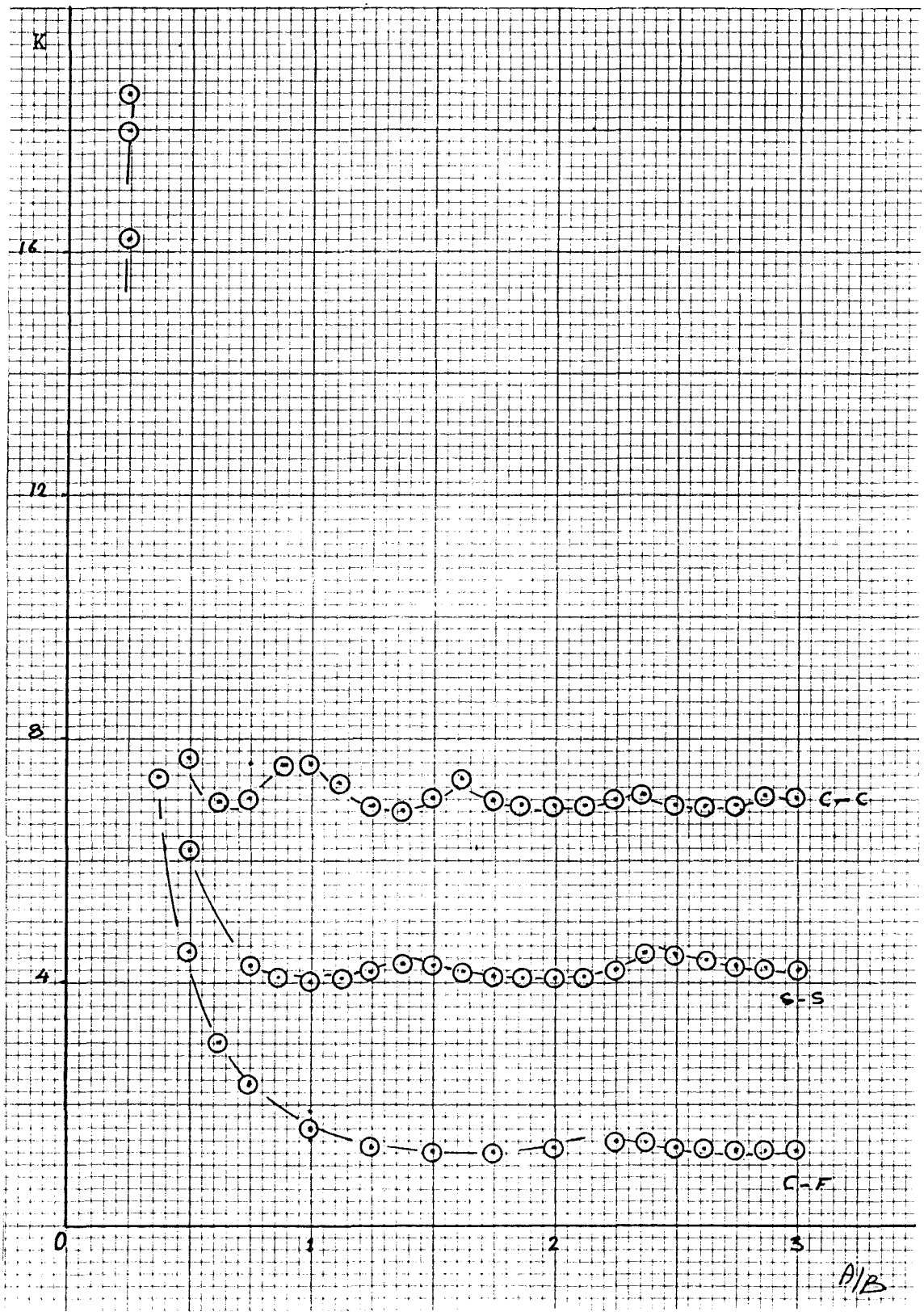

GRAPH (3.5) - ANALYSIS OF ISOTROPIC PLATE BY FINITE STRIP METHOD.

(c) Conclusion:

The finite strip can be used efficiently for the buckling analysis of a plate. If the plate is long then solution procedure (1) should be adopted. For a short plate an accurate result can be obtained only by using solution procedure (2), which has been explained earlier.

3.2.5. Plates Stabilised by Elastic Foundation.

(a) Introduction.

Many problems of considerable practical importance can be related to the solution of plates stabilised by elastic foundations.

Slabs for runways and buildings, concrete pavement of highways ship bottom plates are some well known applications, and a survey of various types of foundation can be found in (52).

Here in this section, in order to investigate the effect of an elastic supporting medium on a plate type structure, the instability of plates simply supported at the ends and with different boundary conditions along the lateral sides which are sandwiched between two blocks of low density elastic material will be studied.

These elastic blocks will be considered to be the foundation for the plate which will react only under compression and the material will be considered as linearly elastic with a stiffness constant K_f.

The problem of the simply supported plate will be studied first by using the principal of conservation of energy.

This will serve as an introduction to the work which follows and, at the same time, will help to illustrate the significance of some of the parameters involved besides providing the means for comparison with the solution obtained by the finite strip method.

The study of long webs stabilised by an elastic medium is conducted theoretically and experimentally to provide an assessment of the accuracy of the analysis and of the validity of the assumptions employed.

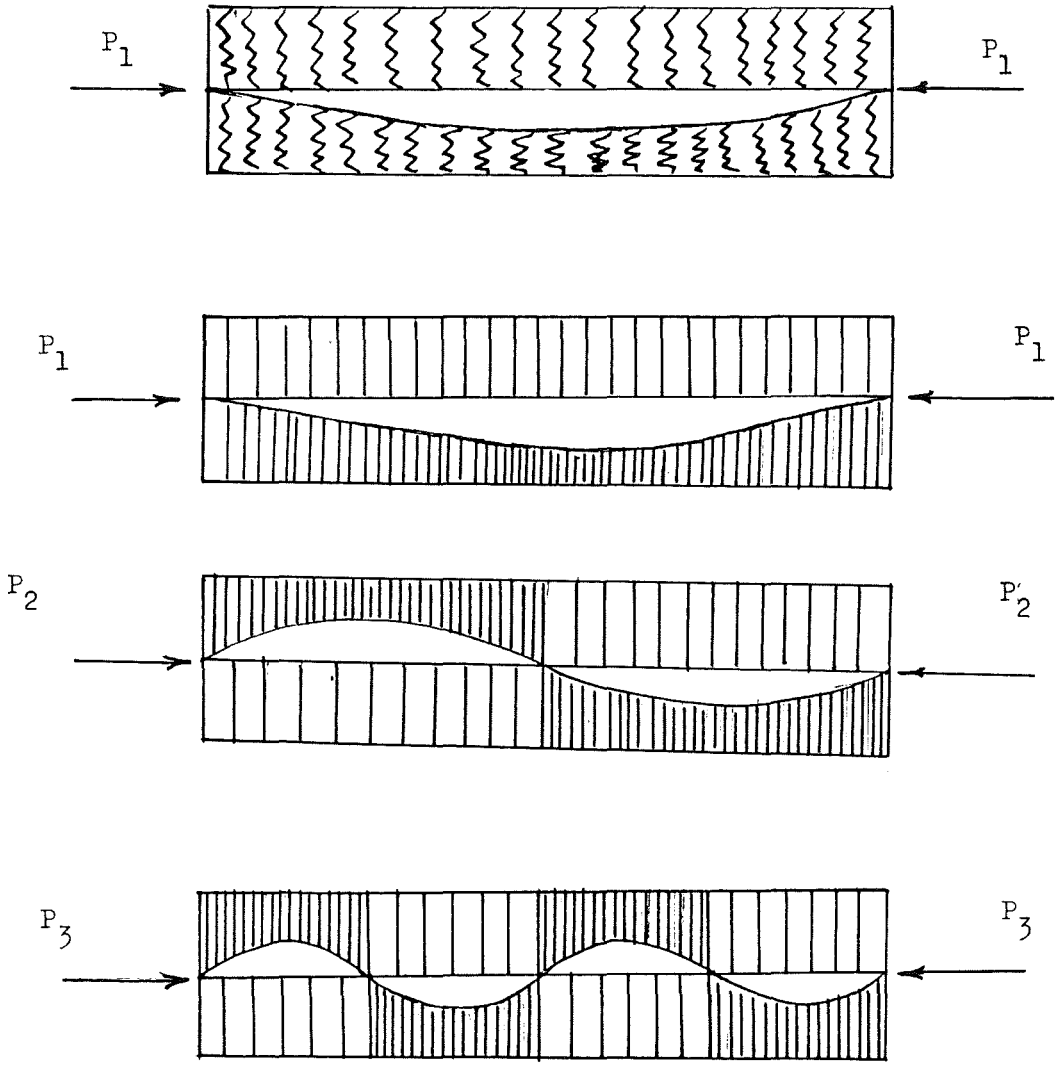

FIGURE (3.14) - BUCKLING PATTERNS FOR PLATE SUPPORTED BY ELASTIC MEDIUM WHICH REACTS IN COMPRESSION.

(b) Elastic Foundation Description:

The foundation which will be assumed for the analysis which follow is imagined to be formed by an infinite number of elastic springs continuously distributed over the span of the plate and acting on both sides of it. The springs are in contact with the surface of the plate but are not attached to it so that when the plate deforms the foundation will react only under compression.

There is no shear interaction between the springs and the lateral loading applied by these springs is proportional to the deflection w of the plate through the constant of proportionality k_f. This constant will be referred to as the foundation modulus or spring constant of the core material and given in N/mm^3.

Figure (3.14) shows the configuration to be studied and the buckling pattern for the plate. It shows also in each case how the foundation deforms, the shaded areas represent compression of the foundation and the light areas represent the uncompressed parts.

For the analysis which follows it is found convenient to present the results in terms of $Z = \frac{k_f}{D}\left(\frac{B}{\pi}\right)^4$ instead of just k_f so that the charts and Tables can have a more general application.

3.2.5.1 Buckling of Plates on Foundation Using the Conservation of Energy Approach,

In this introductory analysis, only the simply supported plate is considered. The thin plate is supported over its two faces by elastic material ,Figure (3.14), which reacts only in compression, foundation modulus is equal to K_f. Following the energy approach, the strain energy of an element of area of the plate is given as:

$$dU_E = dU_b + dU_f$$

where U_b is strain energy due to bending

and U_f is the strain energy due to twisting.

The above expression can be written as:

$$-\tfrac{1}{2}\left(M_x\ \partial^2 w/\partial X^2 + M_y\ \partial^2 w/\partial Y^2 + M_{xy}\ \partial^2 w/\partial X \partial Y\right) dX\, dY$$

From Hooke's law

$$\sigma_x = \left(E/\left(1 - \nu^2\right)\right)\left(\varepsilon_x + \nu\ \varepsilon_y\right)$$

$$\sigma_y = \left(E/\left(1 - \nu^2\right)\right)\left(\varepsilon_y + \nu\ \varepsilon_x\right)$$

$$\tau_{xy} = \left(E/2\ (1 + \nu)\right)\ \gamma_{xy}$$

and, from the strain displacement relation for a plate in bending,

$$\varepsilon_x = -z\ \partial^2 w/\partial X^2$$

$$\varepsilon_y = -z\ \partial^2 w/\partial Y^2$$

$$\gamma_{xy} = -2z\ \partial^2 w/\partial X\, \partial Y$$

Substituting gives:

$$\sigma_x = \left(-Ez/\left(1 - \nu^2\right)\right)\left(\partial^2 w/\partial X^2 + \nu\ \partial^2 w/\partial Y^2\right)$$

$$\sigma_y = \left(-Ez/\left(1 - \nu^2\right)\right)\left(\partial^2 w/\partial Y^2 + \nu\ \partial^2 w/\partial X^2\right)$$

$$\tau_{xy} = -2Gz\ \partial^2 w/\partial X\, \partial Y$$

Since

$$Mx = \int_{-T/2}^{T/2} \sigma_x \; z \, dz \quad , \quad My = \int_{-T/2}^{T/2} \sigma_y \; z \, dz$$

$$Mxy = \int_{-T/2}^{T/2} \tau_{xy} \; z \; dz$$

Substituting for M_x, M_y and M_{xy} in the strain energy expression and integrating gives:

$$U_E = \tfrac{1}{2} D \iint \Big[(\partial^2 w/\partial x^2 + \partial^2 w/\partial y^2)^2 - 2(1-\nu)\{(\partial^2 w/\partial x^2)(\partial^2 w/\partial y^2) - (\partial^2 w/\partial x \partial y)^2\} \Big] \, dx \, dy$$

The contribution of the foundation to the strain energy of the system can be written as

$$U_f = \tfrac{1}{2} K_f \iint w^2 \, dx \, dy$$

The work done by the external forces which in this case are axial forces per unit width Nx is given as

$$w_e = \tfrac{1}{2} \iint Nx \left[\frac{\partial w}{\partial x}\right]^2 dx \, dy.$$

For the simply supported plate, the deflection surface can be represented by

$$w = \sum_{m=1}^{\infty} \sum_{n=1}^{\infty} a_{mn} \sin \frac{m\pi x}{A} \sin \frac{n\pi y}{B}$$

which satisfies the boundary condition at the ends.

Substituting for W in the strain energy expression we have

$$U_E = \frac{D}{2} \int_0^A \int_0^B \Big\{ \sum_1^{\infty} \sum_1^{\infty} a_{mn} \left(\frac{m^2\pi^2}{A^2} + \frac{n^2\pi^2}{B^2}\right) \times$$

$$\times \sin \frac{m\pi x}{A} \sin \frac{n\pi y}{B} \Big\}^2 \, dx \, dy$$

or

$$U_E = \frac{A\,B}{8}\, D \sum_{1}^{\infty}\sum_{1}^{\infty} a_{mn}^2 \left[\frac{m^2\pi^2}{A^2} + \frac{n^2\pi^2}{B^2}\right]^2$$

and that part of the strain energy due to the foundation will be

$$U_f = \tfrac{1}{2}\, K_f \sum_{m=1}^{\infty}\sum_{n=1}^{\infty} a_{mn}^2 \,(A\,B/4)$$

The expression for the total strain energy is

$$U_E + U_f = \frac{A\,B}{8}\left[\pi^4 D \sum_{1}^{\infty}\sum_{1}^{\infty} a_{mn}^2 \left(\frac{m^2}{A^2} + \frac{n^2}{B^2}\right)^2 + K_f \sum_{1}^{\infty}\sum_{1}^{\infty} a_{mn}^2\right]$$

and the external work due to the compressive force N_x becomes

$$w_e = \frac{A\,B}{8}\, N_x \sum_{1}^{\infty}\sum_{1}^{\infty} a_{mn}^2 \,(m\pi/A)^2$$

Equating the external work to the strain energy gives:

$$N_x = \frac{AB/8 \cdot \pi^4 \cdot D \sum\sum a_{mn}^2 ((m/A)^2 + (n/B)^2) + (AB/8)\, K_f \sum\sum a_{mn}^2}{\sum_{1}^{\infty}\sum_{1}^{\infty} a_{mn}^2}$$

The minimum value of Nx is obtained when all but one of the coefficients a_{mn} are zero and $n = 1$ and has the value

$$N_x = \left((\pi A/m)^2 D \left((m/A)^2 + (1/B)^2 \right) + K_f (A/m\pi)^2 \right)$$

or

$$\sigma = \frac{1}{T}\left((\pi A/m)^2 D \left((m/A)^2 + (1/B)^2 \right)^2 + K_f (A/m\pi)^2 \right) \quad (38)$$

which describes the relationship between Nx and K_f and the ratio A / B for each value of m.

Let us find the expression of m for which σ becomes critical:

$$\frac{\partial N_x}{\partial m} = 0$$

$$2 (\pi A)^2 D (m/B^4 - 1/m^3 B^4) - 2 K_f A^2/(m^3 \pi^2) = 0$$

$$2\pi^2 D m/A^2 - (1/m^3)(2\pi^2 A^2 D/B^4 + 2K_f A^2/\pi^2) = 0$$

$$m_{cr}^4 = (A/B)^4 + 2K_f \cdot A^4/(2\pi^4 D)$$

$$m_{cr} = \sqrt[4]{\left(\frac{A}{B}\right)^4 + \frac{K_f}{D}\left[\frac{A}{\pi}\right]^4} \qquad (3.9)$$

If equations (3.8) and (3.9) are solved the critical buckling stress will be obtained.

It is interesting to note that for beam on a Winkler type foundation, the corresponding expression for m_{cr} is:

$$m_{cr} = \frac{L}{\pi}(K_f/EI)^{0.25}$$

The buckling stress coefficient was calculated using equations (3.8) and (3.9) for K_f = 0, 5 and 15 N/mm^3 for a plate which is made of Dural (ν= 0.3, E = 72557 N/mm^2) and which has A/B = 2, B/T = 50 and T = 0.5mm.

The results are presented in Table (3.18) and for a generality nondimensional parameters (K and Z) are used (See page 189 for the definition of Z).

(a) Conclusion:

1. It can be seen that the buckling load and the critical wave length number both increase with Z , which is used to represent the stabiliser stiffness, and the increase in buckling load is quite high.

2. By using Z instead of the dimensional K_f the buckling stress σ can be written as:

$$\sigma/E = f\left(\frac{A}{B}, Z\right)$$

and any other plate which has the same values of the nondimensional parameters A/B, and Z will buckle at the same stress. This property can be used to produce scaled model for experiment or to generalise experimental results for this type of construction.

TABLE (3.18) - BUCKLING ANALYSIS OF ISOTROPIC PLATE STABILISED BY ELASTIC MEDIUM (ENERGY APPROACH).

A/B	Z = 0		$\mathbf{C}_1$		$3\,\mathbf{C}_1$	
	K	m_{cr}	K	m_{cr}	K	m_{cr}
1	3.98	1	12.2	2	18.69	3
2	3.98	2	12.37	5 or 4	19.26	6
3	3.98	3	12.14	7	19.26	9

$$K = \frac{\sigma}{\frac{\pi^2 E}{12(1-\nu^2)} \left(\frac{T}{B}\right)^2}$$

$$Z = (K_f/D)\,(B/\pi)^4$$

$\mathbf{C}_1 = 24.2$

A/B = 2

B/T = 50

3.2.5.2. Finite element Analysis:

The buckling problem for a plate stabilised by an elastic medium as represented in Figure (3.14), consists of finding the buckling stress of a plate which has the strain energy of deformation increased by the amount:

$$U_f = \frac{K_f}{2} \iint w^2 \, dx \, dy \qquad (3.10)$$

Using the finite element strip, the problem will be to find the lowest eigenvalue for the determinental equation

$$\left| \mathbf{K_e} + \lambda \mathbf{K_g^*} \right| = \mathbf{0}$$

where the elastic stiffness is now the sum of the elastic stiffness of the plate and the contribution of the stabiliser represented by the foundation elastic stiffness matrix $\mathbf{k_f}$.

(a) Foundation stiffness matrix derivation:

Using the displacement function assumed for strip analysis:

$$w = \mathbf{N}(y) \sin \frac{\pi x}{A} \mathbf{U}$$

where $\mathbf{N}(Y) = \left[N_1 \quad N_2 \quad N_3 \quad N_4 \right]$

and

$$N_1 = (1 - 3Y^2 + 2Y^3)$$
$$N_2 = (Y - 2Y^2 + Y^3)B$$
$$N_3 = (3Y^2 - 2Y^3)$$
$$N_4 = (-Y^2 + Y^3)B$$

and

and $\mathbf{U} = \{ U_1 \quad U_2 \quad U_3 \quad U_4 \}$

A is the length of the strip.

and a non-dimensional $Y = \frac{y}{B}$ is used, the assumed displacement function can be written as:

$$w = (N_1 U_1 + N_2 U_2 + N_3 U_3 + N_4 U_4) \, s$$

where

$$s = \sin \pi x / A$$

Substituting for w in (3.1 0) gives

$$U_{Ef} = \frac{K_f}{2} \mathbf{U}^T \int_0^A \int_0^B \mathbf{N}^T \mathbf{N}\, s^2\, \mathbf{U}\, dA_r$$

where $dA_r = dx\, dy$

The elements of the foundation stiffness matrix can be computed from

$$\frac{\partial^2 U_{Ef}}{\partial U_i \partial U_j} = K_{Ef}\ (i,j)$$

so that

$$\mathbf{k_f} = K_f \begin{bmatrix} \iint N_1^2 s^2 & & & \text{SYM.} \\ \iint N_1 N s^2 & \iint N_2^2 s^2 & & \\ \iint N_1 N_3 s^2 & \iint N_2 N_3 s^2 & \iint N_3^2 s^2 & \\ \iint N_1 N_4 s^2 & \iint N_2 N_4 s^2 & \iint N_3 N_4 s^2 & \iint N_4^2 s^2 \end{bmatrix} dA_r$$

Then from

$$\int_0^A \sin^2 \frac{\pi x}{A}\, dx = A/2$$

Substituting and integrating with respect to the other variable we obtain the foundation effect matrix given in Table (3.19).

$$\mathbf{k_f} = \frac{K_f A\ B}{840.} \begin{bmatrix} 156. & & & \\ 22B & 4B^2 & \text{Sym.} & \\ 54. & 13B & 156. & \\ -13B & -3B^2 & -22B & 4B^2 \end{bmatrix}$$

where

A is the length of the strip

B is the width

TABLE (3.19) - FOUNDATION STIFFNESS MATRIX.

(b) PRESENTATION OF THE RESULTS:

For better understanding of the phenomena and to get a clear picture of the effect of the different geometric parameters, material, and boundary conditions, the following graphs were plotted:-

1. For each of the following boundary conditions considered
   1. Sides simply supported.
   2. Sides clamped.
   3. One side clamped the other is free.

A graph which represents the relatidn between K, the buckling stress coefficient, Z , and m, the critical wave length was plotted for a plate characterised by $\frac{A}{B} = 2$, $B/T = 50$

See graphs (3.6), (3.7) and (3.8).

2. Three graphs which represent the relation between K, Z and A/B for each of the boundary conditions considered.
See graphs (3.9), (3.10) and (3.11).

3. Graph (3.12) which gives the buckling stress coefficient for a range of values of Z for the three boundary conditions and the plate characterised considered in 1.

4. A graph of $\frac{\sigma}{\sigma_o}$ versus Z plotted for the same plate and for each of the boundary conditions , Graph(3.13) .

The ratio $\frac{\sigma}{\sigma_o}$ represent the buckling stress with stabiliser to the buckling stress of the same plate without stabiliser and the graph shows which boundary conditions profits most from the use of stabiliser material.

5. Finally, to prepare the theoretical results for the compression tests which will follow, graphs giving the buckling stress and the critical curve lengths for long webs with A/B = 9 , and ($\frac{B}{T}$ = 32, 50, 64) were plotted for a range of Z .

See graphs (3.14) and (3.15).

Note In all the graphs the values of Z were given in terms of c_1 where $c_1 = 24.2$.

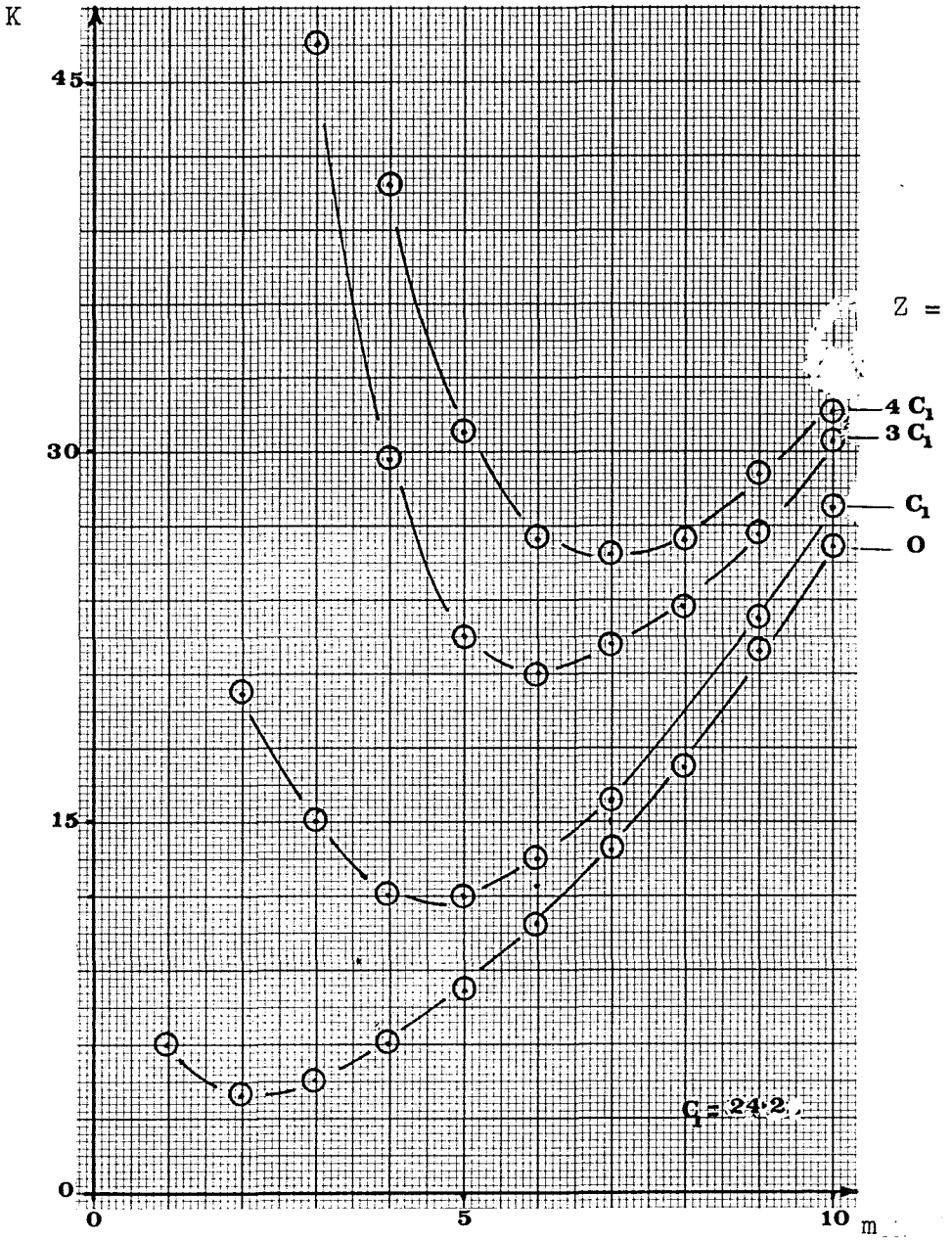

GRAPH (3.6) - BUCKLING OF SIMPLY SUPPORTED PLATE ELASTICALLY SUPPORTED ($A/_B$ = 2, $B/_T$ = 50)

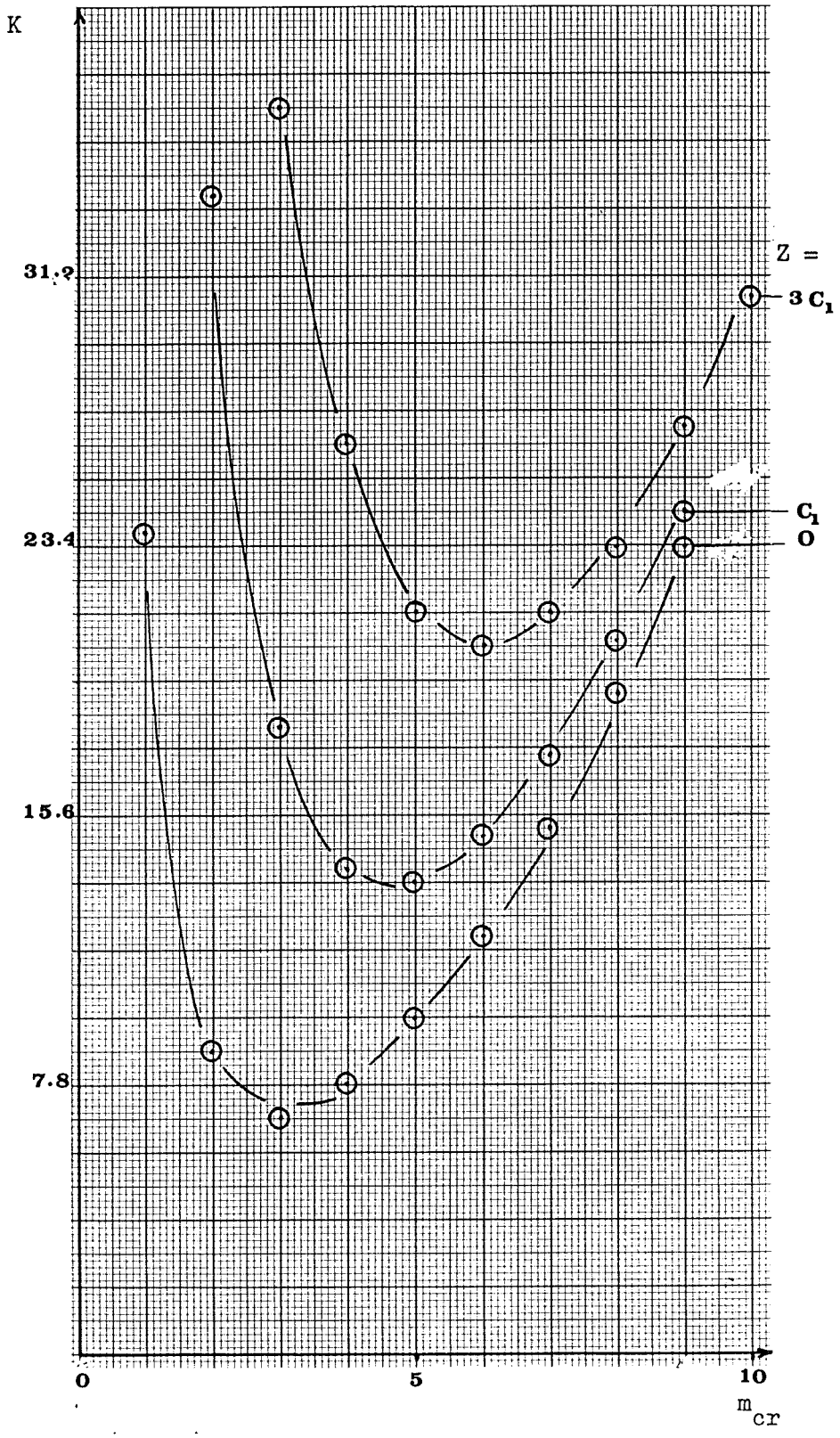

GRAPH (3.7) - BUCKLING OF CLAMPED PLATE ELASTICALLY SUPPORTED ($A/_B$ = 2, $B/_T$ = 50).

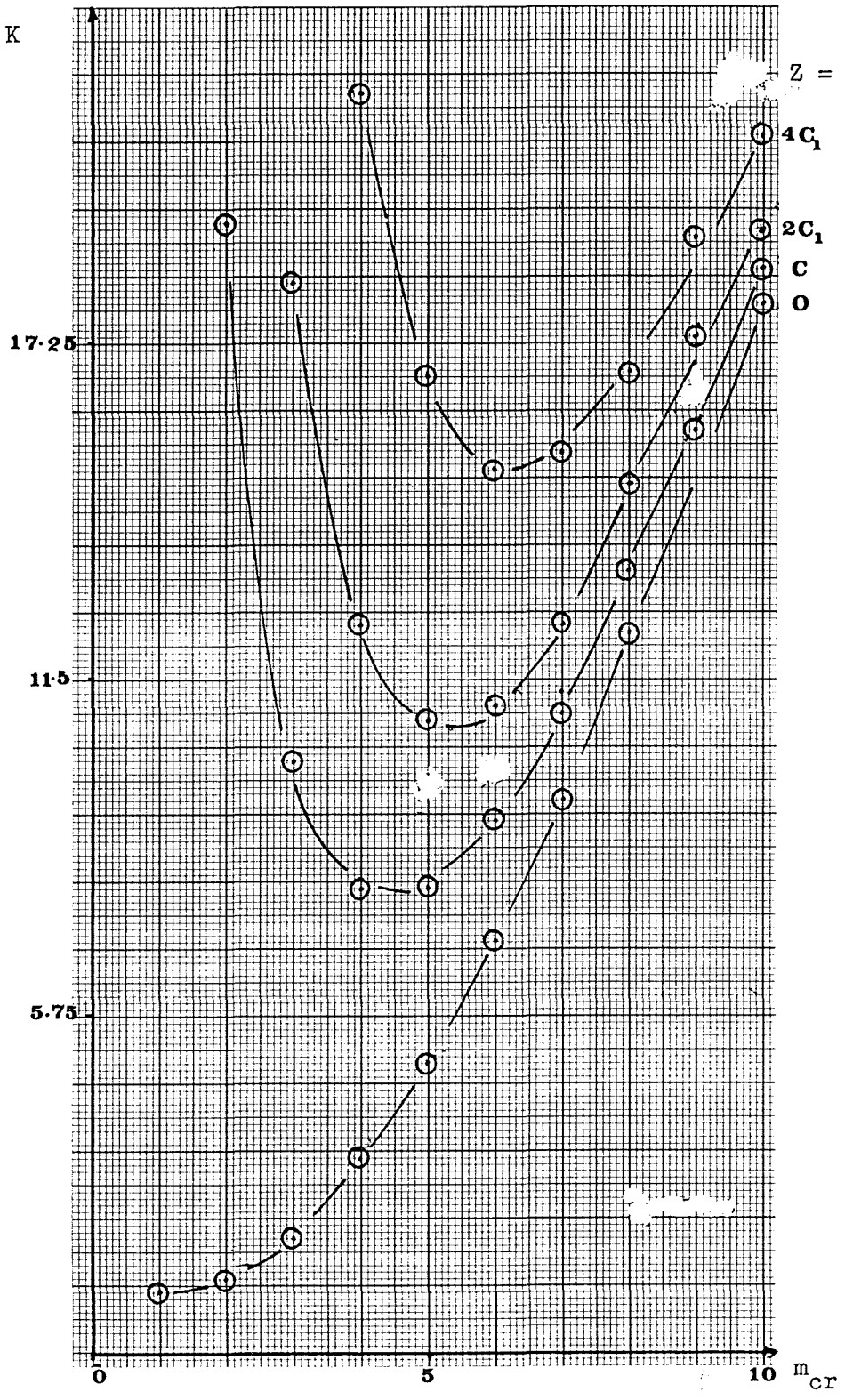

GRAPH (3.8) - BUCKLING OF CLAMPED-FREE PLATE ELASTICALLY SUPPORTED.

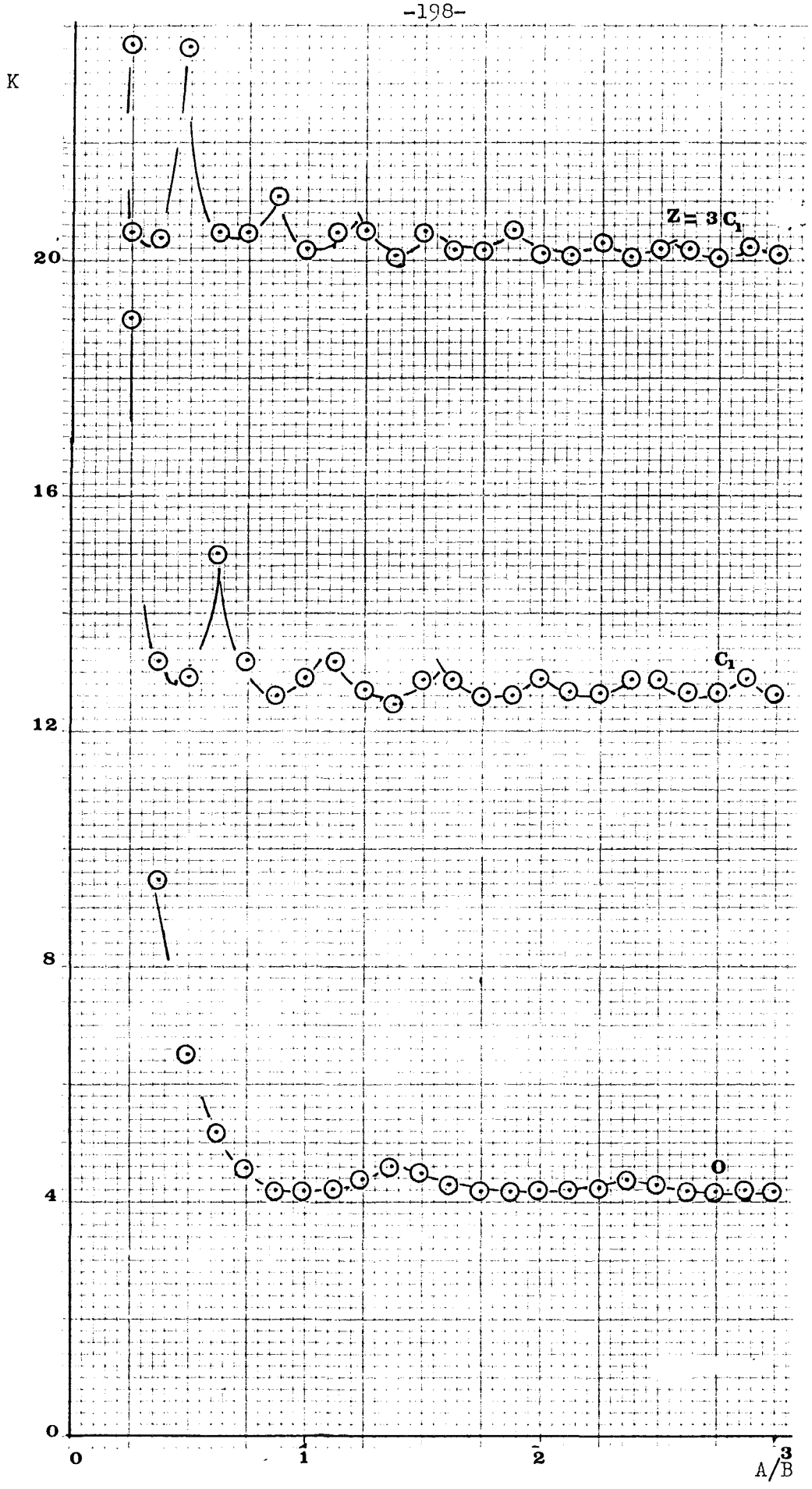

GRAPH (3.9) - BUCKLING ANALYSIS OF SIMPLY SUPPORTED PLATE ELASTICALLY SUPPORTED $B/_T$ = 50, $A/_B$ VARY).

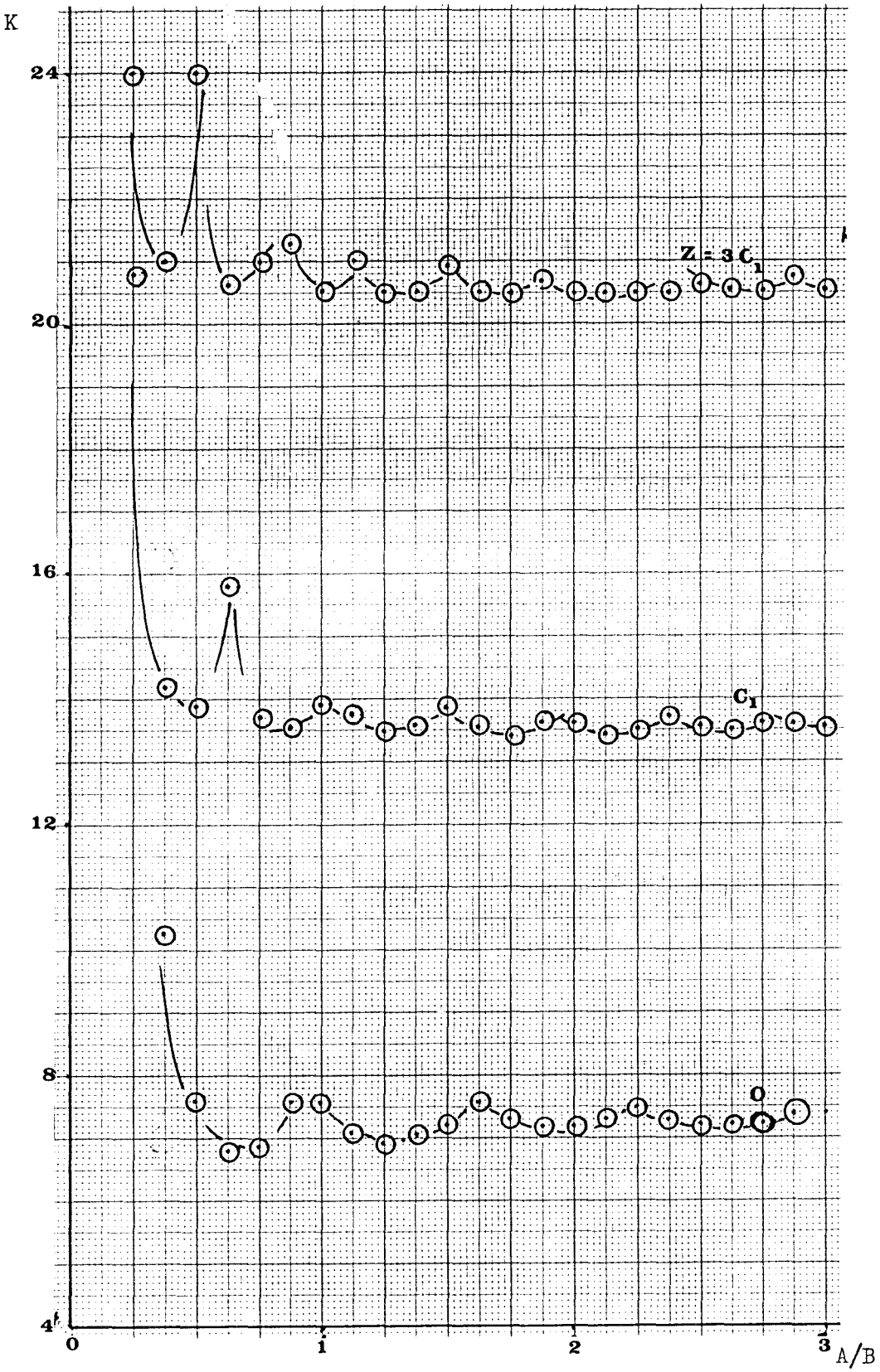

GRAPH (3.10) - BUCKLING ANALYSIS OF CLAMPED PLATE ELASTICALLY SUPPORTED ($B/_T$ = 50, $A/_B$ VARY).

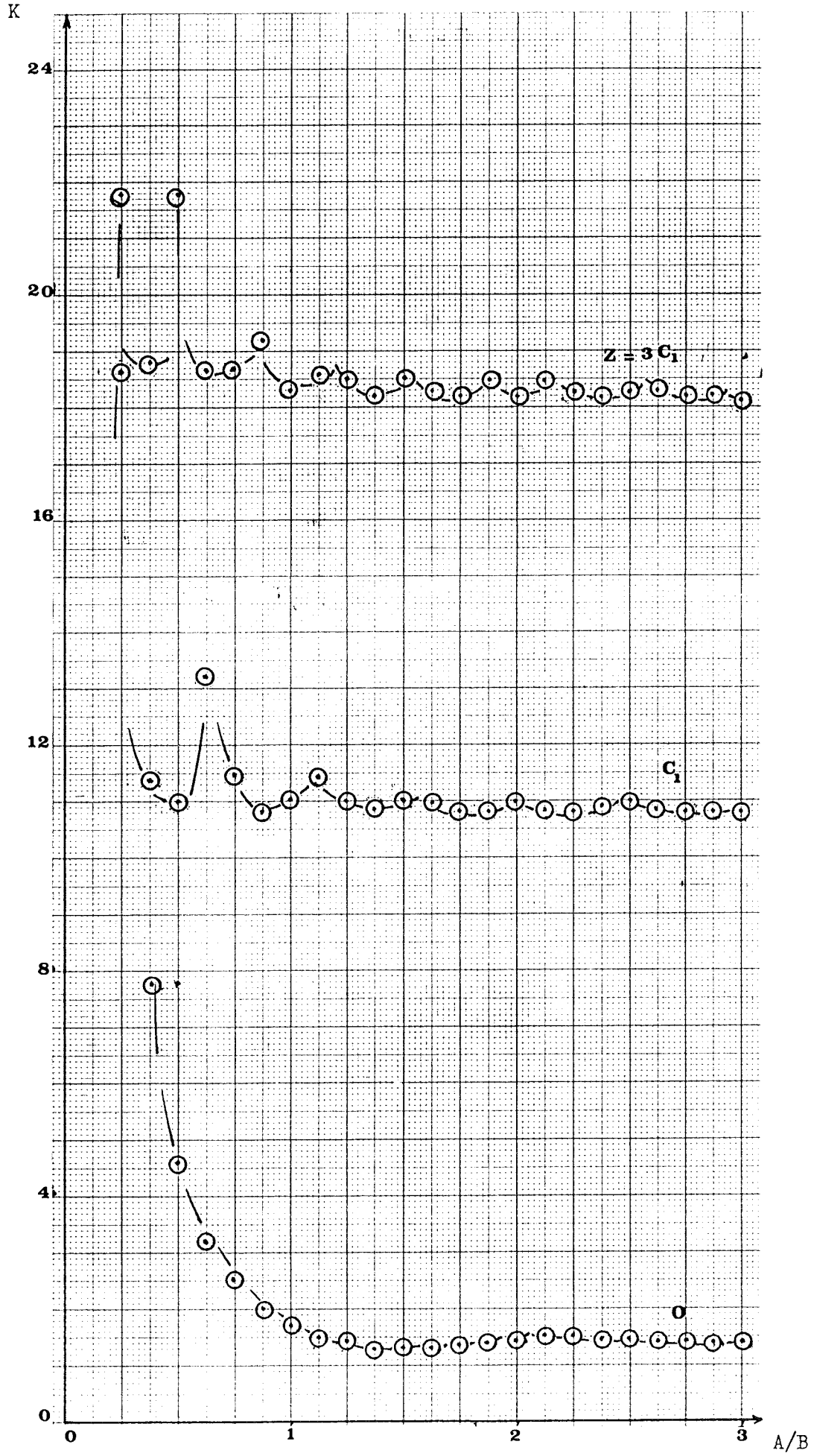

GRAPH (3.11) - BUCKLING ANALYSIS OF CLAMPED-FREE PLATE.

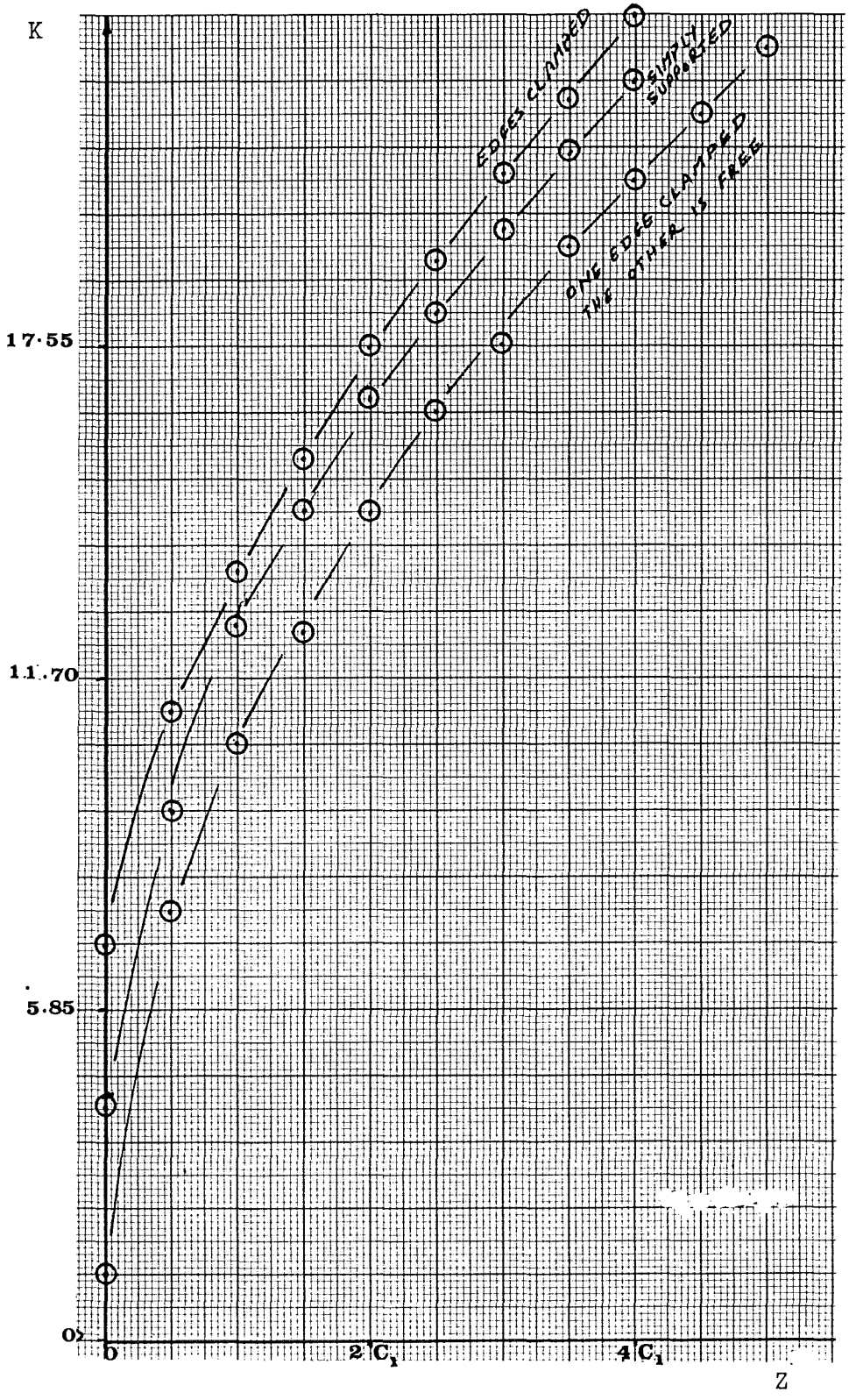

GRAPH (3.12) - BUCKLING ANALYSIS OF PLATE ELASTICALLY SUPPORTED ($A/_B$ = 2, $B/_T$ = 50).

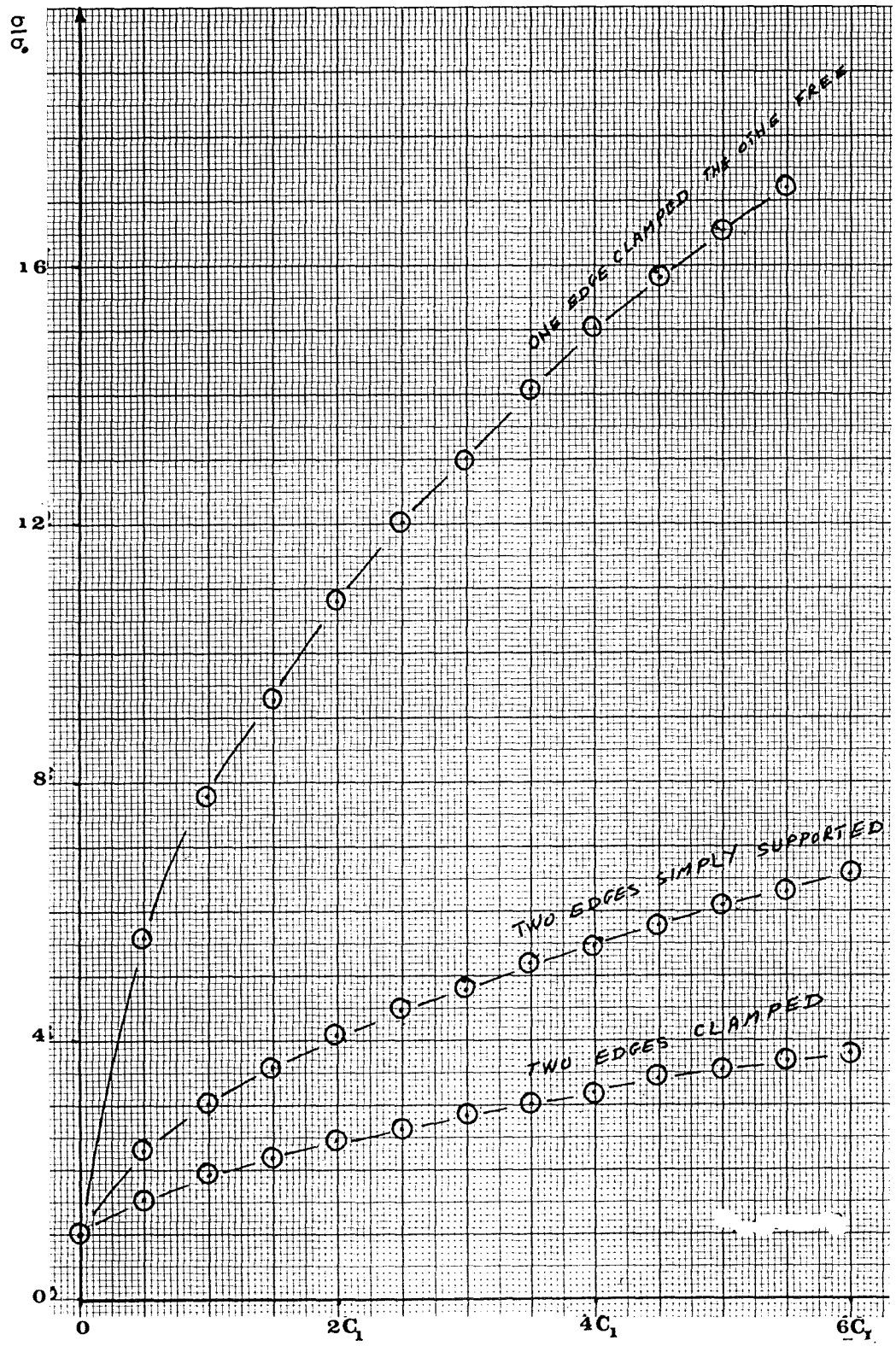

GRAPH (3.13) - RATIO OF BUCKLING STRESS WITH STABILISER TO THE BUCKLING STRESS WITHOUT STABILISER FOR THE SAME PLATE ($A/_B$ = 2, $B/_T$ = 50).

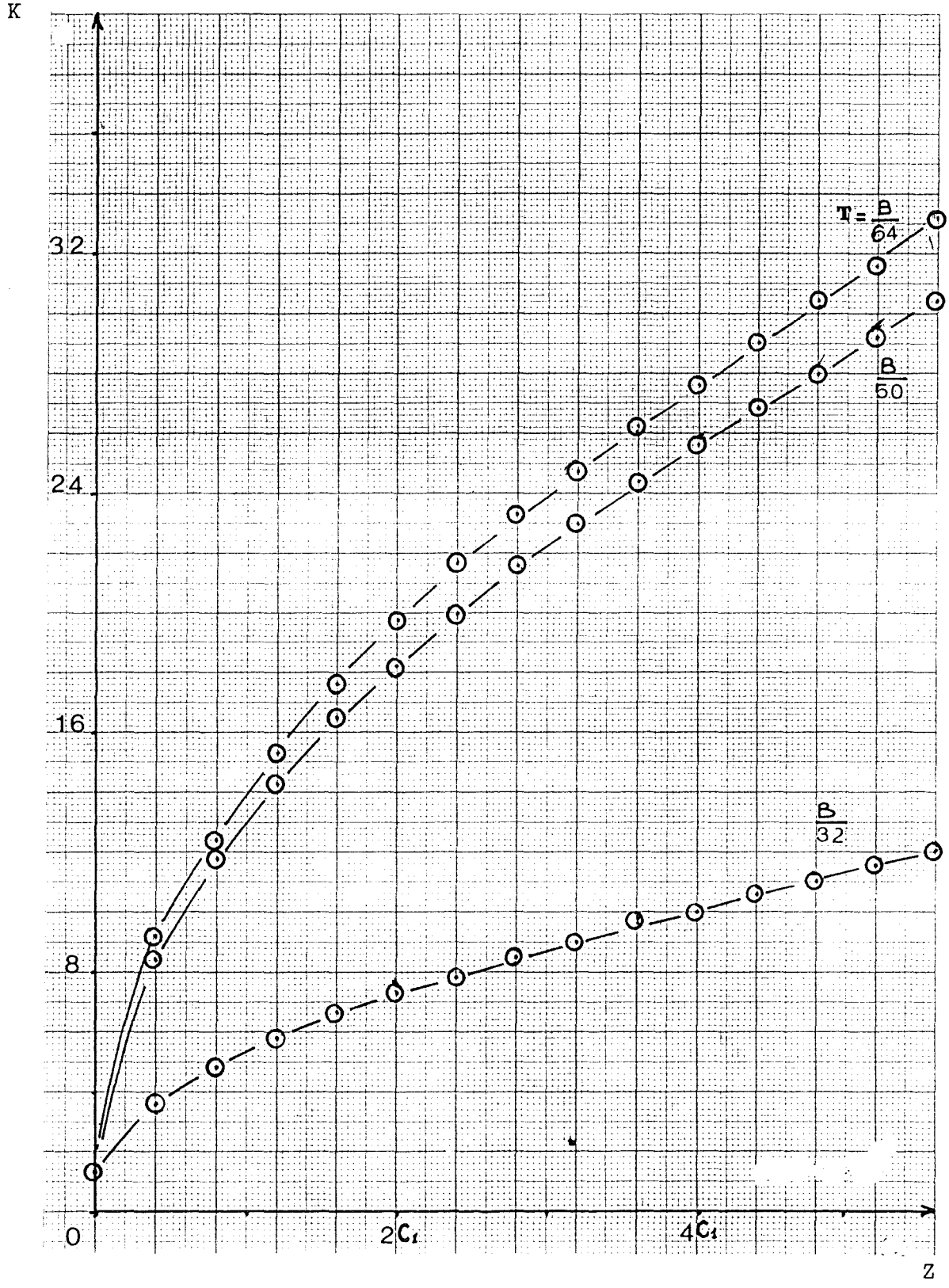

GRAPH (3.14) - BUCKLING STRESS FOR LONG ELASTICALLY SUPPORTED WEBS ($A/_B = 9$).

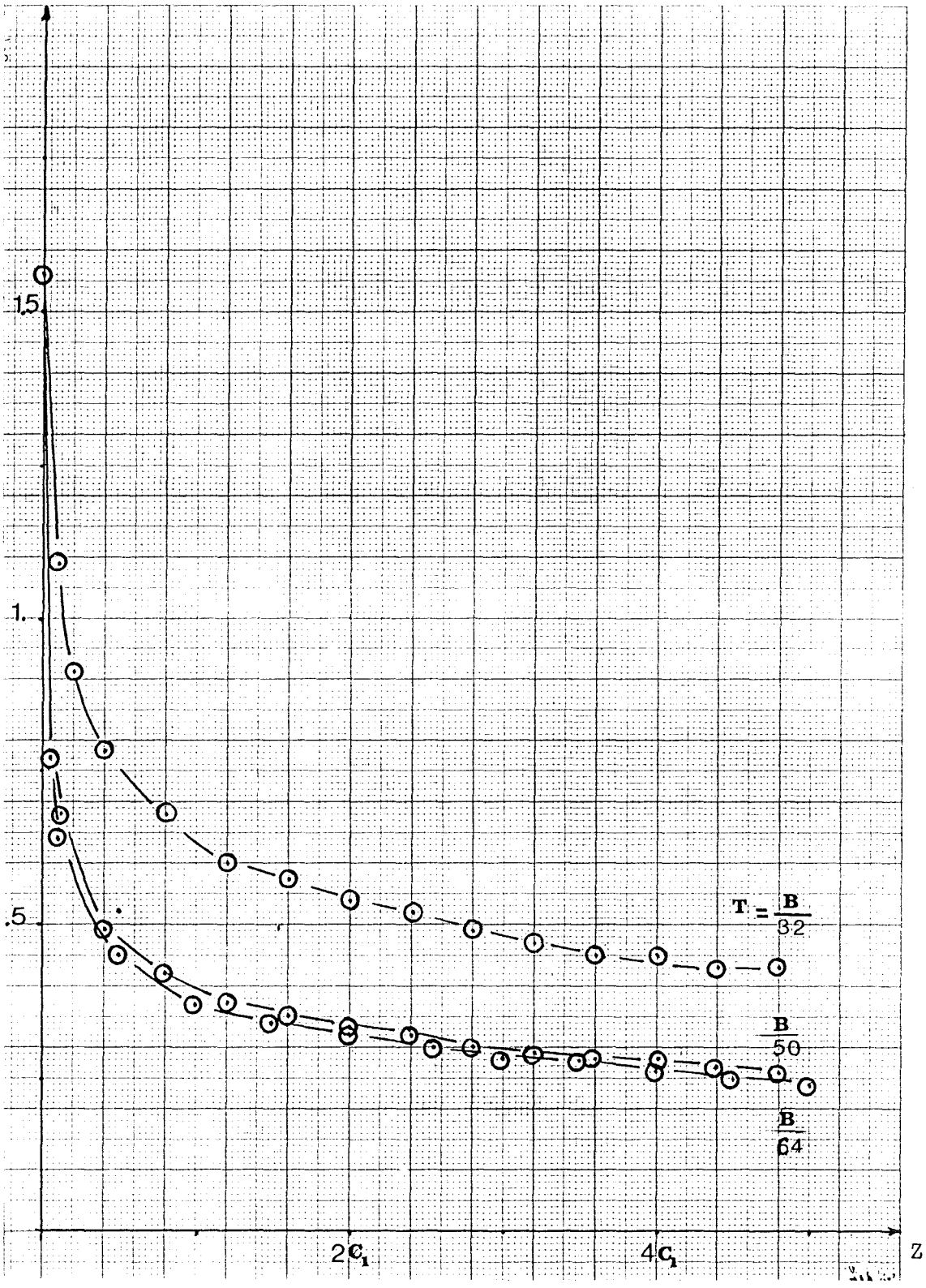

GRAPH (3.15) - BUCKLING ANALYSIS OF ELASTICALLY SUPPORTED WEBS ($A/_B$ = 9) = (CRITICAL WAVE LENGTH).

(c) Results and Conclusions:

1. For a simply supported plate elastically stabilised by an elastic medium the results obtained using the finite strip method agree very well with those obtained by the energy approach of Section (3.2.5.1) .

2. The use of a core material as stabiliser proves to be very effective against buckling of plates and, as can be seen from Graph (3. 6), a very soft material with a small value of Z can increase several times the buckling stress.

3. It is observed that the critical wave length number also increases with increase in the stabiliser stiffness represented by the nondimensional parameter $Z_{..}$

4. The effect of the core is found to reduce the boundary effect and, as can be seen from Graph (3. 12), at the limit the three boundary conditions considered may have the same buckling stress coefficient.

5. The presence of the core increases the stiffness of a clamped-free plate more than in the other two boundary condition cases considered.

As Graph (3.13) shows, the ratio of the buckling stress with infill to that without is highest for clamped-free condition.

6. In Graph (3. 6) the buckling stress as a function of the number of half waves is shown for different values of Z for the same plate.

The critical buckling stress for each value of Z lies at the minimum of the curve.

7. In the study of buckling of stabilised webs as summarised in Graph (3.14), the buckling load increases a great deal especially in the first region after that this increase becomes smaller.

While the critical wave length Graph (3.15), decreases with the increase of support stiffness. It is also interesting to note the dependence of the stabilisation effect on the width-thickness ratio. For the ranges of Z used the benefit increases with the increase of $\frac{B}{T}$.

8. If the elastic modulus of the stabiliser material is given as E_y for the deformation of linearly elastic material under axial pressure we have

$$p = E_y A_r (w/h)$$

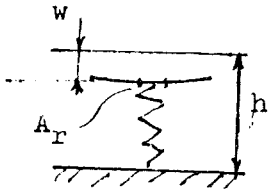

then from spring deformation at the same point

$$p = K_f A_r w$$

equating the two expressions of p

we find:

$$K_f = \frac{E}{h}$$

The validity of this idealisation of the core material will be proved by a series of tests in the next Section before using this assumption in the efficiency study in the next Chapter.

3.2.6. Compression Tests of Webs Supported Along the Faces by Light Weight Core.

Summary:

The results of 21 compression tests on long thin mild steel plates with one long edge clamped and the other free, are presented.

From these tests thirteen were conducted with a light core material acting as a stabiliser for the plates.

The results were compared with the theoretical results obtained using the finite strip method and showed good agreement with the theory.

With a relatively soft support (balsa or polystyrene) a buckling load three to four times higher than the buckling load of an unsupported plate was obtained.

The stabiliser increases the buckling load and the number of half waves in which the plate buckle, and even with relatively large initial deformation present in the plates these buckled into a number of uniform waves very near to the number predicted theoretically.

1. Introduction:

In the previous Section, a study of buckling of plates which are supported on both sides by elastic medium was conducted.

The elastic medium was assumed to behave like a series of closely distributed springs with constant $k_f = E_y/h$ where E_y is the Young's modulus in compression in the direction normal to the faces of the plates, and h is the width of the core material.

Using the finite strip method buckling stresses were computed, and for long plates which has one edge clamped and the other free

/free which are presnet in stiffened types of construction the buckling load was very much increased.

In this Section, the theoretical results obtained are compared with the experimental results and the experimental procedure and apparatus used will be described.

2. Test Specimen :

1. Plates:

The plates are of mild steel, they are 457.mm long and 50.8 mm wide. Eight of them are .79 mm thick and fourteen are 1.59 mm thick.

To determine the material characteristics, in particular σ_p and σ_u tests were made.

a. Determination of σ_p :

Four more plates two of each thickness were used to make the tensile test specimen as shown in Figure (3.15) and Table (3. 20).

The tests were conducted on the Instron machine of G.U.'s Mechanical Engineering Department, which produces plots of load and extension against time. These were combined to give Graph (3.16). The four specimens yielded identical results.

b. Determination of σ_u :

The U.T.S. calculated from tests was found to be 600N/mm^2.

Vichers Hardness tests were conducted on all the compression specimens to detect any variation of properties.

No significant variation was found.

c. The initial deformation of the plates was measured against a straight edge and in Graph (3.17) the plots for three specimen were shown.

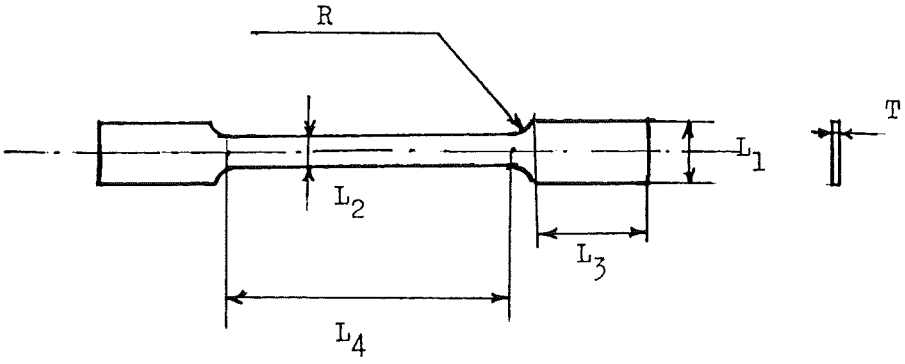

Geometry	Value
L_1	25.4 mm
L_2	12.5
L_3	50.8
L_4	100
T	0.79 (1.59)
R	50.

TABLE (3.20) - DIMENSIONS OF TENSILE TEST SPECIMENS .

GRAPH (3.16) - STRESS-STRAIN DIAGRAM FOR STEEL MATERIAL OF THE WEBS.

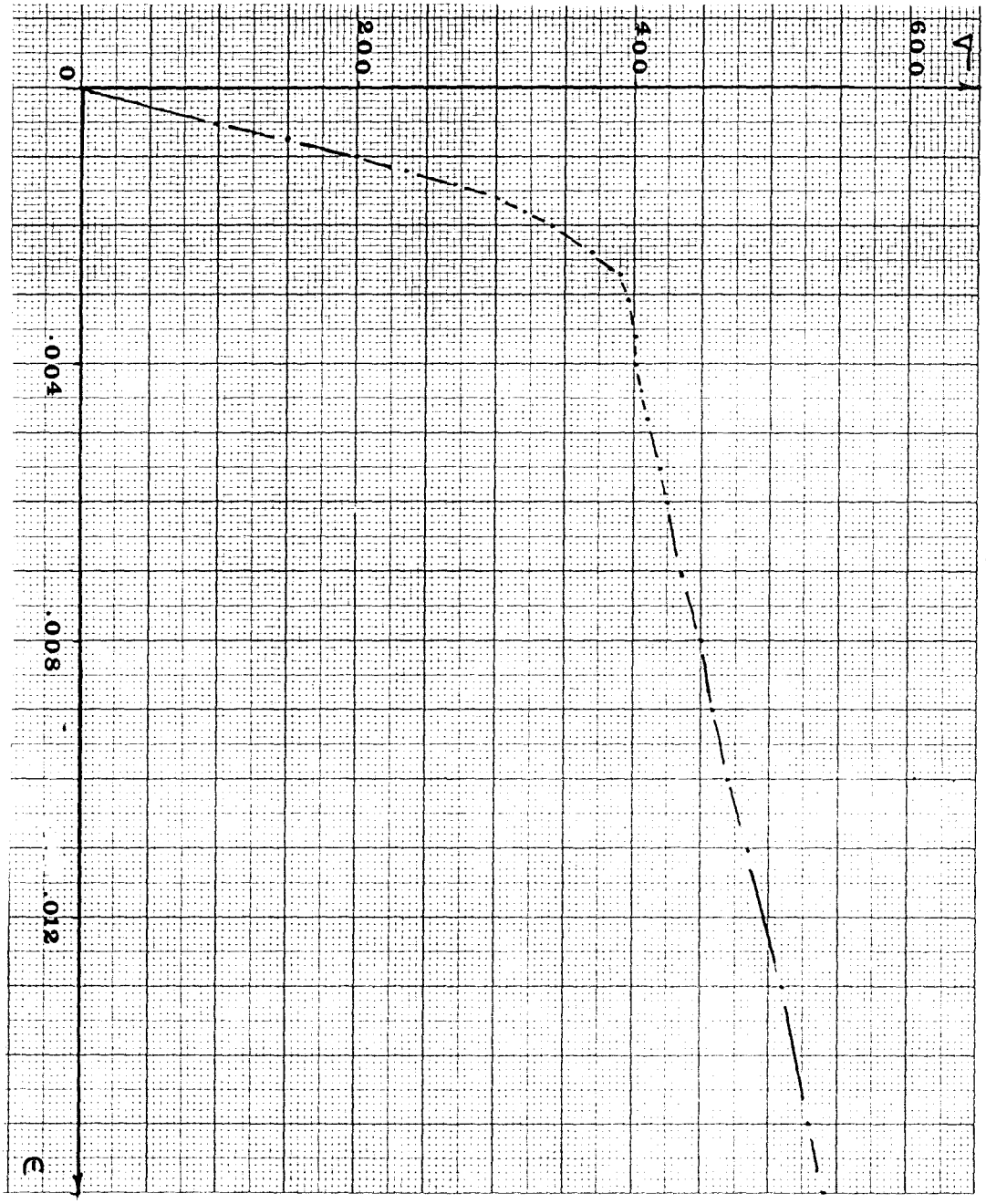

GRAPH (3.17) - INITIAL DEFORMATION OF WEBS.

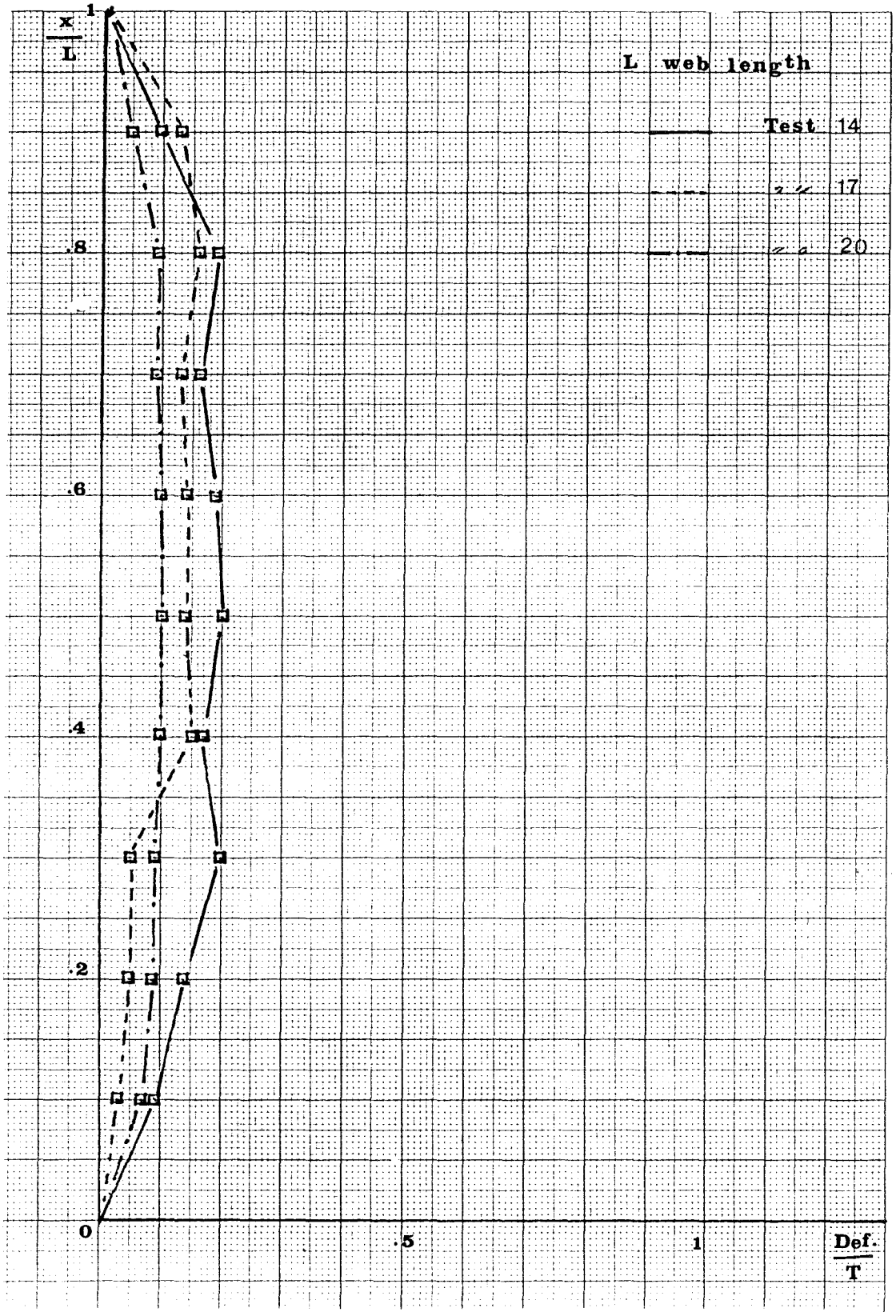

3. Core Materials:

Two types of core material were used:

a. Natural material, balsa wood which was supplied in ten blocks of ($1000 \times 75 \times 75mm^3$) each.

Four blocks were used to produce core material for the 0.79mm thick plates where four tests had to be made, two with core depth equal to 19.705mm, and two with depth equal to 29.705mm. For each test two blocks were required, their length and width being 455mm and 42mm respectively.

For the plates with thickness equal to 1.59mm similar blocks of balsa were prepared for three tests except that here only one depth, 19.205mm was used.

Knowing of the variation of the balsa characteristics, small cubes ($25.4mm^3$) were cut from each block at the time of producing the stabilising blocks. These were tested in compression along three axes to provide the values of Young's Modulus in compression particularly in the direction normal to the face of the plate.

These cubes were also used to find the average density of the balsa used for each test , Figure (3.16) .

In the prepation of the core material high dimensional precision was always preserved by the Department Technician.

b. Artificial Core Material:

This material, a polystyrene type of foam, was available with three types of grains.

Foam 1 - A large grain material, available in a large slab of 35mm thick. From this slab four pieces for two tests were cut, two of thickness 19.205mm and the other two of 29.205mm, the length and width of each being as before.

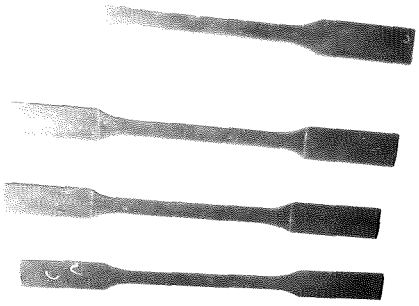

FIGURE (3.15) - SPECIMENS FOR TENSILE TESTS TO FIND (σ - ϵ) PLOT OF WEB MATERIAL.

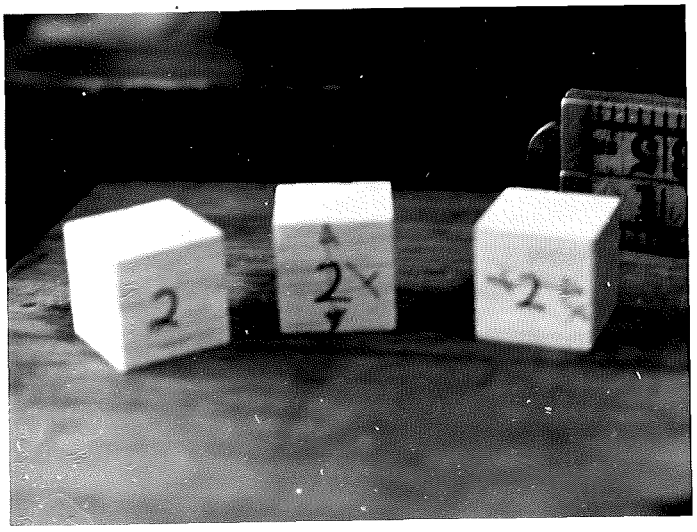

FIGURE (3.16) - CUBES FOR THE DETERMINATION OF YOUNG'S MODULUS OF CORE MATERIAL BY COMPRESSION TESTS.

Foam 2 - Medium grain material, available in wide slabs of 35mm thick.

Also from this slab, four pieces for two tests were cut with dimensions similar to those of Foam 1.

Foam 3 - Fine grain material, available in wide slabs of thickness 45mm. Four pieces for two tests, two of thickness 29.205mm and the other two of thickness 39.205mm, were cut from this material.

For the three foam materials the values of Young's Modulus in compression in the direction normal to the loaded surface, and the density were determined from tests on accurately cut small cubes of the material, ($25.5mm^3$) each.

All the compression tests were conducted using a standard Housnfield Tensometer.

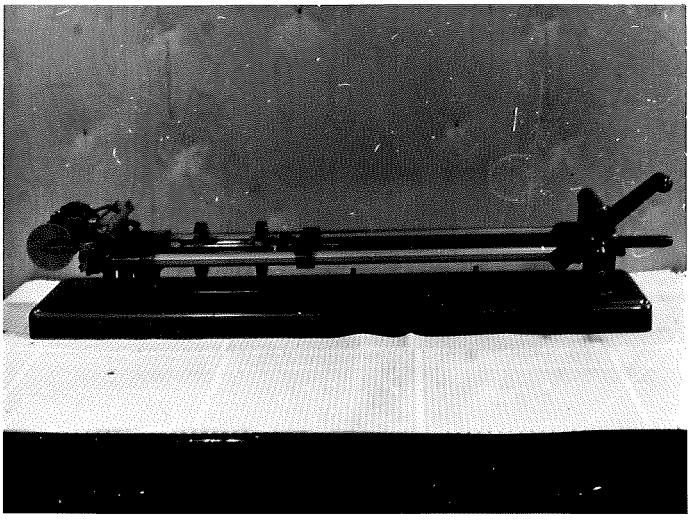

FIGURE (3.17) - HOUSNFIELD TENSOMETER USED TO FIND YOUNG'S MODULUS IN COMPRESSION OF CORE MATERIAL.

4. Test Apparatus:

a. The Loading Machine:

This machine is shown in Figure (3.18). It is manually operated by using the small hand-wheel for loading and the large hand-wheel for unloading.

To apply load the lower platen on which the rig rests moves upward to press the end of the specimen against the upper platen which is constrained by two proving rings, each of nominal capacity 50 kN (5 tons). These were calibrated against the Olsen Testing Machine of the Civil Engineering Department.

Calibration charts for the two ranges 0 - 1 ton, and 0 - 5 tons are shown in Graphs (3.18), (3.19).

b. Testing Rig:

The particulars of the loading rig are shown in Figure (3.20a)

The basis of the rig is two rolled steel channel sections, each with the outer faces of the web and flanges machined flat. The mating flanges were grooved to accommodate the edge constraint strips which were located by steel dowel pins and firmly held by the clamping action of the bolts holding the channels together.

Core support is provided by steel angles bolted to the basic channel sections, provision being made for varying the depth of the core.

At the top there is a plunger, Figure (3.20b) which transmits the load to the specimen. It has ground surfaces and slides between closely fitting guides, themselves with ground surfaces, to ensure as little eccentricity of loading as possible. To ensure uniform/

GRAPH (3.18) - LOADING CELLS CALIBRATION CHART. (RANGE 1 TON).

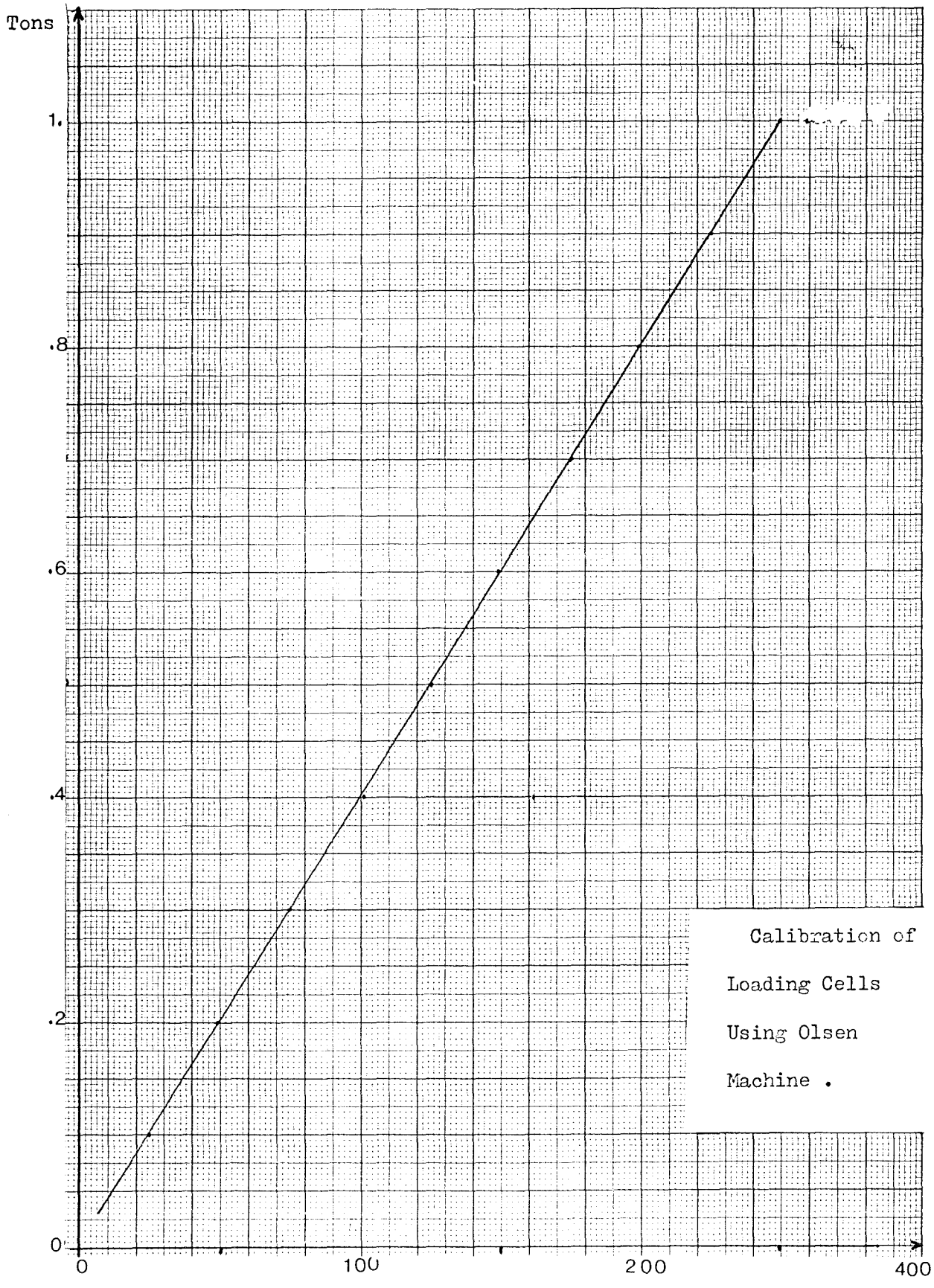

GRAPH (3.19) - LOADING CELLS CALIBRATION CHART. (RANGE 5 TONS).

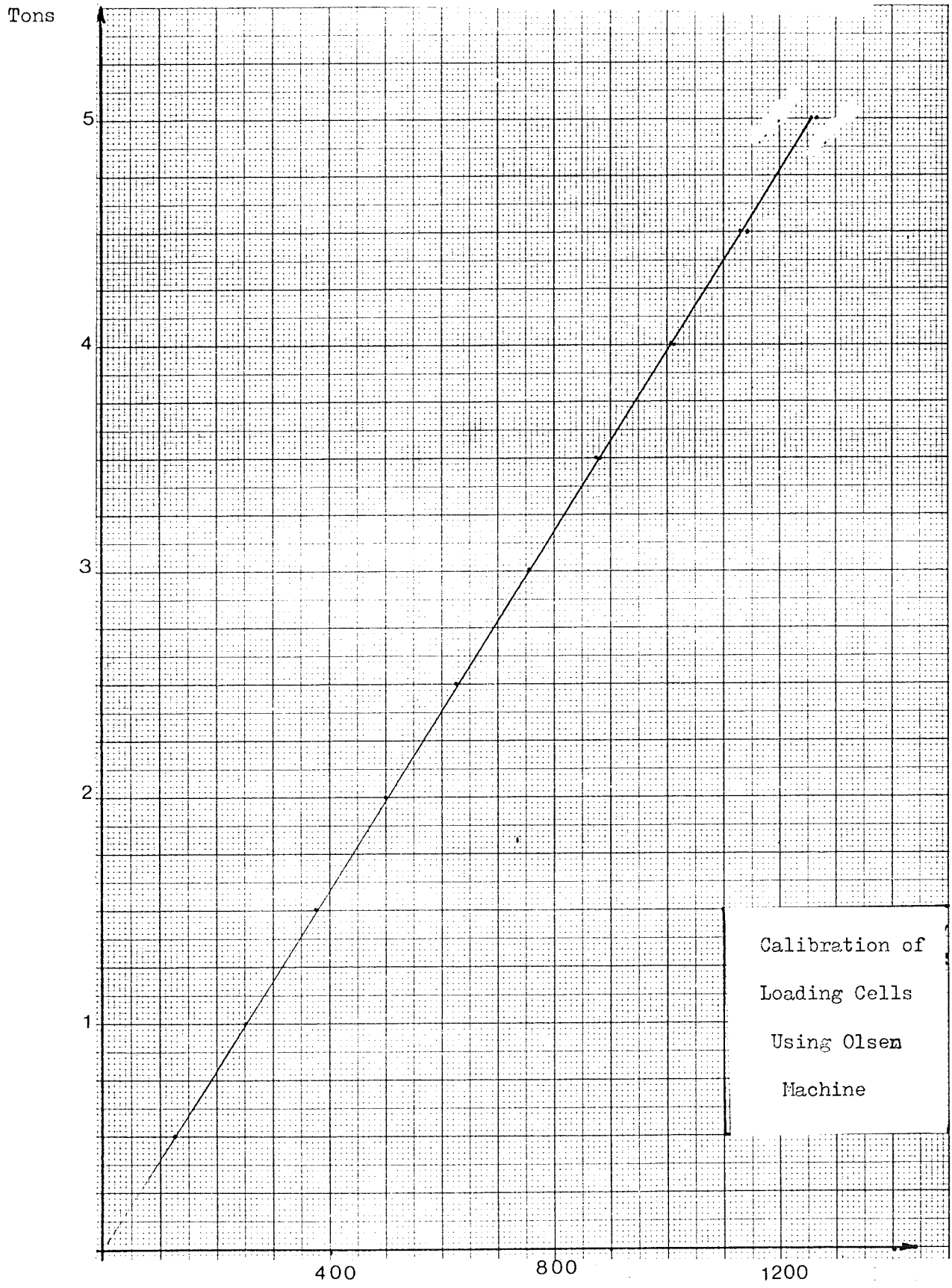

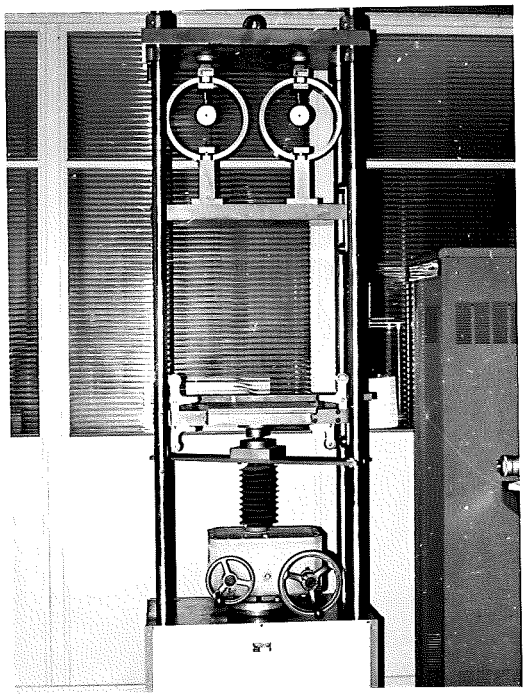

FIGURE (3.18) - COMPRESSION LOADING MACHINE, FULL RANGE = (10 TONS).

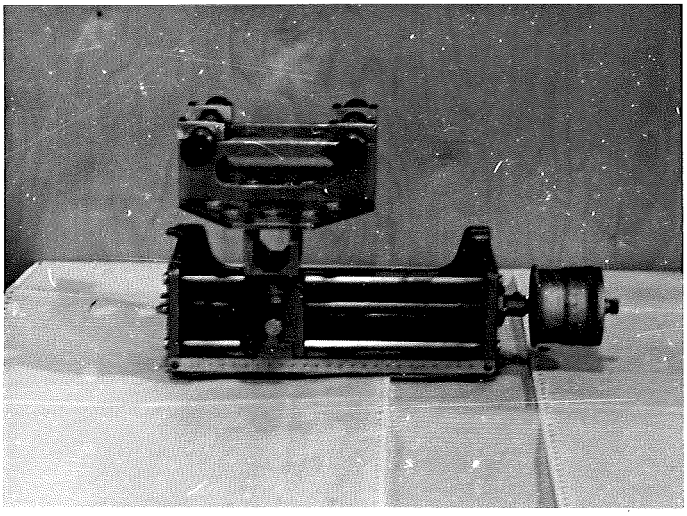

FIGURE (3.19) - TRAVELLING MICROSCOPE, SENSITIVITY (1/200mm).

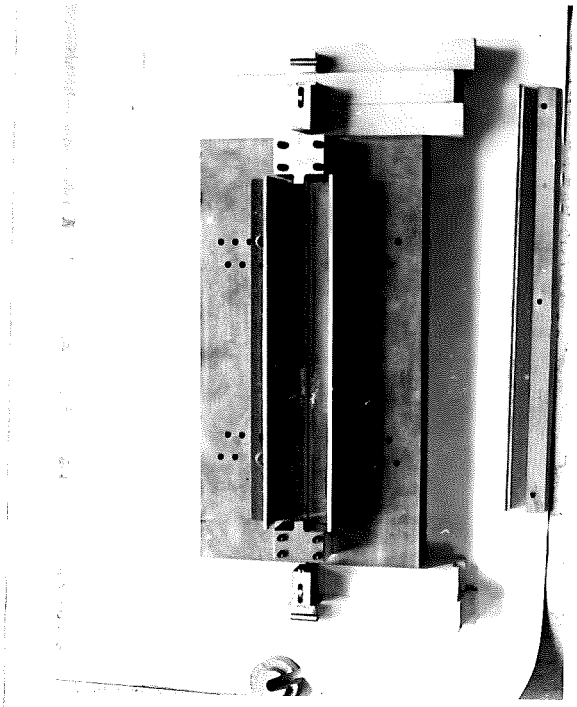

FIGURE (3.20a) - LOADING RIG .

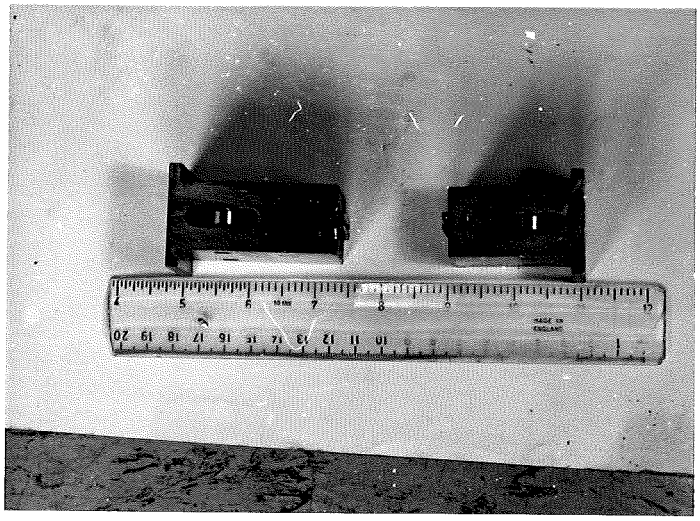

FIGURE (3.20b) - TOP AND BOTTOM PLUNGERS .

/uniform distribution of the load over the full width of the specimen provision has been made for the plunger to rock in the plane of the specimen.

The upper edge of the stringer is inserted into a slotted strip which is a press fit in the plunger.

The bottom loading plunger is essentially similar and both make contact with the loading platens through steel rollers located by shallow transverse grooves positioned at the centre of the loaded width of the specimen.

5. Testing Procedure:

1. The light thinner specimens, each 0.79mm thick, were prepared and cleaned.

2. The rig was assembled and the appropriate edge constraint steel strip inserted and secured.

3. A specimen was fitted and the rig was mounted on the loading platen. In front of the rig provision was made for the travelling microscope to be placed in a position where it could focus clearly on the outer edge of the plate.

4. The loading was carried out and for each step of loading the microscope reading and the level of load was recorded.

5. Four tests were conducted without core material, two with balsa core material 19.705mm thick, and another two with balsa core material 29.705mm thick.

6. After each test was completed, the buckling pattern of the specimen was photographed and the length of the critical wave length measured.

7. The rig was dismantled and the edge constraint strip for the specimens of thickness 1.59mm was fitted and the whole procedure repeated for the remaining thirteen specimens of thickness 1.59mm. Four were tested without core material, three with balsa core of thickness 19.205mm, two with cores of Foam 1 of thickness 19.205mm and 29.205mm respectively, two with cores of Foam 2 of thickness

/thickness 19.205 and 29.205mm, and two with core of Foam 3 of thickness 29.205 and 39.205mm.

8. In all the tests involving cores, the core blocks were slid into place carefully, small adjustments being made to ensure uniform contact between the specimen and the cores without deforming the specimen.

9. In all cases, the value recorded for the buckling load was that needed to produce a clearly defined wave pattern. Although this load was greater than that necessary to initiate instability the increase was small, certainly not more than 5%.

6. Experimental Results:

The results of the compression tests on the plates are given Tables (3.21) to (3.24) . Included in these Tables, is the following information:

1. Geometry and material characteristics of plate material.

2. Geometry and material characteristics of core material.

3. Theoretical buckling load and theoretical critical wave length. Figures (3.22) to (3.43) show the buckled shape of typical specimens.

7. Discussion of the Results and Conclusions:

1. The buckling phenomenon in all tests appeared as a snap into the final buckling shape. the initial displacement did not develop continuously as the load increased but oscillated with amplitude of about $0.2T$, where T is the thickness of the plate.

2. It was intended to use the displacements, as observed through the microscope, to provide the basis for a Southwell type plot, but because of the non-linear behaviour this proved to be impossible. The observation of the displacements did serve to identify the onset of buckling.

3. For the thinner plates the buckling load using the softest balsa was found to be four times that of the buckling load without core, and for the harder type of balsa the factor of improvement increased to 6.

4. For plates of thickness 1.59mm, the balsa type of core produced only twice the buckling load without core, which confirms the idea that the use of the core is more profitable with thinner plates.

5. In all tests the results proved to be in close agreement with the theory developed in the previous Section, using the finite strip.

6. Using the balsa core the buckling wave length was found to be slightly shorter than that predicted theoretically. This might be due to the shear effect which is not accounted for in the theoretical analysis.

7. The value of the K_f constant modulus used in the theoretical analysis as $\frac{E_y}{h}$ was found to be a good and reasonable representation of the core stiffness and the neglect of the shear stiffness contribution of the core does not introduce a large error in the computation for the types of core material considered.

8. Initial deformation of the plates does not seem to affect the outcome of the tests and the buckled shape did not follow the initial deformation of the plates.

9. From the test results for unsupported plates, the thinner plates showed better agreement with the theory.

10. For the plates supported elastically both types showed the same degree of accuracy.

11. For the plates supported by an elastic medium, the experimental buckling wave lengths showed better agreement with the theoretical values than was the case for unsupported plates. this suggests that the presence of the infill material reduces the effect of the initial deformation on the value of the buckling stress.

12. It appears that the balsa core produced results in closer agreement with the calculated values than did the polystyrene core comparing Tests 15 and 18, in which the values of E_y/h are the same.

13. Finally, as was predicted theoretically, the use of a light core material can provide adequate support and can increase the buckling load very considerably even for the weakest type of construction.

The formula used for the estimation of the core stiffness E_y/h is accurate enough and the balsa wood behaves reasonably well as a core material. The core contribution to stiffness extends into the inelastic region as can be observed from Tests 13, 14, 15, 16 and 8.

Note :The theoretical results were taken from Figure (3.14) and Figure (3.15). To take into account the practical approximation to the boundary condition the width was assumed to be the actual width of the plate minus half the width of the slot. This means that the deflection and rotation of the constrained edge are zero along the mid-line of the part of the plate inside the slot.

TABLE (3.21) - THEORETICAL AND EXPERIMENTAL BUCKLING LOADS FOR UNSUPPORTED STEEL PLATES (THICKNESS = 0.79mm).

TEST NO.	PLATE MATERIAL (N/mm^2)			PLATE GEOMETRY (mm)			BUCKLING LOAD (KN)		CRITICAL STRESSES N/mm^2		CRITICAL WAVE LENGTH (mm)		FIGURE
	E	$\sigma_{.2}$	σ_u	A	B	T	P_{TH}	P_{EX}	σ_{TH}	σ_{EX}	λ_{TH}	λ_{EX}	
1	210000.0	400.0	600.0	457.0	50.8	0.79	2.624	2.400	71.76	60.70	72.2	91.4	(3.21
2	210000.0	400.0	600.0	457.0	50.8	0.79	2.624	2.240	71.76	57.70	72.2	91.4	(3.22)
3	210000.0	400.0	600.0	457.0	50.8	0.79	2.624	2.320	71.76	58.70	72.2	91.4	
4	210000.0	400.0	600.0	457.0	50.8	0.79	2.624	2.400	71.76	60.70	72.2	91.4	

TABLE (3.22) - THEORETICAL AND EXPERIMENTAL BUCKLING LOADS FOR UNSUPPORTED STEEL PLATES (THICKNESS = 1.59mm).

TEST	PLATE MATERIAL N/mm^2			PLATE GEOMETRY (mm)			BUCKLING LOAD (TONS)		BUCKLING STRESS (N/mm^2)	BUCKLING WAVE LENGTH (mm)		FIGURE
NO.	E	$\sigma_{.2}$	σ_u	A	B	T	P_{TH}	P_{EX}	σ_{EX}	λ_{TH}	λ_{EX}	
9	210000.0	400.0	600.0	457.0	50.8	1.59	2.061	1.600	201.3	78.0	91.4	(3.27)
10	210000.0	400.0	600.0	457.0	50.8	1.59	2.061	1.600	201.3	78.0	91.4	
11	210000.0	400.0	600.0	457.0	50.8	1.59	2.061	1.884	236.9	78.0	91.4	(3.28)
12	210000.0	400.0	600.0	457.0	50.8	1.59	2.061	1.700	213.8	78.0	91.4	

TABLE (3.23) - THEORETICAL AND EXPERIMENTAL RESULTS OF TESTS ON (0.79mm) STEEL PLATES STABILISED BY ELASTIC MEDIUM.

TEST NO.	CORE TYPE	YOUNG'S MODULUS IN COMPRESSION FOR CORE (N/mm^2)			CORE DENSITY g/mm^3	CORE GEOMETRY mm			SPRING CONSTANT MODULUS N/mm^3	BUCKLING LOAD (TONS)		BUCKLING STRESS N/mm^2	CRITICAL WAVE LENGTH		FIGURE
		Ex	Ez	Ey	ρ_c	A	B	h	$k_f = E_y/h$	P_{TH}	P_{EX}	σ_{EX}	λ_{TH}	λ_{EX}	
5	BALSA	2000.0	107.0	40.0	$1.896\ 10^{-4}$	457.0	50.8	30	1.3	.918	.880	222.0	29.3	30.0	(3.23) , (3.
6	BALSA	2000.0	54.0	45.0	$1.628\ 10^{-4}$	457.0	50.8	20	2.25	1.1009	1.007	253.1	27.9	25.4	
7	BALSA	2400.0	45.0	45.0	$1.445\ 10^{-4}$	457.0	50.8	30	1.5	.914	1.080	243.4	29.6	30.5	
8	BALSA	2400.0	94.0	67.0	$1.781\ 10^{-4}$	457.0	50.8	20	3.35	1.466	1.449	367.0	23.2	26.8	(3-25), (3-26)

TABLE (3.24) - THEORETICAL AND EXPERIMENTAL RESULTS OF TESTS ON (1.59mm) STEEL PLATES STABILISED BY ELASTIC MEDIUM.

TEST NO.	CORE TYPE	CORE MATERIAL YOUNG'S MODULUS IN COMPRESSION N/mm^2			CORE DENSITY g/mm^3	CORE GEOMETRY mm			SPRING MODULUS N/mm^3	CRITICAL LOAD TONS		EXPERIMENTAL AVERAGE STRESS (N/mm^2)	CRITICAL WAVE LENGTH mm		FIGURE
		Ex	Ez	Ey	ρ_c	A	B	h	$k_f = E_y^f/h$	P_{TH}	P_{EX}	σ_{EX}	λ_{TH}	λ_{EX}	
13	BALSA	1600.0	62.0	54.0	$1.176\ 10^{-4}$	457.0	50.8	20	2.7	3.95	3.84	483.8	46.0	35.15	
14	BALSA	1600.0	40.0	40.0	$1.166\ 10^{-4}$	457.0	50.8	20	2.0	3.62	3.20	403.2	47.0	38.08	(3.29),(3.30)
15	BALSA	2000.0	60.0	36.0	$2.665\ 10^{-4}$	457.0	50.8	20	1.8	3.44	3.20	403.2	48.5	38.08	
16	FOAM 1	42.5	42.5	42.5	$.872\ 10^{-4}$	457.0	50.8	20	2.1	3.67	2.90	365.4	47.0	45.7	(3.31),(3.32)
17	FOAM 1	42.5	42.5	42.5	$.872\ 10^{-4}$	457.0	50.8	30	1.4	3.12	2.60	327.6	49.5	45.7	(3.33),(3.34)
18	FOAM 2	36.0	36.0	36.0	$.762\ 10^{-4}$	457.0	50.8	20	1.8	3.44	2.60	327.6	48.5	50.7	(3.35), (3.36)
19	FOAM 2	36.0	36.0	36.0	$.762\ 10^{-4}$	457.0	50.8	30	1.2	3.02	2.60	327.6	47.5	50.7	(3.37),(3.38)
20	FOAM 3	30.0	30.0	30.0	$.682\ 10^{-4}$	457.0	50.8	30	1.0	2.95	2.40	302.4	62.5	65.2	(3.39),(3.40)
21	FOAM 3	30.0	30.0	30.0	$.682\ 10^{-4}$	457.0	50.8	40	0.75	2.78	2.16	272.2	67.5	76.2	(3.41),(3.42)

FIGURE (3. 21) - BUCKLED SHAPE OF 0.79mm STEEL PLATE CLAMPED AT THE INNER EDGE.

TEST 1

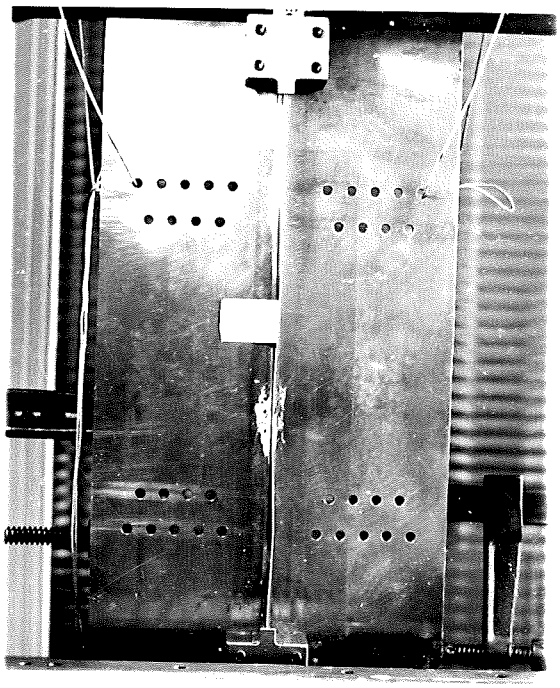

FIGURE (3.22) - BUCKLED SHAPE OF 0.79mm STEEL PLATE CLAMPED AT THE INNER EDGE.

TEST 2.

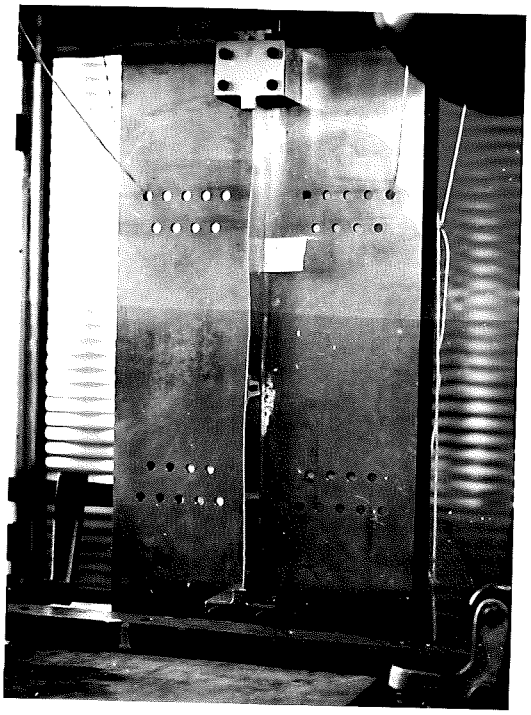

FIGURE (3.23) - BUCKLED SHAPE OF 0.79mm STEEL PLATE SUPPORTED BY BALSA BLOCKS 30 mm WIDE.

TEST 5.

FIGURE (3.24) - BUCKLING WAVE LENGTH OF PLATE.

TEST 5

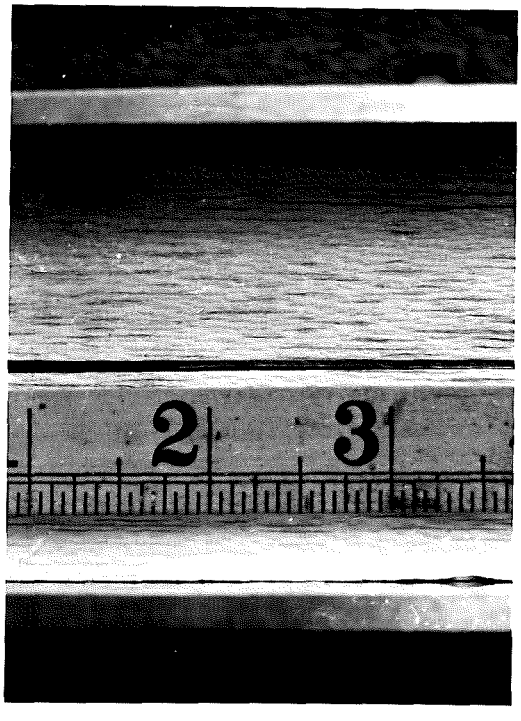

FIGURE (3.25) - BUCKLED SHAPE OF 0.79mm STEEL PLATE SUPPORTED BY BALSA BLOCKS 20mm WIDE.

TEST 8

FIGURE (3.26) - BUCKLING WAVE LENGTH OF TEST 8.

FIGURE (3.27) - BUCKLED SHAPE OF 1.59mm STEEL PLATE CLAMPED AT THE INNER EDGE.

TEST 9

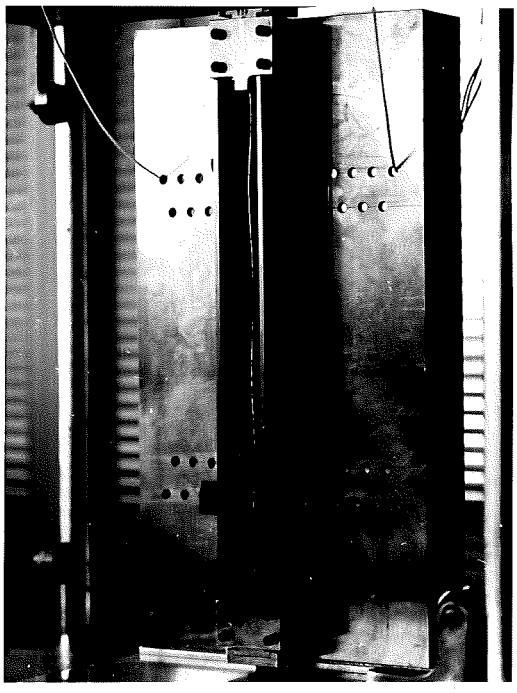

FIGURE (3.28) - BUCKLED SHAPE OF 1.59mm STEEL PLATE CLAMPED AT THE INNER EDGE.

TEST 11

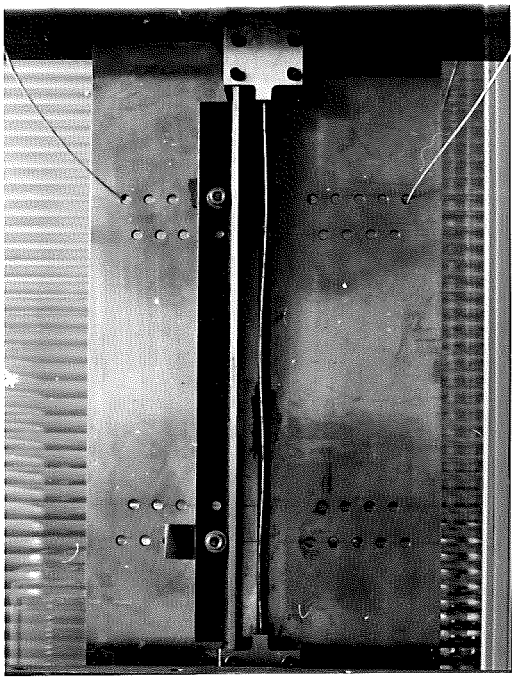

FIGURE (3.29) - BUCKLED SHAPE OF 1.57mm STEEL PLATE SUPPORTED BY BALSA BLOCKS 20mm WIDE.

TEST 14

FIGURE (3.30) - BUCKLING WAVE LENGTH OF PLATE

TEST 14

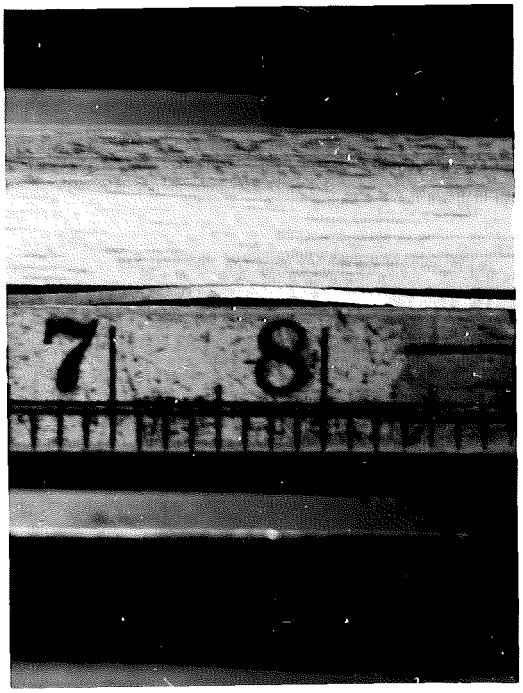

FIGURE (3.31) - BUCKLED SHAPE OF 1.59mm THICK STEEL PLATE SUPPORTED BY BLOCKS OF FOAM MATERIAL TYPE FOAM 1 (20mm) WIDE.

TEST 16

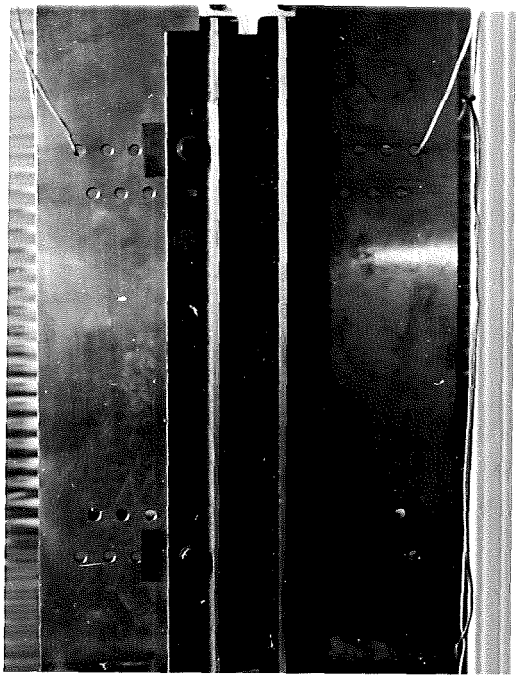

FIGURE (3.32) - BUCKLING WAVE LENGTH OF TEST 16.

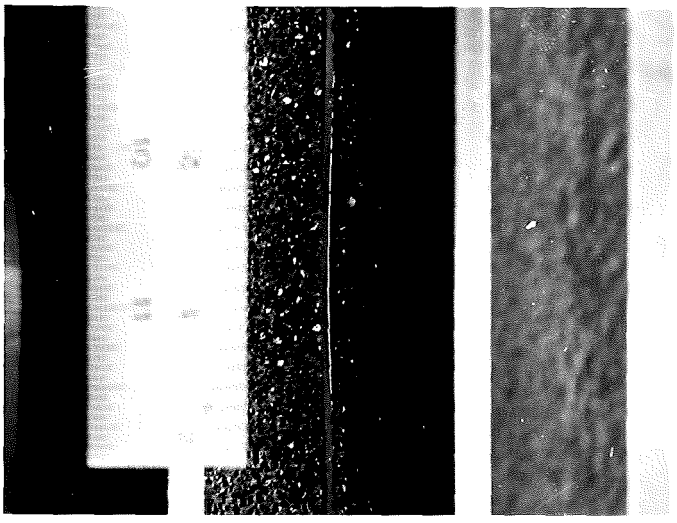

FIGURE (3.33) - BUCKLED SHAPE OF 1.59mm THICK STEEL PLATE SUPPORTED BY BLOCKS OF FOAM 1 (30mm) WIDE.

TEST 17

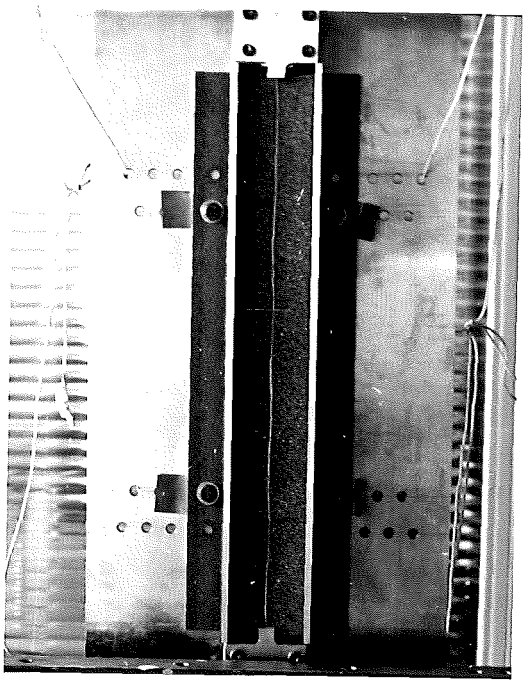

FIGURE (3.34) - BUCKLING WAVE LENGTH OF TEST 17.

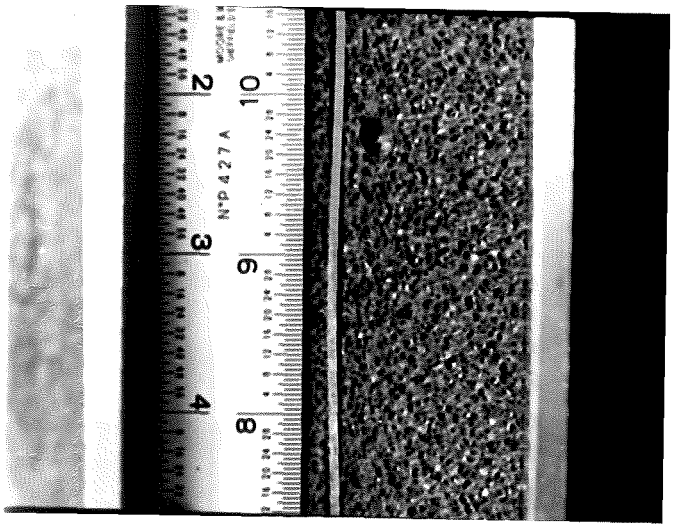

FIGURE (3.35) - BUCKLED SHAPE OF 1.59mm STEEL PLATE SUPPORTED BY FOAM 2 BLOCKS 20mm WIDE.

TEST 18

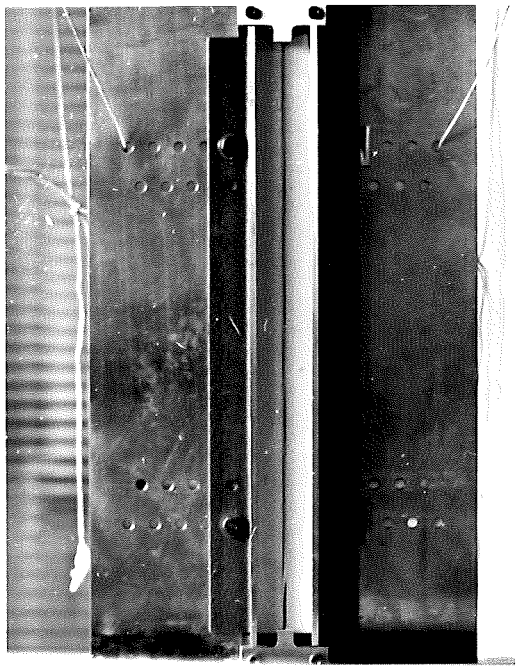

FIGURE (3.36) - BUCKLING WAVE LENGTH OF TEST 18.

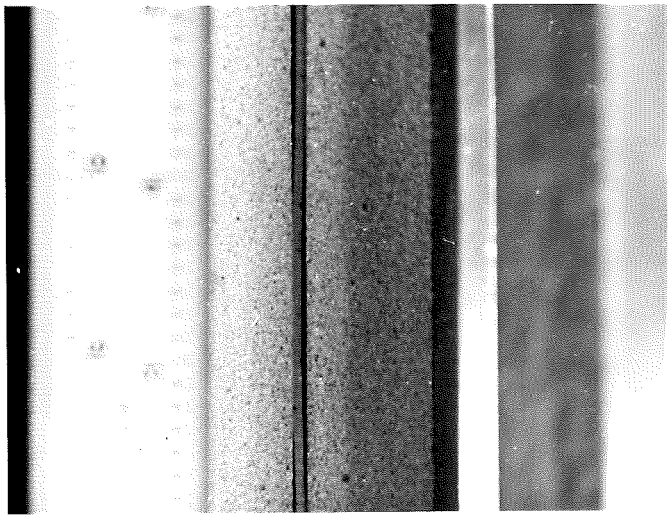

FIGURE (3.37) - BUCKLED SHAPE OF 1.59mm STEEL PLATE SUPPORTED BY FOAM 2 BLOCKS 30mm WIDE.

TEST 19

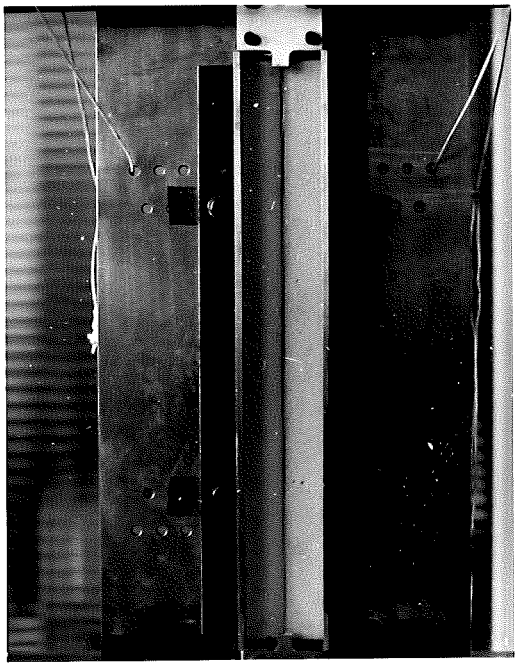

FIGURE (3.38) - BUCKLING WAVE LENGTH OF TEST 19.

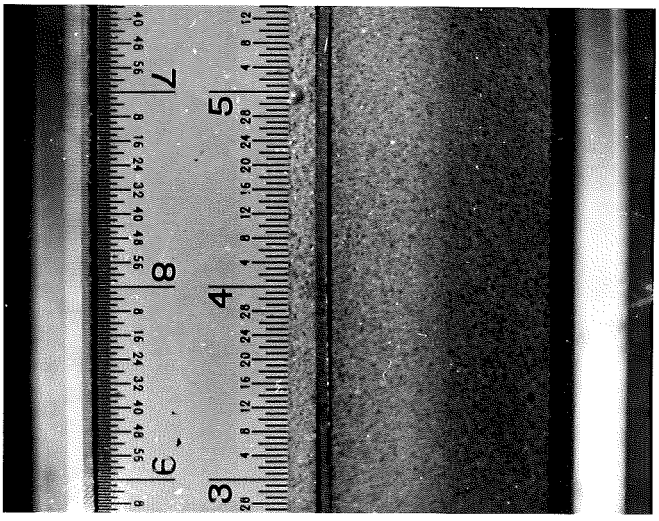

FIGURE (3.39) - BUCKLED SHAPE OF 1.59mm STEEL PLATE SUPPORTED BY FOAM 3 BLOCKS 30mm WIDE.

TEST 20

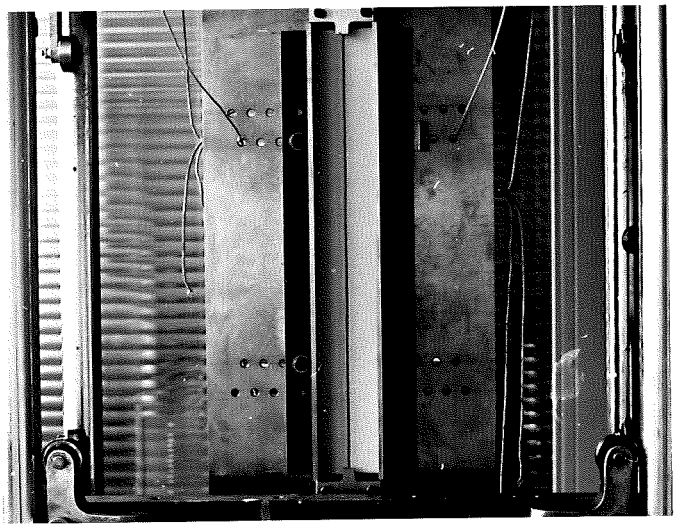

FIGURE (3.40) - BUCKLING WAVE LENGTH OF TEST 20.

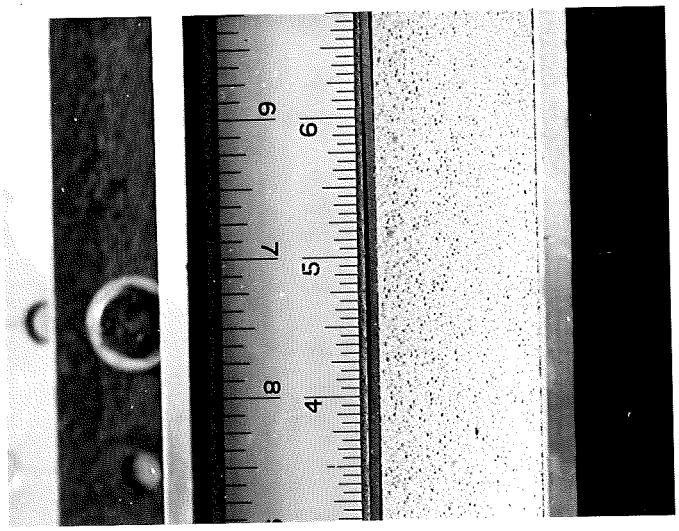

FIGURE (3.41) - BUCKLED SHAPE OF 1.59mm STEEL PLATE SUPPORTED BY FOAM 3 BLOCKS 40mm WIDE.

TEST 21

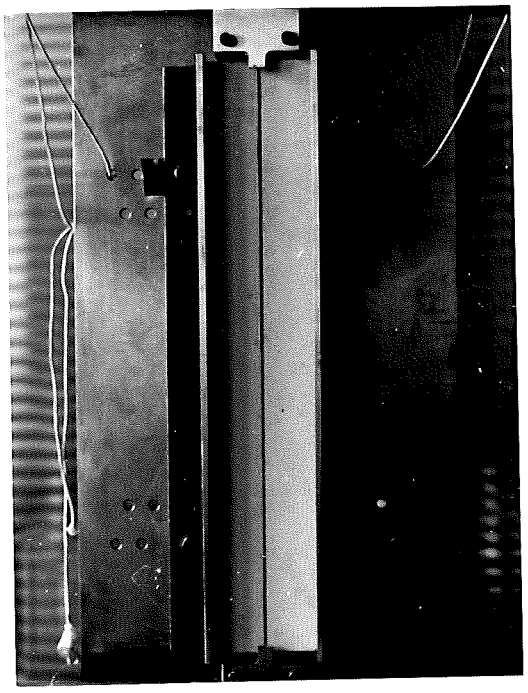

FIGURE (3.42) - BUCKLING WAVE LENGTH OF TEST 21.

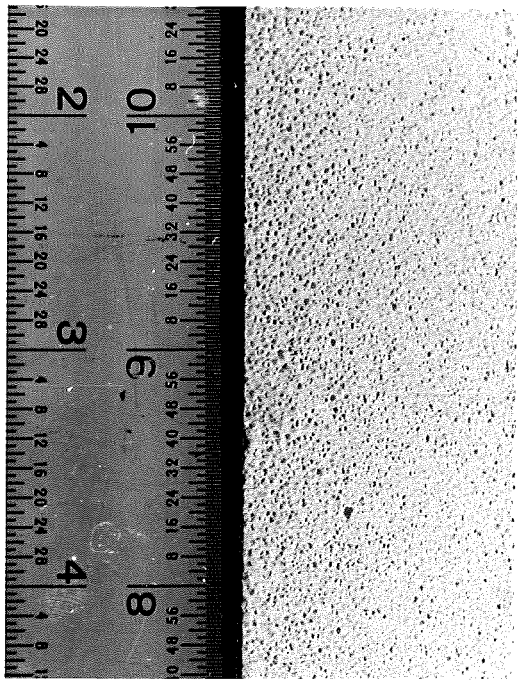

3.2.7. COMPOSITE PANEL.

3.2.7.1. Introduction:

In the study of the local instability of longitudinally stiffened panels it was found that unless T_w/T_s is very large, the buckling stress rapidly decreases as the ratio B_w/B_s increases.

This local buckling behaviour influenced the minimum weight design of such panels and resulted in minimum weight proportions corresponding to short stiffeners of large thickness.

In Ref. (5), these proportions were found to be : T_w/T_s = 2.25, B_w/B_s = 0.65, with total weight distributed as 1.45 in the stiffeners and 1.0 in the skin.

This sturdy geometry resulting for the optimum design suggested that a more efficient panel would be obtained if means could be found to improve the local buckling behaviour.

From the preceding section, in which the instability of plates supported by an elastic medium was studied, and, in particular from the study of long webs, a very useful property has emerged.

It appears that the buckling load for a web or of a narrow strip can be increased a great deal if the web is supported by a continuous elastic medium. This elastic medium can be effective in stabilising such structural elements even if it possesses a low value of Young's Modulus.

This property will be used here to improve the local stability characteristics for longitudinally stiffened panels. A composite panel will be constructed with longitudinal stiffeners separated by an elastic medium arranged between these stiffeners and in this section, the local buckling behaviour will be studied.

It will be seen that this panel proves to be very efficient.

3.2.7.2. Description and Assumptions:

The composite panel to be studied is represented in Figure (3.43). It consists of a plate divided by longitudinal stiffeners with an elastic core material between the stiffeners. The object of the stiffeners is to increase the load capacity by carrying part of the load and also by dividing the plate into a series of narrow strips of low $B/_T$ value.

The core material will primarily act as a stabiliser for the stiffeners against the onset of local buckling.

The local buckling mode considered here is shown in Figure (3.43)., this involves local buckling of the stringers plus distortion of the plate.

Every two consecutive stringers rotate the same amount but in opposite directions, the wave length being of the order of the stringer spacing.

The cross-section will be regarded as made up of thin flat plates joined edge to edge and those which form the stiffeners are assumed to rest on an elastic medium which acts as a foundation. The spring constant (K_f) for this foundation is given as the ratio of the Young's Modulus in the direction normal to the plane of the stiffeners (E_y) to the distance between the stiffener and the midplane plane formed as a result of the buckling shape assumed:

$$\text{i.e.} \quad K_f = \frac{E_y}{0.5B_s} \quad \text{approximately if } \frac{T_w}{B_s} \text{ is small}$$

In the local buckling mode the longitudinal lines of intersection of the mid-lines of the plate and stiffeners remain straight. It is assumed that the side constraint effects are negligible.

3.2.7.3. Finite Element Idealisation:

The finite element grid is shown in Figure (3.12b), together with the numbering system used for the nodes. Six finite strips are used, two for the stringer and two for the plate on each side of it.

The elastic and geometric stiffness matrices are given in Table (3.14), and Table (3.15), the matrix of the spring constant effect of the core material is given in Table (3.19).

The nodal numbering matrix **ND** (I,J) and the matrix of boundary conditions **NB** (I) are given in Table (3.16b) . The computer Programme (PROGRAMME (3.5)), is given in Chapter 5.

The programme yields the buckling shape in the form of an eigenvector and gives also the buckling stress and critical wave length.

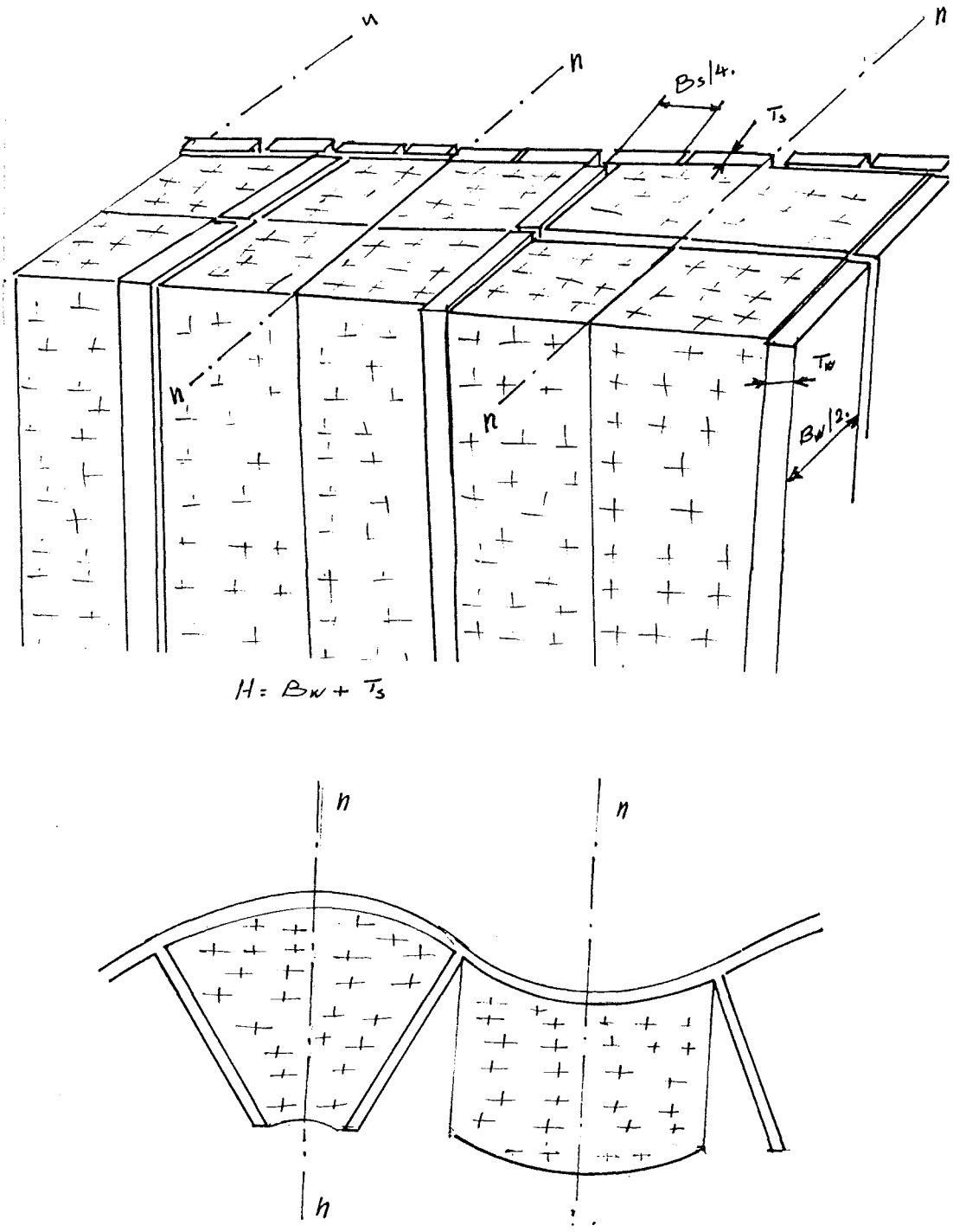

FIGURE (3.43) - COMPOSITE PANEL IDEALISATION AND ASSUMED BUCKLING SHAPE.

3.2.7.4. Presentation of the Results of this Study.

For composite panel of relatively large width, K versus B_w/B_s has been plotted for a range of T_w/T_s and Z.

Where

K = is the local buckling stress coefficient $\dfrac{\sigma}{E\left(\dfrac{T_s}{B_s}\right)^2}$

H = cross-section depth $(B_w + T_s)$

K_f = spring constant of the core material.

E = is the Young's Modulus for the skin material.

$Z = \dfrac{K_f}{D}\left(\dfrac{H}{\pi}\right)^4$

The ratio T_w/T_s is held fixed while B_w/B_s is varied from 0.2 to 1.2 for different values of Z to determine the buckling load and the effectiveness of the core material as a stabiliser and to single out for each combination of $(T_w/T_s,\ B_w/B_s)$ the critical value of Z, which can be considered from a practical point of view as the parameter which represents the minimum stiffness of the core material necessary to fully stabilise the stiffeners against the onset of local instability.

The procedure is repeated for different values of T_w/T_s. In all, values of T_w/T_s of 0.25, 0.5, 0.75, 1.0 and 1.5 are considered.

These plots are given in Graphs (3.20) through (3.24).

GRAPH (3.20) - LOCAL BUCKLING OF COMPOSITE PANEL K IN FUNCTION OF NONDIMENSIONAL CORE STIFFNESS PARAMETER Z (T_w/T_s = 0.25).

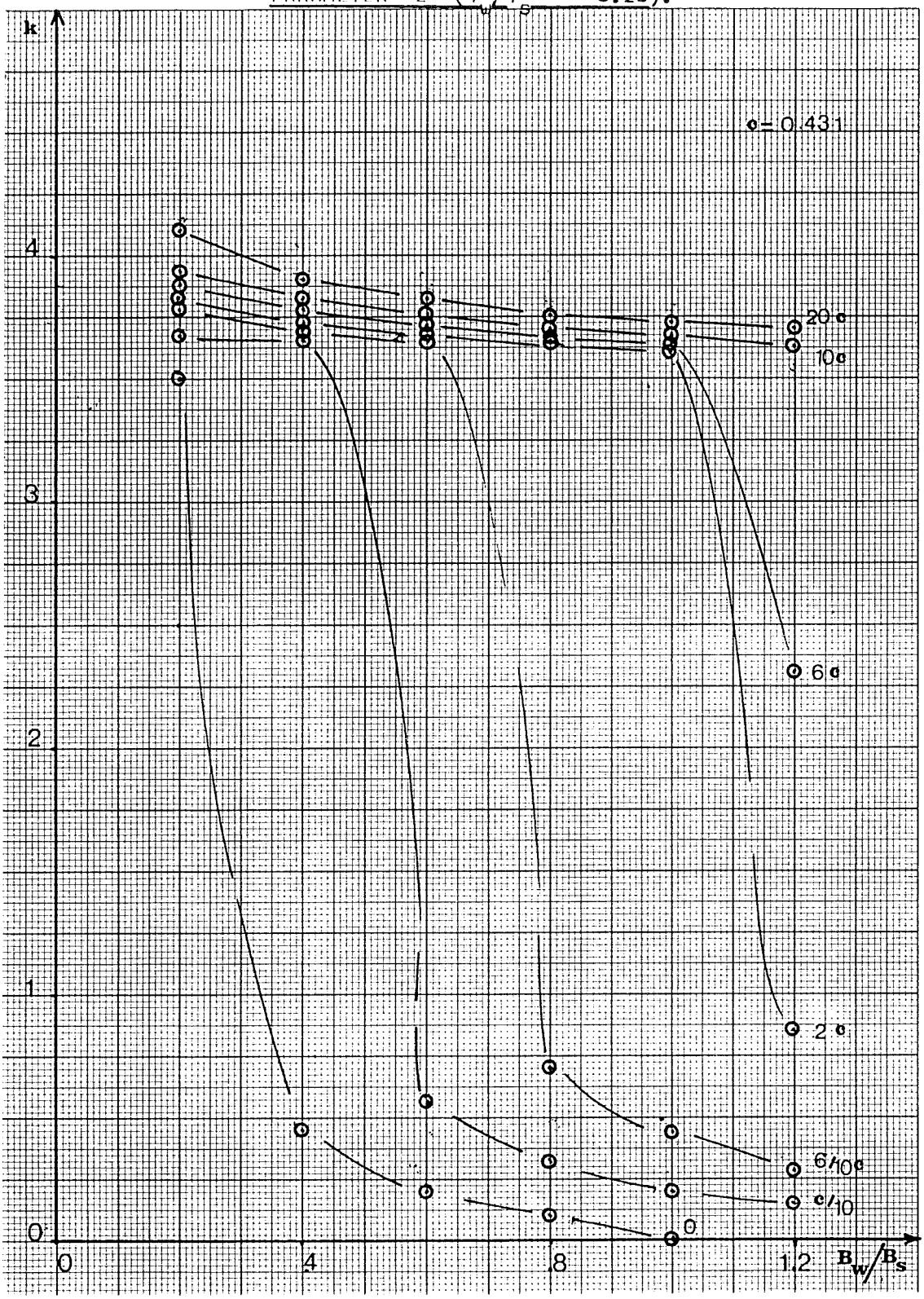

GRAPH (3.21) - LOCAL BUCKLING OF COMPOSITE PANEL K IN FUNCTION OF NONDIMENSIONAL CORE STIFFNESS PARAMETER Z (T_w/T_s = 0.50).

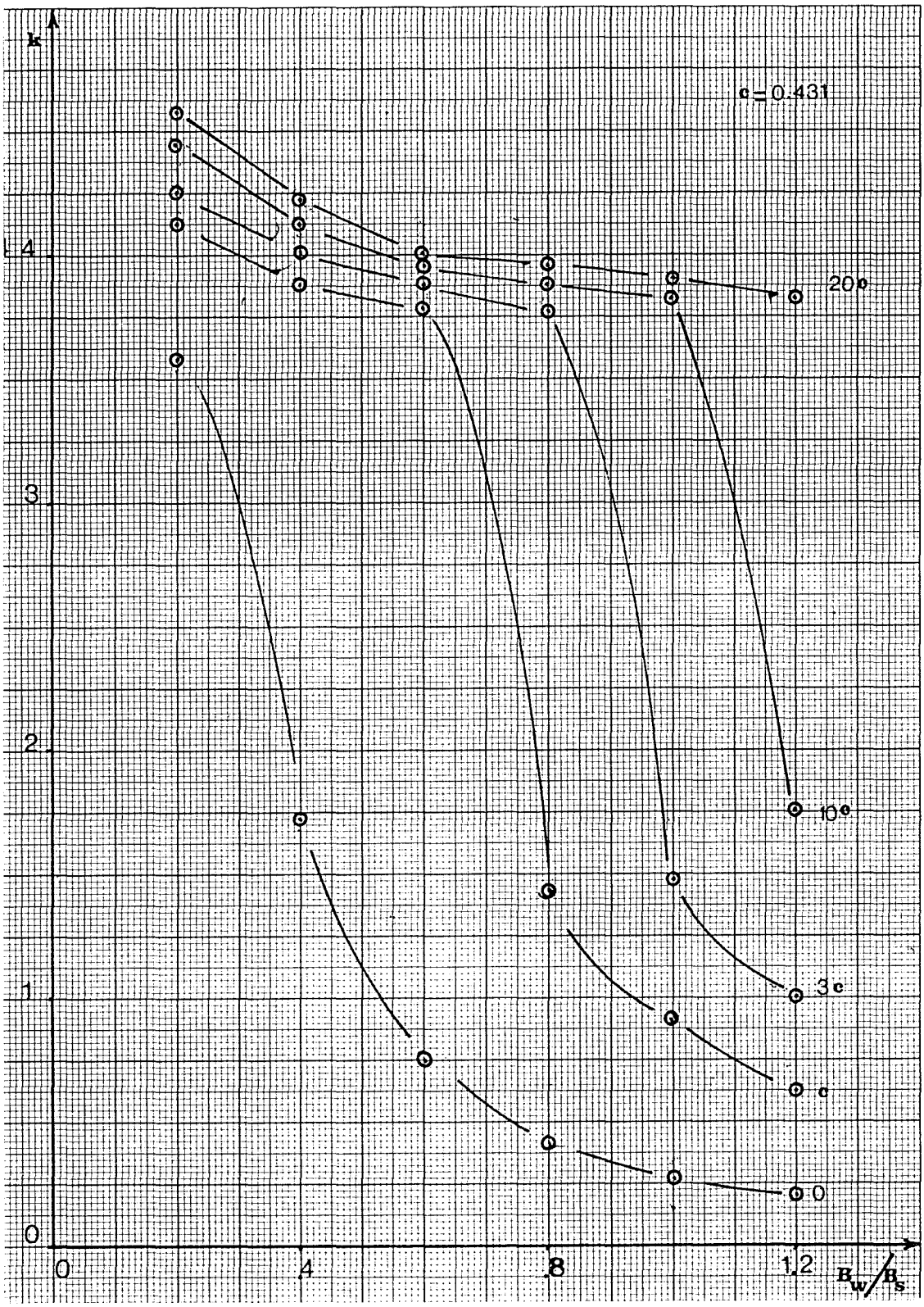

GRAPH (3.22) - LOCAL BUCKLING OF COMPOSITE PANEL K IN FUNCTION OF NONDIMENSIONAL CORE STIFFNESS PARAMETER Z (T_u/T_s = 0.75).

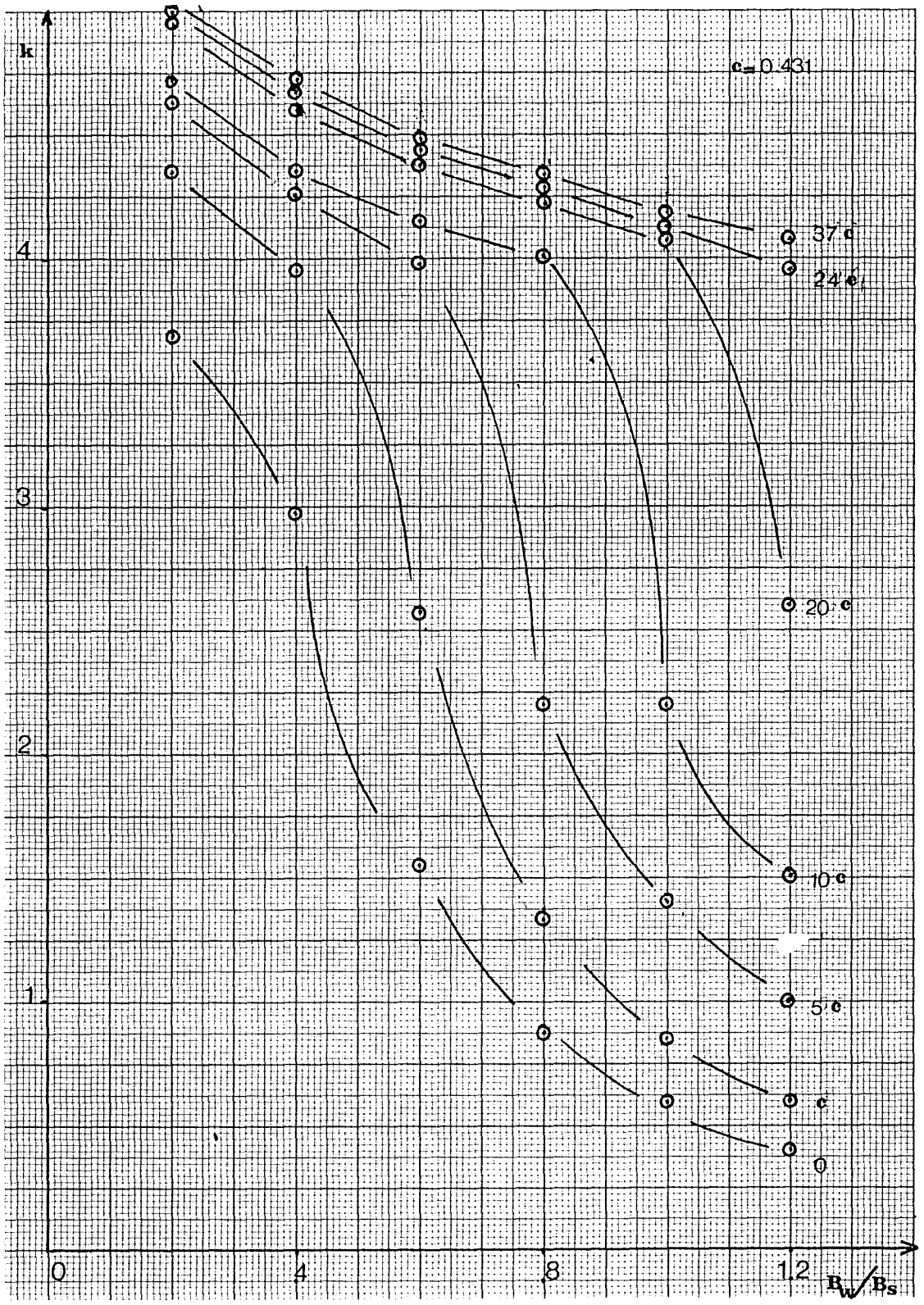

GRAPH (3.23) - LOCAL BUCKLING OF COMPOSITE PANEL K IN FUNCTION OF NONDIMENSIONAL CORE STIFFNESS PARAMETER Z (T_w/T_s = 1.0).

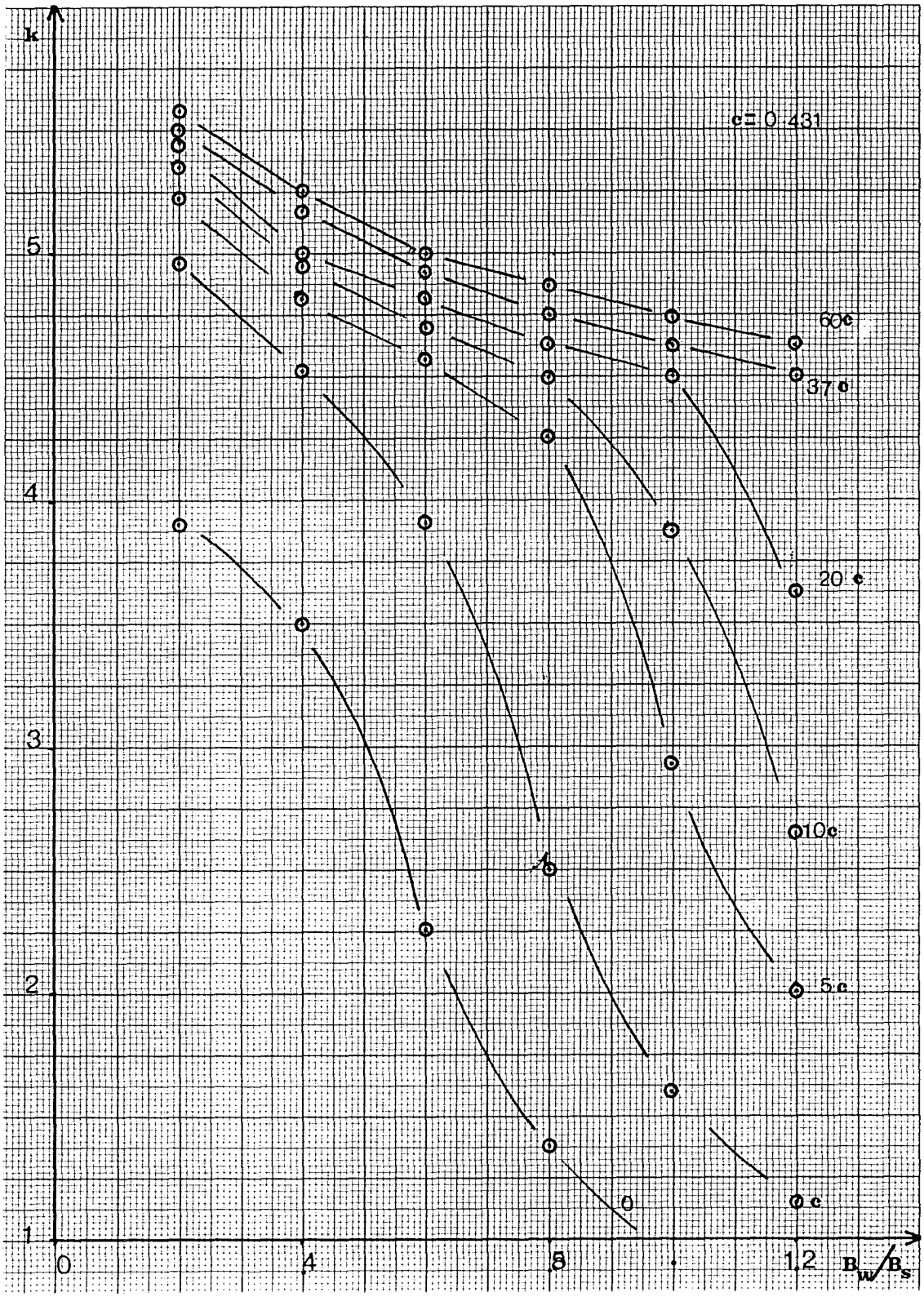

GRAPH (3.24) - LOCAL BUCKLING OF COMPOSITE PANEL K IN FUNCTION OF NONDIMENSIONAL CORE STIFFNESS PARAMETER Z (T_w/T_s = 1.5).

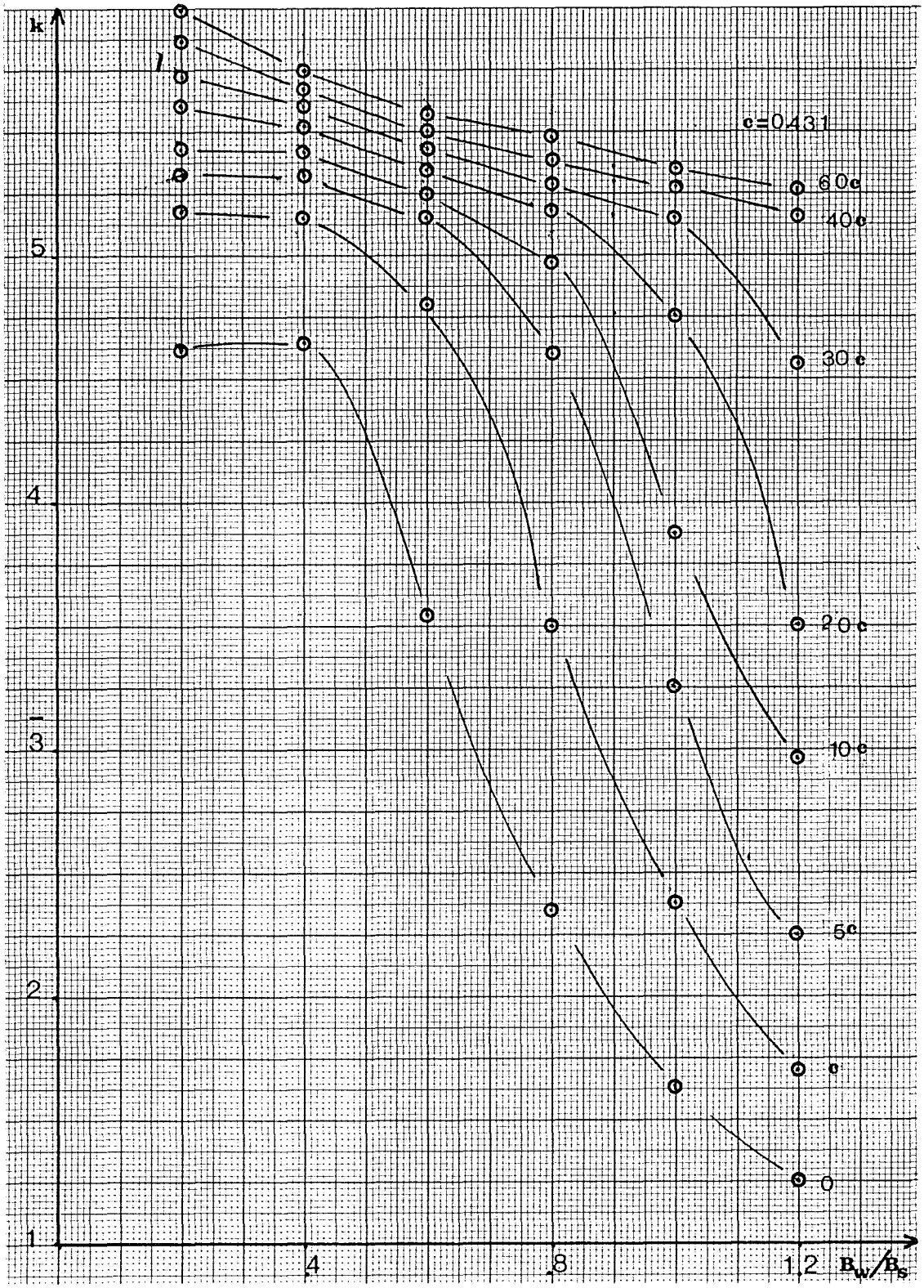

TABLE (3.25) - CRITICAL VALUES OF Z FOR COMPOSITE PANEL.

r_b \ r_t	0.25	0.5	0.75	1.0	1.5
0.2	$\frac{C}{10}$	C	C	C	C
0.4	$\frac{C}{10}$	C	C	C	C
0.6	$\frac{6\,C}{10}$	C	5C	5C	5C
0.8	2C	3C	10C	10C	20C
1.0	2C	10C	20C	20C	30C
1.2	10C	20C	24C	37C	40C

C = 0.431

$r_t = T_w / T_s$

$r_b = B_w / B_s$

3.2.7.5. Approximate Buckling Analysis of Composite Panel.

The previous study of the composite panel was based on the fact that the webs are integral part of the skin, and at buckling compatibility of wave lengths at the line junctions provided some degree of elastic rotational restraint, as a result, the buckling stress coefficient of the web K_w may assume values which are intermediate between the values of K_w of stabilised hinged web and those of stabilised clamped web.

As an approximate buckling analysis of the composite panel, the plate components of the cross-section might be considered as pin-jointed at the line junctions so that the buckling stress coefficient of the panel may assume either the value of K_s, the buckling stress coefficient of simply supported plate skin, or the value of K_w of stabilised hinged web, which whichever is the smallest.

For a simply supported long plate $K_s = 3.65$, for the stabilised hinged free web, K_w is given in function of Z.

Of particular importance are the values of Z at which $K_w = 3.65$, is achieved, See Table (3.26).

TABLE (3.26) - Approximate Buckling Analysis of Composite Panel . Hinged Stabilized Web.

T_w/T_s	Z	K_w
.25	0.0	.43
	.03	2.97
	.06	3.99
.50	.06	1.08
	.22	2.84
	.44	3.73
.75	.44	2.13
	.56	2.47
	1.4	3.65
1.0	2.92	3.43
	3.21	3.57
	3.50	3.72
1.25	3.50	2.42
	4.67	3.16
	6.71	3.69
1.5	6.71	2.96
	8.76	3.26
	11.68	3.70

3.2.7.6. Results and Conclusions:

1. We can see that for each pair of cross-section parameters represented by a combination of $(T_w/T_s,\ B_w/B_s)$ the buckling load increases with the increase of Z until a certain value of Z is reached beyond which the local buckling stress coefficient K ceases to increase even with a large increase of the value of Z.

2. For practical use of the results derived, and in order to establish a criterion for choosing the right core material for use in conjunction with any geometry of composite panel to be constructed, a lower limit of Z is determined so that by using a core material which produces this value, the local buckling stress of the composite panel always will be higher than the local buckling stress for a similarly stiffened panel having the same T_w/T_s, but with $B_w/B_s = 0.2$.

These values of Z are given in Table (3.25).

3. The use of core material as stabiliser for thin stiffeners is very advantageous, and, for the composite panel under study, the local buckling stress was increased by a great deal even in the case of a very thin and high stiffener.

4. The Graphs and the Table are of a general nature. They give the buckling stress and the critical value of Z or E_y for any composite panel which is made of the same material and has the same non-dimensional parameters T_w/T_s, B_w/B_s, and Z.

5. The approximate analysis of the composite panel in which the panel is idealised into plates and stablised webs hinged at the line junctions, showed that for $Z = 11.68$ and $T_w/T_s \leq 1.5$, the buckling stress coefficient K_w can be assumed 3.65 which is the value of buckling stress coefficient for simply supported plate.

Finally, the results suggest that a study of minimum weight design for such a construction would be valuable and this will be the subject of the next Chapter, and as will be seen, a panel constructed from relatively soft core and a metal skin material can be very efficient.

CHAPTER 4.

MINIMUM WEIGHT DESIGN OF COMPOSITE PANEL

4.1. Introduction:

This study was conducted to provide information about the efficiency of a panel made up of two materials. The panel comprises a skin of high strength material with slender integral stiffeners of the same material and a stabilising core or infill of a light material of adequate stiffness.

The object is to produce a structural element which is strong and stiff and, at the same time, weighs less as a result of the combination of the two densities.

In addition to the degree of efficiency which this structural element can provide, it is also possible to incorporate in it such properties as low conductivity, good thermal insulation and fire retardant action, all of which are of great importance in aeronautics.

This study was not meant to be the last word in the field, rather it is hoped to provide a sound basis upon which further research can be based. The study has led to results of a general nature which are applicable to any combination of plate and core material.

First, an efficient study was conducted for a panel with an isotropic core material.

Then, after a preliminary study of the skin and core materials available, a combination of duraluminium and balsa wood was considered.

The results of both cases are then presented in such a way that for any set of design data, i.e. the load per unit width, N, the length of the panel and the Young's Modulus of the material, the optimum characteristics can be found.

The comparison with other types of panels showed a high degree of efficiency. In the first panel, which will be named (P - I), the efficiency study was based on an analysis of the results obtained in Section (3.2.7)

In the second panel (P - II), a numerical procedure was devised using Programme (4.1) with the necessary modification in which the stabilising effect of the core material was incorporated in the overall stiffness matrix as explained before.

In both cases, the minimum weight design is based on the simultaneous buckling criteria, i.e. the overall buckling and local buckling occur simultaneously.

4.2. Minimum Weight Design in Aeronautics.

Although minimum weight design considerations are of great importance in all branches of engineering, either because of the reduction of cost as a result of the minimum weight design or because of the increase in efficiency of the construction, it is in aeronautics that minimum weight design is of vital importance.

A heavier aircraft will require a larger lifting surface which will lead to a bigger power plant with the consequent increases in fuel consumption and runway length for take-off and landing.

The cost of achieving even small saving in weight can be justified economically.

The design requirements are normally set by the necessity of a Company to build an aircraft which will carry a certain load over a certain distance. These design factors will be reflected in the design of every single component.

For example, the wing design parameters will be the overall length, the chord and thickness, and all these are functions of the payload of the prototype, of its range, aerodynamics, and performance.

Sometimes in addition to the performance induced design parameters, there will be other parameters to be considered which are functions of the position of the single component.

The weight of the wing surface plating is a significant part of the total structure weight and considerable sttention must be given to the problem of efficiently using this material Any acceptable proposal for the improvement in the utilisation of the potential strength of the plating must recognise the essential functions of maintaing the aerodynamic shape, sealing the wing interior and, for high speed aircraft, insulating the wing interior from the effects of dynamic heating.

4.3. Composite Panel.

The composite panel which is the object of this study can be seen in Figure (3.43), it consists of a plate made of high strength material divided by a series of very thin longitudinal stiffeners.

The thin stiffeners are separated by a light core material which acts primarily as a stabiliser for the thin stiffeners but which will, in addition, carry part of the load, as in the case of the sandwich construction.

This type of panel was chosen so to achieve the advantages of both the stiffened and sandwich panels.

As will be shown later, this type of construction proves to be more efficient and possibly less expensive than many forms of plate type construction.

4.4. Minimum Weight Design of Composite Panel with Isotropic Core Material.

4.4.1. Introduction:

The minimum weight design study in this Section, is based on information obtained from the study of local buckling of composite panel.

In particular, it was found that for each pair of values of B_w/B_s and T_w/T_s a value of Z is found, where

$$Z = (K_f/D)\,(H/\pi)^4$$

for which the same buckling stress coefficient for web and plate skin can be found (See Section 3.2.7.5.).

Using these results in conjunction with Gerard's Approximate Method (54), the optimum stress and geometry can be found.

This approximate method assumes that the plate components of the cross-section are pinjointed at the line junction, as a result, at optimum the skin and the web buckle at the same stress.

Analytically this can be written as follows:

At Optimum

$$\overline{\sigma}_s = \overline{\sigma}_w$$

$$E\,K_s(T_s/B_s)^2 = E\,K_w\,(T_w/B_w)^2$$

then from Section (3.2.7.6.), for $Z = 11.68$ we may assume

$$K_s = K_w$$

then

$$T_s/B_s = T_w/B_w$$

this relation can be written as

$$T_w/T_s = B_w/B_s$$

or symbolically

$$r_t = r_b$$

4.4.2. Efficiency Coefficient:

It is assumed that when the applied stress reaches the optimum value, the panel fail by simultaneous local and the overall buckling modes.

a. Applied stress

$$\sigma_a = N/\bar{t}$$

where

$$\bar{t} = T_s + (B_w T_w / B_s) + \epsilon$$

and where ϵ is the thickness due to infill which will be considered of negligible value.

So we may write

$$\bar{t} = T_s + (B_w T_w / B_s)$$

b. Overall buckling stress

$$\sigma_E = \eta \pi^2 E (g/L)^2$$

where η is the plasticity factor and g is the radious of gyration.

c. Local buckling stress

$$\sigma_L = \frac{\pi^2 K \eta E}{12(1-\nu^2)} (T_s/B_s)^2$$

For minimum weight

$$\sigma_a = \sigma_E = \sigma_L$$

To obtain the analysis in terms of the structural index $(N / \eta EL)$ the three stresses are combined in the following manner:

$$\sigma = \sqrt[4]{\sigma_E \ \sigma_L \ \sigma_a^2}$$

which gives:

$$\sigma = \pi \eta E (K/12(1-\nu^2))^{\frac{1}{4}} ((N/\eta EL)^2 (g T_s / B_s \bar{t})^2)^{\frac{1}{4}}$$

Where g is the radius of gyration of the cross-section.

This can be written as:

$$\sigma = \alpha \eta E \left(N / \eta EL \right)^{\frac{1}{2}}$$

Where α is the efficiency coefficient which is equal to

$$\alpha = \pi \left(K / 12(1 - \nu^2) \right)^{\frac{1}{4}} \left((g / B_s)(T_s / \bar{t}) \right)^{\frac{1}{2}} \qquad (4.1)$$

Then from

$$g = \sqrt{I / A} = (B_s / (1 + r_b r_t)) \left(r_t r_b^3 \frac{(4 + r_b r_t)}{12} \right)^{\frac{1}{2}} \qquad (4.2)$$

Where

I is the cross-section moment of inertia about axis in the plane of the plate and from

$$\bar{t} / T_s = 1 + r_b r_t$$

Substituting, we obtain:

$$\alpha = \pi \left(K / 12(1 - \nu^2) \right)^{\frac{1}{4}} \left(1 / (1 + r_b r_t) \right) \left((r_b^3 r_t / 12)(4 + r_b r_t) \right)^{\frac{1}{4}}$$

Combining equations (4.1) and 4.2).and for α to be minimum $\partial \alpha / \partial r_b = 0$

We obtain

$$r_b^4 + 5 r_b^2 - 8 = 0$$

Which gives

$$r_b = 1.129$$

and

$$r_t = 1.129$$

which represent the optimum cross-section geometric proportions for composite panel with isotropic core (P - I).

4.4.3. Optimum Efficiency Coefficient.

Substituting with $r_b = r_t = 1.129$ in equation (4.2), we obtain

$$\alpha = 0.986$$

4.4.4. Optimum Stress.

The optimum stress is given as

$$\sigma = 0.986\ \eta E (N/\eta EL)^{\frac{1}{2}} \qquad (4.3)$$

It is to be noticed that:

a. For integrally stiffened panel (55)

$$\sigma = 0.81\ \eta E (N/\eta EL)^{\frac{1}{2}}$$

b. For Z stiffened panel (55)

$$\sigma = 0.95\ \eta E (N/\eta EL)^{\frac{1}{2}}$$

As can be seen, the composite panel (P - I) is more efficient since it develops for the same structural index higher buckling stress.

4.4.5. Optimum Geometry.

From

$$N = \sigma \bar{t} \qquad \text{or} \qquad \bar{t} = N/\sigma$$

Substituting on σ and multiplying by $\sqrt{L} / \sqrt{L}$, we obtain

$$\bar{t}/L = 1.014\ (N/\eta EL)^{\frac{1}{2}}$$

and from

$$\bar{t} = T_s (1 + r_b r_t)$$

$$T_s = 0.445\ L\ (N/\eta EL)^{\frac{1}{2}} \qquad (4.4)$$

and

$$T_w = r_t T_s = 0.502 L (N/\eta EL)^{\frac{1}{2}} \qquad (4.5)$$

Then from

$$\sigma = 3.65 E (T_s/B_s)^2$$

We may write:

$$B_s = (3.65 E T_s^2 / \sigma)^{\frac{1}{2}}$$

and the optimum stiffeners spacing becomes:

$$B_s = 0.856 L (N/\eta EL)^{\frac{1}{4}} \qquad (4.6)$$

and

$$B_w = 0.967 L (N/\eta EL)^{\frac{1}{4}} \qquad (4.7)$$

4.4.6. Optimum Core Material Stiffness.

From the previous Chapter

$$Z = (K_f /D) (H/\pi)^4$$

which can be written as:

$$Z = ((E_y/ 0.5 B_s)/(E T_s^3/12(1 - \nu^2))(B_w/ \pi)^4$$

Where H is replaced by B_w without much error and where E_y is the Young's Modulus of the core material in the transverse direction.

Substituting on Z with the [illegible] value found in the previous Chapter, section (3.2.7.6) which is equal to 11.68 and r_b and r_t being equal to 1.129 we find for the optimum core stiffness the expression:

$$E_y/E = 4.48 (N/\eta EL)^{\frac{3}{4}} \qquad (4.8)$$

4.4.7. Optimum Weight of the Composite Panel.

It consists of the sum of the two parts:

1. The weight of the skin.

2. The weight of the core in which the density is assumed to be proportional to its Young's Modulus.

1. The weight of the skin.

$$w_o = \rho \bar{t} = 1.014\ L\ (N/\eta EL)^{\frac{1}{2}} \rho \qquad Kg/m^2$$

2. The weight of the core.

$$\bar{t}_c = (E_y/E)\ B_w$$

Substituting, we find:

$$w_c = \rho \bar{t}_c = 0.967\ (E_y/E)\ L\ (N/\eta EL)^{\frac{1}{4}} \rho \qquad Kg/m^2$$

The total weight of the panel will be the sum of the weight of the skin and that of the core.

$$w = (1.014\ L\ (N/\eta EL)^{\frac{1}{2}} + 0.967\ (E_y/E)\ L\ (N/\eta EL)^{\frac{1}{4}})\ \rho \qquad Kg/m^2 \qquad (4.9)$$

As will be seen, the second part on the right hand side is very small.

4.4.8. Design Example.

A panel is to be manufactured from material which has

$E = 69000\ N/mm^2$

$\sigma = 392\ N/mm^2$

$\rho = 2.79\ 10^{-3}\ Kg/mm^3$

The panel is square with $L = 950$ mm, the applied load is to be 10^6 N.

From the results previously obtained we find that:

For the structural index

$$(N/EL) = 1.6\ 10^{-5}$$

We have,

Optimum skin thickness T_s = 1.69 mm (eq. (4.4))

Optimum web thickness T_w = 1.91 mm (eq. (4.5))

Optimum web spacings B_s = 51.43 mm (eq. (4.6))

Optimum web height B_w = 58.17 mm (eq. (4.7))

Optimum stress σ = 272 N/mm^2 (eq. (4.3))

Optimum core material stiffness $E_y/E = 13.\ 10^{-4}$

(eq. (4.8))

Optimum panel weight $w = (3.85 + 0.07)\rho$

$= 0.0109\ g/mm^2$ (eq. (4.9))

$W = w L^2 = 9.83$ Kg.

It is to be noticed that in this case, the ratio of core weight to that of skin = (0.07/ 3.85) = 0.018 and can be neglected without appreciable error.

4.4.9. Weight Comparison.

For the purpose of evaluating the efficiency of Panel (P - I) from weight basis represented by $(\bar{t}/L)$ and using the results of Ref. (55) we have:

1. Unstiffened panel

$$\frac{\bar{t}}{L} = 1.067\ (N/\eta EL)^{\frac{1}{3}}$$

2. Unflanged integral stiffened panel

$$\frac{\bar{t}}{L} = 1.234\ (N/\eta EL)^{\frac{1}{2}}$$

3. Z - stiffened panel

$$\frac{\bar{t}}{L} = 1.047\ (N/\eta EL)^{\frac{1}{2}}$$

4. Composite panel (P - I)

$$\frac{\bar{t}}{L} = 1.014\ (N/\eta EL)^{\frac{1}{2}}$$

As can be seen, among the stiffened configurations considered above the composite panel is the lightest.

4.5. Minimum Weight Design of Composite Panel with Orthotropic Core Material (P - II).

4.5.1. Introduction:

In the previous Section, the minimum weight design of a composite panel built up from metal skin and soft core was studied; the optimum stress, geometry, and core stiffness were given in compact form as in functions of the structural index.

In the previous analysis the optimum panel, (P - I), was found to have high slender stiffeners and the weight of the core was found to be negligible.

The stiffness of the core in the direction of loading was not considered in the analysis.

In the following Sections, an efficiency study of a similar composite panel but with an orthotropic core material will be made.

The overall buckling of this panel will be determined as a function of both the skin and core longitudinal stiffness.

The latter was accounted for by applying the reduced modulus to the cross-section of the core.

The numerical procedure adopted in the analysis is based on the determination of the geometric proportions of the panel of least weight which buckles by simultaneous local and overall mode at given load .

This numerical procedure will be described and the computer programme used will be given in the next Chapter PROGRAMME (4.1) together with the flow chart.

4.5.2. Local Buckling of Composite Panel.

The cross-section of the panel is regarded as made up of a number of thin flat strips joined edge to edge. These strips are referred to as the component flat plates. The component flat plates which form the stiffener webs are assumed to rest on an elastic medium.

The elastic medium is considered as a Winkler type foundation, and the spring constant of the core material K_f is given by the equation:

$$K_f = E_y /(0.5B_s)$$

Where E_y is the core material Young's Modulus in the direction normal to the plane of the webs.

B_s is the webs spacing.

The translation stiffness of the component flat plates in their planes is much greater than the rotational stiffness about the edge lines, so it is reasonable to assume that during buckling no component flat plate will translate in its plane, and all edge lines remain straight.

Under these assumptions, all possible modes of deformation will involve only distortion of the cross-section. The component flat plates will rotate around their edge lines, (see Fig. (3.43)), and the only stiffness involved is the stiffness of the component flat plates around their edge lines.

The elastic stiffness and geometric stiffness matrices for the component flat plates and the elastic foundation matrix were derived in previous Chapters.

The procedure for determining the local buckling stress is the same as the procedure used in the last Chapter.

Programme (4.1), which will be explained in the next Chapter, will be used for the minimum weight design computations.

4.5.3. Overall Buckling of Composite Panel.

Since the width of the panel is many times its thickness, the overall buckling mode of the composite panel will be function of the stiffness of the panel relative to the axis which lies in the plane of the skin plating and normal to the stiffeners. Buckling will occur causing the panel to bow with a wave of buckling which has a length of the order of the panel width or multiple of it depending on the type of constraint of the loaded edges.

If it is assumed that the panel is wide enough to neglect the effect from the unloaded edges the composite panel can be treated as a wide column, and the buckling stress for the overall mode can be found by applying the Euler equation for the buckling of a strut.

Although this formula may over estimate the buckling load, as it was found in the previous Chapter, the use of it as a first approximation may be quicker and more economical than using one of the finite elements methods derived in the previous Chapter.

The core material stiffness in the direction of the application of the load is taken into account by applying the consideration of a beam of two materials to the basic strut and the overall buckling of the composite panel will be found as the buckling stress of the strut which has the same B_w , B_s , and T_s but with T_w being the sum of the initial web thickness plus a factor due to the core stiffness (see Figures (4.1a) and (4.1b), and the thickness of the equivalent strut can be given:

$$T_w = T_{w_o} + T_{w_1}$$

Where $$T_{w_1} = B_s \cdot B_w \cdot E_x/(E \cdot B_w)$$

Where the label o refers to the stiffener original thickness.
The buckling stress for the panel is then given:

$$\sigma = c \pi^2 E(g / L)^2$$

Where c is the end constraint coefficient which is given in Figure (4.2) and g is the radius of gyration.

In the following analysis only the simple support conditions is considered.

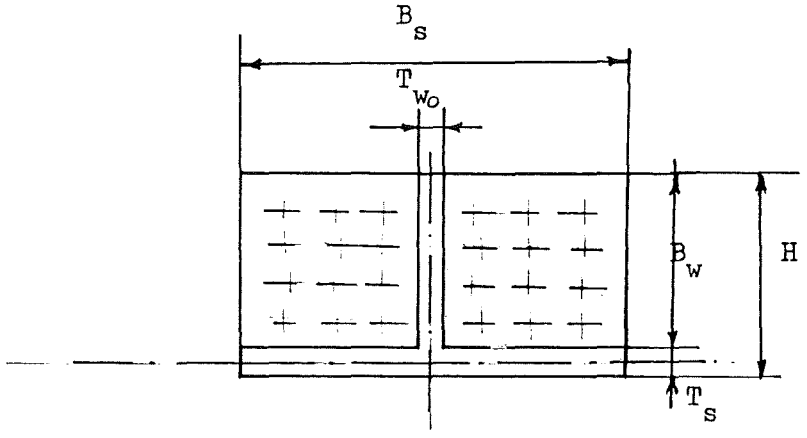

(a)

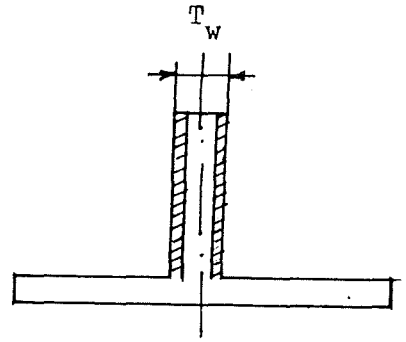

(b)

Fig. (4.1) - Reduction of actual strip of the composite panel to equivalent strip for overall buckling.

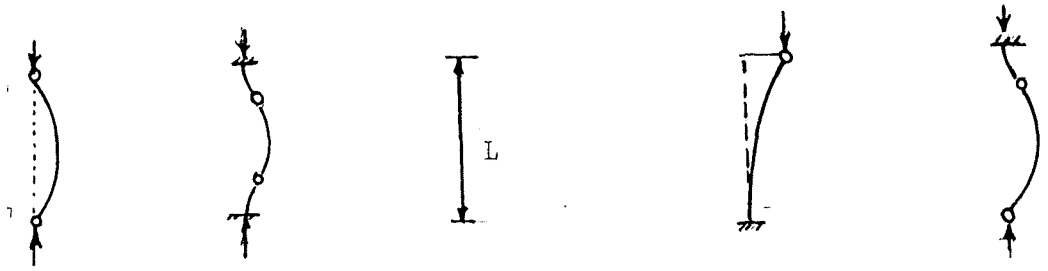

c = 1 c = 4 c = .25 c = 2.04

Fig. (4.2) - End constraint co-efficient c for axially loaded strut of length L .

4.5.4. Core Material. (56), (57).

Although the selection of core material for such types of structure must be governed primarily by having the one which possesses the highest possible value of the ratio E_x / ρ_c where E_x is the Young's Modulus in the longitudinal direction of the core material, and ρ_c is the core material density, the requirement of strength, serviceability and cost are equally important.

In the past, many authors have preferred the use of core material of isotropic structure since this reduced the number of variables in the design process, and consequently facilitated the analysis.

To stabilise the longitudinal stiffeners against local buckling a relatively soft core material, expressed by the spring constant K_f was found to be sufficient.

On the other hand, the requirement for overall buckling of this type of panels is to have a value of Young's Modulus in the direction of loading as high as possible when sliding between the two materials at the contact area, is prevented.

We conclude that in the design of a panel which is based on buckling criteria and where two materials are used, a core material of orthotropic nature is more valuable specially if the Young's Modulus in the transverse direction is proportional to the material density.

There are a variety of core materials available for the industry, some of them are natural like rubber and balsa for example, the others are artifical.

The latter are favourable since their production can be adapted to the needs of the designer, and they can be provided with the/

/the necessary characteristics to suit the variation between panels of different geometries and of the same design.

The balsa wood is chosen for the following analysis as a basis, because of the ease of manufacturing and because of its availability.

Summarising, to have an efficient composite panel the core material used must have the following properties:

a - High Young's Modulus in compression in the direction of loading.

b - The lowest possible density.

c - Relatively low Young's Modulus in compression in the transverse direction.

d - Variable properties to suit different designs.

e - Available, easy to manufacture, and inexpensive.

4.5.4.1. Balsa Wood.

The balsa wood is one of core materials of natural origin, it is orthotropic and relatively light, and it can be found with a certain degree of variation of its average properties.

This variation of properties is due to the fact that the balsa is very sensitive to humidity and its properties depend very much on the way in which the seasoning and storage was accomplished.

In the past, the balsa wood, in addition to its use as a core material for some sandwich construction, has also been used as a structure material because of its high Young's Modulus in the direction of the fibres.

The Young's Modulus in the transverse direction, that is in the direction normal to the grain, can be found of different values depending on the way in which the balsa was cut either radial or tangenial to the growth rings.

In Table (4.1), is listed average values for the balsa properties, and it must be emphasised that if the material is not handled properly, these characteristics may very much be altered.

TABLE (4.1) - AVERAGE PROPERTIES OF BALSA WOOD.

PROPERTIES	AVERAGE VALUE	
Young's Modulus in the direction of the grain. E_x	2393	N/mm^2
Young's Modulus in transverse direction (radial). E_{y_r}	90.7	N/mm^2
Young's Modulus in transverse direction (tangential). E_{y_t}	35	N/mm^2
Density ρ_c	0.9×10^{-7}	Kg/mm^3
E_x / ρ_c	2.65×10^{10}	
E_{y_r} / ρ_c	1.00×10^{9}	
E_{y_t} / ρ_c	3.9×10^{8}	

4.5.5. Skin Material. (58)

These are some of the factors which influence the choice of the skin material:

a - Strength combined with lightness.

b - High value of stiffness.

c - Toughness.

d - Resistance to corrosion.

e - Resistance to fatigue.

f - Ease of manufacturing.

g - Resistance to creep.

h - Availability.

j - Cost.

In the field of aeronautics, several new materials have been developed which have good properties and which satisfy the above requirement, but only the four convential materials based on the following alloys will be considered for the present analysis and these are:

4.5.5.1. Magnesium alloys.

4.5.5.2. Aluminium alloys.

4.5.5.3. Titanium alloys.

4.5.5.4. Steel alloys.

4.5.5.1. Magnesium Alloys.

These alloys are characterised by relatively low specific weight, but also with low value for Young's Modulus. The structural components made of these alloys usually have large thickness to compensate for the small stiffness.

A suitable use is in the core of the wheels where the heat developed can be absorbed by the relatively large volume of large thermic capacity and low weight.

As it will be shown later, this material is best for structures subject to instability type of failure.

These alloys contain about 10% of aluminium and about 2% to 4% of zinc. Elektron is one of magnesium alloys used in aeronautics.

Average principal characteristics are:

$$c_2 = 280.\ N/mm^2 \qquad \rho = 0.18 \times 10^{-5}\ Kg/mm^3 \qquad E = 46000\ N/mm^2$$

4.5.5.2. Aluminium Alloys.

These alloys have higher value of Young's Modulus and density relative to magnesium alloys. It is used in subsonic and transonic aircraft as primary structure material : skin plating, structure frames, control circuits, and landing gear are examples of use of such alloys.

Two of the commonly used aluminium alloys are:

a - Dural which contains in addition to aluminium 4% to 6% of copper, and small percentages of silicio and magnesium.

b - Ergal which contains 3% to 7% of zinc plus copper and magnesium.

These alloys are not very resistant to corrosion and needs special treatment and they are not resistant to heat, above $250^{o}C$. their characteristics start to deteriorate.

Their use for structure subject to failure by stability proves to be quite good as it will be seen later.

Average principal characteristics are:

$$c_2 = 400.\ \text{to}\ 450.\ N/mm \qquad \rho = 0.27 \times 10^{-5} \qquad E = 74000\ N/mm^2$$

4.5.5.3. Titanium Alloys.

Have high value of Young's Modulus and have moderate value of density. Found much use along side the steel in the industry of high speed aircraft and in airspace vehicles. High resistance to temperature. Used in airframes and in skin of wings and fuselage and in discs and plates.

Average principal characteristics:

$$c_2 = 950.\ \text{to}\ 1050.\ N/mm \qquad \rho = 0.45 \times 10^{-5} \qquad E = 105000.\ N/mm^2$$

4.5.5.4. Steel Alloys.

The toughest material for use in aeronautics. High Young's Modulus and high density too. It has been used for skins and fuselage frames of very high speed aircraft.

These alloys contain small percentages of carbon, nickel, chromium and molybdium.

The average principal characteristics:

c_2 = 1000. to 1200. N/mm^2 $\rho = 0.75 \times 10^{-5}$ Kg/mm^3 $E = 21000$ N/mm^2

After this brief introduction to these four principal alloys available for skin construction, it is very important to evaluate their suitability for use in a skin panel where stability condition is predominant, this can be done by finding the figure of merit for a structure subject to instability type of failure.

4.5.6. Figure of Merit.

Because of the importance of bars which have a cross-section of T form, the figure of merit theory developed in Reference (59) will be adopted to analyse these types of bars and to find the figure of merit for the skin materials in the following cases:

4.5.6.1. - Simple compression (shortbar).

4.5.6.2. - Overall elastic buckling.

4.5.6.3. - Local instability.

4.5.6.4. - Simultaneous local and overall buckling.

4.5.6.1. Figure of Merit for Short T-Strut in Simple Compression.

Suppose we consider a number of struts of different materials but of the same length and loaded in simple compression P .

In this case: $P = \sigma A$

Where σ is the stress at failure of the strut under simple compression and A is the cross-section area.

Since $W = \rho A L$

We have

$$P/W = \sigma/\rho L$$

or

$$P/W \sim \sigma/\rho$$

Where $\frac{\sigma}{\rho}$ can be regarded as the figure of merit for simple compression.

If the member is loaded in tension the figure of merit for the strut will be identical to the figure of merit for the material which is given as: σ_u/ρ

and represents the length of a bar of uniform section which is suspended will break under the action of its own weight.

4.5.6.2. Figure of Merit for T-Strut in Overall Elastic Buckling.

Suppose the struts have geometrically similar cross-sections i.e. the struts have the same $(B_w/B_s, T_w/T_s)$.

Further suppose that the struts have the same buckling load and the same length L .

We can write

$$P_E = c\pi^2 E A g^2 / L^2$$

Where c is the constraint co-efficient, and g is the radius of gyration.

or $$P_E \sim E A g^2.$$

Thus, for the same P_E

$$g \sim 1/\sqrt{E}\sqrt{A}$$

The weight

$$W = \rho A L$$

Then

$$P/W \sim E A g^2/\rho A L$$
$$\sim E g^2/\rho$$

The right hand side can be written

$$E \cdot g\, g \,/\rho$$

and substituting for $g = \frac{1}{\sqrt{E}\sqrt{A}}$, this leads to

$$P/W \sim (\sqrt{E}/\rho \quad . \quad g \;/\; \sqrt{A})$$

But for geometrically similar structures:

$$g \,/\sqrt{A} \;=\; \text{const.}$$

So that $P/W \sim \sqrt{E}/\rho$ which will be the figure of merit for overall buckling.

4.5.6.3. Figure of Merit for T-Strut in Local Instability.

Suppose all the struts have the same load at failure and overall length and also have the same $\bar{P}$, B_w/B_s, T_w/T_s. Furthermore, suppose the latter ratio to be fixed equal to unity whilst permitting the thickness to vary.

Then

$$P_L = K\, A\, E\, (T_s/B_s)^2 \quad ,$$

$$= K\, \bar{P}\, T_s\, E\, (T_s/B_s)^2 \quad \text{where} \quad \bar{P} = B_w + B_s$$

from which

$$P_L \sim E\, T_s^{\,3}$$

and for struts which have the same P_L

$$T_s \sim 1./\sqrt[3]{E}$$

The weight in this case is given by

$$W = \rho\, \bar{P}\, T_s\, L$$

or $$W \sim \rho\, T_s$$

Therefore, considering struts subject to local stability and all having the same load at failure P_L,

$$P/W \sim 1./W$$

so that $P/W \sim 1./T_s \rho$

or $P/W \sim \sqrt[3]{E/\rho}$ which is the figure of merit for struts of TSection under local stability.

4.5.6.4. Figure of Merit for T-Struts Subject to Simultaneous Local and Overall Buckling.

Again we suppose P, L, $\bar{p}$ and (B_w/B_s, $T_w/T_s = 1.$) to be the same for all the struts, but $T_s = T$ is allowed to vary.

Putting

$$P_E = P_L$$

gives $c\pi^2 E A g^2 / L^2 = K E A (T_s/B_s)^2$

or $c\pi^2 E \bar{p} T g^2 / L^2 = K E \bar{p} T (T/B_s)^2$

writing

$$B_s = \bar{p} \theta_1$$

and $g = \bar{p} \theta_2$ where θ_1, θ_2 are factors characteristic of the cross-section.

and substituting gives

$$c\pi^2 E \bar{p}^3 T \theta_2^2 / L^2 = K E \bar{p} T^3 / \bar{p}^2 \theta_1^2$$

then

$$\bar{p}^4 \sim T^2$$

or

$$\bar{p}^2 \sim T$$

Then from

$$P = K E \bar{p} T^3 / \theta_1^2 p^2$$
$$p \sim E T_s^3 / \bar{p}$$

then

$$\bar{p} \sim 1. / \sqrt[5]{E}$$

Since

$$W = \rho \bar{p} \; T \; L$$

we have

$$W \sim \rho \bar{p}^3$$

and, as before, for constant P

$$P/W \sim 1./W$$

Then

$$P/W \sim 1./W \sim 1./ \; \rho \bar{p}^3 \sim \sqrt[5]{E^3}/\rho$$

or $P/W \sim \sqrt[5]{E^3}/\rho$ which is the figure of merit for a T-strut which fails by simultaneous overall and local buckling.

TABLE (4.2) VALUES OF FIGURE OF MERIT FOR STRUTS OF DIFFERENT MATERIALS AND UNDER DIFFERENT TYPES OF LOADING.

NO.	MATERIAL	DENSITY	YOUNG'S MODULUS	STRENGTH	SIMPLE COMPRESSION	OVERALL BUCKLING	LOCAL BUCKLING	SIMULTANEOUS BUCKLING
		ρ Kg/mm^3	E N/mm^2	C_2 N/mm^2	σ/ρ	$\sqrt{E}/\rho$	$\sqrt[3]{E}/\rho$	$\sqrt[5]{E^3}/\rho$
1.	STEEL	$.78 \times 10^{-5}$	210000.	1200.	1.538×10^{8}	5.875×10^{7}	7.315×10^{6}	2.00×10^{8}
2.	TITANIUM	$.45 \times 10^{-5}$	116000.	1000.	2.222×10^{8}	7.568×10^{7}	1.042×10^{7}	2.429×10^{8}
3.	DURAL	$.27 \times 10^{-5}$	74000.	450.	1.666×10^{8}	1.007×10^{8}	1.497×10^{7}	3.091×10^{8}
4.	MAGNESIUM	$.18 \times 10^{-5}$	46000.	280.	1.555×10^{8}	1.191×10^{8}	1.920×10^{7}	3.486×10^{8}

4.5.7. Efficiency of Dural-Balsa Composite Panel.

From the study conducted in the previous Chapter, it was found that the local buckling stress for thin plates and for thin walled structures can be increased by supporting the elements of the structure by core material of relatively low stiffness. If this characteristic is combined with low density it may produce an efficient structural element.

The efficiency study which follows and which makes use of Programme (4.1), will use the local stability consideration for thin flat plates as a basis for refining and obtaining the optimum set of cross-section geometric parameters.

The optimum panel length will be found as the critical length of the panel which has the optimum geometric parameters defined by the local instability consideration.

The minimum weight study will proceed as follows:

H, the panel depth, is held fixed

H/T_s has the values 20, 30 and 40.

The material of the skin is dural and the characteristics were given in Graph (4.1).

The core material is balsa, the characteristics were given in Table (4.1).

It is also assumed that the effect of side constraint is negligible and that the panel is simply supported along the loading edges, so that the panel will buckle as a wide column.

The range of variation of T_w/T_s in the programme is 0.25 to 2.0 with interval equal to 0.25.

The range of variation of B_s/B_w in the programme is 0.5 to 4.5 with interval equal to 0.0125 .

4.5.7.1. Analysis Procedure.

a - A value of H/T_s is fixed.

b - A value of stress σ is fixed together with the appropriate value of the reduction factor η .

c - All the sets of T_w/T_s, B_w/B_s values which produce a local buckling equal to the value of stress chosen above will be isolated together with density of the composite panel $\bar{\rho}$.

d - The value of the density is found from this formula:

$$\bar{\rho} = ((B_s T_s + B_w T_w) \rho + (B_s - T_w)(B_w \rho_c))/B_s H$$

e - The optimum set will be the one which has the highest value of $\frac{\sigma}{\bar{\rho}}$.

f - Having determined the cross-section optimum parameters T_w/T_s, and B_w/B_s these values will be used to find the moment of inertia of the cross-section which will be used in Euler formula to find the critical length L as:

$$L = \left[\pi^2 E g^2 / \sigma \right]^{.5}$$

g - At this stage one point on the efficiency curve is found together with the related optimum proportions.

h - Further points will be found by repeating steps, b, c, d, e and f.

i - When the range of stresses up to the proof stress c_2 has been covered in the manner explained above, for the particular value chosen for H/T an efficiency curve can be drawn.

For convenience, the structure index $\frac{N}{\eta EL}$, and the weight index $\frac{\bar{t}}{L}$, the first being the measure of the intensity of loading and the second being the weight parameter, will be used to draw the efficiency curve.

Also the optimum geometric proportions and the optimum stress will be given in function of the structural index.

j - Another value of H/T_s is chosen and another efficiency curve is drawn.

The results of the above analysis are given in Graphs (4.2), (4.3), (4.4) and (4.5).

GRAPH (4.1) - SKIN MATERIAL.

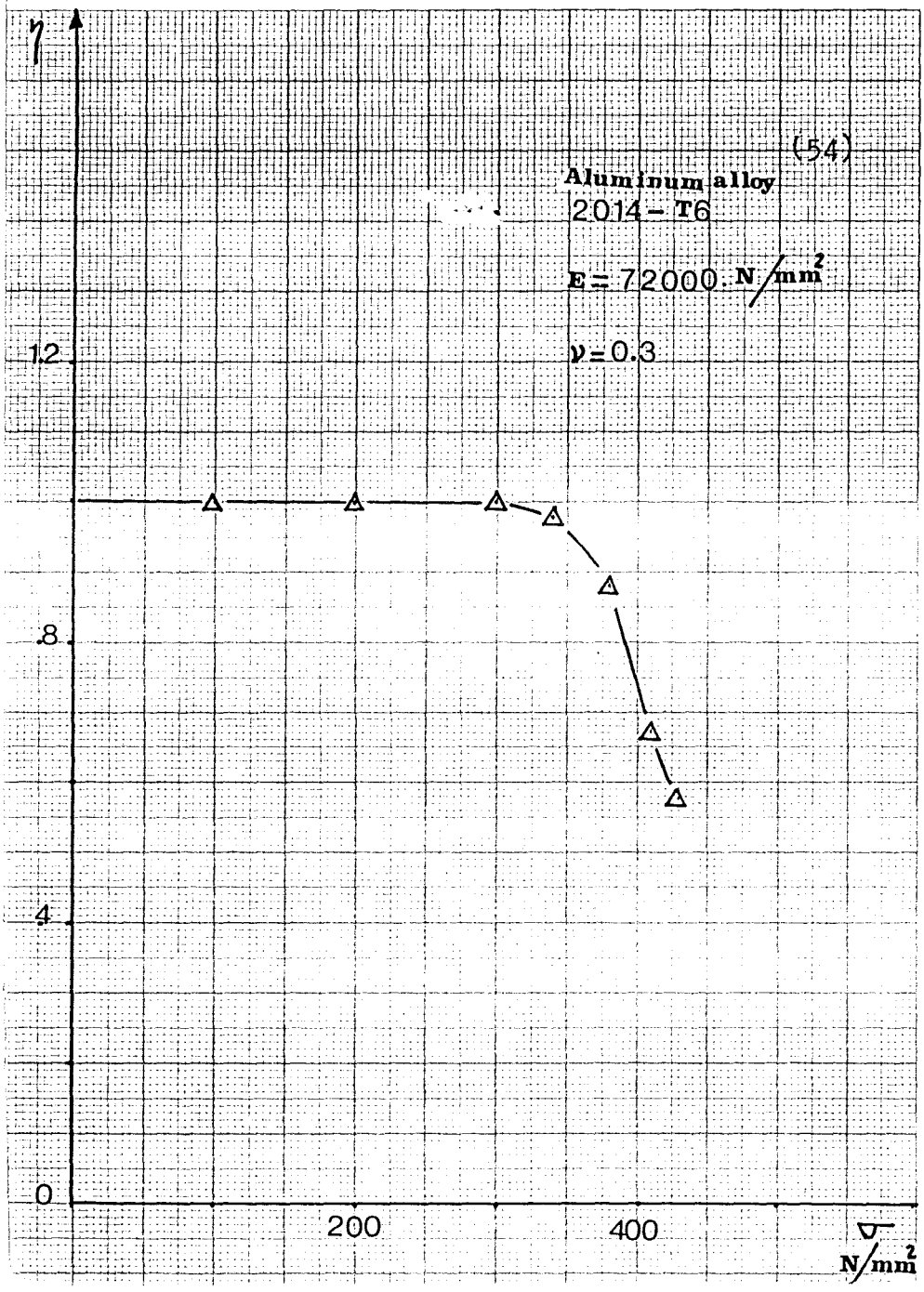

GRAPH (4.2) - OPTIMUM LENGTH TO HEIGHT RATIO OF COMPOSITE PANEL (P - II).

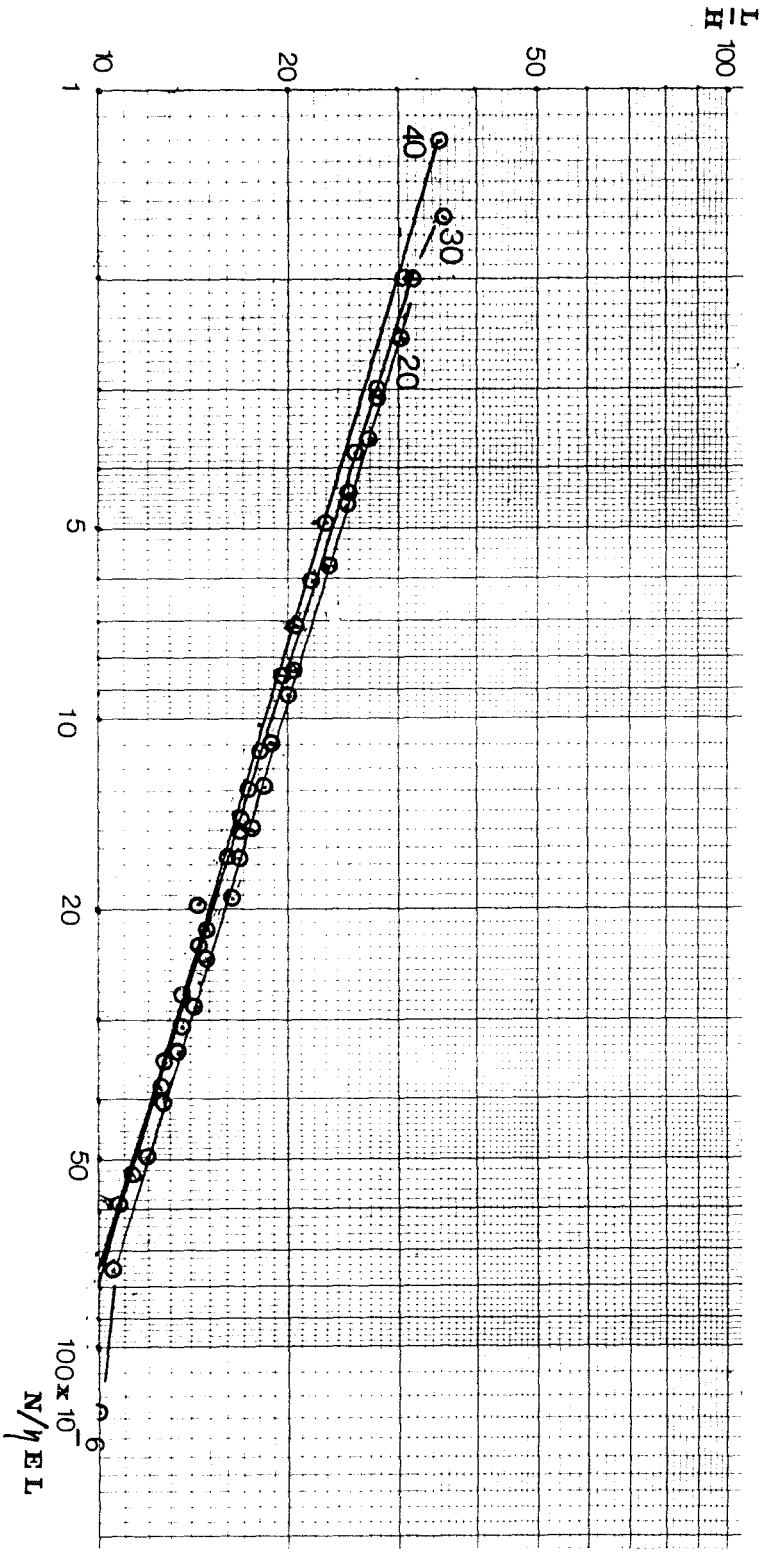

GRAPH (4.3) - OPTIMIMUM CROSS SECTION PROPORTIONS OF COMPOSITE PANEL (P - II).

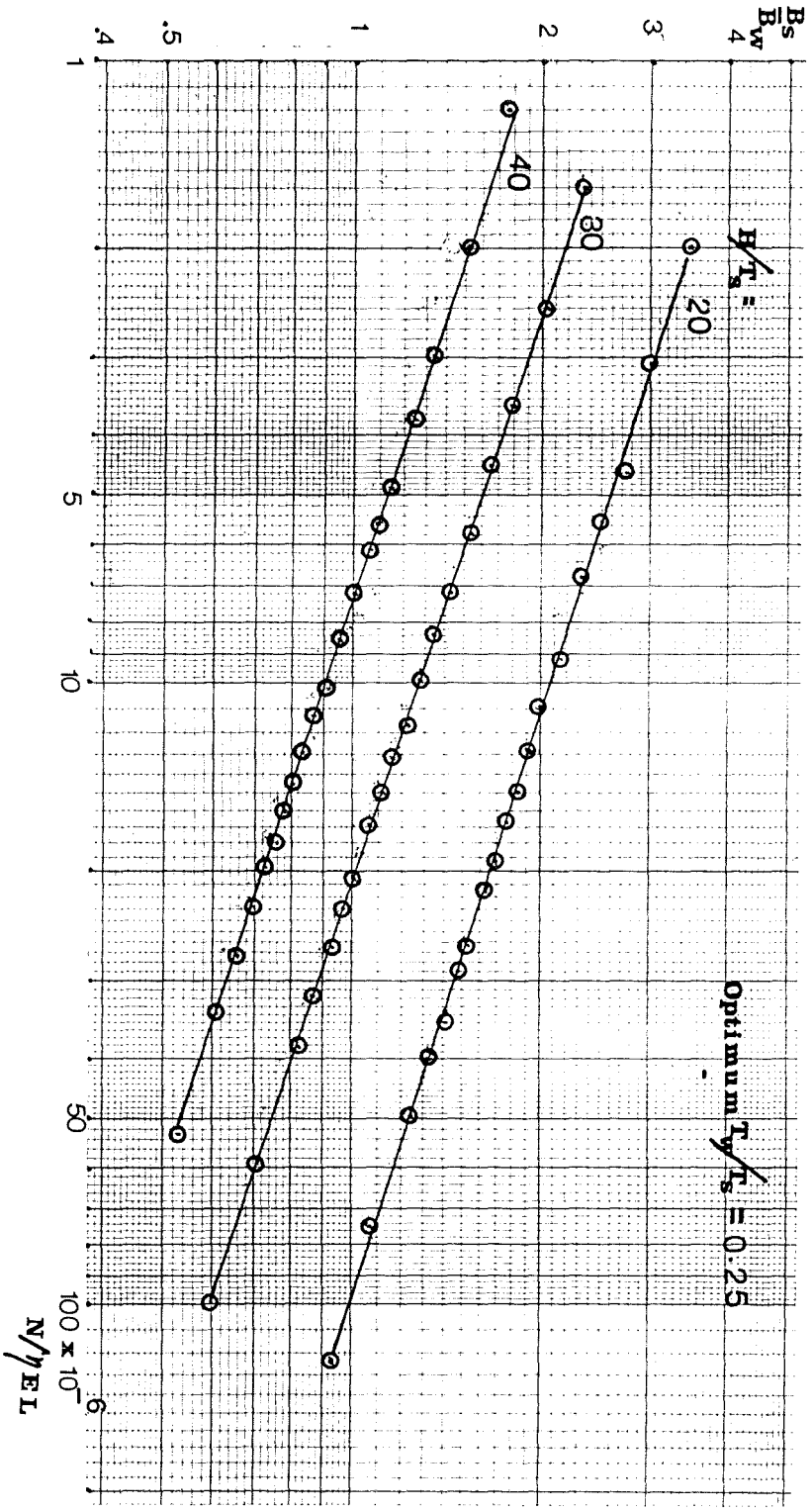

GRAPH (4.4) - WEIGHT EFFICIENCY OF COMPOSITE PANEL (P -II).

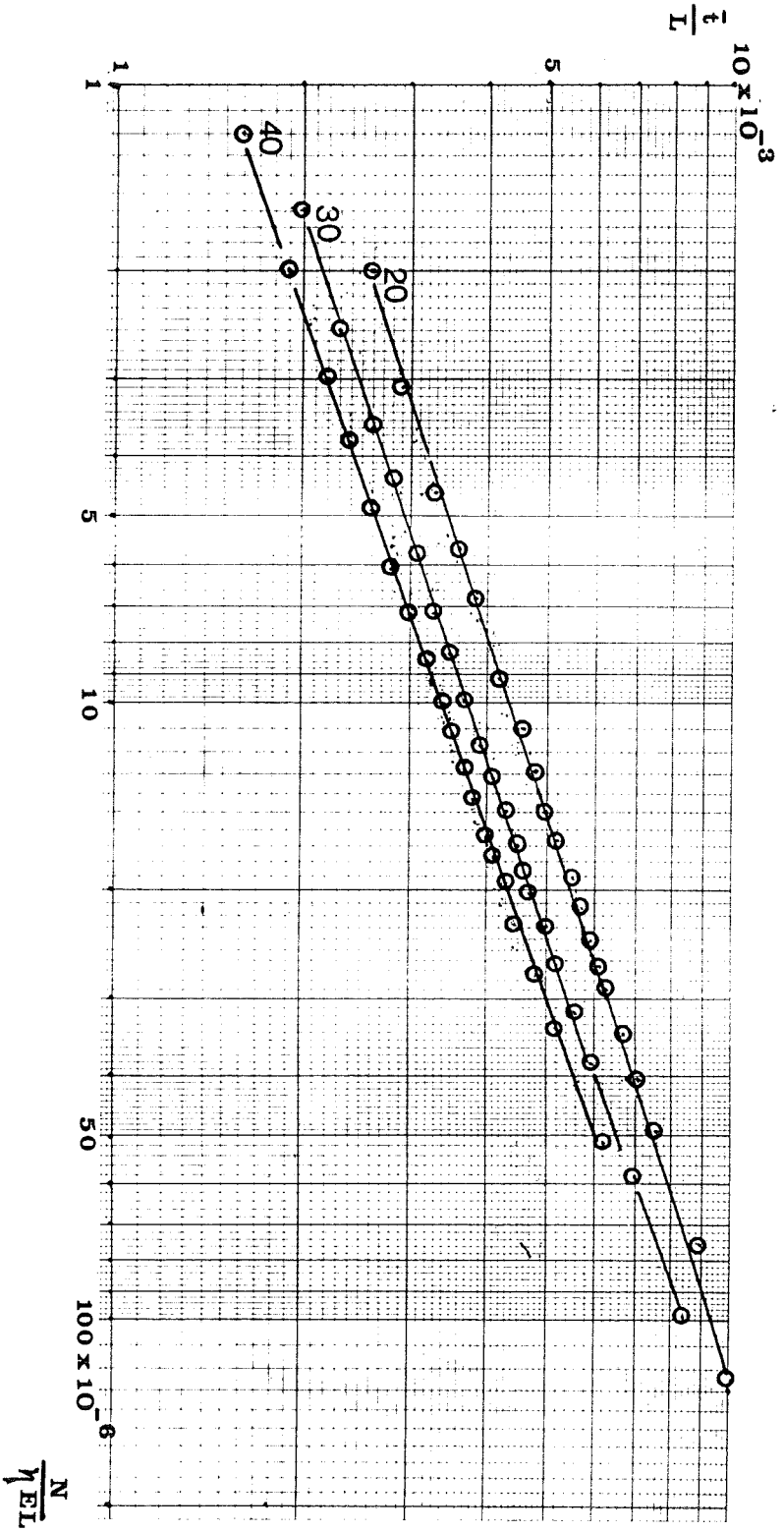

GRAPH (4.5) - OPTIMUM STRESS OF COMPOSITE PANEL (P - II).

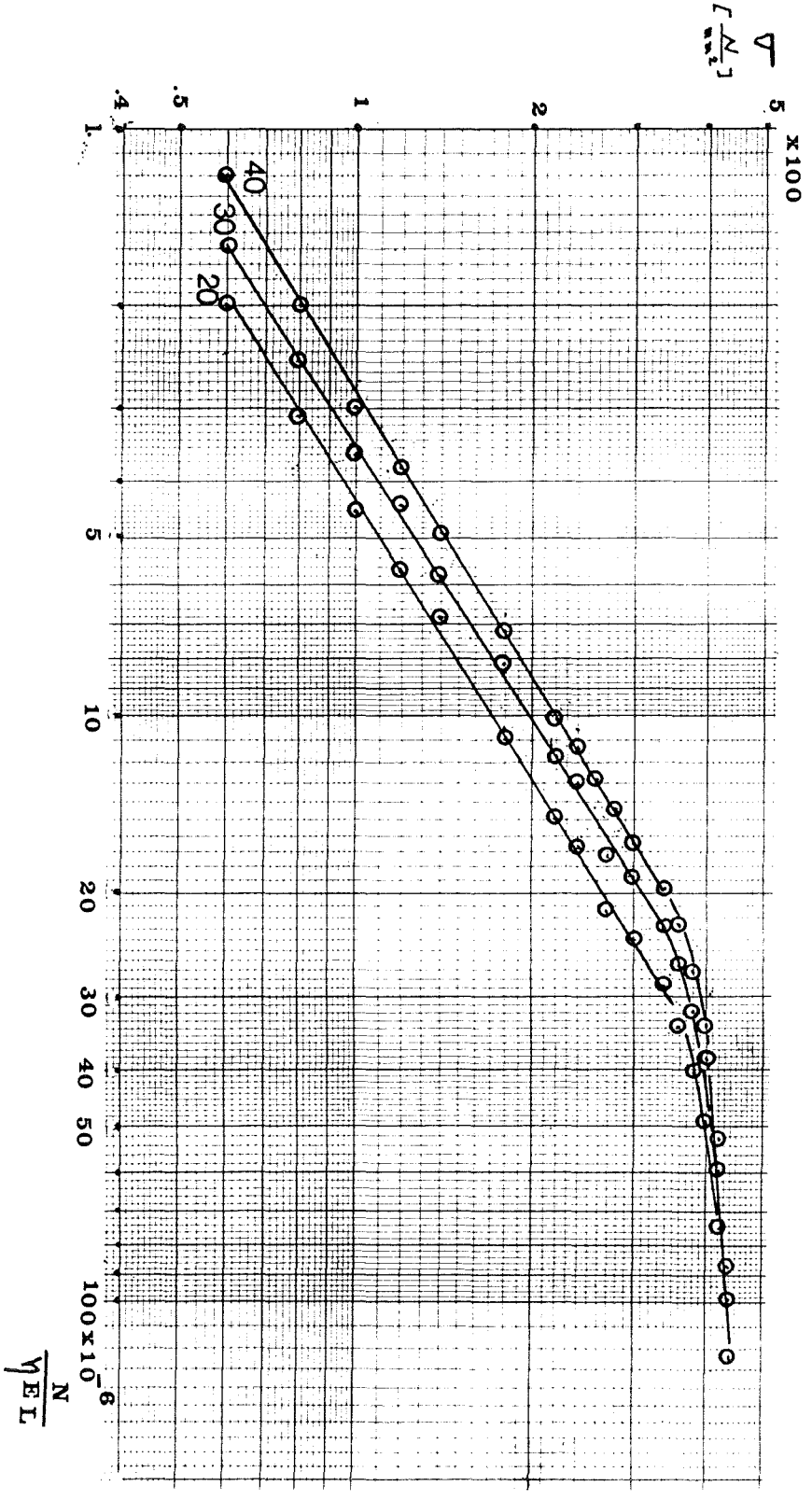

4.5.8. Design Example.

For the same panel considered in Section (4.4), and by using the structural index $N/\eta EL = 1.6\ 10^{-5}$ we find that for $H/T_s = 40$

1.

$L/H = 16.5$ Graph (4.2)

so $H = 57.5$ mm

2.

$B_s/B_w = 0.79$ Graph (4.3)

$B_w = 57.5$ mm

$B_s = 46.0$ mm

$T_s = 1.43$ mm

$T_w = 0.36$ mm

3.

$\bar{t}/L = 0.39\ 10^{-3}$ Graph (4.4)

$\bar{t} = 3.7$ mm

$\bar{t}/\bar{t}_c = 50.8\%$

It is interesting to note that by using $H/T_s = 30$, $\bar{t} = 4.08$

$H/T_s = 20$, $\bar{t} = 4.75$

4. Weight per unit area

$w = \rho \bar{t} = 0.0103$ g/mm

$W = wL^2 = 9.29$ Kg.

5.

$\sigma = 270$ N/mm Graph (4.5)

6.

$E_y/E = 1.3\ 10^{-3}$

GRAPH. (4.6) - WEIGHT EFFICIENCY COMPARISON.

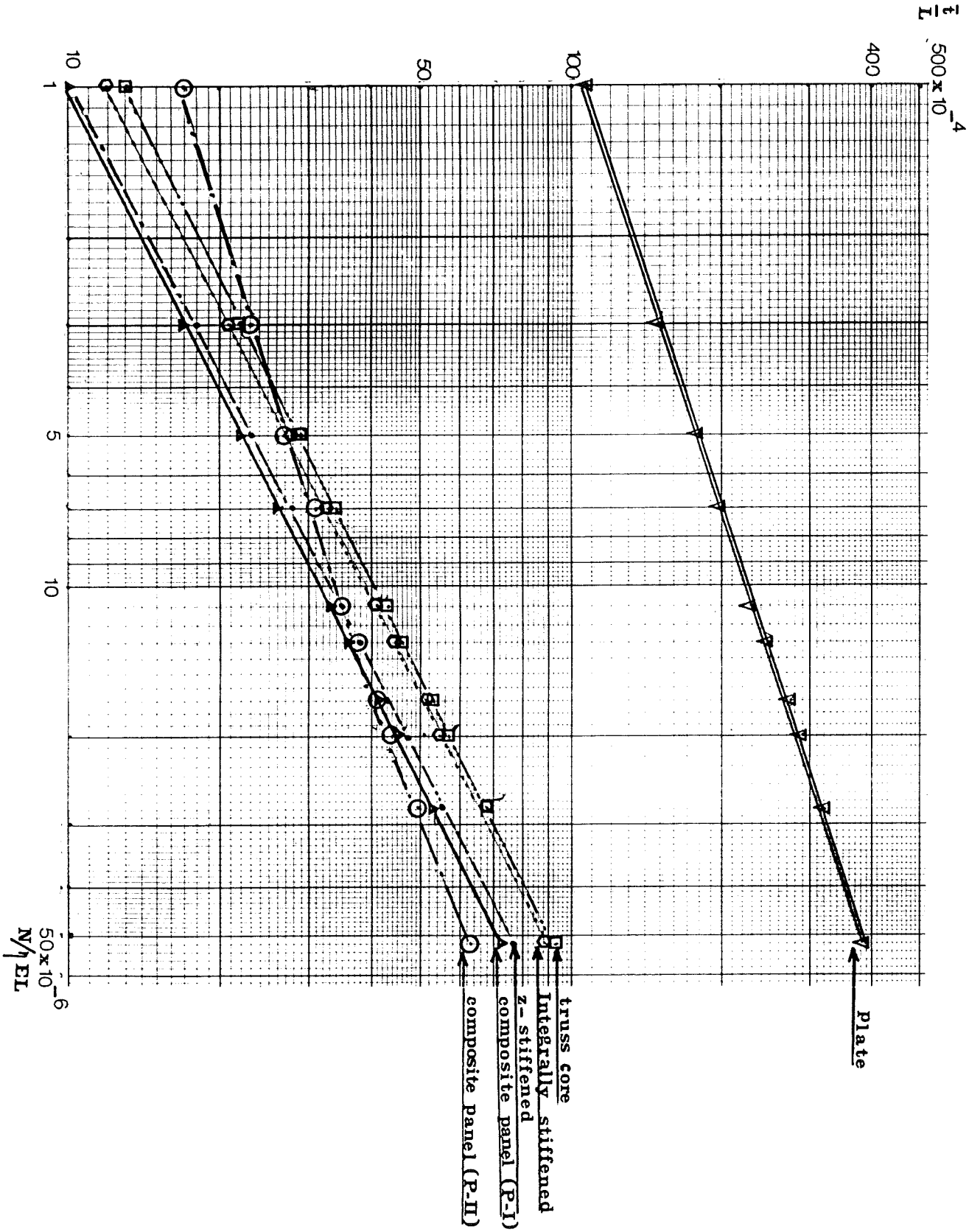

4.6. Conclusions.

1. The two panels which have been studied in this Chapter, are both very efficient.

The first, P - I, as shown in Graph (4.6), is more efficient when the structural index is in the range up to 15×10^{-6} , for higher values of the structural index, Panel P - II is more efficient.

2. It is interesting to note that even the Z - stiffened panel is found to be heavier relative to the two panels considered.

3. Although the panel (P -II) uses less skin material than panel (P - I) the production of such thin stiffeners may prove to be more difficult.

4. The optimum thickness ratio found for panel (P - II), which is equal to 0.25, corresponds to the lowest value of the thickness ratio range considered in the iteration procedure.

5. Although the optimum thickness ratio for panel (P - II) is found to be very small, in reality the panel behaves as if it possesses a large thickness ratio because of the presence of the orthotropic core and its longitudinal stiffness which compensates the apparent value of T_w/T_s .

6. The design examples for the two panels give results which are not much different, this is because the structural index value coincides with the value at which the efficiency curves for the two types of panels coincide.

7. It must be remembered that the composite panel (P - II) plot included in Graph (4.2) is that of $H/T_s = 40$ and the other curves will be heavier.

CHAPTER 5

COMPUTER PROGRAMMES

5.1. Introduction.

In this Chapter, six computer programmes will be presented, three based on the standard finite element method and three based on the finite strip method.

These programmes, which have been used extensively in this project, were developed and checked several times before being used, and the results found to be very satisfactory.

All share the same assembly, the reduction and solving subroutines.

The programmes are classified as follows:

1. Programme (3.1) - This programme is used to find the buckling stress for iostropic plates loaded in-plane.
2. Programme (3.2)- This programme is used to study buckling of orthotropic plates.
3. Programme (3.3) - This programme is used to study the buckling of a stiffened panel idealised into rectangular plates and beams.
4. Programme (3.4) - This programme is used to study buckling of isotropic plates and plates on foundations.
5. Programme (3.5) - This programme is used to study buckling of isotropic plates, and local buckling of panels.
6. Programme (4.1) - This programme is used in minimum weight design of composite panels.

The last three programmes are based on the finite strip for local buckling.

For generality a flow chart for each programme is included except for Programme (4.1) which is obtained from Programme (3. 5).

It is also found helpful to include Section (5.2) in which wymbols appearing in flow charts and programmes are defined.

5.2. SYMBOLS AND DEFINITIONS FOR PROGRAMMES AND FLOW CHARTS.

5.2.1. Programmes Based on Standard Finite Element.

a. Programme (3.1)

AA Total length of structure.

BB Total width of structure.

A Length of finite element.

B Width of finite element.

T Thickness.

U Poison's ratio.

PI Constant value of π

PI Assumed value of π

NEIS Number of elements in the longitudinal direction and transverse directions.

NEL Total number of elements in which the structure is idealised.

LL Number of degrees of freedom per node.

IND Number of independent nodes.

I7 Number of constraint degrees of freedom need to be made equal to zero.

I9 Represents the total degrees of freedom of the constrained structure.

NN Represents the total number of freedom of the unconstrained structure.

RUN is a constant used in the analysis so that when RUN = 1 The geometric stiffnes matrix for one element is computed then assembled and after suppression of the degrees of freedom partinent to the constraints a reduced geometric stiffness for the complete structure is obtained. For RUN = 2 similar operations are conducted on the elastic stiffness matrix.

RUN = 3 the reduced geometric and elastic matrices are introduced into the solving subroutine to find the eigenvalues and the eigenvectors of the problem.

k_e Elastic stiffness matrix for one element, = S for RUN = 1.

k_g Geometric stiffness matrix for one element, = S for RUN = 2.

KS The assembly matrix.

KO The matrix representing the reduced stiffness of the structure.

KG Reduced geometric stiffness of the complete structure.

KE Reduced elastic stiffness of the complete structure.

NB(I) One dimensional matrix contain the numbers of degrees of freedom to be suppressed.

ND(I,J) Is matrix of nodal numbering and it is of order (NEL x NOD)

NOD Number of nodes per element.

R(I) Is the eigenvalue matrix.

Z(I,J) Eigenvector matrices.

F02 AEF Is the standard eigenvalue/eigenvector solving substitute used in the programmes (See Appendix (A. 2).

b. Programme (3.2).

As above except for the following symbols:

DX, DY, DXY, D1)Are the flexural rigidities of the orthotropic plate.

TAV Average thickness of the finite plate element.

SA, SB, SC, SD, SL, SE)Are matrices each is of the order of 12 x 12 used to compute the elastic stiffness matrix.

c. Programme (3.3).

As above except for the following symbols:

BS Stiffener spacings.

BW Stiffener height.

TW Stiffener thickness.

TS Skin thickness.

NPLATES Number of plates used in the idealisation.

NBEAMS Number of beams used in the idealisation.

EE Young's modulus.

5.2.2. Programmes Based on Finite Strip.

a. Programme (3.4).

UN Poisqn's constant.

FLA Estimated critical wave length

FB(I) One dimensional matrix representing the width of each strip.

GK The value of spring constant modulus of the core material.

FK(I) Matrix of core stiffness value for each strip.

QM Iteration counter.

STR(QM) Buckling stress computed at the end of each step.

SGI The required value of the buckling stress.

E Young's modulus.

Ex,Ey Young's modulus in compression for core material.

b. Programme (3.5).

As before except for the following symbols:

IP Is used as a counter for the number of iteration.

QM Is used to count the number of times a predicted buckling stress was computed.

F9(I) Is matrix representing the critical wave lengths.

c. Programme (4.1).

As before except for the following symbols:

GX Young's modulus of core material in the longitudinal direction.

G1 Skin material density.

G2 Core material density.

T(I) Matrix of thickness of single strips.

NS Number of stiffeners.

BB Width of single strip.

BWH Stiffener width.

TH Overall thickness of stiffener.

YIX Moment of inertia.

RAG Square of radius of gyration.

DEN Average density of panel.

PROGRAMME (3.1).

FLOW CHART AND FORTRAN LIST

BUCKLING OF ISOTROPIC PLATES.

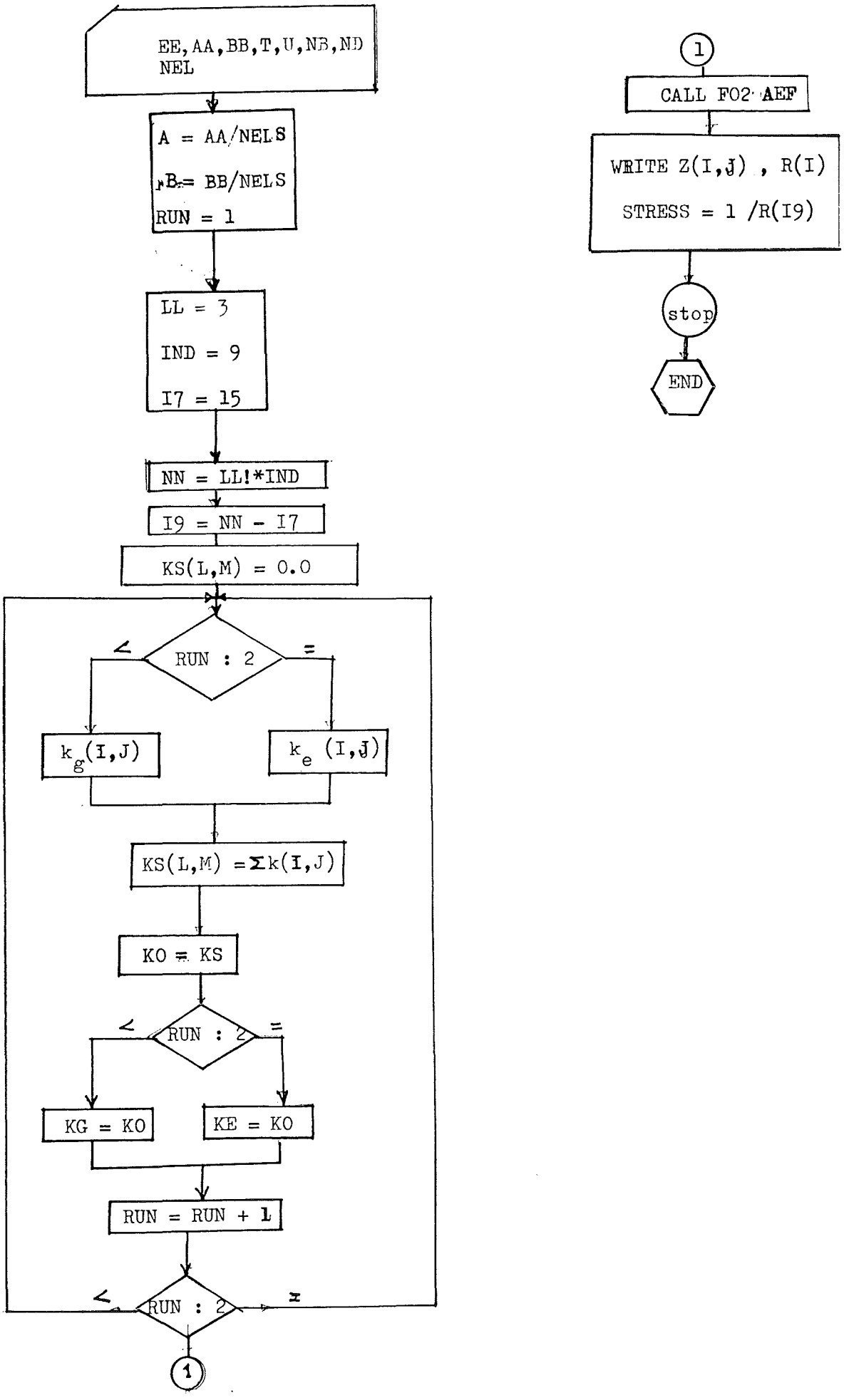
EE, AA, BB, T, U, NB, ND
NEL
A = AA/NELS
B = BB/NELS
RUN = 1
LL = 3
IND = 9
I7 = 15
NN = LL!*IND
I9 = NN - I7
KS(L,M) = 0.0
RUN : 2
k_g(I,J)
k_e (I,J)
KS(L,M) = Σk(I,J)
KO = KS
RUN : 2
KG = KO
KE = KO
RUN = RUN + 1
RUN : 2
1
1
CALL F02 AEF
WRITE Z(I,J) , R(I)
STRESS = 1 /R(I9)
stop
END

```
      DOUBLE PRECISION PI,EE,B,AA,A,S,BB ,SS,KE,KS,KG,DL,Z,Q,R,V,KO,VV,P
      DIMENSION S(12,12),KS(27,27),ND(04,04),NB(15),KO(27,27),KG(12,12),
     5KE(12,12),DL(12),Z(12,12),Q(12),R(12)
      READ(5,1111) EE,AA,BB,T,U
111   FORMAT(1X,9D13.6)
1111  FORMAT(6X,F7.1,1X,2F5.1,1X,2F3.1)
10004  FORMAT(4I4)
      WRITE(6,1111)EE,AA,BB,T,U
      DO 10003 I=1,4
10003 READ(5,10004)(ND(I,J),J=1,4)
       READ(5,*)(NB(I),I=1,15)
      DO 10005 I=1,4
10005 WRITE(6,10004)(ND(I,J),J=1,4)
      WRITE(6,*)(NB(I),I=1,15)
      A=AA/4.
      B=BB/4.
      X=1.-U
      Y=1.+4.*U
      ZZ=14.-4.*U
      RUN=1
 208  NEL=4
      LL=3
      P=B/A
      D=P*P
      IND=9
      I7=15
      NN=LL*IND
      I9=NN-I7
      DO 2 L=1,NN
      DO 2 M=1,NN
2     KS(L,M)=0.0
      I1=1
 33   IF(RUN-2)3,4,632
3     VV=B/(1260.*A)
      S(1,1)=VV*552.
      S(2,1)=VV*B*66.
      S(3,1)=-VV*A*42.
      S(4,1)=VV*204.
      S(5,1)=-VV*B*39.
      S(6,1)=-VV*A*21.
      S(07,1)=-VV*552.
      S(08,1)=-VV*B*66.
      S(09,1)=-VV*A*42.
      S(10,1)=-VV*204.
      S(11,1)=VV*B*39.
      S(12,1)=-21.*A*VV
      S(2,2)=VV*B*B*12.
      S(3,2)=0.0
      S(4,2)=VV*B*39.
      S(5,2)=-VV*B*B*9.
      S(6,2)=0.0
      S(07,2)=-VV*B*66.
      S(8,2) =-VV*B*B*12.
      S(09,2)=0.0
      S(10,2)=-VV*B*39.
```

```
S(11,2)=VV*B*B*9.
S(12,2)=0.0
S(3,3)=56.*A*A*VV
S(4,3)=-21.*A*VV
S(5,3)=0.0
 S(6,3)=28.*A*A*VV
S(07,3)=42.*A*VV
S(08,3)=0.0
S(09,3)=-14.*A*A*VV
S(10,3)=21.*A*VV
S(11,3)=0.0
S(12,3)=-7.*A*A*VV
S(4,4)=552.*VV
S(5,4)=-66.*B*VV
S(6,4)=-42.*A*VV
S(07,4)=-204.*VV
S(08,4)=-39.*B*VV
S(09,4)=-21.*A*VV
S(10,4)=-552.*VV
S(11,4)=66.*B*VV
S(12,4)=-42.*A*VV
S(5,5)=12.*B*B*VV
S(6,5)=0.0
S(07,5)=39.*B*VV
 S(08,5)=9.*B*B*VV
S(09,5)=0.0
S(10,5)=66.*B*VV
S(11,5)=-12.*B*B*VV
S(12,5)=0.0
S(6,6)=56.*A*A*VV
S(07,6)=21.*A*VV
S(08,6)=0.0
S(09,6)=-7.*A*A*VV
S(10,6)=42.*A*VV
S(11,6)=0.0
S(12,6)=-14.*A*A*VV
S(7,7)=552.*VV
S(8,7)=66.*B*VV
S(9,7)=42.*A*VV
S(10,7)=204.*VV
S(11,7)=-39.*B*VV
S(12,7)=21.*A*VV
S(8,8)=12.*B*B*VV
S(9,8)=0.0
S(10,8)=39.*B*VV
S(11,8)=-9.*B*B*VV
S(12,8)=0.0
S(9,9)=56.*A*A*VV
S(10,9)=21.*A*VV
S(11,9)=0.0
S(12,9)=28.*A*A*VV
S(10,10)=552.*VV
S(11,10)=-66.*B*VV
 S(12,10)=42.*A*VV
S(11,11)=12.*B*B*VV
S(12,11)=0.0
```

```
S(12,12)=56.*A*A*VV
GO TO 11
V=EE*(T**3.)/(180.*(1.-U*U)*A*B)
S(1,1)=V*(60.*(D+1./D)+3.*ZZ)
S(2,1)=V*(30./D+3.*Y)*B
S(3,1)=-V*(30.*D+3.*Y)*A
S(4,1)=V*(30.*(D-2./D)-3.*ZZ)
S(5,1)=V*(30./D+3.*X)*B
S(6,1)=V*(-15.*D+3.*Y)*A
S(07,1)=V*(-30.*(2.*D-1./D)-3.*ZZ)
 S(08,1)=V*(15./D-3.*Y)*B
S(09,1)=V*(-30.*D-3.*X)*A
S(10,1)=V*(-30.*(D+1./D)+3.*ZZ)
S(11,1)=V*(15./D-3.*X)*B
S(12,1)=V*(-15.*D+3.*X)*A
S(2,2)=V*(20./D+4.*X)*B*B
S(3,2)=-V*15.*A*B*U
S(4,2)=-S(5,1)
S(5,2)=V*(10./D-X)*B*B
S(6,2)=0.0
S(7,2)=S(8,1)
S(08,2)=V*(10./D-4.*X)*B*B
S(09,2)=0.0
S(10,2)=-S(11,1)
S(11,2)=V*(5./D+X)*B*B
S(12,2)=0.0
S(3,3)=V*(20.*D+4.*X)*A*A
S(4,3)=S(6,1)
S(5,3)=0.0
S(6,3)=V*(10.*D-4.*X)*A*A
S(7,3)=-S(9,1)
S(08,3)=0.0
S(09,3)=V*(10.*D-X)*A*A
S(10,3)=-S(12,1)
S(11,3)=0.0
S(12,3)=V*(5.*D+X)*A*A
S(4,4)=S(1,1)
S(5,4)=-S(2,1)
S(6,4)=S(3,1)
S(7,4)=S(10,1)
 S(8,4)=-S(11,1)
S(9,4)=S(12,1)
S(10,4)=S(7,1)
S(11,4)=-S(8,1)
 S(12,4)=S(9,1)
S(5,5)=S(2,2)
S(6,5)=V*15*U*A*B
S(7,5)=S(11,1)
S(8,5)=S(11,2)
S(09,5)=0.0
S(10,5)=-S(8,1)
S(11,5)=S(8,2)
S(12,5)=0.0
S(6,6)=S(3,3)
S(7,6)=-S(12,1)
S(08,6)=0.0
```

```
      S(9,6)=S(12,3)
      S(10,6)=-S(9,1)
      S(11,6)=0.0
      S(12,6)=S(9,3)
      S(07,07)=S(1,1)
      S(08,07)=S(2,1)
      S(09,07)=-S(3,1)
      S(10,7)=S(4,1)
      S(11,7)=S(5,1)
      S(12,7)=-S(6,1)
      S(08,08)=S(2,2)
      S(9,8)=S(6,5)
      S(10,8)=S(4,2)
      S(11,8)=S(5,2)
      S(12,8)=0.0
      S(09,09)=S(3,3)
      S(10,9)=-S(6,1)
      S(11,9)=0.0
      S(12,9)=S(6,3)
      S(10,10)=S(1,1)
      S(11,10)=-S(2,1)
      S(12,10)=-S(3,1)
      S(11,11)=S(2,2)
      S(12,11)=S(3,2)
      S(12,12)=S(3,3)
11    DO 7 I=1,12
      DO 7 J=1,12
 7    S(I,J)=S(J,I)
      NOD=4
1000   N1=1
52    L1=1
50    DO 90 I=1,LL
      DO 90 J=1,LL
      L2=I+(N1-1)*LL
      M3=J+(L1-1)*LL
      L=LL*ND(I1,N1)-LL+I
      M=LL*ND(I1,L1)-LL+J
90    KS(L,M)=KS(L,M)+S(L2,M3)
      L1=L1+1
      IF(L1-NOD)50,50,51
51    N1=N1+1
      IF(N1-NOD)52,52,53
53    I1=I1+1
      IF(I1-NEL)33,33,320
320   DO 500 L=1,NN
      DO 500 M=1,NN
      KO(L,M)=KS(L,M)
500   CONTINUE
      DO 600 II=1,I7
      K=NB(II)
      K=K-II+1
      ITERM=NN-1
      DO 510 L=K,ITERM
      IP1=L+1
      DO 510 M=1,NN
      KO(L,M)=KS(IP1,M)
```

```
510   CONTINUE
      NM1=NN-1
      DO 540 L=1,NM1
      DO 540 M=1,NN
      KS(L,M)=KO(L,M)
540   CONTINUE
      DO 520 M=K,ITERM
      JP1=M+1
      DO 520 L=1,NN
520   KO(L,M)=KS(L,JP1)
      NN=NN-1
      DO 545 L=1,NN
      DO 545 M=1,NN
      KS(L,M)=KO(L,M)
545   CONTINUE
600   CONTINUE
      IF(RUN-2)16,17,602
16    DO 161 I=1,I9
      DO 161 J=1,I9
161   KG(I,J)=KO(I,J)
      GO TO 207
17    DO 171 I=1,I9
      DO 171 J=1,I9
171   KE(I,J)=KO(I,J)
 207  RUN=RUN+1
      IF(RUN-2)208,208,602
602   IFAIL=0
      CALL F02AEF(KG,I9,KE,I9,I9,R,Z,I9,DL,Q,IFAIL)
      IF(IFAIL.EQ.0) GO TO 1066
      WRITE(6,99994) IFAIL
99994 FORMAT(I2)
      STOP
1066  WRITE(6,106)(R(I),I=1,I9)
 106  FORMAT(/'EIGENVALUES'/,((3X,D13.6)))
      DO 107 J=I9,I9
      WRITE(6,1071)J
      WRITE(6,1072)(Z(I,J),I=1,I9)
107   CONTINUE
 1071 FORMAT (/'EIGENVECTOR NO',I2)
1072  FORMAT(/,(1X,D13.5))
      STRESS=1./R(I9)
      WRITE(6,2093) STRESS
2093  FORMAT(2X,F9.1)
      WRITE(6,1109)
1109  FORMAT(/' MATRIX KE'/)
      DO 1017 I=1,7
1017   WRITE(6,111)(KE(I,J),J=1,7)
      WRITE(6,2223)
2223  FORMAT(/' MATRIX KG'/)
      DO 2222 I=1,7
2222  WRITE(6,111)(KG(I,J),J=1,7)
503   STOP
      END
```

PROGRAMME (3.2).

FLOW CHART AND FORTRAN LIST

BUCKLING OF ORTHOTROPIC PLATES.

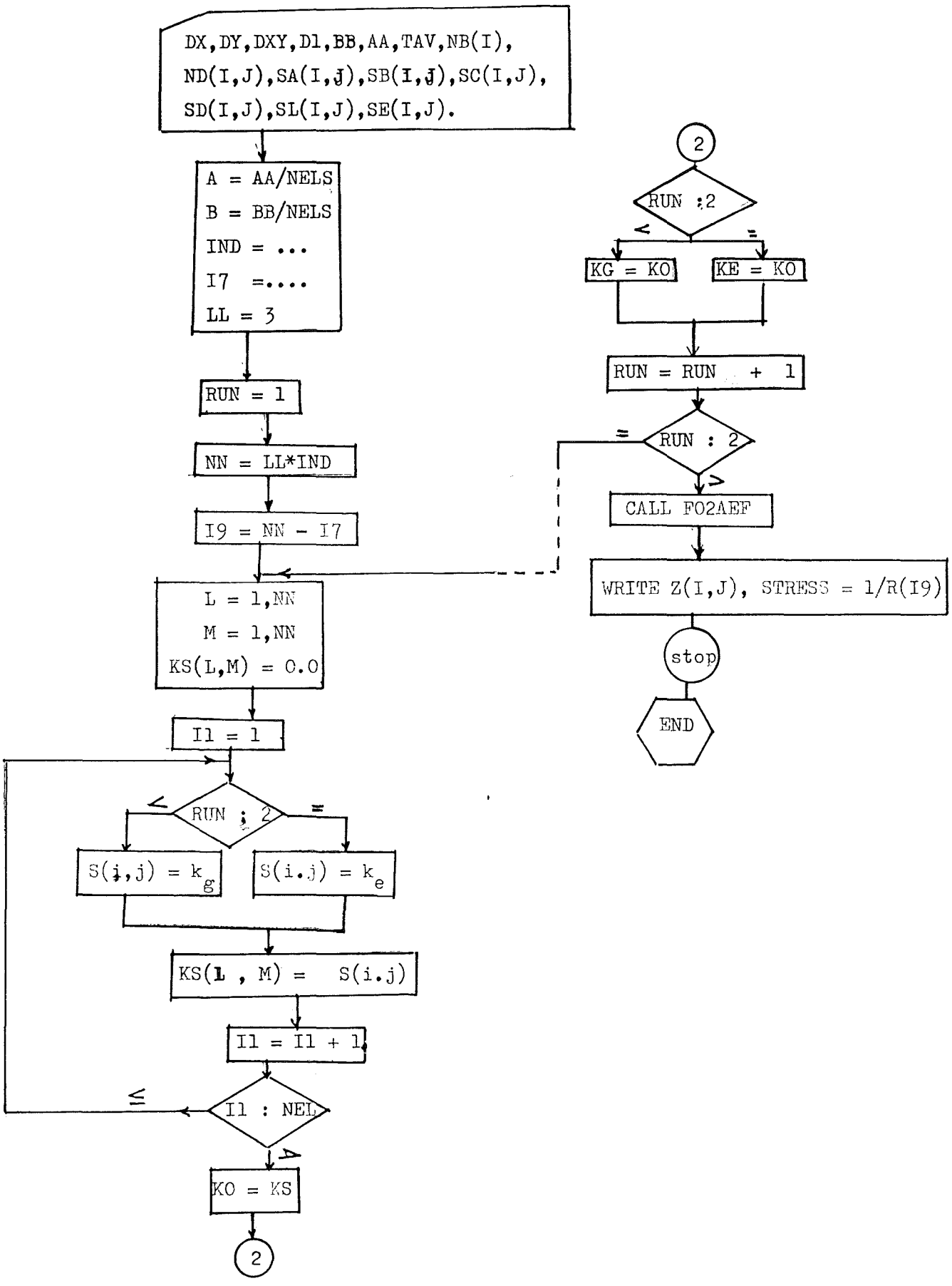
DX,DY,DXY,D1,BB,AA,TAV,NB(I),
ND(I,J),SA(I,J),SB(I,J),SC(I,J),
SD(I,J),SL(I,J),SE(I,J).
A = AA/NELS
B = BB/NELS
IND = ...
I7 =....
LL = 3
RUN = 1
NN = LL*IND
I9 = NN - I7
L = 1,NN
M = 1,NN
KS(L,M) = 0.0
I1 = 1
RUN : 2
S(i,j) = k_g
S(i.j) = k_e
KS(L , M) = S(i.j)
I1 = I1 + 1
I1 : NEL
KO = KS
2
2
RUN : 2
KG = KO
KE = KO
RUN = RUN + 1
RUN : 2
CALL FO2AEF
WRITE Z(I,J), STRESS = 1/R(I9)
stop
END

```
C      ORTHOTROPIC PLATE
C      RECTANGULAR PLATE IDEALIZZATION
       DOUBLE PRECISION PI,EE,B,AA,A,S,BB ,SS,KE,KS,KG,DL,Z,Q,R,V,KO,
      2SA,SB,SC,SD,SL,SM,ST,SU,DX,DY,DXY,D1,TAV,VV,P,SE,SF,SG
        DIMENSION S(12,12),KS(48,48),ND(9,4),NB(28),KO(48,48),KG(20,20),
      5KE(20,20),DL(20),Z(20,20),Q(20),R(20),SA(12,12),SB(12,12),
      7SC(12,12),SD(12,12),SL(12,12),SM(12,12),ST(12,12),SU(12,12),
      9SE(12,12),SG(12,12),SF(12,12)
       READ(5,99)DX,DY,DXY,D1,BB,AA,TAV
99     FORMAT(4X,4F7.1,1X,2F4.1,1X,F4.2)
       WRITE(6,99)DX,DY,DXY,D1,BB,AA,TAV
111    FORMAT(1X,(9D13.6))
1111   FORMAT(12F6.1)
10004  FORMAT(4I4)
       READ(5,*)(NB(I),I=1,28)
       WRITE(6,*)(NB(I),I=1,28)
       DO 10003 I=1,9
10003  READ(5,10004) (ND(I,J),J=1,4)
       DO 1 I=1,12
 1     READ(5,1111) (SA(I,J),J=1,12)
       DO 5  I=1,12
 5     READ(5,1111) (SB(I,J),J=1,12)
       DO 6  I=1,12
 6     READ(5,1111) (SC(I,J),J=1,12)
       DO 9  I=1,12
 9     READ(5,1111) (SD(I,J),J=1,12)
       DO 162I=1,12
162    READ(5,1111)(SL(I,J),J=1,12)
       DO 787 I=1,12
787    READ(5,1111)(SE(I,J),J=1,12)
       DO 12 I=1,12
  12   WRITE(6,1111)(SA(I,J),J=1,12)
       DO 13 I=1,12
  13   WRITE(6,1111)(SB(I,J),J=1,12)
       DO 14 I=1,12
  14   WRITE(6,1111)(SC(I,J),J=1,12)
       DO 15 I=1,12
15     WRITE(6,1111)(SD(I,J),J=1,12)
        DO 163 I=1,12
 163    WRITE(6,1111)(SL(I,J),J=1,12)
       DO 7871 I=1,12
7871   WRITE(6,1111) (SE(I,J),J=1,12)
       DO 10005 I=1,9
10005   WRITE(6,10004)(ND(I,J),J=1,4)
       A=AA/3.
       B=BB/3.
       RUN=1
208    NEL=9
       LL=3
        P=A/B
       IND=16
       I7=28
       NN=LL*IND
       I9=NN-I7
```

```
      DO 2 L=1,NN
      DO 2 M=1,NN
2     KS(L,M)=0.0
      I1=1
 33   IF(RUN-2)3,4,602
3     VV=B/(1260.*A)
      S(1,1)=VV*552.
      S(2,1)=VV*B*66.
      S(3,1)=-VV*A*42.
      S(4,1)=VV*204.
      S(5,1)=-VV*B*39.
      S(6,1)=-VV*A*21.
      S(07,1)=-VV*552.
      S(08,1)=-VV*B*66.
      S(09,1)=-VV*A*42.
      S(10,1)=-VV*204.
      S(11,1)=VV*B*39.
      S(12,1)=-21.*A*VV
      S(2,2)=VV*B*B*12.
      S(3,2)=0.0
      S(4,2)=VV*B*39.
      S(5,2)=-VV*B*B*9.
      S(6,2)=0.0
      S(07,2)=-VV*B*66.
      S(08,2)=-VV*B*B*12.
      S(09,2)=0.0
      S(10,2)=-VV*B*39.
      S(11,2)=VV*B*B*9.
      S(12,2)=0.0
      S(3,3)=56.*A*A*VV
      S(4,3)=-21.*A*VV
      S(5,3)=0.0
       S(6,3)=28.*A*A*VV
      S(07,3)=42.*A*VV
      S(08,3)=0.0
      S(09,3)=-14.*A*A*VV
      S(10,3)=21.*A*VV
      S(11,3)=0.0
      S(12,3)=-7.*A*A*VV
      S(4,4)=552.*VV
      S(5,4)=-66.*B*VV
      S(6,4)=-42.*A*VV
      S(07,4)=-204.*VV
      S(08,4)=-39.*B*VV
      S(09,4)=-21.*A*VV
      S(10,4)=-552.*VV
      S(11,4)=66.*B*VV
      S(12,4)=-42.*A*VV
      S(5,5)=12.*B*B*VV
      S(6,5)=0.0
      S(07,5)=39.*B*VV
       S(08,5)=9.*B*B*VV
      S(09,5)=0.0
      S(10,5)=66.*B*VV
      S(11,5)=-12.*B*B*VV
      S(12,5)=0.0
```

```
      S(6,6)=56.*A*A*VV
      S(07,6)=21.*A*VV
      S(08,6)=0.0
      S(09,6)=-7.*A*A*VV
      S(10,6)=42.*A*VV
      S(11,6)=0.0
      S(12,6)=-14.*A*A*VV
      S(7,7)=552.*VV
      S(8,7)=66.*B*VV
      S(9,7)=42.*A*VV
      S(10,7)=204.*VV
      S(11,7)=-39.*B*VV
      S(12,7)=21.*A*VV
      S(8,8)=12.*B*B*VV
      S(9,8)=0.0
      S(10,8)=39.*B*VV
      S(11,8)=-9.*B*B*VV
      S(12,8)=0.0
      S(9,9)=56.*A*A*VV
      S(10,9)=21.*A*VV
      S(11,9)=0.0
      S(12,9)=28.*A*A*VV
      S(10,10)=552.*VV
      S(11,10)=-66.*B*VV
       S(12,10)=42.*A*VV
      S(11,11)=12.*B*B*VV
      S(12,11)=0.0
      S(12,12)=56.*A*A*VV
      DO 7 I=1,12
      DO 7 J=1,12
 7    S(I,J)=S(J,I)
      DO 707 J=1,12
      DO 727 I=1,12
      SF(I,J)=0.0
      DO 747 K=1,12
      SF(I,J)=SF(I,J)+SE(I,K)*S(K,J)
747   CONTINUE
727   CONTINUE
707   CONTINUE
      DO 757 J=1,12
      DO 767 I=1,12
      SG(I,J)=0.0
      DO 777 K=1,12
      SG(I,J)=SG(I,J)+SF(I,K)*SE(K,J)
777   CONTINUE
767   CONTINUE
757   CONTINUE
      DO 737 I=1,12
      DO 737 J=1,12
737   S(I,J)=SG(I,J)
      GO TO 11
 4    DO 18 I=1,12
      DO 18 J=1,12
18    SU(I,J)=(DX/(P*P))*SA(I,J)+ DY*P*P*SB(I,J)+D1*SC(I,J)+DXY*SD(I,J)
      DO 19 J=1,12
      DO 20 I=1,12
```

```
      ST(I,J)=0.0
      DO 21 K=1,12
      ST(I,J)=ST(I,J)+SL(I,K)*SU(K,J)
21    CONTINUE
20     CONTINUE
19    CONTINUE
      DO 22 J=1,12
      DO 23 I=1,12
      SM(I,J)=0.0
      DO 24 K=1,12
      SM(I,J)=SM(I,J)+ST(I,K)*SL(K,J)
24    CONTINUE
 23   CONTINUE
22    CONTINUE
      DO 25 I=1,12
      DO 25 J=1,12
25    S(I,J)=(4./(60.*A*B))*SM(I,J)
11    NOD=4
1000   N1=1
52    L1=1
50    DO 90 I=1,LL
      DO 90 J=1,LL
      L2=I+(N1-1)*LL
      M3=J+(L1-1)*LL
      L=LL*ND(I1,N1)-LL+I
      M=LL*ND(I1,L1)-LL+J
90    KS(L,M)=KS(L,M)+S(L2,M3)
      L1=L1+1
      IF(L1-NOD)50,50,51
51    N1=N1+1
      IF(N1-NOD)52,52,53
53    I1=I1+1
      IF(I1-NEL)33,33,32
320   DO 500 L=1,NN
      DO 500 M=1,NN
      KO(L,M)=KS(L,M)
500   CONTINUE
      DO 600 II=1,I7
      K=NB(II)
      K=K-II+1
      ITERM=NN-1
      DO 510 L=K,ITERM
      IP1=L+1
      DO 510 M=1,NN
      KO(L,M)=KS(IP1,M)
510   CONTINUE
      NM1=NN-1
      DO 540 L=1,NM1
      DO 540 M=1,NN
      KS(L,M)=KO(L,M)
540   CONTINUE
      DO 520 M=K,ITERM
      JP1=M+1
      DO 520 L=1,NN
520   KO(L,M)=KS(L,JP1)
      NN=NN-1
```

FORTRAN TEXT

```
      DO 545 L=1,NN
      DO 545 M=1,NN
      KS(L,M)=KO(L,M)
545   CONTINUE
600   CONTINUE
      IF(RUN-2)16,17,602
16    DO 161 I=1,I9
      DO 161 J=1,I9
161   KG(I,J)=KO(I,J)
      GO TO 207
17    DO 171 I=1,I9
      DO 171 J=1,I9
171   KE(I,J)=KO(I,J)
207   RUN=RUN+1
      IF(RUN-2)208,208,602
 602  IFAIL=0
      CALL F02AEF(KG,I9,KE,I9,I9,R,Z,I9,DL,Q,IFAIL)
      IF(IFAIL.EQ.0) GO TO 1066
      WRITE(6,99994) IFAIL
99994 FORMAT(I2)
      STOP
 1066 WRITE(6,106)(R(I),I=1,I9)
106   FORMAT(/'EIGENVALUES'/,((3X,D13.6)))
      DO 107 J=I9,I9
      WRITE(6,1071)J
      WRITE(6,1072)(Z(I,J),I=1,I9)
107   CONTINUE
1071  FORMAT(/'EIGENVECTOR NO',I2)
1072  FORMAT(/,(1X,D13.5))
      STRESS=1./R(I9)
      WRITE(6,2093) STRESS
2093  FORMAT(2X,F9.1)
503   STOP
      END
```

PROGRAMME (3.3).

FLOW CHART AND FORTRAN LIST

BUCKLING OF STIFFENED PANEL

PLATE-BEAM IDEALISATION.

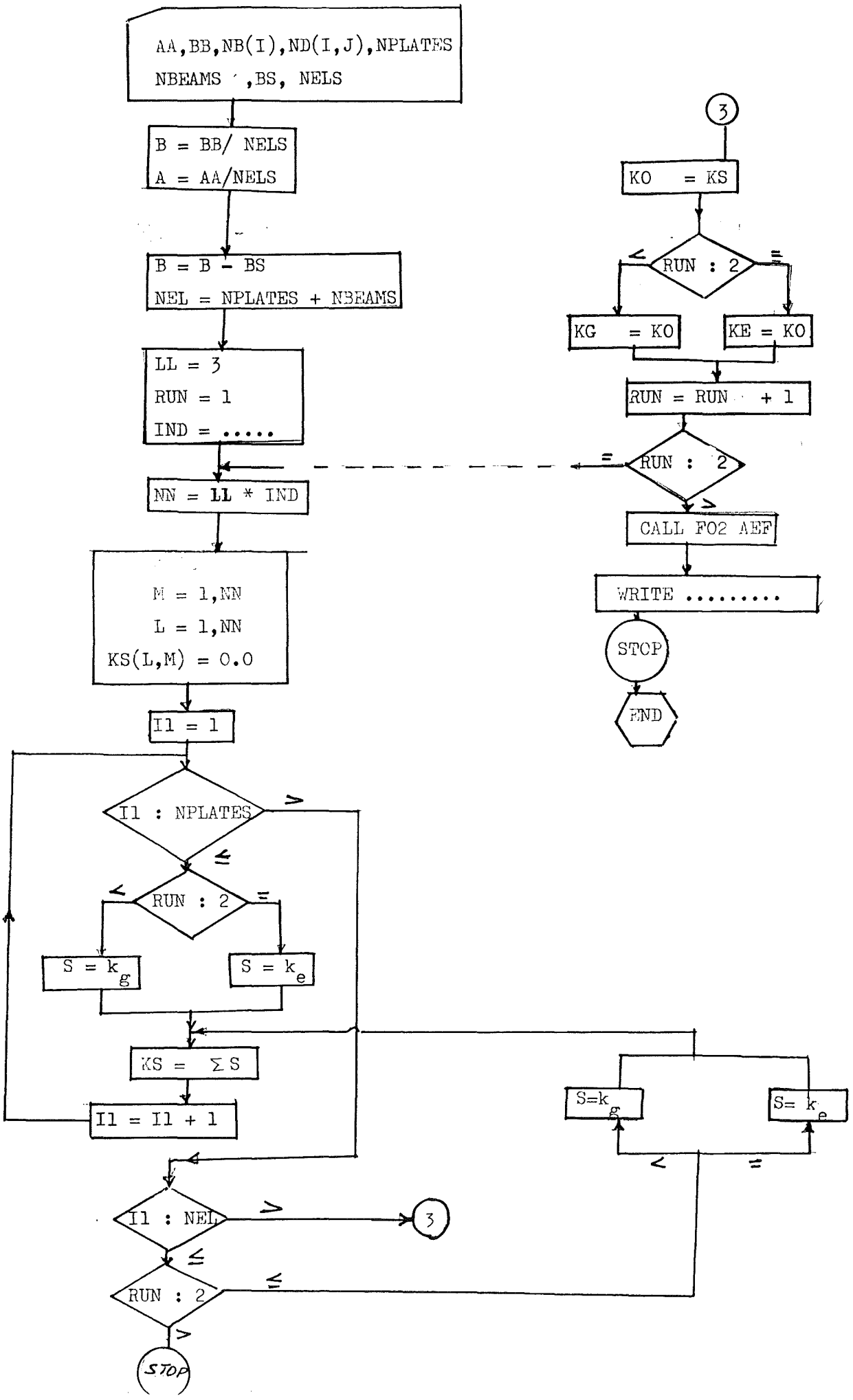
AA,BB,NB(I),ND(I,J),NPLATES
NBEAMS ,BS, NELS
B = BB/ NELS
A = AA/NELS
B = B - BS
NEL = NPLATES + NBEAMS
LL = 3
RUN = 1
IND = ...
NN = LL * IND
M = 1,NN
L = 1,NN
KS(L,M) = 0.0
I1 = 1
I1 : NPLATES
RUN : 2
S = k g
S = k e
KS = Σ S
I1 = I1 + 1
I1 : NEL
RUN : 2
STOP
3
KO = KS
RUN : 2
KG = KO
KE = KO
RUN = RUN + 1
RUN : 2
CALL FO2 AEF
WRITE .....
STOP
END
S=k g
S= k e

```
C       STABILITY OF STIFFENED PLATE BY FINITE ELEMENT METHOD
C       OVERALL BUCKLING
C       IDEALIZATION: PLATE-BEAM
C       EFFECTIVE FLANGE
        DOUBLE PRECISION PI,EE,B,AA,A,S,BB ,SS,KE,KS,KG,DL,Z,Q,R,V,KO,VV,P
         DIMENSION S(12,12),KS(147,147),KO(147,147),ND(78,4),NB(42),
       4KG(105,105),KE(105,105),DL(105),Z(105,105),Q(105),R(105)
        READ(5,1111) EE,AA,BB,T,U,BS,BW,TW
1111    FORMAT(6X,F7.1,1X,2F5.1,1X,2F3.1,F4.1,1X,F4.1,1X,F5.2)
        I7=42
        NBEAMS=24
        NPLATES=36
        NEL=NPLATES+NBEAMS
        NOPEL=4
        DO 1116 I=1,NEL
1116    READ(5,1118)(ND(I,J),J=1,NOPEL)
 1118   FORMAT(4I4)
111     FORMAT(1X,9D13.6)
         READ(5,*)(NB(I),I=1,I7)
        DO 1119 I=1,NEL
1119    WRITE(6,1118) (ND(I,J),J=1,NOPEL)
        WRITE(6,*)(NB(I),I=1,I7)
        AA=241
        BB=178
        B=BB/6.
        BBB1=B
        BS=3.0*T
77777   B=BBB1-BS
```

```
      A=AA/6.
      X=1.-U
      Y=1.+4.*U
      ZZ=14.-4.*U
      B1=TW
      B2=BW
2088  RUN=1
208   LL=3
      P=  B/A
      D=P*P
      GB=EE/(2.+2.*U)
      AR=B2*B1+BS*T
      STA=B1*B2*(B2/2.+T)+T*BS*(T/2.)
      ZCG=STA/AR
      ZX=(BS*(T**3.))/12.+(BS*T)*((ZCG-T/2.)**2.)
      ZY=B1*(B2**3.)/12.+B1*B2*((B2/2.+T-ZCG)**2.)
      ZYY=ZY+ZX
      PHIZ=(12.*EE*ZYY)/(GB*B2*B1*A*A)
      QB=(EE*ZYY)/((1.+PHIZ)*A)
      BJ=(1./3.)*B2*(B1**3.)+BS*(T**3.)*(1./3.)
       WRITE(6,111)AR,STA,ZCG,ZY,ZX,ZYY,PHIZ,QB,BJ,P
      IND=49
      VZ=0.0
      NN=LL*IND
      I9=NN-I7
      DO 2 L=1,NN
      DO 2 M=1,NN
2     KS(L,M)=0.0
```

```
      I1=1
 33   IF(I1.GT.NPLATES) GO TO 303
      IF(RUN-2)3,4,602
3     VV=(B*T)/(1260.*A)
      S(1,1)=VV*552.+2.*VZ
      S(2,1)=VV*B*66.
      S(3,1)=-VV*A*42.
      S(4,1)=VV*204.+VZ
      S(5,1)=-VV*B*39.
      S(6,1)=-VV*A*21.
      S(07,1)=-VV*552.-2.*VZ
      S(08,1)=-VV*B*66.
      S(09,1)=-VV*A*42.
      S(10,1)=-VV*204.-VZ
      S(11,1)=VV*B*39.
      S(12,1)=-21.*A*VV
      S(2,2)=VV*B*B*12.
      S(3,2)=0.0
      S(4,2)=VV*B*39.
      S(5,2)=-VV*B*B*9.
      S(6,2)=0.0
      S(07,2)=-VV*B*66.
      S(8,2) =-VV*B*B*12.
      S(09,2)=0.0
      S(10,2)=-VV*B*39.
      S(11,2)=VV*B*B*9.
      S(12,2)=0.0
      S(3,3)=56.*A*A*VV
      S(4,3)=-21.*A*VV
      S(5,3)=0.0
       S(6,3)=28.*A*A*VV
      S(07,3)=42.*A*VV
      S(08,3)=0.0
      S(09,3)=-14.*A*A*VV
      S(10,3)=21.*A*VV
      S(11,3)=0.0
      S(12,3)=-7.*A*A*VV
      S(4,4)=552.*VV+2.*VZ
      S(5,4)=-66.*B*VV
      S(6,4)=-42.*A*VV
      S(07,4)=-204.*VV-VZ
      S(08,4)=-39.*B*VV
      S(09,4)=-21.*A*VV
      S(10,4)=-552.*VV-2.*VZ
      S(11,4)=66.*B*VV
      S(12,4)=-42.*A*VV
      S(5,5)=12.*B*B*VV
      S(6,5)=0.0
      S(07,5)=39.*B*VV
       S(08,5)=9.*B*B*VV
      S(09,5)=0.0
      S(10,5)=66.*B*VV
      S(11,5)=-12.*B*B*VV
      S(12,5)=0.0
      S(6,6)=56.*A*A*VV
      S(07,6)=21.*A*VV
```

```
      S(08,6)=0.0
      S(09,6)=-7.*A*A*VV
      S(10,6)=42.*A*VV
      S(11,6)=0.0
      S(12,6)=-14.*A*A*VV
      S(7,7)=552.*VV+2.*VZ
      S(8,7)=66.*B*VV
      S(9,7)=42.*A*VV
      S(10,7)=204.*VV+VZ
      S(11,7)=-39.*B*VV
      S(12,7)=21.*A*VV
      S(8,8)=12.*B*B*VV
      S(9,8)=0.0
      S(10,8)=39.*B*VV
      S(11,8)=-9.*B*B*VV
      S(12,8)=0.0
      S(9,9)=56.*A*A*VV
      S(10,9)=21.*A*VV
      S(11,9)=0.0
      S(12,9)=28.*A*A*VV
      S(10,10)=552.*VV+2.*VZ
      S(11,10)=-66.*B*VV
       S(12,10)=42.*A*VV
      S(11,11)=12.*B*B*VV
      S(12,11)=0.0
      S(12,12)=56.*A*A*VV
      WRITE(6,1111) EE,A,B,T,U,BS,BW,TW
      GO TO 11
4     V=EE*(T**3.)/(180.*(1.-U*U)*A*B)
      S(1,1)=V*(60.*(D+1./D)+3.*ZZ)
      S(2,1)=V*(30./D+3.*Y)*B
      S(3,1)=-V*(30.*D+3.*Y)*A
      S(4,1)=V*(30.*(D-2./D)-3.*ZZ)
      S(5,1)=V*(30./D+3.*X)*B
      S(6,1)=V*(-15.*D+3.*Y)*A
      S(07,1)=V*(-30.*(2.*D-1./D)-3.*ZZ)
       S(08,1)=V*(15./D-3.*Y)*B
      S(09,1)=V*(-30.*D-3.*X)*A
      S(10,1)=V*(-30.*(D+1./D)+3.*ZZ)
      S(11,1)=V*(15./D-3.*X)*B
      S(12,1)=V*(-15.*D+3.*X)*A
      S(2,2)=V*(20./D+4.*X)*B*B
      S(3,2)=-V*15.*A*B*U
      S(4,2)=-S(5,1)
      S(5,2)=V*(10./D-X)*B*B
      S(6,2)=0.0
      S(7,2)=S(8,1)
      S(08,2)=V*(10./D-4.*X)*B*B
      S(09,2)=0.0
      S(10,2)=-S(11,1)
      S(11,2)=V*(5./D+X)*B*B
      S(12,2)=0.0
      S(3,3)=V*(20.*D+4.*X)*A*A
      S(4,3)=S(6,1)
      S(5,3)=0.0
      S(6,3)=V*(10.*D-4.*X)*A*A
```

```
      S(7,3)=-S(9,1)
      S(08,3)=0.0
      S(09,3)=V*(10.*D-X)*A*A
      S(10,3)=-S(12,1)
      S(11,3)=0.0
      S(12,3)=V*(5.*D+X)*A*A
      S(4,4)=S(1,1)
      S(5,4)=-S(2,1)
      S(6,4)=S(3,1)
      S(7,4)=S(10,1)
       S(8,4)=-S(11,1)
      S(9,4)=S(12,1)
      S(10,4)=S(7,1)
      S(11,4)=-S(8,1)
       S(12,4)=S(9,1)
      S(5,5)=S(2,2)
      S(6,5)=V*15*U*A*B
      S(7,5)=S(11,1)
      S(8,5)=S(11,2)
      S(09,5)=0.0
      S(10,5)=-S(8,1)
      S(11,5)=S(3,2)
      S(12,5)=0.0
      S(6,6)=S(3,3)
      S(7,6)=-S(12,1)
      S(08,6)=0.0
      S(9,6)=S(12,3)
      S(10,6)=-S(9,1)
      S(11,6)=0.0
      S(12,6)=S(9,3)
      S(07,07)=S(1,1)
      S(08,07)=S(2,1)
      S(09,07)=-S(3,1)
      S(10,7)=S(4,1)
      S(11,7)=S(5,1)
      S(12,7)=-S(6,1)
      S(08,08)=S(2,2)
      S(9,8)=S(6,5)
      S(10,8)=S(4,2)
      S(11,8)=S(5,2)
      S(12,8)=0.0
      S(09,09)=S(3,3)
      S(10,9)=-S(6,1)
      S(11,9)=0.0
      S(12,9)=S(6,3)
      S(10,10)=S(1,1)
      S(11,10)=-S(2,1)
      S(12,10)=-S(3,1)
      S(11,11)=S(2,2)
      S(12,11)=S(3,2)
      S(12,12)=S(3,3)
11    DO 7 I=1,12
      DO 7 J=1,12
7     S(I,J)=S(J,I)
      NOD=4
      GO TO 1000
```

```
303     NOD=2
        IF(RUN-2)301,304,602
 301    S5=AR/(30.*A)
        S(1,1)=S5*36.
        S(2,1)=0.0
        S(3,1)=-S5*3.*A
        S(4,1)=-S5*36.
        S(5,1)=0.0
        S(6,1)=S(3,1)
         S(2,2)=0.0
        S(3,2)=0.0
        S(4,2)=0.0
        S(5,2)=0.0
        S(6,2)=0.0
        S(3,3)=S5*4.*A*A
        S(4,3)=-S(3,1)
        S(5,3)=0.0
        S(6,3)=-S5*A*A
        S(4,4)=S(1,1)
         S(5,4)=0.0
        S(6,4)=-S(3,1)
        S(5,5)=0.0
        S(6,5)=0.0
        S(6,6)=S(3,3)
        GO TO 110
 304    S(1,1)=(12.*QB)/(A*A)
        S(2,1)=0.0
         S(3,1)=(-6.*QB)/A
        S(4,1)=(-12.*QB)/(A*A)
        S(5,1)=0.0
        S(6,1)=-6.*QB/A
        S(2,2)=(GB*BJ)/A
        S(3,2)=0.0
        S(4,2)=0.0
        S(5,2)=-(GB*BJ)/A
        S(6,2)=0.0
        S(3,3)=(4.+PHIZ)*QB
        S(4,3)=(6.*QB)/A
        S(5,3)=0.0
        S(6,3)=(2.-PHIZ)*QB
        S(4,4)=(12.*QB)/(A*A)
        S(5,4)=0.0
        S(6,4)=(6.*QB)/A
        S(5,5)=(GB*BJ)/A
        S(6,5)=0.0
        S(6,6)=(4.+PHIZ)*QB
110      DO 71 I=1,6
        DO 71 J=1,6
71      S(I,J)=S(J,I)
1000     N1=1
52      L1=1
50      DO 90 I=1,LL
        DO 90 J=1,LL
        L2=I+(N1-1)*LL
        M3=J+(L1-1)*LL
        L=LL*ND(I1,N1)-LL+I
```

```
      M=LL*ND(I1,L1)-LL+J
90    KS(L,M)=KS(L,M)+S(L2,M3)
      L1=L1+1
      IF(L1-NOD)50,50,51
51    N1=N1+1
      IF(N1-NOD)52,52,53
53    I1=I1+1
      IF(I1-NEL)33,33,320
320   DO 500 L=1,NN
      DO 500 M=1,NN
      KO(L,M)=KS(L,M)
500   CONTINUE
      DO 600 II=1,I7
      K=NB(II)
      K=K-II+1
      ITERM=NN-1
      DO 510 L=K,ITERM
      IP1=L+1
      DO 510 M=1,NN
      KO(L,M)=KS(IP1,M)
510   CONTINUE
      NM1=NN-1
      DO 540 L=1,NM1
      DO 540 M=1,NN
      KS(L,M)=KO(L,M)
540   CONTINUE
      DO 520 M=K,ITERM
      JP1=M+1
      DO 520 L=1,NN
520   KO(L,M)=KS(L,JP1)
      NN=NN-1
      DO 545 L=1,NN
      DO 545 M=1,NN
      KS(L,M)=KO(L,M)
545   CONTINUE
600   CONTINUE
      IF(RUN-2)16,17,602
16    DO 161 I=1,I9
      DO 161 J=1,I9
161   KG(I,J)=KO(I,J)
      GO TO 207
17    DO 171 I=1,I9
      DO 171 J=1,I9
171   KE(I,J)=KO(I,J)
 207  RUN=RUN+1
      IF(RUN-2)208,208,602
602   IFAIL=0
      CALL F02AEF(KG,I9,KE,I9,I9,R,Z,I9,DL,0,IFAIL)
      IF(IFAIL.EQ.0) GO TO 1066
      WRITE(6,99994) IFAIL
99994 FORMAT(I2)
      STOP
1066  WRITE(6,106)(R(I),I=1,I9)
 106  FORMAT(/'EIGENVALUES'/,((3X,D13.6)))
      DO 107 J=I9,I9
      WRITE(6,1071)J
```

```
      WRITE(6,1072)(Z(I,J),I=1,I9)
107   CONTINUE
 1071 FORMAT (/'EIGENVECTOR NO',I2)
1072  FORMAT(/,(1X,D13.5))
      STRESS=1./R(I9)
      WRITE(6,2093) STRESS
2093  FORMAT(2X,F9.1)
503   BS=BS+2.5*T
      BAV=2*B-2.5*TS
      IF(BS.GT.BAV) GO TO 77771
      GO TO 77777
77771 STOP
      END
```

PROGRAMME (3.4).

FLOW CHART AND FORTRAN LIST

BUCKLING ANALYSIS OF PLATES

USING FINITE STRIP IDEALISATION.

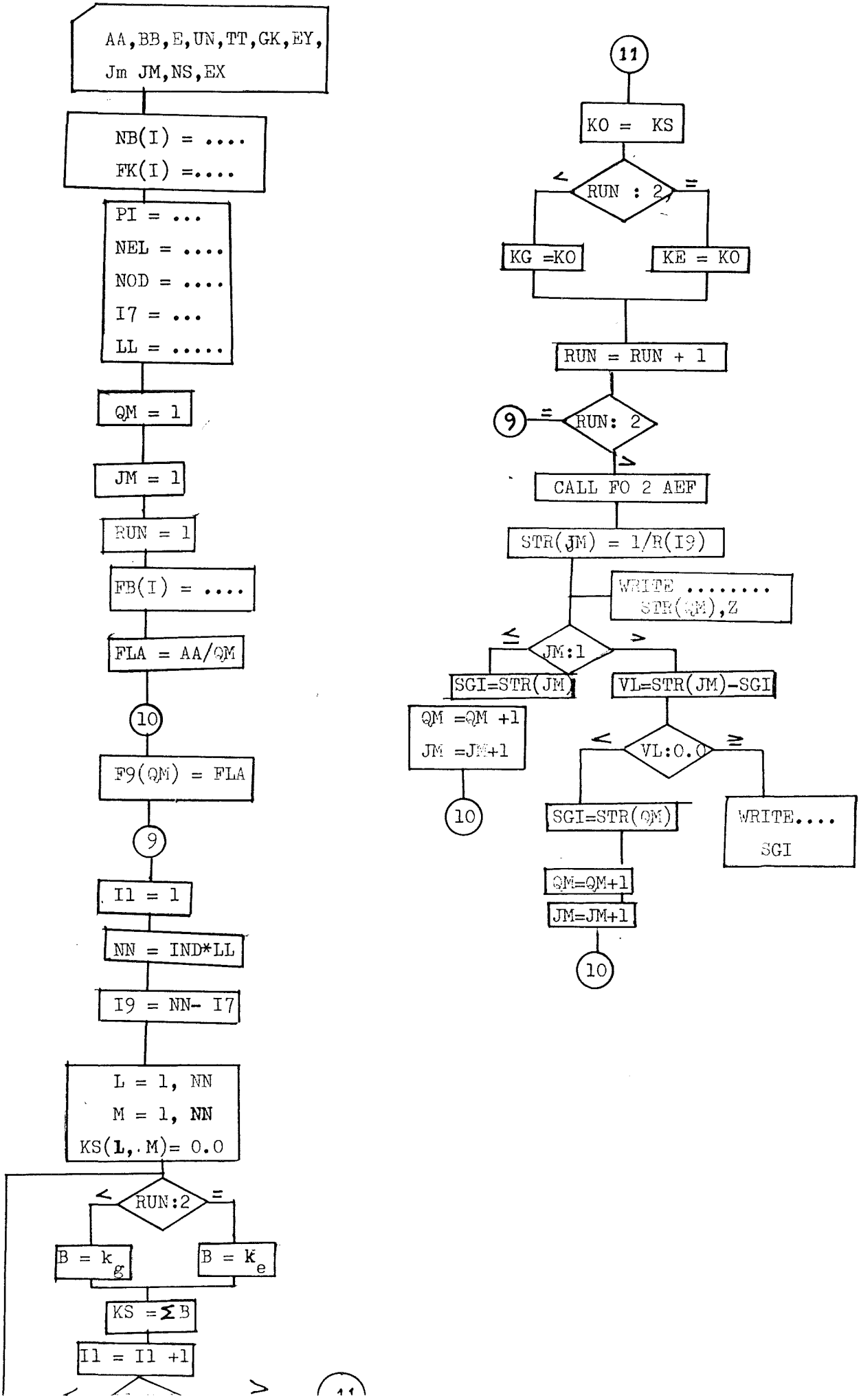
AA,BB,E,UN,TT,GK,EY,
Jm JM,NS,EX
NB(I) = ...
FK(I) =....
PI = ...
NEL = ...
NOD = ...
I7 = ...
LL = ...
QM = 1
JM = 1
RUN = 1
FB(I) = ...
FLA = AA/QM
10
F9(QM) = FLA
9
I1 = 1
NN = IND*LL
I9 = NN- I7
L = 1, NN
M = 1, NN
KS(L,.M)= 0.0
RUN:2
B = k g
B = k e
KS = Σ B
I1 = I1 +1
11
KO = KS
RUN : 2
KG =KO
KE = KO
RUN = RUN + 1
9
RUN: 2
CALL FO 2 AEF
STR(JM) = 1/R(I9)
WRITE .....
STR(QM),Z
JM:1
SGI=STR(JM)
VL=STR(JM)-SGI
QM =QM +1
JM =JM+1
10
VL:0.0
SGI=STR(QM)
WRITE....
SGI
QM=QM+1
JM=JM+1
10

```
C      BUCKLING ANALYSIS OF ISOTROPIC PLATE WITH FINITE LENGTH
C      FINITE STRIP METHOD
C      FINITE ELEMENT GRID: SIX ELEMENTS
       DOUBLE PRECISION PI,PHA,PHB,PHC,PHD,FLA,FLB,FLC,B,KO,KG,KE,KS,DL,
      2Z,Q,R,E,DET,EF,K,FB,T,GK,V4,V5,RATIO,BB,TT,STR,F9,DUA,DUB,DUC,FLU,
      4EMAX,FLS,GX,G1,G2,DEN,X7,Y7,BWH,TH,TAV
       INTEGER QM,RUN
       DIMENSION B(4,4),KO(14,14),KG(13,13),KE(13,13),DL(13),
      1Z(13,13),Q(13),R(13),KS(14,14),ND(6,2),NB(1),FB(6),T(6),FK(6),
      3STR(40),F9(40)
        READ(5,99) BB,E,UN,TT,GK,EY,QM,NS,AA,EX
99     FORMAT(2X,F5.2,1X,F7.1,1X,F3.1,1X,F4.2,1X,F4.2,1X,F5.2,1X,I2,1X,
      2I2,1X,F6.2,1X,F7.2)
       READ(5,*)((ND(I,J),J=1,2),I=1,6)
       WRITE(6,*)((ND(I,J),J=1,2),I=1,6)
       GK=0.0
        TT=1.
       BW=6.*BB
```

```
      AA=3.*BW
305   I7=1
      V5=0.25
99066 V4=1.
99591 TS=TT
      BS=BW
      PI=3.14
      IP=1
      NEL=6
      NOD=2
      LL=2
      IND=7
307   UN=0.3
C     BOUNDRY CONDITION INTRODUCTION
      NB(1)=1
C     EFFECT OF ELASTIC SUPPORT
      FK(1)=GK
      FK(2)=GK
      FK(3)=GK
      FK(4)=GK
      FK(5)=GK
      FK(6)=GK
C     THICNESS OF SINGLE STRIPS
      T(1)=TT*V5
      T(2)=TT*V5
      T(3)=TT*V5
      T(4)=TT*V5
      T(5)=TT*V5
      T(6)=TT*V5
      QM=1
      JM=1
306   FLA=AA/QM
 303  RUN=1
C     WIDTH OF SINGLE FLAT STRIPS
      FB(1)=BB
      FB(2)=BB
      FB(3)=BB
      FB(4)=BB


      FB(5)=BB
      FB(6)=BB
      F9(QM)=FLA
208   PI=3.141593
      I1=1
      NN=IND*LL
      I9=NN-I7
 1000 DO 2 L=1,NN
      DO 2 M=1,NN
 2    KS(L,M)=0.0
```

```
C       COMPUTATIONS OF STIFFNESSES OF SINGLE FLAT PLATE
30C     PHA=(PI**4.)*E*FB(I1)*(T(I1)**3.)/(10080.*(1.-UN*UN)*(FLA**3.))+
       3FK(I1)*FLA*FB(I1)/640.
        PHB=PI*PI*E*(T(I1)**3.)/(360.*(1.-UN*UN)*FB(I1)*FLA)
        PHC=E*FLA*(T(I1)**3.)/(24.*(1.-UN*UN)*(FB(I1)**3.))
        PHD=PI*PI*FB(I1)*T(I1)/(840.*FLA)
 33     IF(RUN-2)3,4,602
C       GEOMETRIC STIFFNESS OF SINGLE STRIP
3       B(1,1)=PHD*156.
        B(2,1)=PHD*22.*FB(I1)
        B(3,1)=PHD*54.
        B(4,1)=PHD*(-13.)*FB(I1)
        B(2,2)=PHD*4.*FB(I1)*FB(I1)
        B(3,2)=PHD*13.*FB(I1)
        B(4,2)=PHD*(-3.)*FB(I1)*FB(I1)
        B(3,3)=PHD*156.
        B(4,3)=PHD*(-22.)*FB(I1)
        B(4,4)=PHD*FB(I1)*FB(I1)*4.
        GO TO 11
C       ELASTIC STIFFENESSS OF SINGLE STRIP
4       B(1,1)=PHA*156.+PHB*36.+PHC*12.
        B(2,1)=PHA*22.*FB(I1)+PHB*(3.+15.*UN)*FB(I1)+PHC*6.*FB(I1)
        B(3,1)=PHA*54.+PHB*(-36.)+PHC*(-12.)
        B(4,1)=PHA*(-13.)*FB(I1)+PHB*(+3.)*FB(I1)+PHC*6.*FB(I1)
        B(2,2)=4.*FB(I1)*FB(I1)*(PHA+PHB+PHC)
        B(3,2)=PHA*13.*FB(I1)+PHB*(-3.)*FB(I1)+PHC*(-6.)*FB(I1)
        B(4,2)=PHA*FB(I1)*FB(I1)*(-3.)+PHB*FB(I1)*FB(I1)*(-1.)+
       7PHC*FB(I1)*FB(I1)*2.
        B(3,3)=PHA*156.+PHB*36.+PHC*12.
        B(4,3)=PHA*(-22.)*FB(I1)+PHB*(-3.-15.*UN)*FB(I1)+PHC*(-6.)*FB(I1)
        B(4,4)=4.*FB(I1)*FB(I1)*(PHA+PHB+PHC)
```

```
 11   DO 7 I=1,4
      DO 7 J=1,4
 7    B(I,J)=B(J,I)
111   FORMAT(1X,(9D13.6))
C     ASSEMBLY OF THE MATRIX FROM SINGLE COPONENTS
      N1=1
52    L1=1
50    DO 90 I=1,LL
      DO 90 J=1,LL
      L2=I+(N1-1)*LL
      M3=J+(L1-1)*LL
      L=LL*ND(I1,N1)-LL+I
      M=LL*ND(I1,L1)-LL+J
90    KS(L,M)=KS(L,M)+B(L2,M3)
      L1=L1+1
```

```
      IF(L1-NOD)50,50,51
51    N1=N1+1
      IF(N1-NOD)52,52,53
53    I1=I1+1
      IF(I1-NEL)300,300,320
320   DO 500 L=1,NN
      DO 500 M=1,NN
      KO(L,M)=KS(L,M)
500   CONTINUE
      DO 600 II=1,I7
      K=NB(II)
      K=K-II+1
      ITERM=NN-1
      DO 510 L=K,ITERM
      IP1=L+1
      DO 510 M=1,NN
      KO(L,M)=KS(IP1,M)
510   CONTINUE
      NM1=NN-1
      DO 540 L=1,NM1
      DO 540 M=1,NN
      KS(L,M)=KO(L,M)
540   CONTINUE
      DO 520 M=K,ITERM
      JP1=M+1
      DO 520 L=1,NN
520   KO(L,M)=KS(L,JP1)
      NN=NN-1
      DO 545 L=1,NN
      DO 545 M=1,NN
      KS(L,M)=KO(L,M)
545   CONTINUE
600   CONTINUE
      IF(RUN-2)16,17,602
C     GEOMATRIC STIFFENESS
16    DO 161 I=1,I9
      DO 161 J=1,I9
161   KG(I,J)=KO(I,J)
      GO TO 207
C     ELASTIC STIFFENESS
17    DO 171 I=1,I9
      DO 171 J=1,I9
171   KE(I,J)=KO(I,J)
 207  RUN=RUN+1
      IF(RUN-2)208,208,602
C     INTRODUCTION OF SOLVING SUBROUTIN
602   IFAIL=0
      CALL F02AEF(KG,I9,KE,I9,I9,R,Z,I9,DL,Q,IFAIL)
      IF(IFAIL.EQ.0) GO TO 1066
      WRITE(6,99994) IFAIL
99994 FORMAT(I2)
      STOP
1066   STR(JM)=(1./R(I9))
1067  DO 107 J=I9,I9
      WRITE(6,1071)J
```

```
      WRITE(6,1072)(Z(I,J),I=1,I9)
107   CONTINUE
 1071 FORMAT (/'EIGENVECTOR NO',I2)
1072  FORMAT(/,(1X,9D13.5))
2053   FORMAT(D13.6,3X,D13.6,3X,3F7.3,3X,I2,3X,F5.2,3X,D13.6)
      TW=TT*V5
      X7=STR(JM)/(E*((TW/BW)**2.))
      Y7=F9(JM)/BW
      ALFA=0.0
        WRITE(6,111) STR(JM),F9(JM),V4,V5,TT,GK,X7,Y7,ALFA
      IF(JM.GT.1) GO TO 1078
      SGI=STR(JM)
      QM=QM+1
      JM=JM+1
      GO TO 306
1078  VL=STR(JM)-SGI
      IF(VL.GT.0.0) GO TO 2933
      SGI=STR(JM)
      QM=QM+1
      JM=JM+1
      GO TO 306
2933  WRITE(6,9900) SGI
9900  FORMAT(D13.6)
      V5=V5+0.25
      IF(V5.GT.2) GO TO 55501
      GO TO 99066
55501 GK=GK+0.5
      IF(GK.GT.10.) GO TO 99998
      GO TO 309
99998 STOP
      END
```

PROGRAMME (3.5).

FLOW CHART AND FORTRAN LIST

LOCAL BUCKLING OF THIN WALLED STRUCTURES.

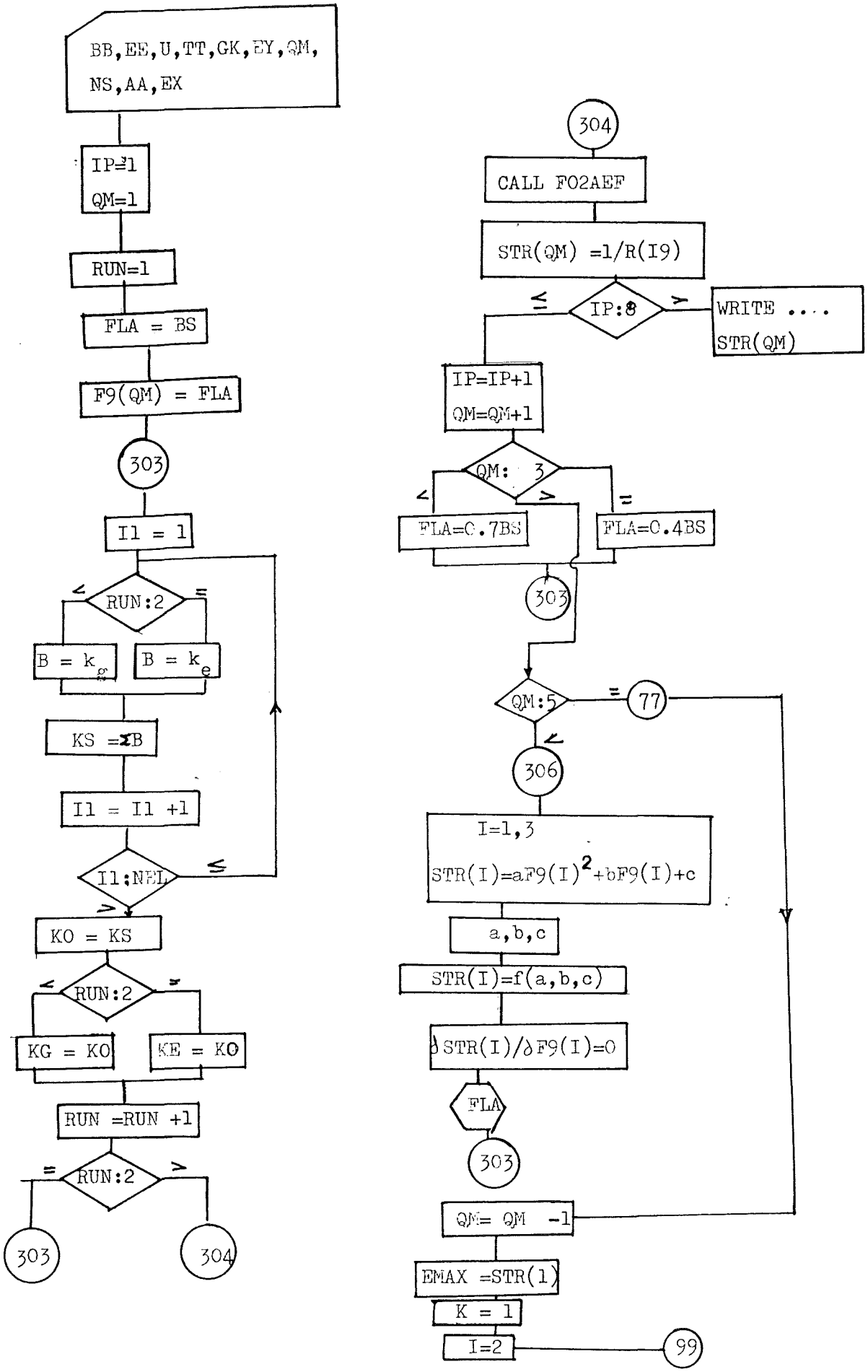
BB,EE,U,TT,GK,EY,QM,
NS,AA,EX
IP=1
QM=1
RUN=1
FLA = BS
F9(QM) = FLA
303
I1 = 1
RUN:2
B = k_g
B = k_e
KS =ΣB
I1 = I1 +1
I1:NEL
KO = KS
RUN:2
KG = KO
KE = KO
RUN =RUN +1
RUN:2
303
304
304
CALL FO2AEF
STR(QM) =1/R(I9)
IP:8
WRITE ....
STR(QM)
IP=IP+1
QM=QM+1
QM: 3
FLA=0.7BS
FLA=0.4BS
303
QM:5
77
306
I=1,3
STR(I)=aF9(I)²+bF9(I)+c
a,b,c
STR(I)=f(a,b,c)
∂STR(I)/∂F9(I)=0
FLA
303
QM= QM -1
EMAX =STR(1)
K = 1
I=2
99

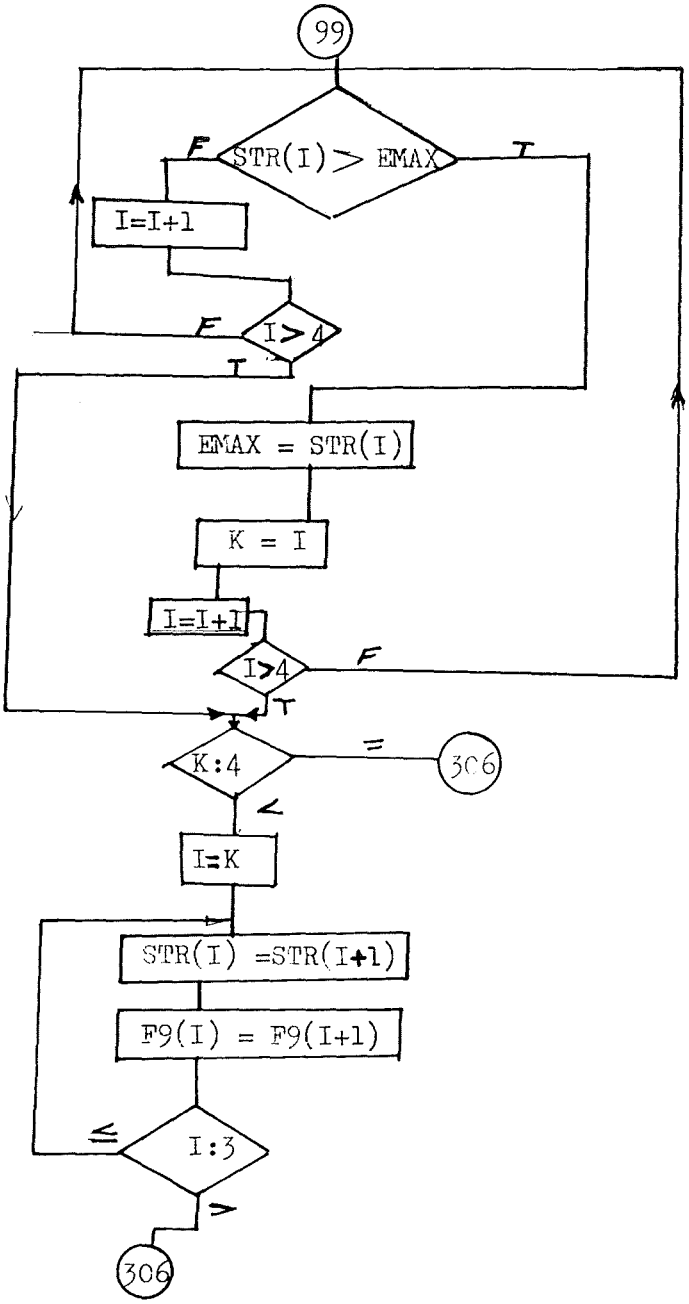
99
STR(I) > EMAX
F
T
I=I+1
I>4
F
T
EMAX = STR(I)
K = I
I=I+1
I>4
F
T
K:4
=
306
<
I=K
STR(I) =STR(I+1)
F9(I) = F9(I+1)
≤
I:3
>
306

```
C       LOCAL BUCKLING ANALYSIS

C       FINITE STRIP METHOD
C       FINITE ELEMENT GRID: SIX ELEMENTS
        DOUBLE PRECISION PI,PHA,PHB,PHC,PHD,FLA,FLB,FLC,B,KO,KG,KE,KS,DL,
       2Z,Q,R,E,DET,EF,K,FB,T,GK,V4,V5,RATIO,BB,TT,STR,F9,DUA,DUB,DUC,FLU,
       4EMAX,FLS,GX,G1,G2,DEN,X7,Y7,BWH,TH,TAV
        INTEGER QM,RUN
        DIMENSION B(04,04),KO(14,14),KG(11,11),KE(11,11),DL(11),
       1Z(11,11),Q(11),R(11),KS(14,14),ND(6,2),NB(3),FB(6),T(6),FK(6),
       3STR(04),F9(04)
         READ(5,99) BB,E,UN,TT,GK,EY,QM,NS,AA,EX
99      FORMAT(2X,F5.2,1X,F7.1,1X,F3.1,1X,F4.2,1X,F4.2,1X,F5.2,1X,I2,1X,
       2I2,1X,F6.2,1X,F7.2)
        READ(5,*)((ND(I,J),J=1,2),I=1,6)
        WRITE(6,*)((ND(I,J),J=1,2),I=1,6)
        GK=0.0
         TT=1.
        H=4.*BB
        BW=H-TT
309      I7=3
        V5=0.25
99066   V4=0.20
99991   TS=TT
        BS=BW/V4
        PI=3.14
        IP=1
        NEL=6
        NOD=2
```

```
      LL=2
      IND=7
307   UN=0.3
C     BOUNDRY CONDITION INTRODUCTION
      NB(1)=2
      NB(2)=5
       NB(3)=14
C     THICNESS OF SINGLE STRIPS
      T(1)=TT
      T(2)=TT
      T(3)=TT*V5
      T(4)=TT*V5
      T(5)=TT
      T(6)=TT
      NWAVE=1
306   FLA=BS*NWAVE
      QM=1
 303  RUN=1
C     EFFECT OF ELASTIC SUPPORT
      FK(1)=0.0
      FK(2)=0.0
      FK(4)=GK
      FK(3)=GK
      FK(5)=0.0
      FK(6)=0.0
C     WIDTH OF SINGLE FLAT STRIPS
      FB(1)=BS/4.
```

```
      FB(2)=BS/4.
      FB(3)=BW/2.
      FB(4)=BW/2.
      FB(5)=BS/4.
      FB(6)=BS/4.
      F9(QM)=FLA
208   PI=3.141593
      I1=1
      NN=IND*LL
      I9=NN-I7
 1000 DO 2 L=1,NN
      DO 2 M=1,NN
 2    KS(L,M)=0.0
C     COMPUTATIONS OF STIFFNESSES OF SINGLE FLAT PLATE
300   PHA=(PI**4.)*E*FB(I1)*(T(I1)**3.)/(10080.*(1.-UN*UN)*(FLA**3.))+
     3FK(I1)*FLA*FB(I1)/840.
      PHB=PI*PI*E*(T(I1)**3.)/(360.*(1.-UN*UN)*FB(I1)*FLA)
      PHC=E*FLA*(T(I1)**3.)/(24.*(1.-UN*UN)*(FB(I1)**3.))
      PHD=PI*PI*FB(I1)*T(I1)/(840.*FLA)
 33   IF(RUN-2)3,4,602
C     GEOMETRIC STIFFNESS OF SINGLE STRIP
3     B(1,1)=PHD*156.
      B(2,1)=PHD*22.*FB(I1)
      B(3,1)=PHD*54.
      B(4,1)=PHD*(-13.)*FB(I1)
      B(2,2)=PHD*4.*FB(I1)*FB(I1)
      B(3,2)=PHD*13.*FB(I1)
      B(4,2)=PHD*(-3.)*FB(I1)*FB(I1)
      B(3,3)=PHD*156.
      B(4,3)=PHD*(-22.)*FB(I1)
      B(4,4)=PHD*FB(I1)*FB(I1)*4.
```

```
      GO TO 11
C     ELASTIC STIFFENESSS OF SINGLE STRIP
4     B(1,1)=PHA*156.+PHB*36.+PHC*12.
      B(2,1)=PHA*22.*FB(I1)+PHB*(3.+15.*UN)*FB(I1)+PHC*6.*FB(I1)
      B(3,1)=PHA*54.+PHB*(-36.)+PHC*(-12.)
      B(4,1)=PHA*(-13.)*FB(I1)+PHB*(+3.)*FB(I1)+PHC*6.*FB(I1)
      B(2,2)=4.*FB(I1)*FB(I1)*(PHA+PHB+PHC)
      B(3,2)=PHA*13.*FB(I1)+PHB*(-3.)*FB(I1)+PHC*(-6.)*FB(I1)
      B(4,2)=PHA*FB(I1)*FB(I1)*(-3.)+PHB*FB(I1)*FB(I1)*(-1.)+
     7PHC*FB(I1)*FB(I1)*2.
      B(3,3)=PHA*156.+PHB*36.+PHC*12.
      B(4,3)=PHA*(-22.)*FB(I1)+PHB*(-3.-15.*UN)*FB(I1)+PHC*(-6.)*FB(I1)
      B(4,4)=4.*FB(I1)*FB(I1)*(PHA+PHB+PHC)
 11   DO 7 I=1,4
      DO 7 J=1,4
 7    B(I,J)=B(J,I)
111   FORMAT(1X,(9D13.6))
C     ASSEMBLY OF THE MATRIX FROM SINGLE COPONENTS
      N1=1
52    L1=1
50    DO 90 I=1,LL
      DO 90 J=1,LL
      L2=I+(N1-1)*LL
      M3=J+(L1-1)*LL
      L=LL*ND(I1,N1)-LL+I
```

```
      M=LL*ND(I1,L1)-LL+J
90    KS(L,M)=KS(L,M)+B(L2,M3)
      L1=L1+1
      IF(L1-NOD)50,50,51
51    N1=N1+1
      IF(N1-NOD)52,52,53
53    I1=I1+1
      IF(I1-NEL)300,300,320
C     ELIMINATION OF DEGREES OF FREEDOM CORRESPONDENT TO CONSTRAINT
320   DO 500 L=1,NN
      DO 500 M=1,NN
      KO(L,M)=KS(L,M)
500   CONTINUE
      DO 600 II=1,I7
      K=NB(II)
      K=K-II+1
      ITERM=NN-1
      DO 510 L=K,ITERM
      IP1=L+1
      DO 510 M=1,NN
      KO(L,M)=KS(IP1,M)
510   CONTINUE
      NM1=NN-1
      DO 540 L=1,NM1
      DO 540 M=1,NN
      KS(L,M)=KO(L,M)
540   CONTINUE
      DO 520 M=K,ITERM
      JP1=M+1
```

```
      DO 520 L=1,NN
520   KO(L,M)=KS(L,JP1)
      NN=NN-1
      DO 545 L=1,NN
      DO 545 M=1,NN
      KS(L,M)=KO(L,M)
545   CONTINUE
600   CONTINUE
      IF(RUN-2)16,17,602
C     GEOMATRIC STIFFENESS FOR THE HALL PLATE
16    DO 161 I=1,I9
      DO 161 J=1,I9
161   KG(I,J)=KO(I,J)
      GO TO 207
C     ELASTIC STIFFENESS MATRIX FOR THE HALL PLATE
17    DO 171 I=1,I9
      DO 171 J=1,I9
171   KE(I,J)=KO(I,J)
 207  RUN=RUN+1
      IF(RUN-2)208,208,602
C     INTRODUCTION OF SOLVING SUBROUTIN TO FIND THE EIGEN VALUE -EIGEN VECTOR
602   IFAIL=0
      CALL F02AEF(KG,I9,KE,I9,I9,R,Z,I9,DL,Q,IFAIL)
      IF(IFAIL.EQ.0) GO TO 1066
      WRITE(6,99994) IFAIL
99994 FORMAT(I2)
      STOP
```

```
1066    STR(QM)=(1./R(I9))
          IF(IP.EQ.08) GO TO 1067
        GO TO 1068
1067    DO 107 J=I9,I9
        WRITE(6,1071)J
        WRITE(6,1072)(Z(I,J),I=1,I9)
107     CONTINUE
 1071   FORMAT (/'EIGENVECTOR NO',I2)
1072    FORMAT(/,(1X,9D13.5))
2093     FORMAT(D13.6,3X,D13.6,3X,3F7.3,3X,I2,3X,F5.2,3X,D13.6)
        X7=STR(QM)/(E*((TT/BS)**2.))*(1.1)
        Y7=F9(QM)/BS
        ALFA1=PI*(X7/(12.*(1.-UN*UN)))**0.25
        ALFA2=1./(1.+V4*V5)
        ALFA3=(((V4**3.)*V5/12.)*(4.+V4*V5))**0.25
        ALFA=ALFA1*ALFA2*ALFA3
         WRITE(6,111) STR(QM),F9(QM),V4,V5,TT,GK,X7,Y7,ALFA
1068    IP=IP+1
        IF(IP-08)2933,2933,9903
2933    QM=QM+1
        IF(QM-3)3033,3035,9900
C       CRAMMER RULL INTRODUCTION TO FIND THE MINIMUM OF THE CURVE(ST.-L)
3033    FLA=0.8*BS
        GO TO 303
3035    FLA=0.6*BS
         GO TO 303
9900     IF(QM-5)9902,9901,9903
9902    DUA=STR(1)*(F9(2)-F9(3))
        DUB=STR(2)*(F9(1)-F9(3))
        DUC=STR(3)*(F9(1)-F9(2))
```

```
      FLU=2.*(DUA-DUB+DUC)
      FLS=+(F9(1)*F9(1)*(STR(2)-STR(3))-F9(2)*F9(2)*(STR(1)-STR(3))+
     7F9(3)*F9(3)*(STR(1)-STR(2)))
      FLA=-(F9(1)*F9(1)*(STR(2)-STR(3))-F9(2)*F9(2)*(STR(1)-STR(3))+
     7F9(3)*F9(3)*(STR(1)-STR(2)))/(2.*(STR(1)*(F9(2)-F9(3))-STR(2)*
     8(F9(1)-F9(3))+STR(3)*(F9(1)-F9(2))))
      GO TO 9907
9907   IF(FLA.LE.0.0000000000000000) GO TO 9903
      GO TO 9909
9909  IF(QM.GT.10) GO TO 9903
      GO TO 303
9901  QM=QM-1
      EMAX=STR(1)
      K=1
      DO 501 I=2,4
      IF(STR(I).GT.EMAX) GO TO 502
      GO TO 501
502    EMAX=STR(I)
      K=I
501   CONTINUE
      IF(K.EQ.4) GO TO 503
      DO 504 I=K,3
      STR(I)=STR(I+1)
      F9(I)=F9(I+1)
504   CONTINUE
503   CONTINUE
```

```
      GO TO 9902
 9903 WRITE(6,111 ) F9(1),F9(2),F9(3),STR(1),STR(2),STR(3),FLA,FLU,FLS
      IP=1
      V4=V4+0.2
      IF(V4.GT.1.4) GO TO 99993
      GO TO  99991
99993   V5=V5+0.25
      IF(V5.GT.1.5) GO TO 99997
      GO TO 99066
99997 GK=GK+0.5
      IF(GK.GT.5.) GO TO 99998
      GO TO 309
99998 STOP
      END
```

PROGRAMME (4.1).

FORTRAN LIST

EFFICIENCY STUDY OF COMPOSITE PANEL

```
C      FINITE STRIP METHOD
C      FINITE ELEMENT GRID: SIX ELEMENTS
       DOUBLE PRECISION PI,PHA,PHB,PHC,PHD,FLA,FLB,FLC,B,KO,KG,KE,KS,DL,
      2Z,Q,R,E,DET,EF,K,FB,T,GK,V4,V5,RATIO,BB,TT,STR,F9,DUA,DUB,DUC,FLU,
      4EMAX,FLS,GX,G1,G2,DEN,X7,Y7,BWH,TH,TAV
       INTEGER QM,RUN
       DIMENSION B(04,04),KO(14,14),KG(11,11),KE(11,11),DL(11),
      1Z(11,11),Q(11),R(11),KS(14,14),ND(6,2),NB(3),FB(6),T(6),FK(6),
      3STR(4),F9(4)
       READ(5,99) BB,E,UN,TT, BG,GK,QM,NS,AA,GX
99     FORMAT(2X,F5.2,1X,F7.1,1X,F3.1,1X,F4.2,1X,F6.2,1X,F5.2,1X,I2 ,
      21X,I2,1X,F6.2,1X,F7.2)
       READ(5,*)((ND(I,J),J=1,2),I=1,6)
       WRITE(6,*)((ND(I,J),J=1,2),I=1,6)
       NWAVE=1
99066   G1=0.00002696
       G2=0.00000093
        V4=0.2
309    I7=3
       V5=0.75
       IP=1
       NEL=6
       NOD=2
       LL=2
       IND=7
       UN=0.3
       NB(1)=2
       NB(2)=5
       NB(3)=14
       FK(1)=0.0
       FK(2)=0.0
       FK(3)=GK
       FK(4)=GK
       FK(5)=0.0
       FK(6)=0.0
       T(1)=TT
       T(2)=TT
       T(3)=TT*V5
       T(4)=TT*V5
       T(5)=TT
       T(6)=TT
306    FLA=4.*BB*NWAVE
       QM=1
 303   RUN=1
       FB(1)=BB
       FB(2)=BB
       FB(3)=BB*V4
       FB(4)=BB*V4
       FB(5)=BB
        FB(6)=BB
       F9(QM)=FLA
208    PI=3.141593
       I1=1
```

```
      NN=IND*LL
      I9=NN-I7
 1000 DO 2 L=1,NN
      DO 2 M=1,NN
 2    KS(L,M)=0.0
300   PHA=(PI**4.)*E*FB(I1)*(T(I1)**3.)/(10080.*(1.-UN*UN)*(FLA**3.))+
     3FK(I1)*FLA*FB(I1)/840.
      PHB=PI*PI*E*(T(I1)**3.)/(360.*(1.-UN*UN)*FB(I1)*FLA)
      PHC=E*FLA*(T(I1)**3.)/(24.*(1.-UN*UN)*(FB(I1)**3.))
      PHD=PI*PI*FB(I1)*T(I1)/(840.*FLA)
 33   IF(RUN-2)3,4,602
3     B(1,1)=PHD*156.
      B(2,1)=PHD*22.*FB(I1)
      B(3,1)=PHD*54.
      B(4,1)=PHD*(-13.)*FB(I1)
      B(2,2)=PHD*4.*FB(I1)*FB(I1)
      B(3,2)=PHD*13.*FB(I1)
      B(4,2)=PHD*(-3.)*FB(I1)*FB(I1)
      B(3,3)=PHD*156.
      B(4,3)=PHD*(-22.)*FB(I1)
      B(4,4)=PHD*FB(I1)*FB(I1)*4.
      GO TO 11
4     B(1,1)=PHA*156.+PHB*36.+PHC*12.
      B(2,1)=PHA*22.*FB(I1)+PHB*(3.+15.*UN)*FB(I1)+PHC*6.*FB(I1)
      B(3,1)=PHA*54.+PHB*(-36.)+PHC*(-12.)
      B(4,1)=PHA*(-13.)*FB(I1)+PHB*(+3.)*FB(I1)+PHC*6.*FB(I1)
      B(2,2)=4.*FB(I1)*FB(I1)*(PHA+PHB+PHC)
      B(3,2)=PHA*13.*FB(I1)+PHB*(-3.)*FB(I1)+PHC*(-6.)*FB(I1)
      B(4,2)=PHA*FB(I1)*FB(I1)*(-3.)+PHB*FB(I1)*FB(I1)*(-1.)+
     7PHC*FB(I1)*FB(I1)*2.
```

```
      B(3,3)=PHA*156.+PHB*36.+PHC*12.
      B(4,3)=PHA*(-22.)*FB(I1)+PHB*(-3.-15.*UN)*FB(I1)+PHC*(-6.)*FB(I1)
      B(4,4)=4.*FB(I1)*FB(I1)*(PHA+PHB+PHC)
 11   DO 7 I=1,4
      DO 7 J=1,4
 7    B(I,J)=B(J,I)
 111  FORMAT(1X,(9D13.6))
      N1=1
52    L1=1
50    DO 90 I=1,LL
      DO 90 J=1,LL
      L2=I+(N1-1)*LL
      M3=J+(L1-1)*LL
      L=LL*ND(I1,N1)-LL+I
      M=LL*ND(I1,L1)-LL+J
90    KS(L,M)=KS(L,M)+B(L2,M3)
      L1=L1+1
      IF(L1-NOD)50,50,51
51    N1=N1+1
      IF(N1-NOD)52,52,53
53    I1=I1+1
      IF(I1-NEL)300,300,320
320   DO 500 L=1,NN
      DO 500 M=1,NN
      KO(L,M)=KS(L,M)
500   CONTINUE
```

```
      IP1=L+1
      DO 510 M=1,NN
      KO(L,M)=KS(IP1,M)
510   CONTINUE
      NM1=NN-1
      DO 540 L=1,NM1
      DO 540 M=1,NN
      KS(L,M)=KO(L,M)
540   CONTINUE
      DO 520 M=K,ITERM
      JP1=M+1
      DO 520 L=1,NN
520   KO(L,M)=KS(L,JP1)
      NN=NN-1
      DO 545 L=1,NN
      DO 545 M=1,NN
      KS(L,M)=KO(L,M)
545   CONTINUE
600   CONTINUE
      IF(RUN-2)16,17,602
16    DO 161 I=1,I9
      DO 161 J=1,I9
161   KG(I,J)=KO(I,J)
      GO TO 207
17    DO 171 I=1,I9
      DO 171 J=1,I9
171   KE(I,J)=KO(I,J)
207   RUN=RUN+1
      IF(RUN-2)208,208,602
 602  IFAIL=0
      CALL F02AEF(KG,I9,KE,I9,I9,R,Z,I9,DL,Q,IFAIL)
      IF(IFAIL.EQ.0) GO TO 1066
      WRITE(6,99994) IFAIL
99994 FORMAT(I2)
      STOP
1066  DO 107 J=I9,I9
      WRITE(6,1071)J
      WRITE(6,1072)(Z(I,J),I=1,I9)
107   CONTINUE
1071  FORMAT(/'EIGENVECTOR NO',I2)
1072  FORMAT(/,(1X,9D13.5))
      BWH=FB(3)+FB(4)
      TH=T(4)+4.*BB*(GX/E)
      BS=4.*BB
      TAV=TT+TH*BWH/(4.*BB)
      AEX=(TH*BWH)+(TT*BS)
```

```
      YIS=(TH*(BWH**3.))/12.+(TH*BWH)*(((BWH/2.+TT)-ZGX)**2.)
      YIP=((BS*(TT**3.))/12.) +(TT*BS)*((ZGX-TT/2.)**2.)
      YIX=YIS+YIP
      RAG=YIX/AEX
      SXX=(PI**2.)*E*RAG*(1./(AA*AA))
      X7=STR(QM)*(BWH+TT)*(1./BG)
      X8=SXX*(TT+BWH)*(1./BG)
      VU=((BWH+TT)*BG)
      DEN=((BWH*T(4)+4.*BB*TT)*NS*G1+(BWH*4.*BB)*NS*G2)/VU
      Y7=((TT+BWH)*DEN)/BG
      RATIO=V4/2.
      X9=DEN*BG*AA*(BWH+TT)/(X8*BG*BG)
      WRITE(6,90101)  NWAVE
90101 FORMAT(I2)
      WRITE(6,99)BB,E,UN,TT, BG,GK,QM,NS,AA,GX
      WRITE(6,111)X7,X8,Y7,VU,DEN,GK,TT,TH,RAG
      WRITE(6,2093)STR(QM),SXX,F9(QM),RATIO,V5,IP,TAV,X9
2093   FORMAT(D13.6,3X,D13.6,3X,3F7.2,3X,I2,3X,F5.2,3X,D13.6)
 1068 IF(QM.LE.3) GO TO 9904
9904   IP=IP+1
      IF(IP-08)2933,2933,9903
2933   QM=QM+1
      IF(QM-3)3033,3035,9901
3033   FLA=0.9*NWAVE*4.*BB
      GO TO 303
3035   FLA=0.8*NWAVE*4.*BB
       GO TO 303
9900    IF(QM-5)9902,9901,9903
9902   DUA=STR(1)*(F9(2)-F9(3))
      DUB=STR(2)*(F9(1)-F9(3))
      DUC=STR(3)*(F9(1)-F9(2))
      FLU=2.*(DUA-DUB+DUC)
      FLS=+(F9(1)*F9(1)*(STR(2)-STR(3))-F9(2)*F9(2)*(STR(1)-STR(3))+
     7F9(3)*F9(3)*(STR(1)-STR(2)))
      FLA=-(F9(1)*F9(1)*(STR(2)-STR(3))-F9(2)*F9(2)*(STR(1)-STR(3))+
     7F9(3)*F9(3)*(STR(1)-STR(2)))/(2.*(STR(1)*(F9(2)-F9(3))-STR(2)*
     8(F9(1)-F9(3))+STR(3)*(F9(1)-F9(2))))
      GO TO 9907
9907    IF(FLA.LE.0.0000000 .0000000) GO TO 9903
      GO TO 9909
9909   IF(QM.GT.10) GO TO 9903
      GO TO 303
9901   QM=QM-1
      EMAX=STR(1)
      K=1
      DO 501 I=2,4
      IF(STR(I).GT.EMAX) GO TO 502
      GO TO 501
502     EMAX=STR(I)
      K=I
501    CONTINUE
      IF(K.EQ.4) GO TO 503
      DO 504 I=K,3
      STR(I)=STR(I+1)
      F9(I)=F9(I+1)
504    CONTINUE
```

```
503    CONTINUE
       GO TO 9902
 9903  WRITE(6,111 ) F9(1),F9(2),F9(3),STR(1),STR(2),STR(3),FLA,FLU,FLS
       IP=1
       V4=V4+0.2
       IF(V4.GT.2.2) GO TO 99055
       GO TO 309
99055  NWAVE=NWAVE+1
       IF(NWAVE.EQ.4) GO TO 99077
       GO TO 99066
99077   STOP
       END
```

CHAPTER SIX

6.1. Conclusions.

1. The finite element method is a technique of general application and once elastic and geometric stiffness matrices have been formulated a variety of problems encountered in structural analysis can be dealt with.

2. Its application to stability has been found to be accurate and efficient.

3. Because it can use elements of different shapes and sizes, the finite element method can be used in the analysis of structures with very complicated geometries, and analysis of which using alternative analytical methods can only be accomplished if a great deal of simplification is introduced.

4. The force method and Argyris' approach to the displacement method are dependent on the transformation matrices $\mathbf{B}_o$, $\mathbf{B}_1$, $\mathbf{A}_o$ and $\mathbf{A}_1$ and because these matrices are dependent in turn on the choice of the internal force system, the direct displacement method found to be more straight forward to apply and much easier to programme.

5. Since the setting up of computer programme may take a considerable time, it is important that it should be as general as possible, so that, once established a variety of problems can be dealt with in a very short computer time.

6. Elastic stiffness formulation of non-isotropy is dealt with without any increase in cost or complexity.

7. Effect of thermal strain distribution is included in the element stiffness so that the analysis can be conducted for a structure composed of parts which have different temperature changes by assigning to each element properties which are consistent with the temperature change of that element.

8. Displacement boundary conditions can be described by suppressed degrees of freedom, by elastic springs introduced at the effected nodes and through special elements that are formulated to account for the type of support at the boundary. This can intoduce a broad interpretation of the effect of constraint.

9. The existence of different approaches to the formulation of the elastic and geometric stiffnesses for the finite elements used to construct the finite element model called for a unified approach. This has been accomplished by using the formula derived in Chapter 2 which gives the elastic and geometric stiffness matrices in terms of the shape functions. This formula has been found to be very simple and less cumbersome to use than the existing methods and its application to particular problems gave results in agreement with those obtained by existing methods.

10. From the examination of the analytical methods used in the determination of buckling loads it was found that they either require the differential equation with the associated boundary conditions or the analytical expression for the total potential energy; unless the structural form is simple,neither can be determined readily.

11. For the analytical methods, once the expression of total potential energy or the differential equation are obtained and the appropriate boundary conditions set up, the solution still requires the proper choice of displacement function representing as closely as possible the true deflection shape by satisfying as many as possible of the boundary conditions. This further adds to the difficulty of employing these methods.

12. The use of finite element method in structure stability studies found to be very efficient.

13. The application of the finite element method to overall and local stability of some structural elements in Chapter 3 showed very good agreement with existing solutions.

14. For the overall buckling of beams loaded in-plane, a one-element idealisation was found to give only a very small error.

15. For a beam in pure torsion, because the derivation of element stiffnesses was based on a third degree polynomial, the boundary conditions corresponding to zero rotation and zero warping could not be incorporated in the analysis and, as a result, a relatively larger error was found.

16. For the analysis of isotropic and orthotropic plates it was found that the best results can be obtained by using thirt six finite elements representing one quarter of the plate.

17. For the determination of the overall buckling load of stiffened plates it was found that the use of the orthotropic analogy is much more economical than the use of plate-beam combinations.

18. The finite strip approach offers a large reduction of time and cost of computer use as compared to the standard finite element method.

19. The exact finite strip offers also the advantage of predicting, the lowest buckling mode regardless of its type, and can be used for vibration as well as in buckling.

20. The approximate finite strip (Cheung), uses a standard eigenvalue/eigenvector programme, and can be applied to linear elasticity, buckling, and vibration but needs more storage space and uses more elements to represent the structure as compared to the exact finite strip.

21. The finite strip for local stability is suitable for the study of local buckling. It uses a standard eigenvalue/eigenvector subroutine, and can be used very efficiently and with minimum of computer time in the study of the buckling of plates with finite length, the buckling of plates on an elastic foundation, and the

/the local buckling of panels.

22. The study of plates stabilised by elastic core material revealed that:

a. The buckling load can be increased to several times its stabilised value even with a relatively soft core.

b. As the core stiffness increased, there was less variation in the buckling stress for the different boundary conditions which may suggest that the stabiliser material reduces the effect of side constraint.

c. The results for a simply supported plate on an elastic foundation using Timoshenko's method were the same as those obtained by the finite strip method.

d. The experimental verification using 21 steel strips stabilised by cores made of balsa wood and polystyrene with one end clamped the other free showed close agreement with the theory.

e. The core stiffness seems to contribute to the stiffness of the plates when the buckling stress approaches the yield stress, some plates showing a higher stiffness than that predicted from their stress-strain diagram.

f. Although the plates have a relatively large initial deformation, they failed by buckling and not by continuous deformation as might have been expected.

23. The local buckling of a composite panel made up of two materials can be increased very much even with a soft core material.

24. For each pair of parameters defining the cross-section geometry of a composite panel there is a value defining the stiffness of the core necessary to produce the highest possible buckling stress and any increase in the core stiffness beyond that value does not produce any significant increase in the buckling stress. These values are given in Table (3.25).

25. The efficiency study conducted in Chapter 4 showed that:

a. The panel constructed from light core material and metal skin can be very efficient.

b. Panel (P - I) which was constructed from an isotropic core material and a metal skin is more efficient than either the integrally stiffened panel, the sandwich panel or the z stiffened panel.

c. Panel (P - II) which is constructed with a balsa core is more efficient in the region of higher structural index and less efficient in the lower region.

6.2. Future Work.

As in any scientific work, this study has lead to new problems emerging which may require a larger amount of effort to solve.

The following are some points which I believe, need to be looked at further:

1. A comparative study between the standard finite element approaches and an evaluation of their accuracy by applying the procedures to a range of problems so providing specific proof of which method is the more efficient.

2. The effect of a core on the stability of a plate in the presence of initial deformation of the plate.

3. Investigation of the core material effect on the stiffness of the plates in the region of yield stress.

4. Investigation of the effect of initial deformation of the plate components on the stability of a composite panel.

5. Buckling tests on composite panel.

6. The study of minimum weight design of a composite panel with initial deformation.

7. A study of the design of an aircraft wing made of composite panels and the effect of the core on the torsional and flexural stiffness of the wing.

8. Generalisation of the computer programmes which have been developed by using a library of element stiffness and combining the local and overall buckling in one unified programme.

A P P E N D I X (A.1).

Theorems based on the principal of virtual work and on the principal of complementary virtual work:

1. Definition:

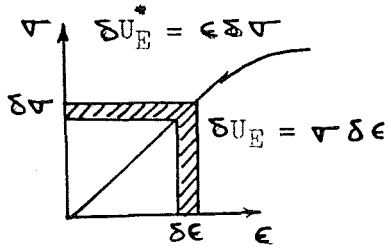

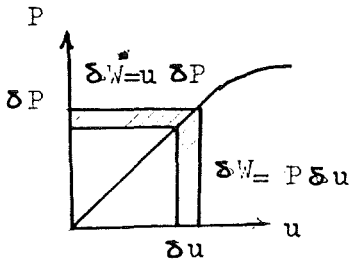

As can be seen from Figures (a) and (b).

a. Virtual work is given as $\delta W = P \delta u$. If n concentrated loads are applied then

$$\delta W = \mathbf{P}^T \delta \mathbf{U}$$

Where $\delta \mathbf{U}$ is a column of virtual displacements in the direction of $\mathbf{P}$.

b. Complementary virtual work $\delta W^* = u \delta P$

and similarly for n concentrated forces

$$\delta W^* = \mathbf{U}^T \delta \mathbf{P}$$

It must be noted that for linearly elastic system $W = W^*$.

c. Virtual strain energy:

$$\delta U_E = \sigma \delta \epsilon$$

d. Virtual complementary strain energy:

$$\delta U_E^* = \epsilon \delta \sigma$$

2. Principal of virtual displacement : (16)

"An elastic structure is in equilibrium under a given system of loads if for any virtual displacement δu from a compatible state of deformation u the virtual work is equal to the virtual strain energy".

$$(\delta W = \delta U_E)$$

It is used to find the forces necessary to maintain equilibrium in a structure for which the true stresses are known.

a. Continuous structure.

Suppose the true stresses are known and given as σ then if for each applied force P_i a virtual displacement δU_i is applied at the point of application and in the direction of P_i then from the principal virtual work

$$P_i \delta U_i = \int_V \sigma^T \delta \epsilon_i \, dV$$

in elastic structure

$$\delta \epsilon_i = \underline{b}_i \delta U_i$$

where $\underline{b}_i$ represent compatible strains due to unit displacement $U_i = 1$ applied in the direction of P_i.

Substituting gives:

$$P_i = \int_V \sigma^T \underline{b}_i \, dV$$

b. Discreet-element system:

The virtual work is given as $\delta W = \delta \mathbf{U}^T \mathbf{P}$

The virtual strain energy is given as the sum of products of discreet-element forces $\mathbf{F}i$ by their respective virtual displacements/

/displacements $\bar{\mathbf{U}}_i$

$$\delta U_E = \sum_i \delta \bar{\mathbf{U}}_i^T \mathbf{F}_i$$

and in matrix form we may write

$$\delta U_E = \delta \bar{\mathbf{U}}^T \mathbf{F}$$

$\bar{\mathbf{U}}$ is the element displacement and is related to the complete structure displacement $\mathbf{U}$ by

$$\bar{\mathbf{U}} = \mathbf{A}\,\mathbf{U}$$

applying the principal of virtual work

$$\delta U = \delta U_E$$

$$\delta \mathbf{U}^T \mathbf{P} = \delta \bar{\mathbf{U}}^T \mathbf{F}$$

substituting on $\delta \bar{\mathbf{U}}^T$ we find

$$\mathbf{P} = \mathbf{A}^T \mathbf{F}$$

3. Principal of virtual forces:

"An elastic structure is in compatible state of deformation under a given system of loads if for any virtual stresses away from the equilibrium state of stress the virtual complementary work is equal to the virtual complementary strain energy".

$$\delta W^* = \delta U_E^*$$

It is used to find the displacement U in a structure for which the distribution of true total strains are known.

a. Continuous structure.

Suppose the strains ϵ are known

If a virtual force δP_i is applied in the direction of U_i then

$$U_i \, \delta P_i = \int_V \epsilon^T \delta \sigma_i$$

In elastic structure

$$\delta \sigma_i = \bar{\sigma}_i \delta P_i$$

where $\bar{\sigma}_i$ are statically equivalent stresses due to unit load ($\delta P_i = 1$) applied in direction of U_i .

Substituting

$$U_i = \int_V \epsilon^T \bar{\sigma}_i \, dV$$

b. Discreet-element system.

If $\mathbf{U}$ represent the displacements and $\mathbf{P}$ the external applied loads then the complementary work

$$\delta W^* = \mathbf{U}^T \delta \mathbf{P}$$

Indicating $\mathbf{S}_i$ the internal forces and $\mathbf{V}_i$ are the internal displacements then the complementary strain energy for one element

$$\delta U_E^* = \delta \mathbf{S}_i^T \mathbf{V}_i$$

for the structure

$$\delta U_E^* = \delta \mathbf{S}^T \mathbf{V}$$

for linear elastic system

$$\delta \mathbf{S} = \mathbf{B} \delta \mathbf{P}$$

where $\mathbf{B}$ represent element forces that are in equilibrium with unit load $\delta P = 1$

From

$$\delta W^* = \delta U^*$$

We obtain

$$\mathbf{U} = \mathbf{B}^T \mathbf{V}$$

A P P E N D I X (A.2).

Subroutine (F02 AEF).

This subroutine is used to calculate all the eigenvalues and eigenvectors of $Az = Bx$, where A is a real symmetric matrix and B is a real symmetric positive definite matrix.

This subroutine operates as follows:

1. The problem is reduced to the standard symmetric eigenproblem using Cholesky's method to decompose B into triangular matrices

$$B = L L^t$$

where L is lower triangular matrix.

As a result, the equation

$$Ax = Bx$$

becomes

$$(L^{-1} A L^{-t}) \ (L^t x) = (L^t x)$$

which can be written as

$$P y = y$$

where $P = L^{-1} A L^{-t}$ is the symmetric matrix.

2. Householder's method is used to tranform the matrix P into tridiagonal matrix.

3. Then the QL algorithm is used to find the eigenvalues and the eigenvectors z, these eigenvectors are related to those of the original problem x by

$$z = L^t x.$$

The eigenvectors z are normalised so that $z^* z = 1$, and the eigenvectors of the original problem are normalised so that $x^T B x = 1$.

For further study consultations may be made to computer documentations NAGFLIB: 991 /379

and to WILKINSON, J.H. and REINSCH, C.

Handbook for Automatic Computation V-II - Linear Algebra

Springer - Verlag, 1971.

REFERENCES.

(1) J.H. Argyris, "Energy Theorems and Structural Analysis", Aircraft Engineering J., Vol. 26 - 27, 1954, 1955.

(2) P.H. Denk, "Nonlinear and Thermal Effects on Elastic Vibration", Agardograph, 72, Matrix Methods of Structural Analysis, Ed. B. Fraeijs de Veubeke, 1964.

(3) M.J. Turner, R.W. Clough, H.C. Martin, and R.J. Melosh, "Stiffness and Deflection of Complex Structure", Aeronautical Science J., Vol. 23, No. 9, 1956.

(4) M.J. Turner, E.H. Dill, H.C. Martin, and R.J. Melosh, "Large Deflection of Structures Subjected to Heating and External Loads, Aero/Space Science J., Vol. 27, No. 2, 1960.

(5) D. William, D.M. Leggatt, and H.G. Hopkins, "Flat Sandwich Panels under Compressive End Loads", Aeronautical Research Council, R. & M., No. 1987, June, 1941.

(6) W.H. Wittrick, "A Theoretical Analysis of the Efficiency of Sandwich Construction under Compressive End Load", R. & M. No. 2016, April, 1945.

(7) J.S. Archer, "Consistent Matrix Formulation for Structural Analysis Using Finite Element Technique", A.I.A.A. J., Vol. 3, No. 10, 1965.

(8) J.S. Przemieniecki, "Discrete-Element Methods for Stability Analysis of Complex Structures", The Aeronautical J., Vol. 72, No. 696, 1968.

(9) R.H. Gallaghar and J. Padlog, "Discrete Element Approach to Structural Instability Analysis", A.I.A.A. J., Vol. 1, No. 6, 1965.

(10) J.H. Argyris, "On the Analysis of Complex Structures", Appl. Mech. Rev., Vol., 11, pp 331, 1958.

(11) R.D. Cook, "Concepts and Applications of Finite Element Analysis", John Wiley & Sons, 1974.

(12) T.Y. Yang, "A Finite Element Procedure for Large Deflection Analysis of Plates with Initial Deflections", A.I.A.A. J., Vol., 9, No. 8, 1971.

(13) R.H. Gallaghar, R. Gellatly, J. Padlog, and R. Mallet, "A Discrete Element Procedure for Thin-Shell Instability Analysis", AI.A.A. J., Vol., 5, pp 138, 1967.

(14) O.C. Zienkiewcz, "The Finite Element Method, Third Edition", McGrae-Hill, London, 1977.

(15) R.H. Gallaghar, "A Correlation Study of Methods of Matrix Structural Analysis", Agardograph 69, Pergamon Press, 1964.

(16) J.S. Przemieniecki, "Theory of Matrix Structural Analysis", McGraw-Hill, New York, 1968.

(17) R.H. Gallaghar, "Finite Element Fundamentals", Prentice-Hall, New Jersey, 1975.

(18) R.J. Melosh, "Basis for Derivation of Matrices for the Direct Stiffness Method", A.I.A.A. J., Vol., 1, No. 7, 1963.

(19) O.C. Zienkiewcz, and Y.K. Cheung, "The Finite Element Method for Analysis of Elastic Isotropic and Orthotropic Slabs", Pro. Inst. Civ. Eng., Vol., 28, No. 6726, pp 471, 1964.

(20) A. Chajes, "Principal of Structural Stability Theory", Prentice-Hall, New Jersey, 1974.

(21) R.S. Barsoum, and R.H. Gallaghar, "Finite Element Analysis of Torsional and Lateral Instability Problems", International J. Num. Meth. Eng., Vol., 2, No. 3, pp335, 1970.

(22) H. Ziegler, "Principals of Structural Stability", Blaisdell Publishing Company, London, 1968.

(23) D. William, "Theory of Aircraft Structures", E. Arnold Pub., London, 1960.

(24) G.H. Bryan, "On Stability of a Plane Plate Under Thrusts in its Own Plane with Application to the Buckling of the sides of a Ship", Proceedings of London Mathematical Society, Vol., 22, 1891.

(25) F. Bleich, "Buckling Strength of Metal Structures", McGraw-Hill, New York, 1952.

(26) N.J. Hoff, "A Strain Energy Derivation of the Torsional-Flexural Buckling Loads of Straight Columns of Thin-Walled Open Sections", Quarterly of Applied Mathematics, Vol., 1, No. 4, 1944.

(27) S.P. Timoshenko, "The Collected Papers of Stephen P. Timoshenko", pp 1, McGraw-Hill, New York, 1954.

(28) S.P. Timoshenko, and J. Gere, "Theory of Elastic Stability", McGraw-Hill, Second Edition, London, 1961.

(29) S.H. Crandall, "Engineering Analysis", McGraw-Hill, London, 1956.

(30) W.J. Duncan, "The Galerkin Method for the Approximate Solutions of Linear Differential Equations", R. & M. No. 1798, August, 1937.

(31) M.G. Salvadori, and M. Baron, "Numerical Methods in Engineering", Prentice-Hall, Englewood, 1961.

(32) W.P. Rodden, J.P. Jones, and P.G. Bhuta, "A Matrix Formulation of the Transverse Structural Influence Coefficients for an Axially Loaded Timoshenko Beam", A.I.A.A. J., Vol., 1, pp 225, 1963.

(33) R.F. Hearmon, and E.H. Adams, "The Bending and Twisting of Anisotropic Plates", British J. of Applied Physics, Vol., 3, 1952.

(34) W.H. Wittrick, "Correlation Between Some Stability Problems for Orthotropic and Isotropic Plates Under Bi-Axial and Uni-axial Direct Stress", The Aeronautical Quarterly, Vol., 4, August, 1952.

(35) D.J. Ferrar, "The Design of Compression Structures for Minimum Weight", J. Royal Aeronautical Society, Vol., 53, pp 1041, 1949.

(36) G. Gerard, "Minimum Weight Analysis of Orthotropic Plates Under Compressive Loading", J. Aero/Space Science, January, 1960.

(37) "Unpublished Experimental Results of Buckling of Integrally Stiffened Panels", British Aircraft Corporation, London, 1960.

(38) K.L. Legg, "A Survey and an Experiment", J. of Royal Aeronautical Society, Vo., 58, pp 485, 1954.

(39) W.H. Wittrick, "A Unified Approach to the Initial Buckling of Stiffened Panels in Compression", The Aeronautical Quarterly, Vol., 19, Part 3, 1968.

(40) Y.K. Cheung, "The Finite Strip Method in Structural Analysis", Pergamon Press, 1976.

(41) J.S. Przemieniecki, "The Finite Element Structural Analysis of Local Instability", A.I.A.A. J., Vol., 11, No. 1, 1973.

(42) N.J. Huffinton, "Theoretical Determination of Rigidity Properties of Orthogaonally Stiffened Plates", J. Applied Mechanics, March, 1956.

(43) S.P. Timoshenko, and Woinowsk-Krieger, "Theory of Plates and Shells, McGraw-Hill, London, 1959.

(44) F.W. William, and W.H. Wittrick, "Computational Procedure for a Matrix Analysis of the Stability and Vibration of Thin-Flat-Walled Structures in Compression", J. Mech., Sci., Vol., 11, pp 979, 1969.

(45) F.W. William, and W.H. Wittrick, "Numerical Results for Initial Buckling Loads of Prismatic Plate Assemblies", J. of Sound and Vibration, Vol., 21, pp 87, 1972.

(46) F.W. William, and W.H. Wittrick, and R.J. Plank, "Critical Buckling Loads of Some Prismatic Plate Assemblies", Buckling of Structures, IUTAM Symposium, Cambridge, U.S.A. 1984, Ed. Bernard Budiansky, Springer-Verlag, 1976.

(47) Y.K. Cheung, "Finite Strip Method in the Analysis of Elastic Plates with Two Simply Supported Ends", Pro., Inst., Civ., Eng., Vol., 40, 1968.

(48) Y.C. Loo, and A.R. Cusens, "Finite Strip Method in Bridge Engineering", Viewpoint Pub., 1978.

(49) A.H. Chilver, "A Generalised Approach to the Local Instability of Certain Thin Walled Struts", Aeronautical Quarterly, Vol., 4, pp 245, 1953.

(50) H.L. Cox, "Computation of Initial Buckling Stress for Sheet-Stiffener Combinations", J. of The Royal Aeronautical Society, Vol., 58, pp 364, 1954.

(51) R.M. Rivello, "Theory and Analysis of Flight Structures", McGraw-Hill, London, 1969.

(52) M. Hetenyi, "Beams and Plates on Elastic Foundations and Related Problems", Applied Mechanics Review, Vol., 19, pp 95, 1966.

(53) E.J. Catchpole, "The Optimum Design of Compression surfaces having Unflanged Integral Stiffeners", J. of Royal Aeronautical Society, Vol., 58, November, 1954.

(54) G. Gerard, "Introduction to Structural Stability", McGraw-Hill, New York, 1962.

(55) R.F. Crawford, and A. Burns, "Minimum Weight Potentials for Stiffened Plates and Shells", A.I.A.A., Vol., 1, pp 879, 1963.

(56) F.T. Barwell, "Sandwich Construction and Core Materials", Part 1, Aeronautical Research Council, R. &. M. No. 2123 1945.

(57) R.H. Warring, "Engineering Properties of Balsa", Wood J., February, 1966, Issued by Solarbo Limited, Commerce Way, Lacing, Sussex.

(58) T.H. Megson, "Aircraft Structures for Engineering Students", Edward Arnold, Pub., 1977.

(59) G. Gabrielli, Lezione Sulla Scienza Del Progetto Degli Aeromobili, Seconda Edizione, Levrotto e Bella, Torino, 1974.